MC
..2.
e
QC
879.5
.U45
no.32
c.2

DEPARTMENT OF COMMERCE
WEATHER BUREAU

WEATHER BUREAU

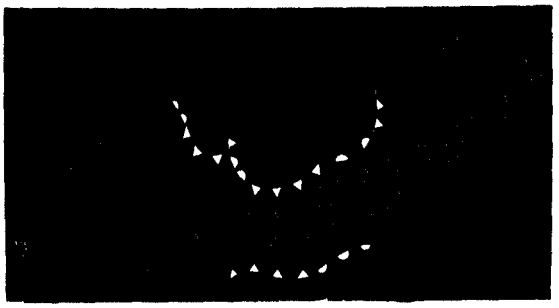

# METEOROLOGICAL SATELLITE LABORATORY
# REPORT NO. 32

## Tiros Photographs and Mosaic Sequences of Tropical Cyclones in the Western Pacific During 1962

WASHINGTON, D. C.
JULY 1964

## METEOROLOGICAL SATELLITE LABORATORY REPORTS

(1-20, 23, 26, 30 are available through the Office of Technical Services, U. S. Department of Commerce, Washington 25, D. C. The OTS number and price follow each entry.)

Number

1. Cloud Conference Summary, L. F. Whitney, Jr., (July, 1960) PB 163 727 $2.60

*2. Analysis of Project Hugo Test, Firing, Dec. 5, 1958, L. F. Hubert, (August, 1960) PB 163 728 $5.60

*3. Preliminary Studies of Atmospheric Energy Parameters, J. S. Winston, (January, 1961) PB 163 729 $3.60

4. Open

5. TIROS I - Camera Attitude Data, Analysis of Location Errors, and Derivation of Correction for Calibration, L. F. Hubert, (April, 1961) N 6211116 $6.60
Supplement to 5: Canadian Grids for TIROS I, Additional Orientation Data, Errata, L. F. Hubert, (June , 1961) N6211117 $4.60

*6. Nimbus Data Utilization Plan, (Anon), (April, 1961) PB 163 732 $2.60

7. Identification of Cloud Forms from TIROS I Pictures, C. O. Erickson and L. F. Hubert, (June, 1961) N 62 14286 $7.60

8. Ice Photography from the Meteorological Satellites TIROS I and TIROS II, D. Q. Wark and R. W. Popham, (March, 1962) PB 163 734 $4.60

*9. Documentation for TIROS III Television Data, L. F. Hubert, (March, 1962) PB 163 735 $6.60

*10. Infrared Flux and Surface Temperature Determinations from TIROS Radiometer Measurements, D. Q. Wark, G. Yamamoto, and J. H. Lienesch, (August, 1962) N 63 11881 $8.60
Supplement to MSL Report No. 10, (April, 1963) PB 165 208 $1.10

11. Perspective Locator Grids for TIROS Pictures, M. H. Frankel and C. L. Bristor, (October, 1962) PB 163 737 $4.60

12. Catalog of Supplemental Meteorological Data Concurrent with TIROS Satellite Observations (TIROS I-V), R. L. Pyle, (August, 1962) PB 163 738 $4.60

*13. Conference on Sferics Measurements, S. Soules (Ed.), (October, 1962) PB 163 739 $5.60

14. A Technique for Precise Analysis for Satellite Data - Vol. 1, Photogrammetry, T. Fujita, (February, 1963) PB 163 740 $9.60

15. Calibration of Image Distortion in TIROS Wide Angle Photography, R. C. Doolittle, (July, 1963) PB 163 741 $5.60

16. Documentation for TIROS IV Television Data, R. L. Pyle, (May, 1963) PB 163 742 $8.10

(Continued on inside of back cover)

* Out of Print

This paper has been printed as a manuscript report for the information of selected interested organizations. As this reproduction does not constitute formal scientific publication, any reference to it in published articles and scientific literature should identify it as a manuscript of the U. S Weather Bureau, National Weather Satellite Center.

U. S. DEPARTMENT OF COMMERCE

Luther H. Hodges, Secretary

U. S. WEATHER BUREAU

Robert M. White, Chief

METEOROLOGICAL SATELLITE LABORATORY

REPORT NO. 32

# TIROS PHOTOGRAPHS AND MOSAIC SEQUENCES OF TROPICAL CYCLONES IN THE WESTERN PACIFIC DURING 1962

by Robert W. Fett*

* Captain, USAF
AWS Member
National Weather Satellite Center

LIBRARY

N.O.A.A.
U S Dept. of Commerce

Washington, D. C.
July 1964

129 428

QC
879.5
U45
no. 32
c. 2

# National Oceanic and Atmospheric Administration
# TIROS Satellites and Satellite Meteorology

## ERRATA NOTICE

One or more conditions of the original document may affect the quality of the image, such as:

Discolored pages
Faded or light ink
Binding intrudes into the text

This has been a co-operative project between the NOAA Central Library and the Climate Database Modernization Program, National Climate Data Center (NCDC). To view the original document contact the NOAA Central Library in Silver Spring, MD at (301) 713-2607 x124 or Library.Reference@noaa.gov.

HOV Services
Imaging Contractor
12200 Kiln Court
Beltsville, MD 20704-1387
January 26, 2009

TABLE OF CONTENTS


| | | Page |
|---|---|---|
| I. | INTRODUCTION | 1 |
| II. | ACKNOWLEDGEMENTS | 2 |
| III. | REFERENCES | 2 |
| IV. | LIST AND DESCRIPTION OF FIGURES | 3-22 |

| | | Figure Number |
|---|---|---|
| V. | TROPICAL CYCLONE PHOTOGRAPHIC AND ANALYSIS SECTION | |
| a. | IRIS | 1 |
| b. | JOAN | 2 |
| c. | OPEL | 3 |
| d. | PATSY | 4-6 |
| e. | RUTH | 7-24 |
| f. | SARAH | 25-31 |
| g. | THELMA | 32-42 |
| h. | VERA | 43-54 |
| i. | WANDA | 55-63 |
| j. | AMY | 64-78 |
| k. | CARLA | 79 |
| l. | DINAH | 80 |
| m. | EMMA | 81-82 |
| n. | FREDA | 83-90 |
| o. | GILDA | 91 |
| p. | IVY | 92-95 |
| q. | JEAN | 96-113 |
| r. | KAREN | 114-125 |

# TIROS PHOTOGRAPHS AND MOSAIC SEQUENCES OF TROPICAL CYCLONES IN THE WESTERN PACIFIC DURING 1962

## I. INTRODUCTION

Of the 24 major Western Pacific typhoons of the 1962 season the TIROS meteorological satellite obtained good views of at least 18. The storms were viewed during various stages of development, and frequently on consecutive days. Some of the mosaics constructed for these storms have been published [1, 2, 3]. but for the most part only incomplete series demonstrating significant characteristics have been shown. The other views, of course, are also extremely interesting containing not only views of tropical systems but those of higher latitudes as well. This report contains an extensive and nearly complete series of the TIROS views of the major tropical cyclones of the Western Pacific during 1962.[1] The report is intended to be more than a catalogue of the various views obtained. The relationship of the appearance of the cyclone to flow patterns suggested by cirrus striations and the direction of shear of cumulonimbus anvils, for example, is discussed. The question of development and changes in appearance with changes in intensity are also described. For this type of documentation data derived through the efforts of the Joint Typhoon Warning Center at Guam and summarized in the Annual Typhoon Report, 1962 [6] , have proven especially valuable and these are frequently referred to.[2] At the same time it was not fully possible to document all of the interpretive aspects involved in these discussions though many analyses and time-sections are attached. Further, more definitive documentation of most of these aspects has been given in the references listed. The following definitions of the various stages of typhoon development adopted from Dunn and Miller [4] are used in this report:

Tropical disturbance - Rotary circulation slight or absent at the surface but possibly better-developed aloft. There are no closed isobars and no strong winds. This type of disturbance is common throughout the tropics.

Tropical depression - One or more closed surface isobars. Wind force equal or less than 33 knots.

---

1 TIROS views of un-named storms or weaker disturbances are not included in this collection except in association with a named storm. Some of the views of decaying storms or storms which have become extra-tropical in association with frontal zones have not been included. And, finally, further investigation may reveal formative stages of the storms considered, which were viewed by TIROS, but were not recognized as a formative stage by the author - and these are not included.

2 From this source the best estimate of maximum sustained surface wind speed is given whenever available. This estimate is generally a smoothed value derived through post-analysis which attempts to correlate and make consistent all sources of maximum wind speed data obtained from a particular storm at a given time.

Tropical storm - Closed surface isobars, wind force 34-63 knots.

Typhoon - Wind force 64 knots or more.

The storms are presented chronologically commencing with Typhoon Iris on May 27, 1962 and ending with Typhoon Karen on November 14, 1962.[3] In this brief period TIROS V and TIROS VI obtained this fascinating series of pictures which are unequaled to this date in terms of completeness and quality of view. It is anticipated that this collection will have great value for comparison with views of other storms obtained in years to come.

## II. ACKNOWLEDGMENTS

The mosaics in this report were prepared with the assistance of S/Sgt Robert T. Furnas and A1C Thomas F. Hayes. The TIROS photographs were developed and painstakingly processed by Norman W. Springer. Without the active support of these individuals and that of Mrs. Margie DiNenna in preparing the manuscript this report would not have been possible.

## III. REFERENCES

1. R. W. Fett, "Aspects of Hurricane Structure: New Model Considerations Suggested by TIROS and Project Mercury Observations, "Monthly Weather Review, vol. 92, No. 9, Feb. 1964, pp. 43-60.

2. R. W. Fett, "Characteristics of the Formative Stage of Typhoon Development: A Satellite Study," Presented at the National Conference on Physics and Dynamics of Clouds, Chicago, Ill., 24-2 March 1964. Unpublished Weather Bureau manuscript.

3. R. W. Fett, "TIROS V Views Final Stages in the Life of Typhoon Sarah August 1962, "Monthly Weather Review, vol. 91, No. 8, Aug. 1963, pp. 367-373.

4. G. E. Dunn and B. I. Miller, Atlantic Hurricanes, Louisiana State University Press, Baton Rouge, La., 1960, 326 pp. (see p. 31).

5. H. Riehl, Tropical Meteorology, McGraw-Hill Book Co., Inc., New York

6. Kotsch, Hutchinson and Staff, "Annual Typhoon Report, 1962," Fleet Weather Central, Joint Typhoon Warning Center Publication, 305 pp.

3 Please note that when more than one typhoon is visible in a given section this same mosaic is duplicated for ease of discussion in the appropriate section dealing with the other storm. (See Table of Contents)

## IV. LIST OF FIGURES

***IRIS***

FIGURE 1. A TIROS IV mosaic of Typhoon Iris on May 27, 1962. Maximum sustained surface winds were near 65 kt . (smoothed) and decreasing.

***JOAN***

FIGURE 2. A TIROS V mosaic of Tropical Storm Joan on July 8, 1962. The center of circulation lies on the western edge of the storm. This asymmetry of the center of circulation with respect to the major cloud shield is typical of storms in the formative or less intense phase. Joan formed on the 6th of July, attained tropical storm intensity on the 7th, and was reported to have had maximum sustained surface winds of near 60 kt. (smoothed) at the time of this TIROS view. These winds are unusually strong for a storm with such pronounced asymmetry [2] .

***OPEL***

FIGURE 3. A TIROS V mosaic of Typhoon Opel, on August 4, 1962. Maximum winds were 110 kt. (smoothed). The well defined eye interior to the major cloud shield, as in this example, appears to be almost always indicative of an intense typhoon. The outflow aloft is well revealed in the cirrus striations which suggest northerly flow over the storm's eastern quadrants.

***PATSY***

FIGURE 4. A TIROS V mosaic of a formative stage of Typhoon Patsy on August 4, 1962. Patsy had been tracked as an easterly wave into the area shown in the TIROS view by the Joint Typhoon Warning Center.[4] Their postanalysis of this storm [6, p. 111] indicates that the initial impetus which caused further development was the result of a "surge from westerlies into easterlies and MPT (Mid-Pacific Trough) at the 200 mb level". The TIROS pictures of Opel (Figure 3) suggesting northerly upper-level flow in the cirrus striations on the eastern side of this storm suggest that this may have been the direction from which the surge came in a manner also observed in the development of a vortex trailing Hurricane Carla, 1961 [1, p. 54] and in the development of Typhoon Vera, described later in this series.

FIGURE 5. A TIROS V mosaic of a formative stage of Typhoon Patsy on August 5, 1962. The upper-level flow, from Typhoon Opel to the area of Patsy is evident in this sequence of pictures through the marked striations in the cirrus cloudiness and can also be deduced from the direction of shear of the visible cumulonimbus anvils. Patsy at this time formed a closed surface vortex and was listed as tropical depression number 51 by the Joint Typhoon Warning Center.

---

[4] Analyses utilized by the Joint Typhoon Warning Center were prepared by members of the U. S. Fleet Weather Central, U.S. Navy.

FIGURE 6. A TIROS V mosaic of Patsy as a tropical depression on August 6, 1962. Easterly wave, numbered 52 by the Joint Typhoon Warning Center is visible far to the east trailing Patsy. Patsy intensified to 40 knots by 2250 GMT on this day. No further TIROS views were obtained of this storm.

***RUTH***

FIGURE 7. A TIROS V mosaic of an early stage of Typhoon Ruth, on August 13, 1962. The vortex near 25°N, 161°E. was also of tropical depression intensity.

FIGURE 8. The Joint Typhoon Warning Center's 2000-ft. streamline analysis for August 13, 1962. This analysis reveals that Ruth had a well defined low level circulation at the time of the TIROS V photos of Figure 7.

FIGURE 9. The Joint Typhoon Warning Center's 200-mb. analysis for August 13, 1962. This analysis reveals a diffluent zone above the formative stage of Ruth. That this pattern was favorable for intensification is shown in Figure 10.

FIGURE 10. A TIROS V mosaic of Tropical Storm Ruth, on August 14, 1962. Maximum winds were near 60 kt . Note the enhancement of convection in the convergent band along 12°N. latitude. A tropical depression is visible near 25°N, 158°E.

FIGURE 11. The Joint Typhoon Warning Center's 2000-ft. streamline analysis for August 14, 1962. Note the convergence asymptotes to the south of Ruth corresponding to the area of enhanced convection in Figure 10.

FIGURE 12. The Joint Typhoon Warning Centers 200-mb. analysis for August 14, 1962. The anticyclone aloft over the storm is well revealed by this analysis. Black arrows indicate wind direction suggested by the cirrus striations in Figure 10. The agreement of these indications with the 200-mb. streamlines is quite good.

FIGURE 13. A TIROS V mosaic of Typhoon Ruth, on August 15, 1962. Maximum winds were near 80 kt. (smoothed). A pronounced clear zone (annular zone of subsidence) is visible along the northern rim of the cloud shield. Note the extensive trailing convective cloudiness to the south. Remains of the tropical depression to the north are visible along latitude 26°N.

FIGURE 14. An individual frame from the orbit of Figure 13 showing some of the details of the internal banding of Ruth. The center of circulation is highly asymmetrical with respect to the cloud shield and is located to the left of the center fiducial mark in the photograph. This asymmetry appears to be a continuation of the similar asymmetrical distribution apparent on the preceding day in Figure 10. The expanding cloud shield extending far to the northeast of the center of circulation suggests a rapidly intensifying condition which has also been noted in other storms. Maximum sustained winds increased from near 80 kt. at the time of this picture to 140 kt. before 24 hours had elapsed.

FIGURE 15. A TIROS V mosaic showing a peripheral view of Typhoon Ruth, on August 16, 1962. The symmetrical appearance of the cloud shield of Ruth even in this high nadir angle view suggests that it was an intense storm. Maximum sustained winds computed by the Joint Typhoon Warning Center (JTWC) were 150 knots (smoothed).

FIGURE 16. An individual frame from the orbit of Figure 15 showing the edge of Typhoon Ruth in relation to the flow at 200 mb . It can be seen that a relatively open channel extends from NE to SW under the shear line at 200 mb separating northeasterly flow over Japan from the southwesterly outflow of Typhoon Ruth.

FIGURE 17. A TIROS V mosaic of Typhoon Ruth on August 18, 1962. Maximum sustained winds were near 95 knots (smoothed). Note the symmetry of the eye with respect to the major cloud shield. This appears to be characteristic of the more intense storm in a more or less steady state condition.

FIGURE 18. An individual frame from the orbit of Figure 17 showing more clearly the concentric eye of the storm.

FIGURE 19. A TIROS V mosaic of the southern edge of Typhoon Ruth on August 19, 1962. Maximum sustained winds were near 90 kt. (smoothed). Note the excellent agreement of the 200-mb. wind at Iwo Jima (indicated on the nephanalysis) to the northeasterly flow suggested by the cirrus striations over the same area (near 25°N, 141°E).

FIGURE 20. A TIROS V mosaic of the western edge of Typhoon Ruth on August 19, 1962.

FIGURE 21. A TIROS V mosaic of Typhoon Ruth on August 20, 1962. The eye is apparent near the center of the cloud shield. Maximum sustained winds were near 85 kt. (smoothed). Cumulonimbus clouds between latitudes 5°-20°N. are sheared to the west-southwest by east-northeasterly upper level winds.

FIGURE 22. A TIROS V mosaic of Typhoon Ruth on August 21, 1962. The eye is apparent near the center of the cloud shield. Maximum sustained winds were near 75 kt. (smoothed). The frontal zone appears intense in the TIROS pictures but was not indicated on the Honolulu surface analysis.

FIGURE 23. A TIROS V mosaic of Typhoon Ruth on August 22, 1962. This mosaic shows Ruth inter-acting with the polar front which was markedly visible in Figure 22.

FIGURE 24. A TIROS V mosaic of Ruth on August 23, 1962, as it merged with the polar front.

***SARAH***

FIGURE 25. A TIROS V mosaic of Sarah on August 14, 1962, 24 hours prior to initial reconnaissance. The pronounced low level banding defining a center of circulation obscured by a relatively small upper cloud shield is characteristic of a tropical cyclone which is approaching tropical storm intensity [2].

FIGURE 26. A TIROS V mosaic of Typhoon Sarah on August 16, 1962. Maximum surface winds were near 70 kt (smoothed). Note the cirrus cloudiness radiating out over the annular zone of subsidence on the north side of the storm, merging with an outer convective band or pre-hurricane squall line.

FIGURE 27. A TIROS V mosaic of Typhoon Sarah on August 19, 1962. Maximum sustained winds were near 70 kt (smoothed). Note the apparent subsident effect sharply inhibiting convective cloudiness over Korea and Kyushu, Japan. Cumulonimbus activity was pronounced along the coast of China, apparently a result of the frictional convergence of the storm circulation over the land area.

FIGURE 28. A TIROS V mosaic of Sarah on August 21, 1962 with maximum sustained winds near 50 knots (smoothed). The northern edge of Sarah was pressed against the island of Kyushu, Japan at this time and terrain effects resulted in the "clear" notch cutting into the northern rim of the cloud shield [3]. The frontal zone appears intense in the TIROS pictures but was not indicated on the Honolulu surface analysis.

FIGURE 29. This figure shows an enlarged view of Sarah from the orbit of Figure 28. The center of circulation and possible eye appears to be located in the middle of the southern half of the storm.

FIGURE 30. A TIROS V mosaic of Sarah in the decaying stage over the islands of Japan on August 22, 1962. Note the flatter and less reflective appearance of the cloud shield of Sarah in this view as opposed to that of Figures 28 and 29. This appears to be indicative of a decrease in the depth of cirrus cloudiness over the storm and relates well to the similar lessening of storm intensity noted during this same period.

FIGURE 31. A final TIROS V view of Sarah on August 23, 1962, as the storm was all but obliterated.

***THELMA***

FIGURE 32. A TIROS V mosaic showing an early stage of Thelma on August 19, 1962. The position of Thelma with respect to Vera should be noted for comparison with the next figure.

FIGURE 33. A TIROS V mosaic of Thelma on August 20, 1962, 24 hours prior to initial reconnaissance. The cloud shield over the center of circulation suggests that it was approaching tropical storm intensity [2]. Note the squall line formation in the storm's southwestern quadrant.

FIGURE 34. A TIROS V mosaic of Thelma approaching typhoon intensity on August 21, 1962. A pre-hurricane squall line is well developed along the western side of the storm. The storm was moving toward the northwest at the time of the TIROS pictures.

FIGURE 35. A TIROS V mosaic of Thelma on August 22, 1962. Maximum sustained surface winds decreased to near 50 kt (smoothed).

FIGURE 36. A TIROS V mosaic of Typhoon Thelma on August 23, 1962. The well defined eye interior to the cloud shield suggests an intense mature storm. This is verified by the Joint Typhoon Warning Center's estimate of maximum winds near 105 knots (smoothed).

FIGURE 37. A TIROS V mosaic of Typhoon Thelma on August 24, 1962 with maximum sustained winds near 90 knots (smoothed).

FIGURE 38. An individual frame from the orbit of Figure 37 showing details of the structure of Typhoon Thelma. The spiral band structure is well revealed in this photograph which also shows pronounced squall lines along the northern edge of the cloud shield. Cirrus cloudiness radiating outward along the eastern side of the storm appears closely aligned with the 200-mb. flow as indicated by Iwo Jima's wind of 320 degrees at 30 knots for August 24 at 0000 GMT. (See the nephanalysis, Figure 37).

Figure 39. A TIROS V mosaic of Typhoon Thelma on August 25, 1962 with maximum sustained winds near 120 kt. (smoothed). The cloud patch in Thelma's south-eastern quadrant should be compared with a similar development to the south of Ruth in Figure 19.

FIGURE 40. A TIROS V view of Thelma on August 26, 1962. Maximum sustained winds were near 60 kt. (smoothed).

FIGURE 41. A TIROS V view of the decaying stage of Thelma on August 27, 1962. Maximum sustained winds were less than 35 kt. (smoothed).

FIGURE 42. A TIROS V mosaic of the eastern edge of Thelma on August 27, 1962.

***VERA***

FIGURE 43: A TIROS V mosaic of the formative stage of Typhoon Vera on August 19, 1962. Vera apparently formed under the diverging northerly 200-mb. outflow of Typhoon Ruth (see Figure 44).

FIGURE 44. A 200-mb. streamline analysis showing the relationship of the cloud masses of Vera and Thelma from the preceding figure, to the upper level flow pattern for 0000 GMT on the same day. The cloud mass associated with Vera is in a position postulated by Riehl as being ideal for intensification [4, p. 333].

FIGURE 45. A TIROS V mosaic of the formative stage of Typhoon Vera on August 20, 1962. Note the similarity of appearance of Vera on this day to that of the preceding day in Figure 43. Vera at this time was just approaching Iwo Jima (near 25°N, 141°E).

FIGURE 46. A time cross-section for Iwo Jima during the period August 19-23, 1962. Effects of the passage of Vera late on August 20, 1962 are well revealed in this analysis. The falling 24-hour height changes prior to passage of the disturbance followed by rising 24-hour height changes, as well as the wind shifts especially pronounced from 700 to 500 mb., reflect this passage.

FIGURE 47. A TIROS V mosaic of the formative stage of Typhoon Vera on August 22, 1962. Some low level banding effects are visible in the northern quadrants of the disturbance.

FIGURE 48. A TIROS V mosaic of Vera on August 23, 1962. Evidence of low level banding - an important indicator of intensification, still seems quite weak. Ship reports in the area were indicating very light winds.

FIGURE 49. A TIROS V mosaic of Vera on August 24, 1962. Vera at this time developed moderate low level banding with its center of circulation in the northern extremity of the disturbed area. Note the pronounced annular zone of probable subsidence and the long outer convective band which delineates the limit of this zone. Nine hours after these pictures were taken reconnaissance reported "feeder bands formed SW to NE". The initial appearance of these bands has been found to be a useful indicator of intensity. In the Pacific it is felt that "when feeder bands first begin to appear on the radar scope, the tropical system will develop to storm proportion or greater. This stage is usually indicative of winds of 30 to 40 knots". (1964 Interdepartmental Typhoon Meeting.) Vera was reported to have maximum winds of 45 kt by August 25 at 0654 , slightly more than 24 hours after the view shown in this figure.

FIGURE 50. An individual frame from the orbit of the preceding figure showing details in the structure of Vera. The apparent center of circulation can be seen in the northwest quadrant of the center fiducial mark.

FIGURE 51. A TIROS V mosaic of Vera as a tropical storm on August 25, 1962. Maximum sustained winds were near 45 kt (smoothed). The small circulation area of Vera suggested by the TIROS photos, was verified by surface analyses (see Figure 53). In fact, Vera was undetected by conventional means until August 25 according to the Joint Typhoon Warning Center "even though the area was more than adequately covered by surface ship observations".

FIGURE 52. A TIROS V mosaic of Typhoon Vera on August 26, 1962. Vera attained maximum intensity of approximately 75 knots on this day.

FIGURE 53. A comparison of the circulation area of Typhoon Vera, August 1962 with that of Tropical Depression No. 90, December 1962 (from Annual Typhoon Report, 1962). This figure shows that intense storms (high maximum sustained surface wind speeds) do not always have large circulation areas. On the other hand, storms with large circulation areas do not always have high surface winds. The pictures of Vera also suggest the possibility of a close correspondence of the major overcast area of a tropical cyclone to the circulation area. This is also suggested in Figure 22 showing Typhoons Sarah and Ruth and the accompanying surface analysis.

FIGURE 54. A TIROS V mosaic showing the western edge of Vera on August 27, 1962, as maximum sustained winds decreased to near 60 kt. (smoothed).

***WANDA***

FIGURE 55. A TIROS V mosaic of a formative stage of Typhoon Wanda on August 24, 1962. Reconnaissance on this day placed a center near 7.2°N. and 153.5°E. with maximum surface winds of only 10 kt. There was a pronounced anticyclone at 200 mb. over the disturbance at the time of the TIROS photos. This is also suggested by the direction of shear of the cumulonimbus anvils being toward the east in the overcast patch near 5°N.

FIGURE 56. A TIROS V mosaic of a portion of Wanda on August 26, 1962. Reconnaissance placed a center on this day near 10.8°N, 142.8°E. with maximum surface winds near 15 kt. The center of circulation is not obvious on this mosaic.

FIGURE 57. A TIROS V mosaic of Wanda on August 27, 1962. Maximum sustained winds were estimated at 25 kt. The well marked bands leading to the apparent center of circulation in the northeast and southwest quadrants; the small cloud shield over the obscured center of circulation; and the pronounced outflow suggested by the cirrus striations make this an "ideal" example of a tropical cyclone which is approaching or has just attained tropical storm intensity [2]. Wanda was reported to have had surface winds of 40 kt. (smoothed) less than 25 hours after these pictures were taken.

FIGURE 58. The 200-mb. analysis prepared by the Joint Typhoon Warning Center for 0000 GMT, August 27, 1962. The outline of Wanda as viewed by TIROS in the preceding figure has been superimposed upon this analysis. It can be seen that Wanda at this time had a well developed anticyclone aloft. The black arrows on this figure represent the suggested upper level flow der ived from the TIROS photographs. These fit the JTWC's analysis quite well. The shear line or col area at 200 mb. on the north side of the storm coincides with a clear area near 18°N in the TIROS photos on the north side of the northernmost spiral arm and suggests that this area may also have been one of appreciable subsidence.

FIGURE 59. A TIROS V mosaic of Typhoon Wanda on August 29, 1962. The cirrus striations from the cloud shield and cumulonimbus anvils depict the anticyclonic turning of the wind above Wanda extremely well. High level easterly winds are apparent from the TIROS photos from the southern edge of Wanda down almost to the equator (see Figure 60).

FIGURE 60. Details of the preceding figure are shown in these two frames. The lower left frame shows an outer convective band along the southwestern edge of Wanda. Similar bands are commonly found delineating the edge of the annular zone of subsidence [1]. The frame in the upper right gives perhaps the best view of Wanda. This frame indicates that the center of circulation lies within the overcast cloudy area of the southernmost overcast cloud group.

FIGURE 61. A TIROS V mosaic of Typhoon Wanda on August 30, 1962 with maximum sustained winds near 85 knots (smoothed). Note the odd shape near the center of the storm suggesting a possible double eye. Double eyes have been observed to occur within the lowest pressure area of a storm primarily in the less intense phase. Concentric eyes, on the other hand are characteristic of the more intense storm with maximum sustained winds of over 120 kt. [5, p. 271].

FIGURE 62. A TIROS V mosaic of Wanda on August 31, 1962. Maximum sustained winds were near 95 kt. (smoothed). These photos suggest northerly upper level flow on the east side of Wanda and southerly upper level flow on the west side of Amy with a col area or shear line between the two storms. This deduction is verified by the 200-mb. analysis for August 31, 1962 (not shown).

FIGURE 63. A TIROS V mosaic of Typhoon Wanda on September 1, 1962 just prior to striking Hong Kong with maximum sustained winds near 85 kt. (smoothed).

***AMY***

FIGURE 64. A TIROS V mosaic showing the eastern edge of the formative stage of Typhoon Amy on August 27, 1962. The direction of shear of the cumulonimbus

anvils associated with Amy is toward the southeast. This suggests that the TIROS photo is of the northeastern quadrant of Amy where upper-level anticyclonic winds from the northwest might be anticipated.

FIGURE 65. A TIROS V mosaic of a formative stage of Typhoon Amy on August 28, 1962. Maximum sustained surface winds were estimated at 30 kt. The upper anticyclone over the storm is well revealed by the direction of shear of the cumulonimbus anvils, which indicate westerly winds on the north side of the storm and easterlies on the south side of the storm (see Figure 66).

FIGURE 66. A 200-mb. streamline analysis prepared by the Joint Typhoon Warning Center coinciding closely in time to the TIROS pictures of the preceding figure. This analysis verifies the upper anticyclonic conditions above Amy suggested by the cirrus striations in the TIROS photos. Some of these have been indicated by means of black arrows superimposed on the JTWC analysis.

FIGURE 67. A TIROS V mosaic of Amy on August 29, 1962 as a tropical storm with maximum sustained winds of 55 kt. (smoothed). This view offers a very interesting comparison to that of 24-hr. prior (Figure 65). The storm was still separated into two distinctive cloudy areas - one to the north and the other to the south. However, the northernmost cloudy area developed a dense cirrus shield which obscured much of the lower level cloudiness, visible on the preceding day. The expanding cirrus shield was clear evidence of further intensification. Such evidence would be quite useful operationally - although it was not employed for that purpose at the time the pictures were obtained.

FIGURE 68. A TIROS V mosaic of Typhoons Wanda and Amy on August 31, 1962. Inter-relationships of upper level flow between two adjacent typhoons is well shown in this example. The upper anticyclone over each of the typhoons is shown by the direction of shear of the cumulonimbus anvils and cirrus striations. These imply northerly flow on the east side of typhoon Wanda ( max. winds 95 kt.) and southerly flow on the west side of typhoon Amy (max. winds 75 kt.). A col area exists between the two storms.

FIGURE 69. A TIROS V mosaic of Typhoon Amy on August 31, 1962. Maximum winds were near 110 kt. (smoothed). Marked squall lines are evident along the northern quadrants of the storm. The storm was moving toward the west at 10 kt. at the time of these pictures. Some outer band debris appears to have been "left behind" in the wake of the storm in the eastern quadrants as the storm progressed toward the west.

FIGURE 70. Individual frames of Typhoon Amy from the orbit of the preceding figure. These pictures demonstrate, in an exceptionally fine manner, the continuous nature of the high cirrus cloud shield through which much of the underlying convective structure of the storm can still be seen.

FIGURE 71. A TIROS V mosaic of Typhoon Amy on September 1, 1962. The storm reached maximum intensity at this time with winds of 140 kt. (smoothed). The squall line area, visible between latitudes 15°-20°N. and longitudes 140°-145°E. resembles very closely the formation shown in the eastern storm quadrants on the preceding day (Figures 69 and 70). However, if it is the same formation it has been further separated from the storm which continued its westward movement at a speed approximately 12 kt. during the preceding 24-hour period. Another possible explanation for this cloud band is that it was an ITC effect on both days. The charts of the Joint Typhoon Warning Center indicate an ITC in each instance leading up to the storm from the eastern quadrants and out from the storm area in the western quadrants.

FIGURE 72. Individual frames from the orbit of the preceding figure. The squall line formation as well as the very symmetrical appearance of the cloud shield with respect to the eye is seen in these views of Typhoon Amy in its most intense phase with maximum sustained surface winds of 140 kt. (smoothed). Note the horizontal cloud alignment near the bottom edge of these pictures. These lines coincide in direction with strong easterly flow indicated at this time on maps at the 200-mb. level (analyses not shown).

FIGURE 73. Two selected frames from TIROS V, orbit 1081, at 2226 GMT on September 2, 1962. These views show Typhoon Amy with maximum sustained surface winds near 135 kt. (smoothed). The large symmetrical high cloud shield surrounding the storm is also suggestive of a very intense circulation. The brighter cloud band along 140°E. longitude approximates the location analysed as the ITC by the Joint Typhoon Warning Center. Guam, located near 13.5°N, 145°E, recorded passage of a small cyclonic circulation in its surface analysis, at approximately the time of these pictures. Generation of trailing cyclonic vortices following intense tropical cyclones appears to be a common occurrence (see figures 4-6, 19, 39, 82, 92, and Reference 1, p. 54).

FIGURE 74. Two selected frames from TIROS V, orbit 1096 at 2326 GMT on September 3, 1962. These views show Typhoon Amy with maximum sustained surface winds near 130 kt. (smoothed). The eastern edge of the storm appears "broken-up" - a probable lee effect of the island of Luzon located just to the southwest of the storm. It is interesting that the reconnaissance estimate of maximum winds showed a significant drop in speed to 70 kt. at this time in contrast to the smoothed estimate on the post-analysis. The TIROS view would tend to support the lower reconnaissance estimate.

FIGURE 75. A TIROS V mosaic of Typhoon Amy on September 4, 1962. Maximum sustained winds were near 130 kt. (smoothed) as the storm interacted with a frontal zone, the cloud band of which is visible extending northeastward from Amy.

FIGURE 76. Two individual frames from the orbit of the preceding figure. These pictures show detailed views of the frontal band extending into the northwestern quadrant of Amy in addition to an enlarged view of the storm area. Note the squall line in the northeastern quadrant of Amy. The storm was moving toward the northwest. This is a good example of why efforts to relate direction of storm movement to the quadrant in which a squall line or convective band is located have failed. These outer bands appear to be related to subsiding effects at the rim of the major overcast cloud shield. The subsiding effects apparently result in low level convergence visibly expressed as convective bands parallel to the rim of the high cloud shield [1]. Such bands appear to be continually regenerated as older bands, subject to steering currents other than those of the main body of the storm, are "left behind" or move outward on independent trajectories. Figures 69, 71, and 75 all support this hypothesis.

FIGURE 77. A TIROS V mosaic of the western edge of Amy on September 5, 1962. Maximum sustained surface winds were near 40 kt. (smoothed). Most of the visible cloudy area associated with Amy in this mosaic was over land. The reduction in the depth of the overlying cirrus shield is apparent in the coarser appearance of the cloudiness. (Compare with Figure 70 for example).

FIGURE 78. Individual frames of Amy from the orbit of the preceding figure. Note the long shadow produced by dense cirrus associated with a jet stream from the southeast. Transverse banding of the cirrus is well shown in the photograph on the upper right of this figure (see a similar effect at the edge of another typhoon in Figure 108).

***CARLA***

Figure 79. Individual frames from TIROS V, orbit 1288 R/O 1286 showing a formative stage of Typhoon Carla as a tropical depression at 0557 GMT on September 17, 1962.

****DINAH***

FIGURE 80. A picture of Dinah as a tropical storm with maximum winds near 55 kt. (smoothed). This picture was taken by TIROS VI on orbit 173 R/O 172 at 2338 GMT, September 29, 1962. The pronounced outflow effects, visible in the cirrus striations and cumulonimbus anvils, coupled with the extensive large diameter cirrus shield also visible, suggest an intense storm. Northerly winds aloft implied by the cirrus striations relate well to the 200-mb. analysis for 0000 GMT, September 30, 1962 (not shown).

***EMMA***

FIGURE 81. A TIROS VI photograph of a formative stage of Typhoon Emma on September 27, 1962 at 2352 GMT. The picture was obtained on orbit 144 R/O 140. Cloudiness over the disturbed area is associated with an easterly wave which had been tracked to this location by the Joint Typhoon Warning Center. Westerly winds aloft are implied by the cirrus striations over the northern portion of the disturbance.

FIGURE 82. A TIROS VI mosaic showing the eastern edge of Typhoon Emma on October 3, 1962. Maximum sustained winds were near 110 kt (smoothed). Cirriform cloudiness extends southeastward from the high cloud shield of Emma in response to the upper anticyclonic flow over the storm and forms an interconnecting link with Freda (see discussion of Typhoon Freda, Figures 83-90).

***FREDA***

FIGURE 83. An individual frame of the formative stage of Typhoon Freda on September 26, 1962. This picture was taken by TIROS V on orbit 1415 R/O 1412 at 0055 GMT. The storm was analysed as a junction vortex on the ITC by the Joint Typhoon Warning Center at the time of the TIROS photos. The sharp indentation along the depression's southern boundary stretching from SW to NE along latitude 5° N. suggests the subsident peripheral condition frequently found in developing tropical cyclones.

FIGURE 84. An individual frame showing the extreme northeastern quadrant of Freda in its formative stage. The picture was taken by TIROS VI on orbit 158 R/O 152 on September 28, 1962 at 2255 GMT. Good evidence for strong upper level westerlies is provided by the evidence from the cirrus cloudiness. Neither Freda nor the small low level vortex shown in this picture were readily apparent from the map analyses over this area.

FIGURE 85. A TIROS VI mosaic of Freda as a tropical depression on September 30, 1962. The center of circulation of the storm was in the extreme western quadrant. Reconnaisssance indicated no cloud center. This view of Freda exemplifies the "Comma Configuration" typical of tropical depressions with a maximum central isotach of less than 20 kt. [2] . Reconnaissance crews reported maximum surface winds of 15 kt. approximately 8 hours after these TIROS photos. Trailing cloudiness from Emma is visible between latitudes 15-20°N. on the west side of this mosaic.

FIGURE 86. Two TIROS VI views of a formative stage of Typhoon Freda on October 1, 1962 at 2142 GMT. The pictures were taken on orbit 201 R/O 197.

FIGURE 87. A TIROS V mosaic of a formative stage of Typhoon Freda on October 2, 1962. Freda at this time developed marked low level cloud banding defining a center of circulation very near the edge of major overcast cloudiness in the northwest quadrant of the storm. The obscuration of the center of circulation by an upper cloud shield indicates that Freda had intensi- from previous views. If one compares Figure 85 with Figure 87 this change is immediately apparent. Freda in the latter mosaic would be classified as a "Tropical Depression II" type cyclone with maximum central isotach near 30 kt [2] . This classification is partially substantiated by a ship report near the center, slightly more than an hour after the TIROS pictures, reporting 30 kt. The Joint Typhoon Warning Center estimated maximum sustained surface winds of 40 kt. (smoothed) commencing on October 3, at 0600 GMT Another notable characteristic of this mosaic is the visible chain of convective cloudiness extending northwestward from Freda to the area of Typhoon

Emma. A fainter connecting band of cirriform cloudiness is visible to the north of this band, apparently derived from the outflow of Typhoon Emma (see also Figure 82).

FIGURE 88. A TIROS VI mosaic of Typhoon Freda on October 3, 1962, with maximum sustained surface winds near 70 kt. (smoothed). Figures 85, 87 and 88 present an unusually fine series showing the development of an individual typhoon from a tropical depression (Figure 85) to a near tropical storm (Figure 87) and finally to a full typhoon (Figure 88). The importance of this series is that it demonstrates, in an unusually fine example, that the center of circulation of a tropical cyclone progressively tends to a more symmetrical position with respect to the major overcast cloud shield as the maximum surface wind speeds increase in value. Relative movement of the center of circulation with respect to the cloud shield is from the west to the east.

FIGURE 89. Individual frames from the orbit of Figure 88. The cirrus cloudiness extending southeastward in the outflow of Typhoon Emma is well seen in this Figure, and may be associated with an upper level jet from the north [1]. The eye of Typhoon Freda is also more clearly visible. A tropical depression southwest of Typhoon Freda is visible in the frame at lower left.

FIGURE 90. Selected frames from TIROS VI orbit 273 R/O 269 on October 6, 1962 at 2013 GMT. These views show Freda as a mature typhoon with maximum sustained surface winds near 90 kt. (smoothed).

***GILDA***

FIGURE 91. Two selected views of Typhoon Gilda on October 28, 1962 at 0620 GMT. These pictures were taken by TIROS VI on orbit 582 R/O 581. Gilda had maximum winds of 105 kt. (smoothed) at the time of these pictures and was moving toward the northeast at 12 kt.

***IVY***

FIGURE 92. Individual frames from TIROS VI, orbit 596 R/O 595 on October 29, 1962, at 0522 GMT. The elongated cloud mass in the central portion of the frames is in the area reported to be occupied by Typhoon Ivy. According to the Joint Typhoon Warning Center, Ivy, centered near latitude 20°N, longitude 138°E, possessed winds of 70 kt. at the time of these pictures. This does not relate at all well to the TIROS views which in this case do not even suggest a vortex at that location. The very edge of Typhoon Gilda, with winds of 90 kt , is recognizable as a vortex even in these high nadir angle views, appearing at the edge of the TIROS photo to the far northwest. Ivy was reported to have dissipated 12 hours after these pictures, being absorbed by Typhoon Gilda. The short history of Ivy, its rapid decrease in intensity over the open ocean, and the lack of correspondence between the TIROS pictures and the reported intensity, suggest that the storm may have been weaker than the initial and near final reconnaissance estimate. The question as to the final disposition of this storm also appears to be open to discussion (see Figures 93-95).

FIGURE 93. A TIROS VI mosaic showing the possible remains of Typhoon Ivy on October 30, 1962 (see Figure 94).

FIGURE 94. Individual frames from the orbit of the preceding figure. These views show a cloud mass centered near latitude 10°N, longitude 150°E. which looks suspiciously like the final view of Typhoon Ivy in Figure 92. They are separated by 10 degrees of longitude and 24 hours of time. The trailing edge of Typhoon Gilda which was centered near latitude 29°N longitude 141°E at the time of these pictures is also suggested in these photos as it was in Figure 92. If the cloud mass which looks similar to Ivy in this figure is indeed the remains of that storm an easterly trajectory of approximately 600 miles taking it over the island of Guam (approx. 13.5°N, 145°E) would have been necessary. A time cross-section for this station is shown in the next figure.

FIGURE 95. A time cross-section for Guam during the period October 28, 1962 till November 2, 1962. An intense upper level disturbance apparently passed the station from west to east during the 29th and 30th of October in agreement with the requirement for the cloud mass centered near latitude 10°N, longitude 140°E. on October 29, 1962 (Figure 92) to pass this station in order to achieve a position near latitude 10°N, longitude 150°E. on October 30, 1962 (Figure 94). Note the strong northwesterly upper-level flow over Guam on the 28th and 29th of October. These winds reflecting the outflow of Typhoon Gilda would favor a rapid eastward or southeastward movement of an upper-level disturbance embedded in this flow.

***JEAN***

FIGURE 96. A TIROS VI mosaic of a formative stage of Typhoon Jean on November 1, 1962. The position of the cloud mass centered near 5°N. and 140°E. on this mosaic coincides with the position of a tropical depression which had formed from an easterly wave that had been tracked into this area by the Joint Typhoon Warning Center. The effects of this wave passing Guam on October 31, 1962 can be seen in Figure 95.

FIGURE 97. A time cross-section for the island of Yap (near 9.5°N, 138°E) during the period October 30, 1962 through November 4, 1962. This time-section reveals some interesting characteristics regarding the structure of Jean. Evidence from this analysis indicates passage of the low level circulation of Jean at approximately 1200 GMT on November 3, 1962. However, the extreme western edge of the cloud shield of Jean passed Yap much earlier, between 1200 GMT, on October 31, and 1200 GMT, on November 1, 1962. Evidence of this passage on the time-section is shown by the wind shifts between 200 and 110 mb. during this period. The TIROS view in Figure 96 on November 1, at 0400 GMT indicates that Yap, at the time of orbit 638, was located at the very edge of the major overcast cloud shield associated with Jean. Backing of the winds at 200 mb. from southeast (2 Nov 1200 GMT) to northeast (4 Nov 1200 GMT) during the period of the passage of Jean also indicates that the storm in this early formative stage was capped by an anticyclone. The pattern of an upper level shear line preceding storm center passage by 2-3 days is a common occurrence also noted in the mature storm [1]. The anticyclone aloft, positioned over a lower level incipient disturbance is known to be a favorable pattern for intensification.

FIGURE 98. A TIROS V mosaic of a formative stage of Typhoon Jean on November 2, 1962. The center of low level circulation is apparent in this mosaic near the center of the hook-shaped cloud formation in the northeastern portion of the disturbed area. The estimated position is near latitude 19°N, longitude 143°E. A northerly movement of the depression is thus indicated from its previous position in Figure 96. This center had not yet passed Yap (near 9.5°N, 138°E) as is also apparent from the time cross-section for this station (Figure 97).

FIGURE 99. A TIROS VI mosaic showing the western side of the disturbed area of Jean on November 3, 1962.

FIGURE 100. A TIROS V mosaic showing the eastern side of the disturbed area of Jean on November 3, 1962.

FIGURE 101. A TIROS V mosaic showing the extreme eastern side of the disturbed area of Jean on November 4, 1962. The cumulonimbus cloud masses aligned in an east-west band along latitude 10°N. reveal shear patterns in the cirrus striations indicating northwesterly upper-level flow. This can be verified by comparing the 200-mb. streamline analysis over this area for 0000 GMT, November 4, 1962, with the TIROS photo (analysis not shown).

FIGURE 102. A TIROS VI mosaic of Jean 24 hours prior to reaching tropical storm intensity. Jean at this time was inter-acting with a frontal band extending northeastward from Jean's northwest quadrant. The cirrus outflow pattern in this mosaic is striking and has been noted in other storms during periods of rapid intensification. A comparison of this figure with the earlier view obtained on the 2nd of November in Figure 98 will result in the conclusion that, aside from the small cloud shield over the central area and enhanced cirrus outflow in the later view, the storms are practically identical in appearance! This conservation of general appearance was maintained despite the passage of 3 days in time and a movement of over 700 miles in distance.

FIGURE 103. This figure shows enlarged views of the storm's central area revealing the enhanced cirrus outflow. This outflow pattern should be compared with Figure 104, a 200-mb. streamline analysis which shows excellent agreement with the TIROS indications of upper level outflow.

FIGURE 104. A 200-mb. streamline analysis prepared by the author for 0000 GMT on November 5, 1962. The cloudy area associated with Jean in Figure 103 has been superimposed on this analysis. Black arrows indicate the direction of upper level flow deduced from the cirrus striations over the area of Jean in Figure 103.

FIGURE 105. A TIROS V view of the formative stage of typhoon Jean approximately one hour after the TIROS VI view of the same area shown in Figure 103.

FIGURE 106. A TIROS V mosaic showing Jean on November 6, 1962. Maximum sustained winds at this time had increased to near 50 kt. (smoothed). From the nephanalysis it can be seen that the main body of the storm was moving over the Philippines and this fact undoubtedly accounts for the winds being limited to these lower intensities. The fact that Jean had intensified from much weaker values only after interacting with the frontal zone visible on this mosaic is an observation of some importance. As discussed in the Annual Typhoon Report, 1962 [6, pp 36-40], "For development (of a typhoon) to take place, there must be a pre-existing surface perturbation and a large increase of divergence aloft to provide the "kick" to start the heat engine". Jean had been tracked as a low level perturbation and Figure 105 indicates that upper level divergence was well developed, thus fulfilling these first two criteria. The report continues, "The apparent complement to these two criteria is the need for the energy level of the easterlies to be increased above normal. This additional energy is usually derived from the westerlies." Jean apparently is an excellent example of the low level, polar trough and easterly wave interaction which results in intensification of many tropical cyclones. This type of interaction was originally described by Riehl [5, p 227]. An examination of the surface and upper-level charts reveals that the "trough" associated with the frontal band in Figure 105 was not characterized by a marked change in wind direction at lower levels. The band visible in the TIROS photos represents the trailing edge of a front which was much more pronounced to the northeast. Strong, generally easterly or northeasterly winds prevailed on both sides of the band as a result of the combined effect of the tropical depression to the south and the encroaching anticyclone behind the front. This physical arrangement of the two pressure systems apparently permitted the "energy transfer", discussed in the Typhoon Report, from the westerlies on the north side of the anticyclone, to the easterlies of the tropical depression. We may conclude according to the preceding argument, that the TIROS photos of Figure 105 combined with the conventional data available, might have been very effectively combined to produce a forecast calling for the intensification which did indeed occur.

FIGURE 107. A TIROS V mosaic of Typhoon Jean on November 8, 1962 with maximum sustained surface winds near 90 kt. (smoothed). The storm was moving toward the WNW at approximately 10 kt. Easterly flow aloft is suggested by the shear of anvil tops from cumulonimbus clouds between the equator and 10°N. latitude.

FIGURE 108. Selected frames from TIROS VI, orbit 756 R/O 756 on November 9, 1962 at 0447 GMT. These views show Typhoon Jean with maximum sustained surface winds near 90 kt. (smoothed). The eye of the storm can still be discerned in spite of the high nadir angle view. To the north of Jean a jet stream cirrus band is evident over the Chinese mainland. The shadow of this band on the ground is also clearly evident as it was in the remarkably similar view of a jet stream associated with Typhoon Amy (Figure 78).

FIGURE 109. Two TIROS V views of Typhoon Jean showing areas not visible in the TIROS VI view of Figure 108. Pictures were taken on orbit 2045 R/O 2044, November 9, 1962 at 0403 GMT. What appears to be the ITC is visible along latitude 5°N.

FIGURE 110. A TIROS VI view of the remains of Typhoon Jean on November 13, 1962 at 0235 GMT. The picture was taken on orbit 813 R/O 813. The lack of an upper cloud shield is evidence of the decreased intensity. Surface ship reports indicated maximum winds of 20 to 25 kt near the storm center. An anticyclone was still evident at upper levels on conventional analyses and is also supported by the cirrus striations in the TIROS photo which indicate southerly flow on the west side of the vortex.

FIGURE 111. A TIROS VI picture from orbit 856 R/O 856 of the remains of Jean on November 16, 1962 at 0120 GMT. The depression stagnated over the China Sea and in this view, 3 days after the view in Figure 109, still shows a well developed low level circulation with increased convective activity.

FIGURE 112. Two selected TIROS V views from orbit 2166 R/O 2158 of the remains of Jean on November 17, 1962 at 0120 GMT. Jean at this time shows obvious signs of re-intensification. Numerous ship reports show a well developed low level circulation with speeds of 20-30 kt.

Figure 113. Two final TIROS VI views of Tropical Depression Jean on November 18, 1962 at 0103 GMT. Pictures were taken on orbit 893 R/O 885. The mainland of Indo-China is visible near longitude 110°E.

***KAREN***

FIGURE 114. An early view of a formative stage of Typhoon Karen taken by TIROS V on November 5, 1962. Karen is visible on the western horizon near 5°N, longitude 115°E, just north of what appears to be the ITC. The vortex, in this high nadir angle view, appears quite symmetrical. This is unusual for formative storms unless they are: (1) either very weak with no closed surface circulation; or (2) have already attained near tropical storm intensity with maximum winds approaching 35 kt. [2]. This latter possibility seems the most reasonable when one considers the view of Karen on the following day (Figure 115).

FIGURE 115. A TIROS V mosaic of Karen on November 6, 1962. Without the benefit of the TIROS information the Joint Typhoon Warning Center in a post-typhoon summary reported that "On the 6th Nov., the Truk-Ponape area was suspect, ....". Had this picture been received at the readout stations during the summer of 1964 it would have prompted an advisory to the hurricane and typhoon forecast centers that a tropical cyclone possessing the attributes of a tropical storm had been detected by the TIROS satellite. Karen, at the time of these pictures, shows pronounced low level banding, definite indications of anticyclonic outflow, and its center is obscured by a cloud shield of 3 to 5 degrees in diameter. These indications are typical of a tropical storm with maximum surface winds approaching at least 40 kt. [2]. The first tropical cyclone warning was issued concerning Karen on the following day (November 7, 1962) at 1800 GMT when Karen was reported to be a tropical storm with maximum winds of 40 kt . The inset picture of Figure 115 shows that the ITC band south of Karen extended far to the east. Another ITC band is apparent at approximately 10°N. and also extends far to the east as can be seen from pictures obtained on a TIROS VI orbit (Figure 116).

FIGURE 116. A TIROS VI mosaic taken on November 6, 1962 showing the continuation of ITC bands east from the area of tropical cyclone Karen. Karen was located at the time of this mosaic near 5°N, 161°E. (See Figure 115).

FIGURE 117. A TIROS VI mosaic of Karen on November 7, 1962. Karen was reported to have winds of 40 kt. by 1800 GMT on this day.

FIGURE 118. A TIROS VI mosaic of Typhoon Karen on November 9, 1962. Maximum sustained surface winds had at this time increased to 155 kt. (smoothed). This increase in intensity is quite obvious in the TIROS pictures if one compares the view in Figure 117 with Figure 118. The latter view shows much more pronounced outflow which is revealed by the cirrus striations, and spiral banding present forms smoother, more continuous lines. The rectified size of the overcast cloud shield also shows a significant increase in areal extent.

FIGURE 119. A TIROS VI mosaic of Typhoon Karen with maximum surface winds near 150 kt. (smoothed). The eye of the storm is visible in the lower left hand corner of the separate frame. It should be noted that the curvature of this mosaic gives the impression that cloudiness of the storm on the north side extends more in an east-west than a north-south direction as is shown in the nephanalysis. Karen, at this time, began to move more rapidly in a westerly direction having previously moved slowly toward the north-northeast. The small vortex near 31°N, 17°E. was analyzed as a developing wave on a frontal band which extended toward the NE and SW of the vortex center.

FIGURE 120. A TIROS V mosaic of Typhoon Karen slightly more than one hour after the view shown in Figure 119. This mosaic shows a cloudy area due west of Karen separated from the storm by a more open zone. Guam located near 13.5°N, 145°E. was under the cloudy area at the time of these pictures. Time cross-section analyses of Guam during this period are quite interesting (Figures 121 and 122).

FIGURE 121. A time cross-section for Guam during the period of the approach of Typhoon Karen to this station from 6-11 November 1962. The eye of Typhoon Karen crossed Guam on the 11th of November near 1200 GMT. Sustained winds of 150 kt. with gusts to 180 kt. were estimated as Karen crossed the island. This time-section shows some of the characteristics of Karen which have also been found to typify other mature storms [1]. An upper-shear line apparently passed Guam near 45,000 ft. during the 7th of November. This was the first indication of outflow from the storm area. Karen moved generally northward at a distance of approximately 500 miles east of Guam during the period 7-9 November. Late on the 9th of November, Karen turned sharply westward and moved directly toward Guam increasing its speed from 7 kt. to about 19 kt. as it struck the island. A trough line is apparent below the outer edge of the outflow of the storm as can be seen on the time-section. The axis of this trough passed Guam during the 8th of November. Wind shifts were especially pronounced near the 400-mb. level, changing from northeast on November 7th

at 1200 GMT to southeast 24 hr. later. As Karen moved northward during the 9th of November Guam remained under the influence of southeasterly flow at the 400 and 500-mb. levels in the eastern portion of this trough. The view of Karen at 0146 GMT on November 10, 1962 shows Guam to be just emerging from the cloudy area which was apparently associated with this trough. Rainfall amounts as indicated on the time-section show that over 1 3/4" of rain fell on Guam from 1200 GMT, November 9th until 1200 GMT on November 10th. As Guam emerged from the trough area and the major edge of the cloud shield of Karen approached the station during the 10th of November the atmosphere through a deep layer became very dry and warm. Height rises at upper elevations in coincidence with steadily falling surface pressure after 1200 GMT on November 10th indicate the probability of fairly intense subsidence at the edge of storm cloudiness (see Figure 122).

FIGURE 122. A time cross-section for Guam during the period 6-11 November 1962. Isopleths of relative humidity have been labeled for the values 25, 50 and 75%. It can be seen that maximum relative humidity early on the 10th of November associated with the trough (Figure 121) was replaced by a pronounced minimum by 1200 GMT on the 10th of November. This was in turn followed by a sharp increase as the edge of the overcast cloud shield of Karen moved over the station. The minimum moisture indication on the 10th of November coincides with pronounced warning throughout the middle and upper troposphere. Values of warming (24-hr. changes) in excess of 1 deg. C. have been indicated by stippling. The other lined areas on the chart indicate areas of cooling (24-hr. changes). The 24-hr. changes of temperature and height have been plotted and analyzed in the central portion of the 24-hr. time period to more adequately indicate the instantaneous change tendency. Of major importance, note that the edge of the dry zone and the beginning of the moist area by 0000 GMT on the 11th of November coincides with the passage of the major overcast cloud shield of Karen over Guam and that this passage also delineates the edge of maximum sustained surface wind speeds of 20 kt or greater (see Figure 123). To summarize the time-section indications:

1. The first indication of Karen's circulation at Guam was the arrival of an upper shear-line associated with the outflow of the storm.
2. A trough or squall area preceded arrival of a pronounced area of subsidence. Atmospheric cooling was associated with passage of the trough. Warming with very dry conditions attended the zone of subsidence.
3. The edge of the major overcast cloud shield of Karen coincided with the commencement of maximum surface winds of 20 kt. or greater.

Similar conditions have been found to appear quite commonly in other mature storms [1].

FIGURE 123. A TIROS VI mosaic of Typhoon Karen on November 11, 1962. Maximum sustained surface wind speeds were approximately 150 kt. (smoothed). Guam (near 13.5°N, 145°E) at the time of these pictures, had just passed under the

first major spiral band of the storm. The eye of Karen passed over Guam approximately 11 hours after this TIROS VI observation. This view shows that circulation effects of Karen extended from at least 20°N. to 7°S. - a distance of over 1500 n.mi.

FIGURE 124. A TIROS VI mosaic of Typhoon Karen on November 13, 1962.

FIGURE 125. A TIROS VI mosaic of Typhoon Karen on November 14, 1962. Maximum sustained surface winds were near 140 kt (smoothed). Karen at this time was inter-acting with a frontal zone extending northeastward from the northern edge of the storm. The eye of Karen on the original film strip shows a "doughnut" shape, typical of the concentric eye and of a very intense storm.

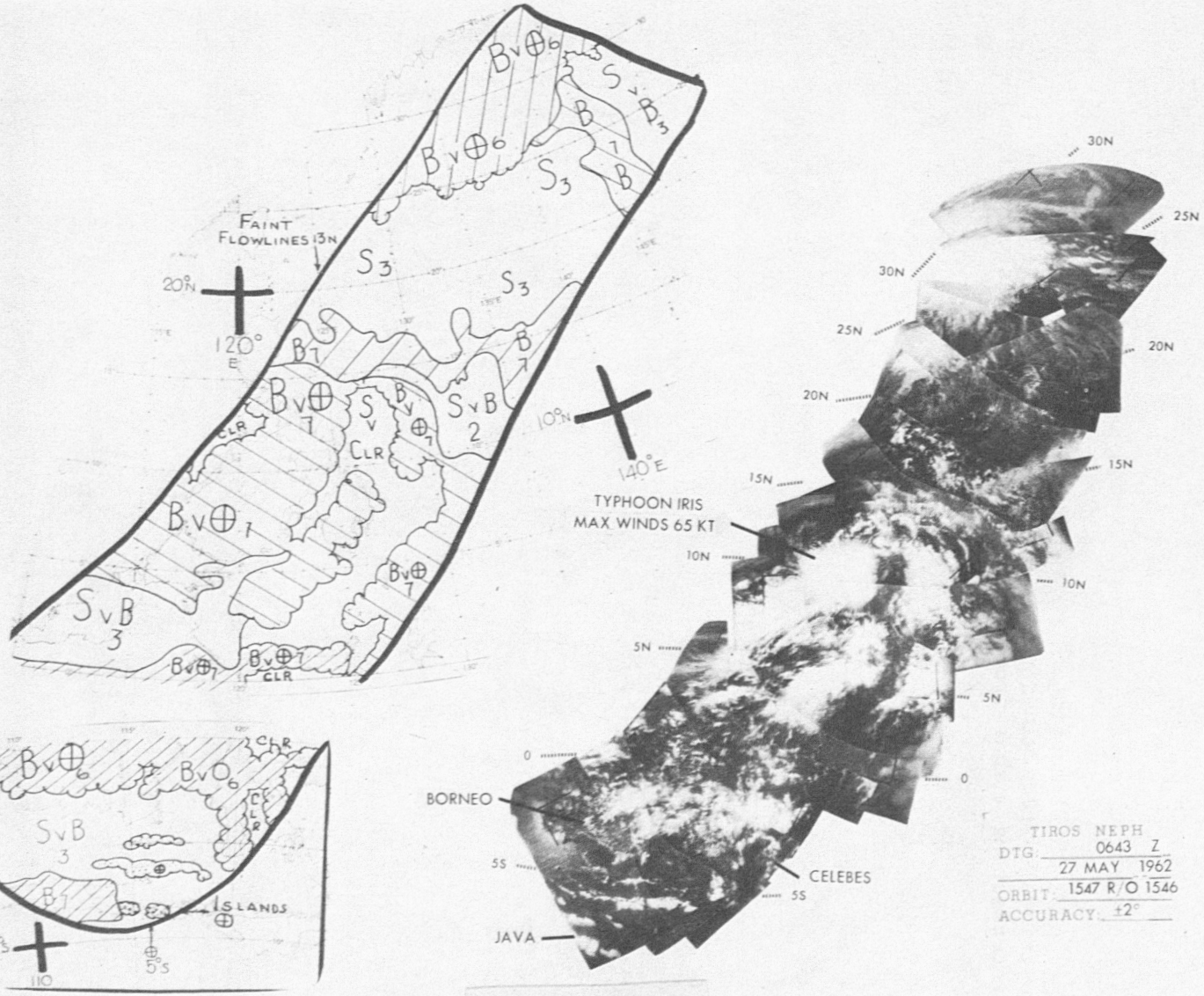
FAINT FLOWLINES 13N
20°N
120° E
10°N
140°E
TYPHOON IRIS
MAX WINDS 65 KT
30N
25N
20N
15N
10N
5N
0
5S
BORNEO
CELEBES
JAVA
ISLANDS
10°S
5°S
110
TIROS NEPH
DTG: 0643 Z
27 MAY 1962
ORBIT: 1547 R/O 1546
ACCURACY: ±2°

FIGURE 1

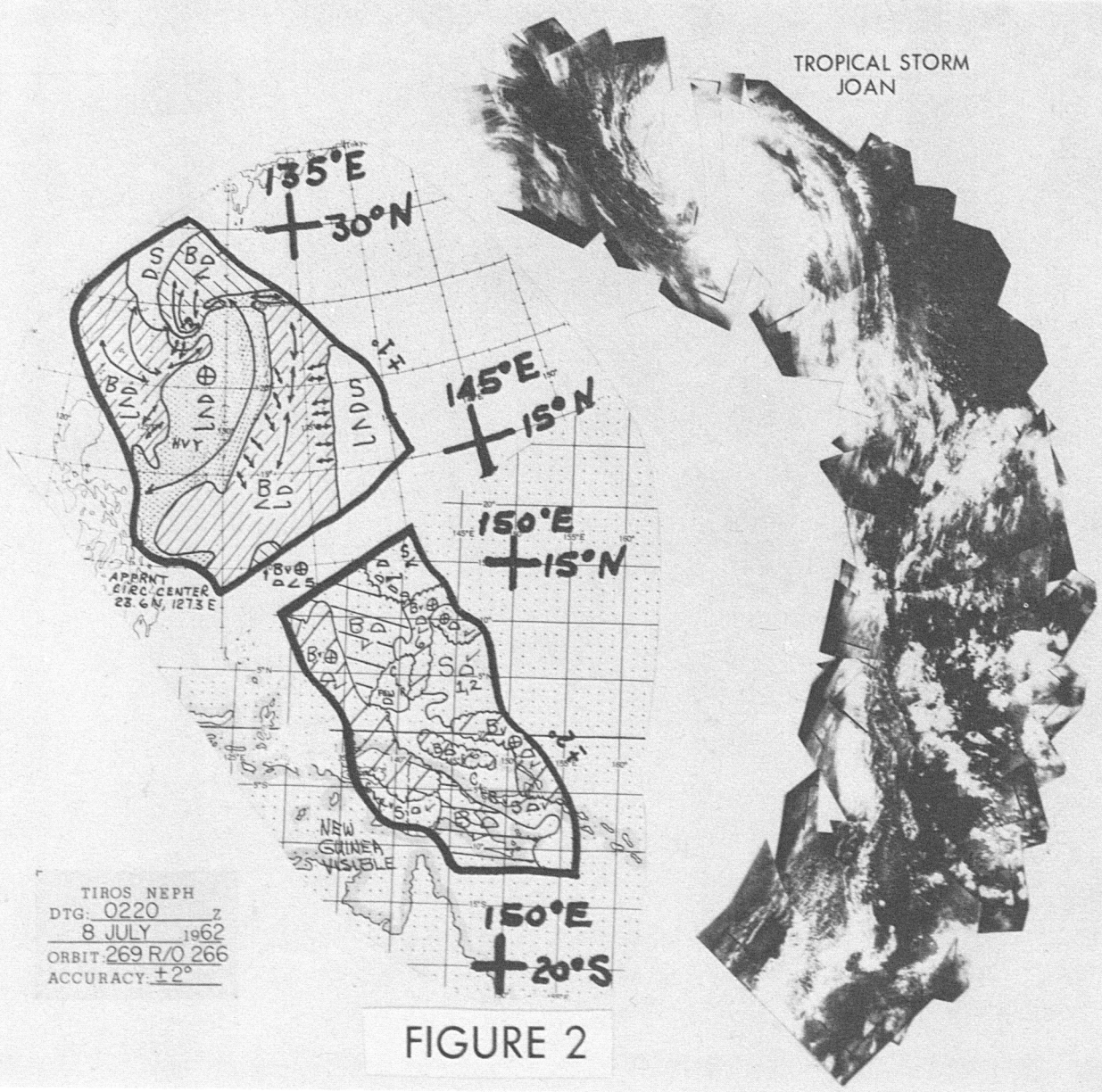
TROPICAL STORM
JOAN
135°E
30°N
145°E
15°N
150°E
15°N
150°E
20°S
APPRNT
CIRC CENTER
28.6N, 127.3E
NEW
GUINEA
VISIBLE
TIROS NEPH
DTG: 0220 Z
8 JULY 1962
ORBIT 269 R/O 266
ACCURACY: ±2°

FIGURE 2

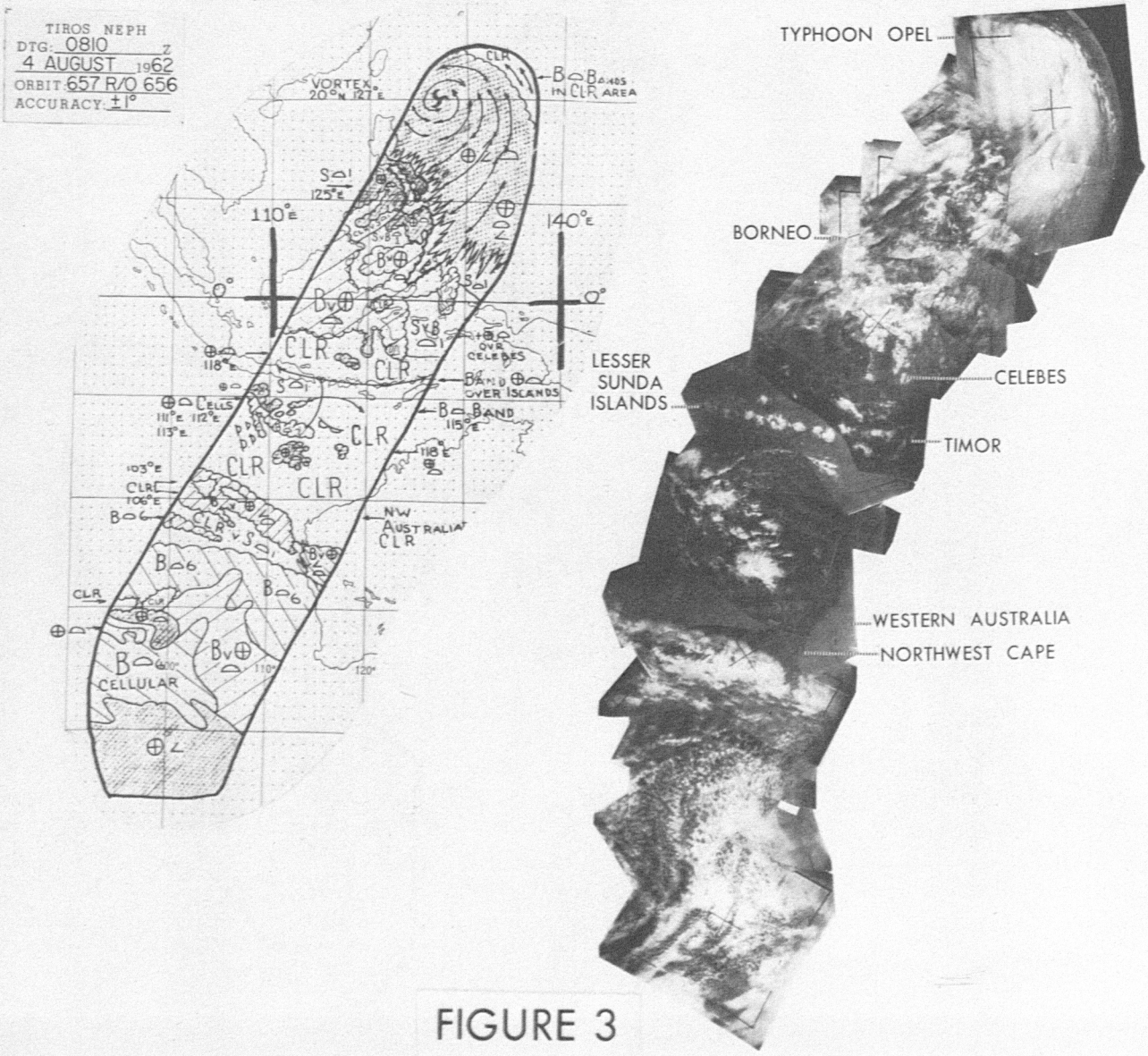
TIROS NEPH
DTG: 0810 Z
4 AUGUST 1962
ORBIT: 657 R/O 656
ACCURACY: ±1°
VORTEX 20°N 127°E
CLR
B Bands IN CLR AREA
Sc
125°E
110°E
140°E
0°
Bv
Sc
Sv
B
CLR
118°E
+B OVER CELEBES
B BAND OVER ISLANDS
Cells
111°E 112°E
113°E
B BAND
115°E
118°E
103°E
CLR
106°E
B
NW AUSTRALIA CLR
B6
CLR
B
CELLULAR
Bv
110°
120°
TYPHOON OPEL
BORNEO
LESSER SUNDA ISLANDS
CELEBES
TIMOR
WESTERN AUSTRALIA
NORTHWEST CAPE

FIGURE 3

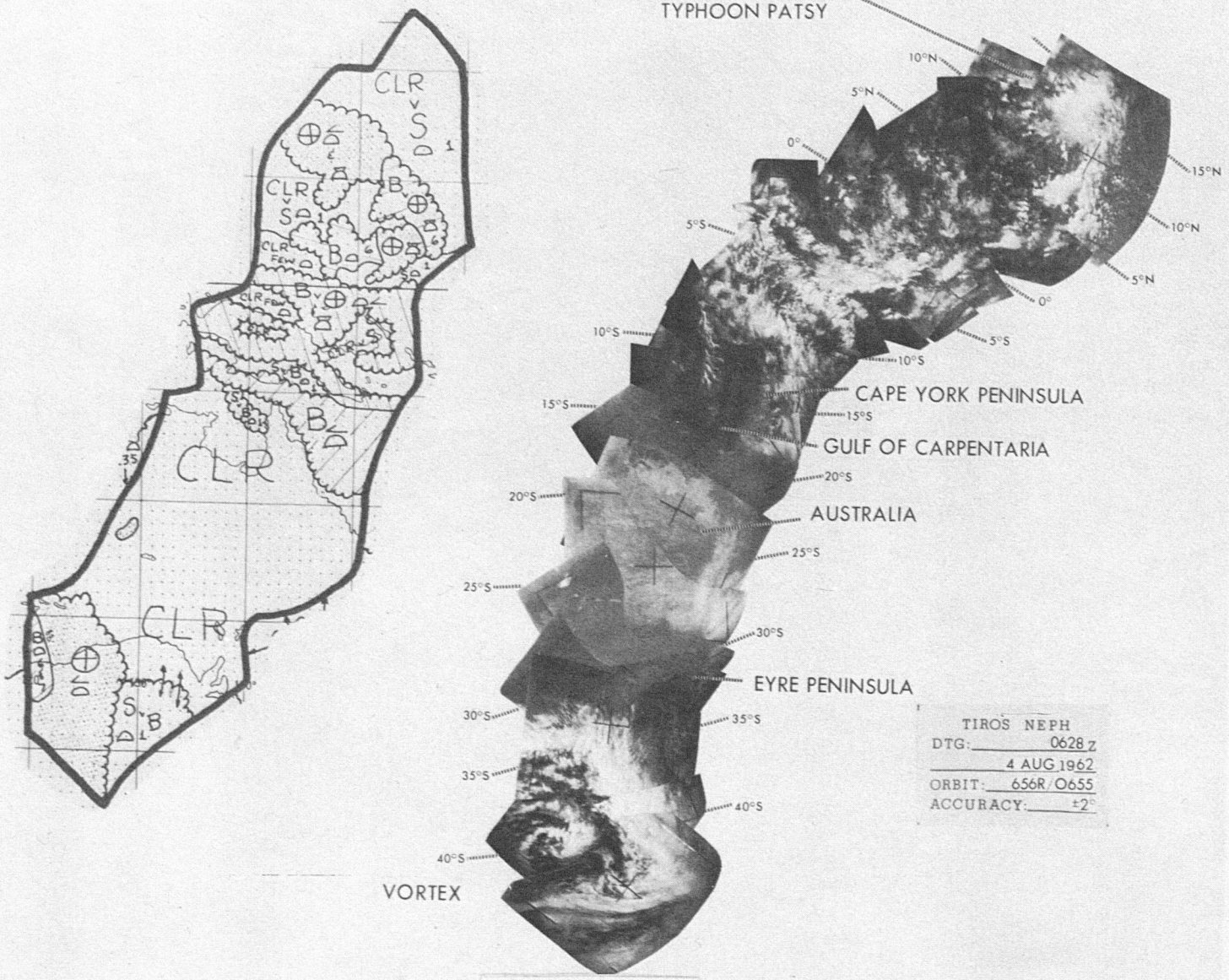
FORMATIVE STAGE
TYPHOON PATSY
10°N
5°N
0°
5°S
10°S
15°S
20°S
25°S
30°S
35°S
40°S
15°N
10°N
5°N
0°
5°S
10°S
15°S
20°S
25°S
30°S
35°S
40°S
CAPE YORK PENINSULA
GULF OF CARPENTARIA
AUSTRALIA
EYRE PENINSULA
VORTEX
CLR
TIROS NEPH
DTG: 0628 Z
4 AUG 1962
ORBIT: 656R/0655
ACCURACY: ±2°

FIGURE 4

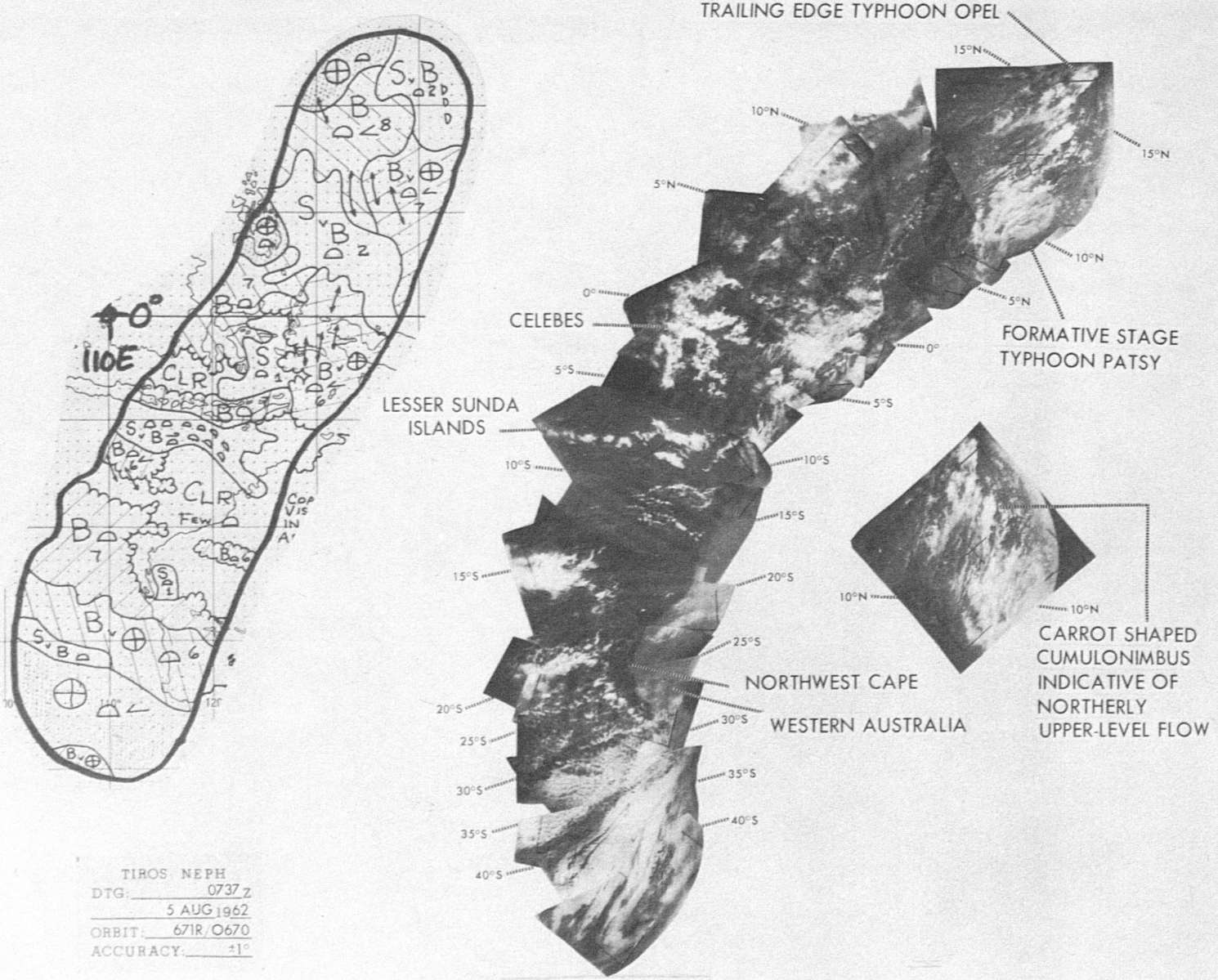
TRAILING EDGE TYPHOON OPEL
15°N
10°N
5°N
0°
5°S
10°S
15°S
20°S
25°S
30°S
35°S
40°S
110E
CELEBES
LESSER SUNDA ISLANDS
FORMATIVE STAGE TYPHOON PATSY
CARROT SHAPED CUMULONIMBUS INDICATIVE OF NORTHERLY UPPER-LEVEL FLOW
NORTHWEST CAPE
WESTERN AUSTRALIA
CLR
Few
TIROS NEPH
DTG: 0737 Z
5 AUG 1962
ORBIT: 671R/0670
ACCURACY: ±1°

FIGURE 5

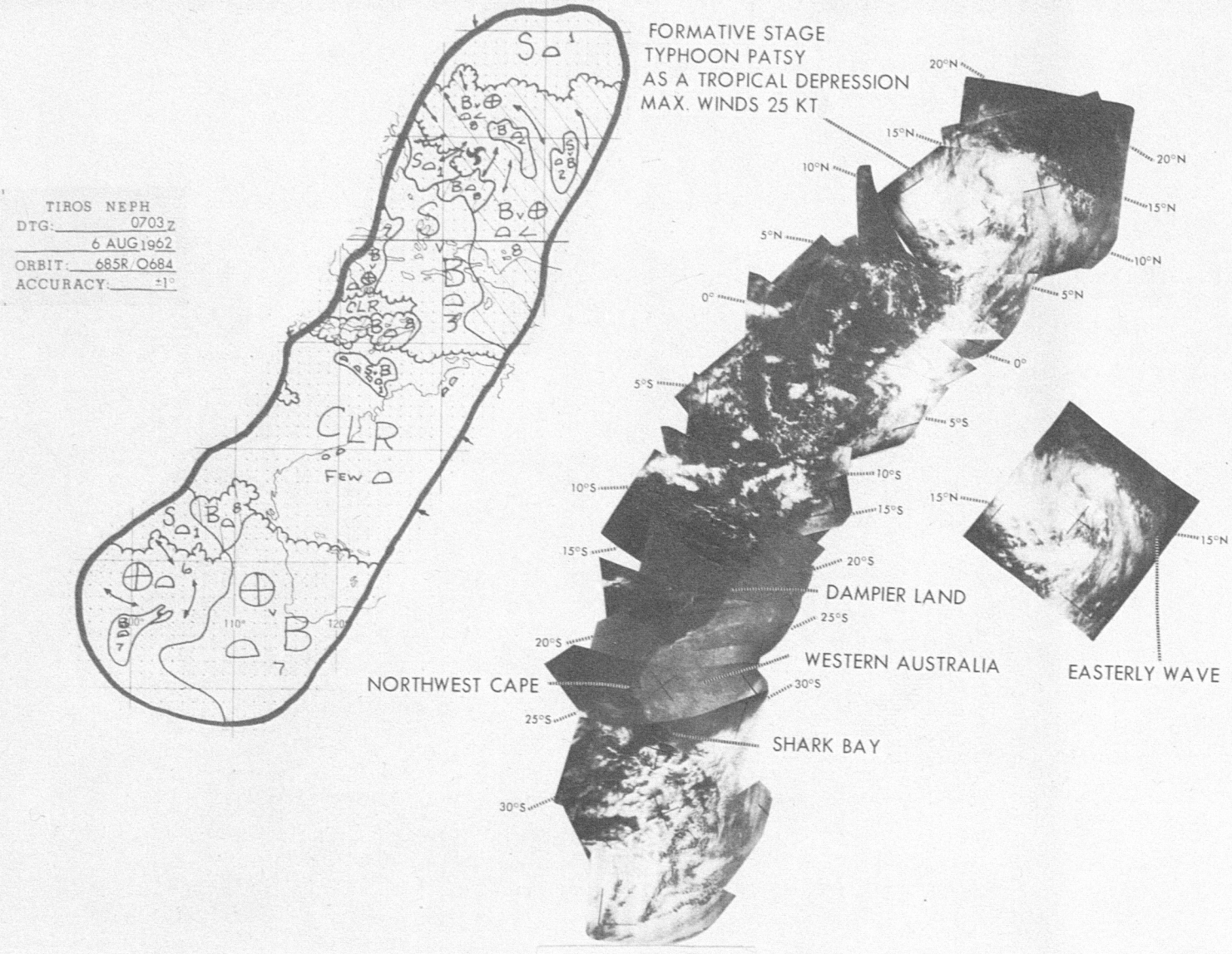
TIROS NEPH
DTG: 0703Z
6 AUG 1962
ORBIT: 685R/O684
ACCURACY: ±1°
FORMATIVE STAGE
TYPHOON PATSY
AS A TROPICAL DEPRESSION
MAX. WINDS 25 KT
CLR
FEW
20°N
15°N
10°N
5°N
0°
5°S
10°S
15°S
20°S
25°S
30°S
DAMPIER LAND
WESTERN AUSTRALIA
NORTHWEST CAPE
SHARK BAY
EASTERLY WAVE

FIGURE 6

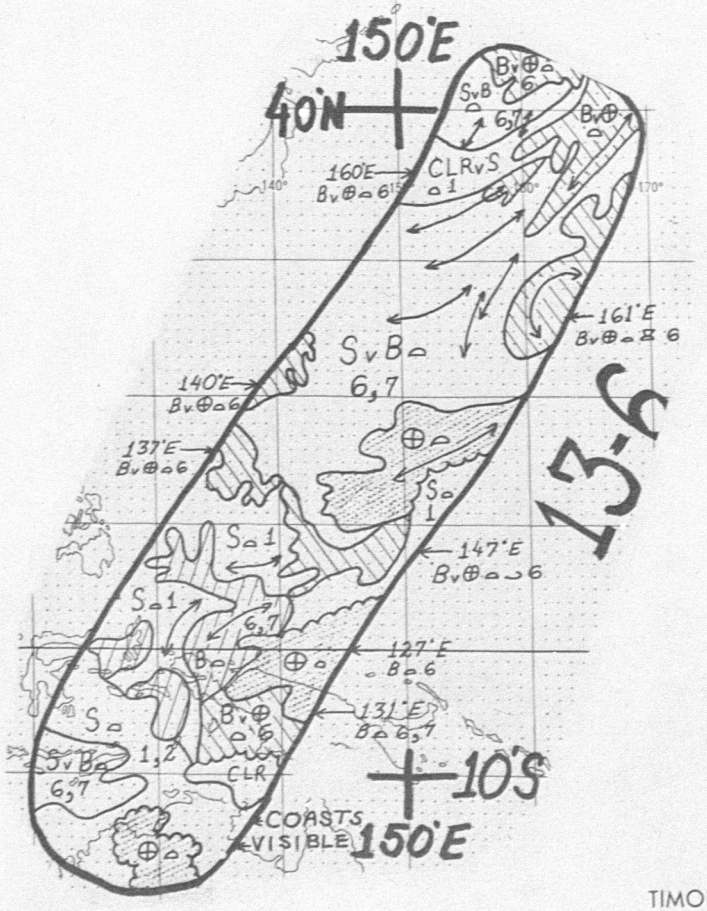
150°E
40°N
160°E
CLR v S
161°E
S v B
6,7
140°E
137°E
147°E
127°E
131°E
S
1,2
CLR
10°S
COASTS VISIBLE
150°E
13-6

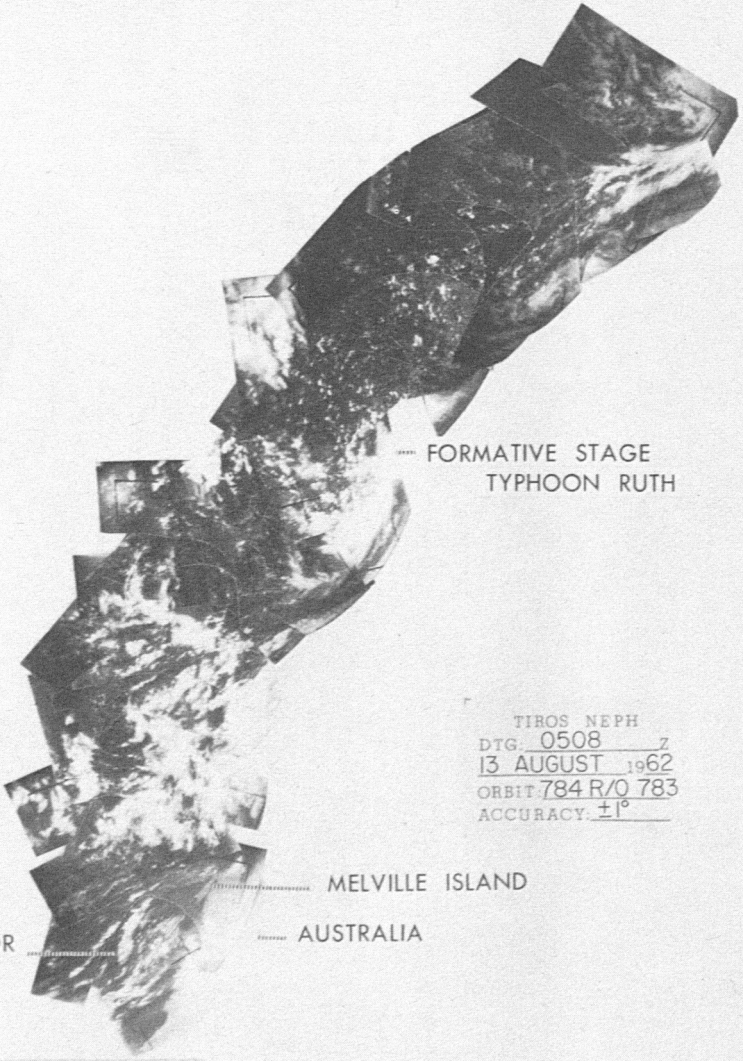
FORMATIVE STAGE
TYPHOON RUTH
TIROS NEPH
DTG: 0508 Z
13 AUGUST 1962
ORBIT 784 R/O 783
ACCURACY: ±1°
MELVILLE ISLAND
AUSTRALIA
TIMOR

FIGURE 7

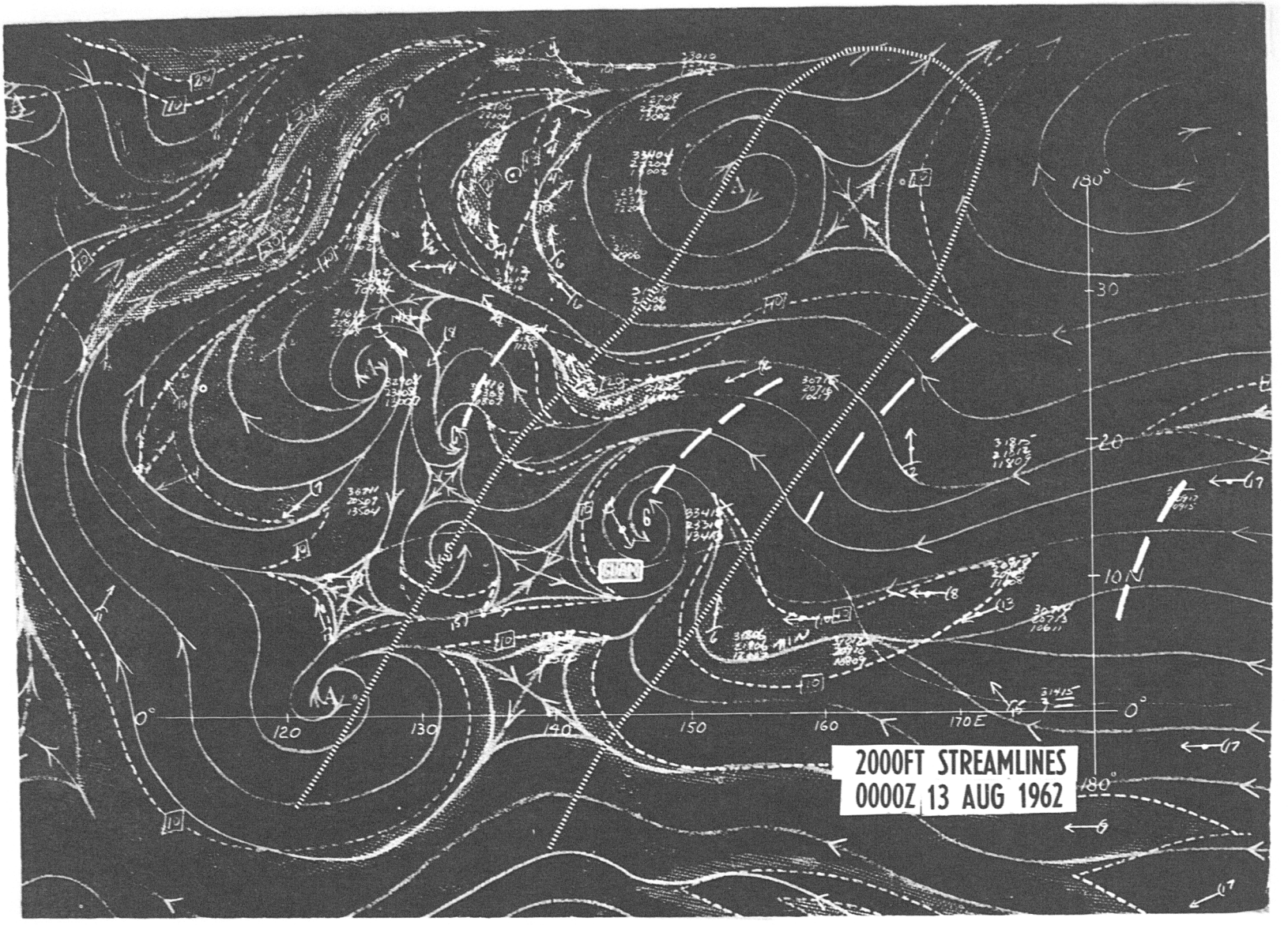
180°
30
20
10N
0°
120
130
140
150
160
170E
0°
180°
2000FT STREAMLINES
0000Z 13 AUG 1962

FIGURE 8

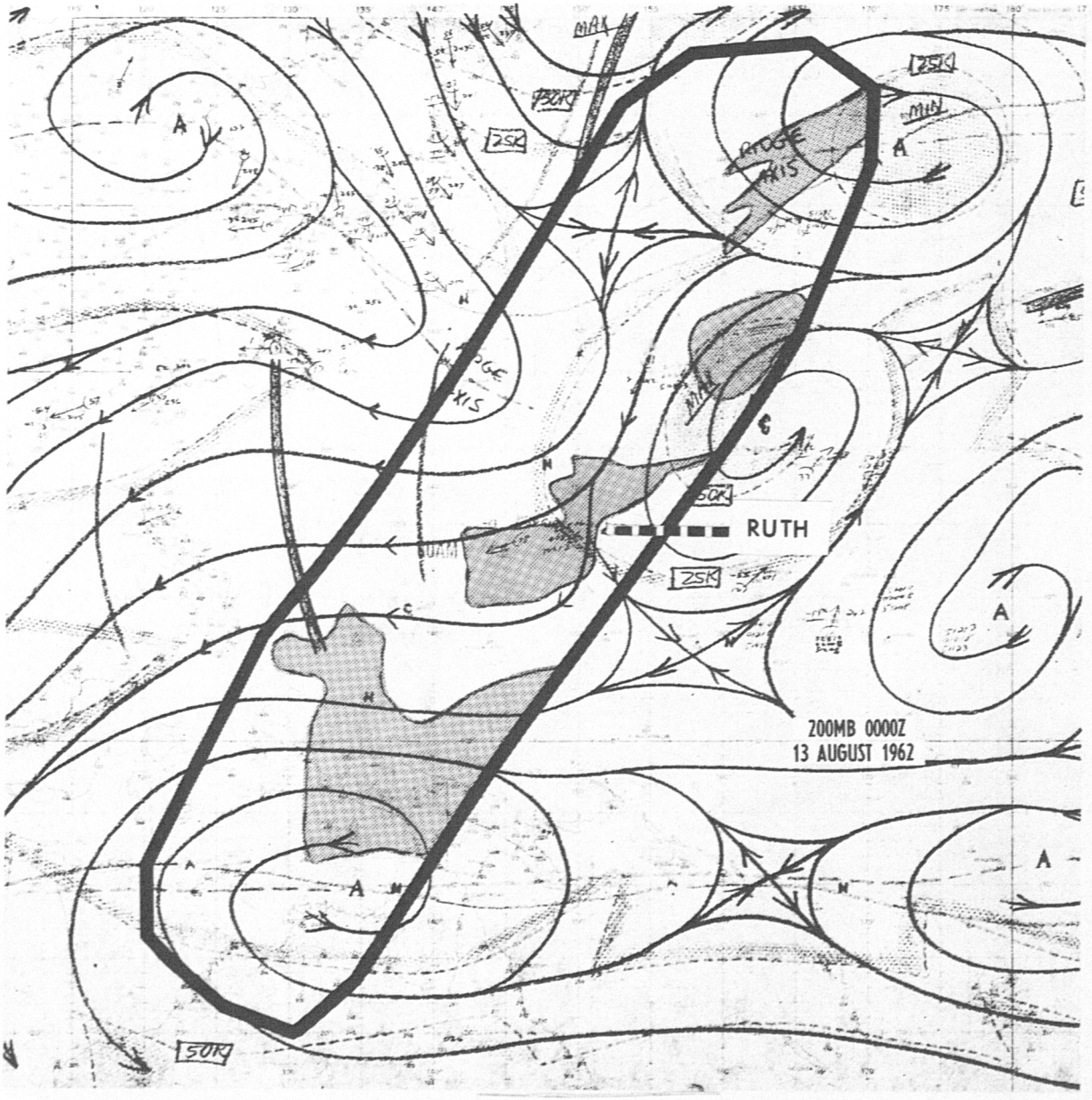


FIGURE 9

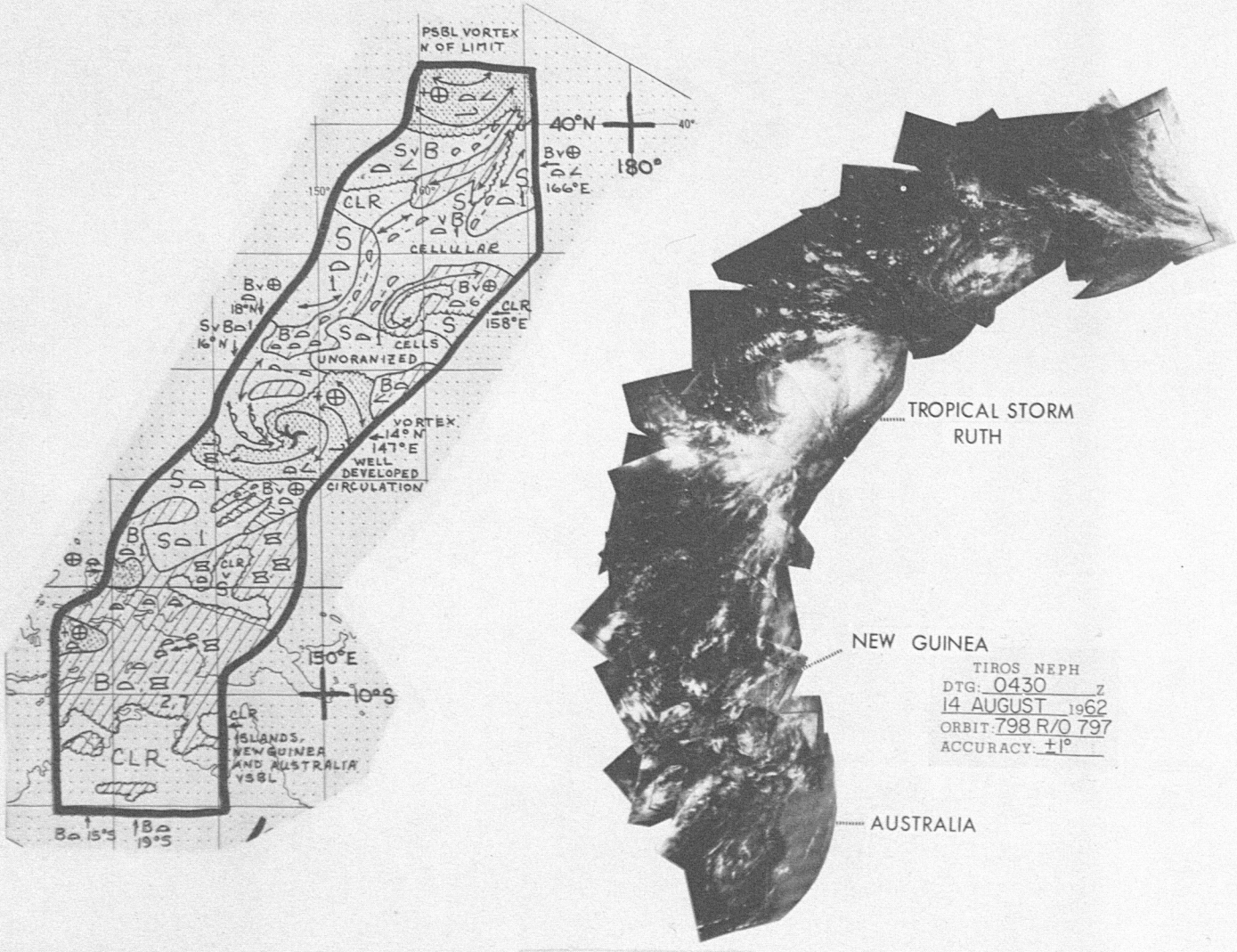
PSBL VORTEX
N OF LIMIT
40°N
40°
180°
SvB
Bv⊕
166°E
150°
160°
CLR
S
VB
CELLULAR
Bv⊕
18°N
SvBa
16°N
CLR
158°E
CELLS
UNORANIZED
VORTEX
14°N
147°E
WELL
DEVELOPED
CIRCULATION
Sa
B
CLR
150°E
10°S
ISLANDS,
NEW GUINEA
AND AUSTRALIA
VSBL
Ba 15°S
18
19°S
TROPICAL STORM
RUTH
NEW GUINEA
AUSTRALIA
TIROS NEPH
DTG: 0430 Z
14 AUGUST 1962
ORBIT: 798 R/O 797
ACCURACY: ±1°

FIGURE 10

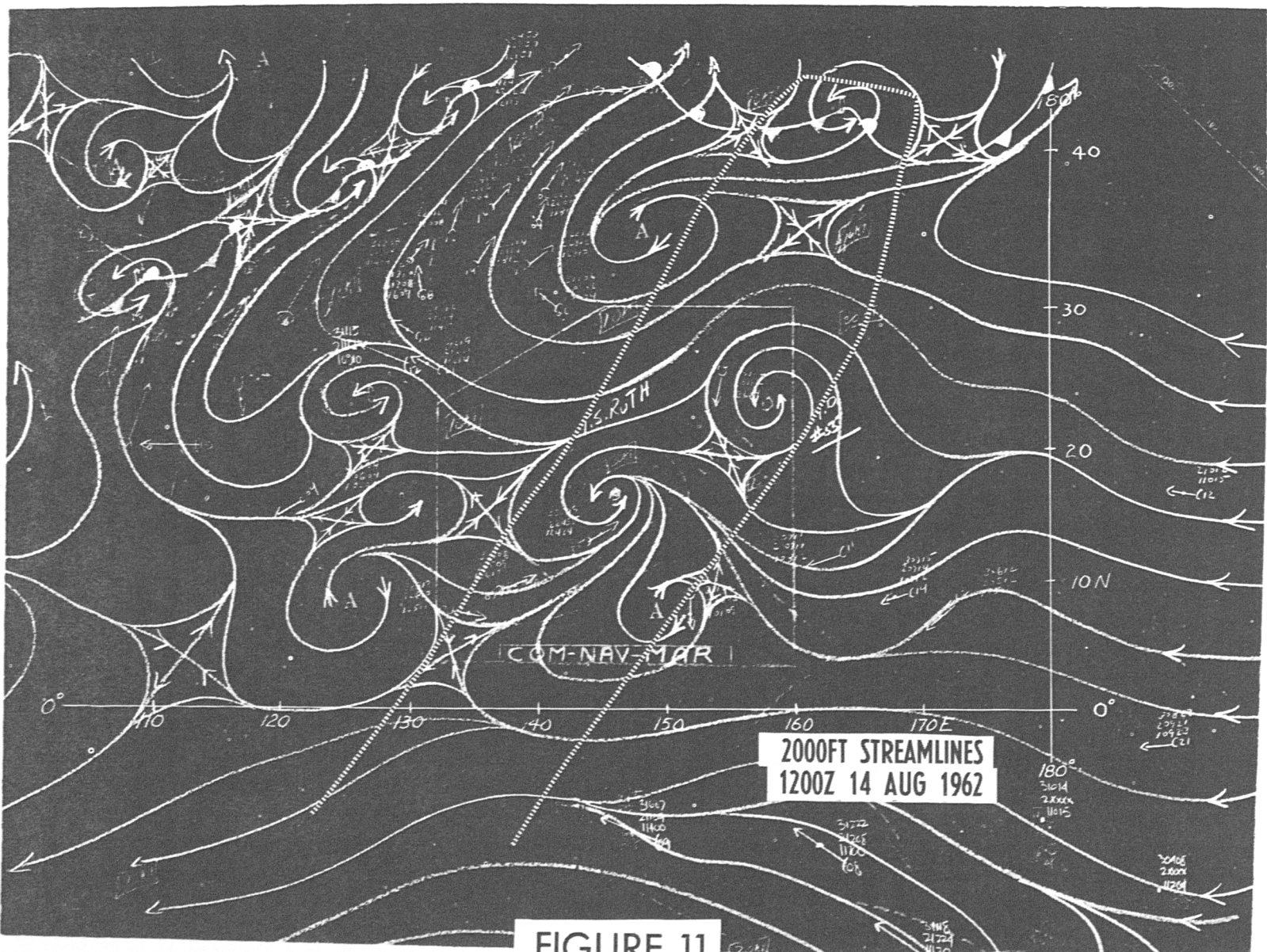
160°W
40
30
20
10N
0°
110
120
130
40
150
160
170E
180°
0°
S. ROTH
COM-NAV-MAR
2000FT STREAMLINES
1200Z 14 AUG 1962

FIGURE 11

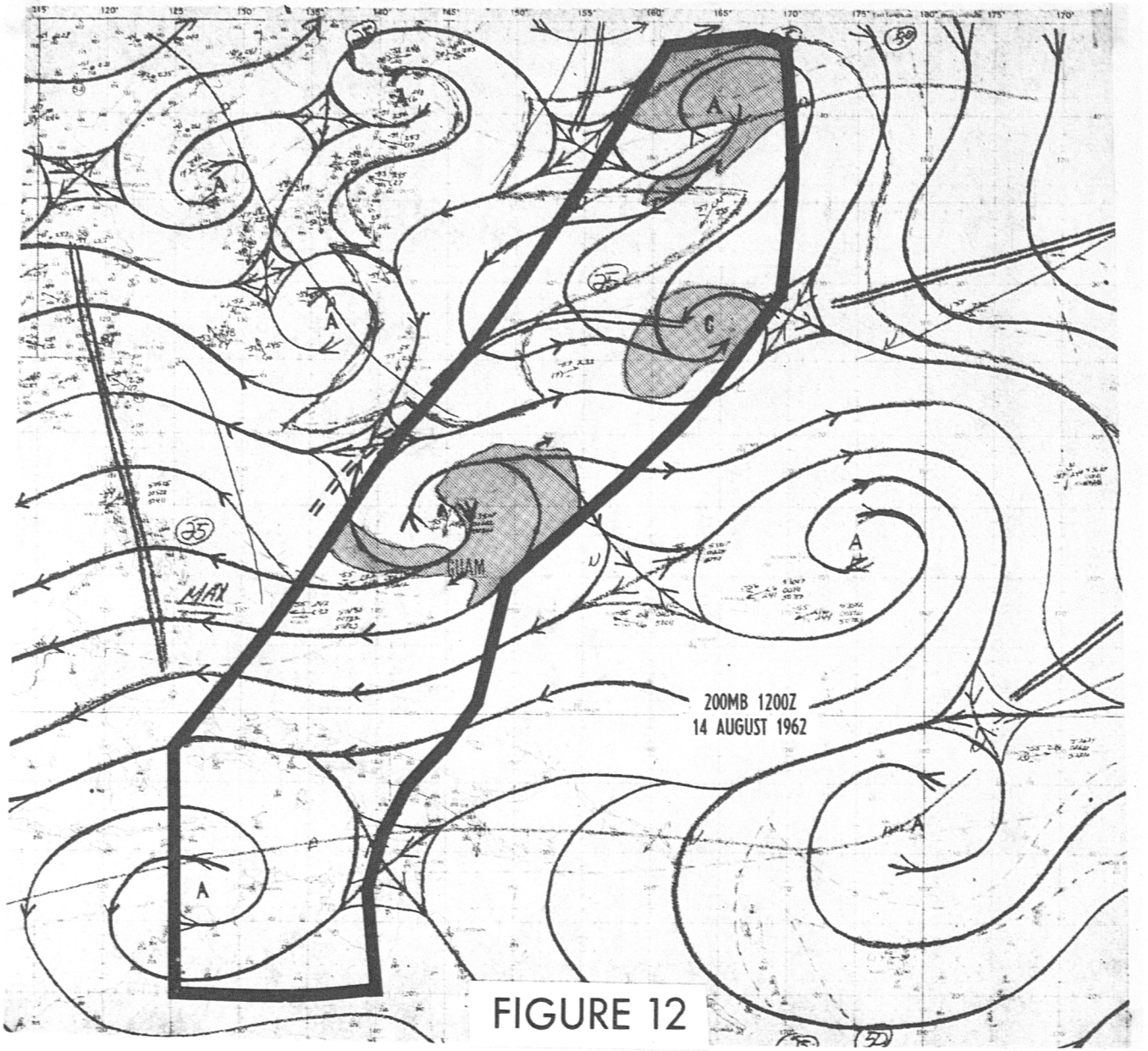


FIGURE 12

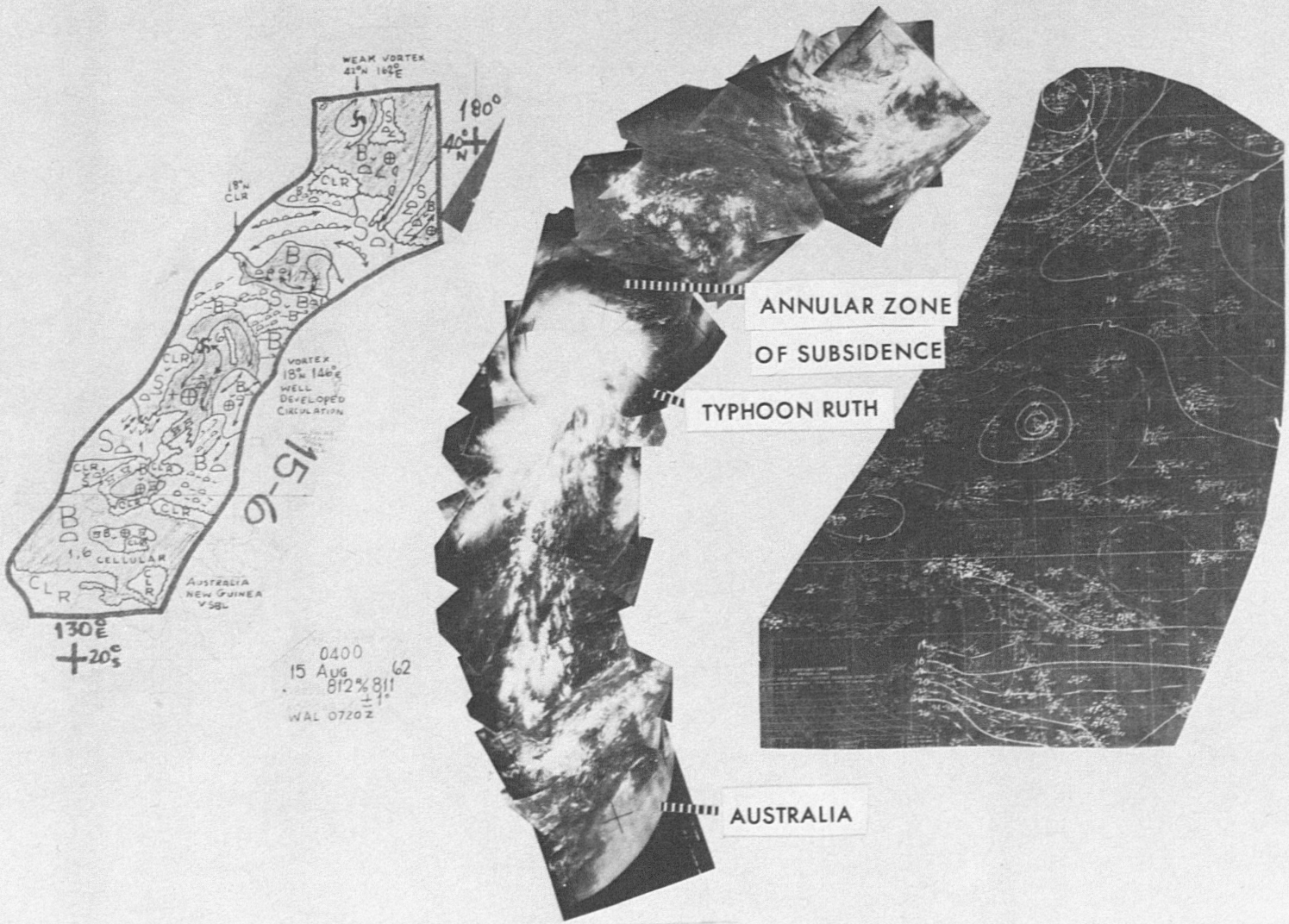
WEAK VORTEX
41°N 160°E
180°
40°N
18°N
CLR
VORTEX
18°N 146°E
WELL
DEVELOPED
CIRCULATION
15-6
1,6
CELLULAR
AUSTRALIA
NEW GUINEA
VSBL
130°E
20°S
0400
15 AUG 62
812 % 811
±1°
WAL 0720Z
ANNULAR ZONE
OF SUBSIDENCE
TYPHOON RUTH
AUSTRALIA

FIGURE 13

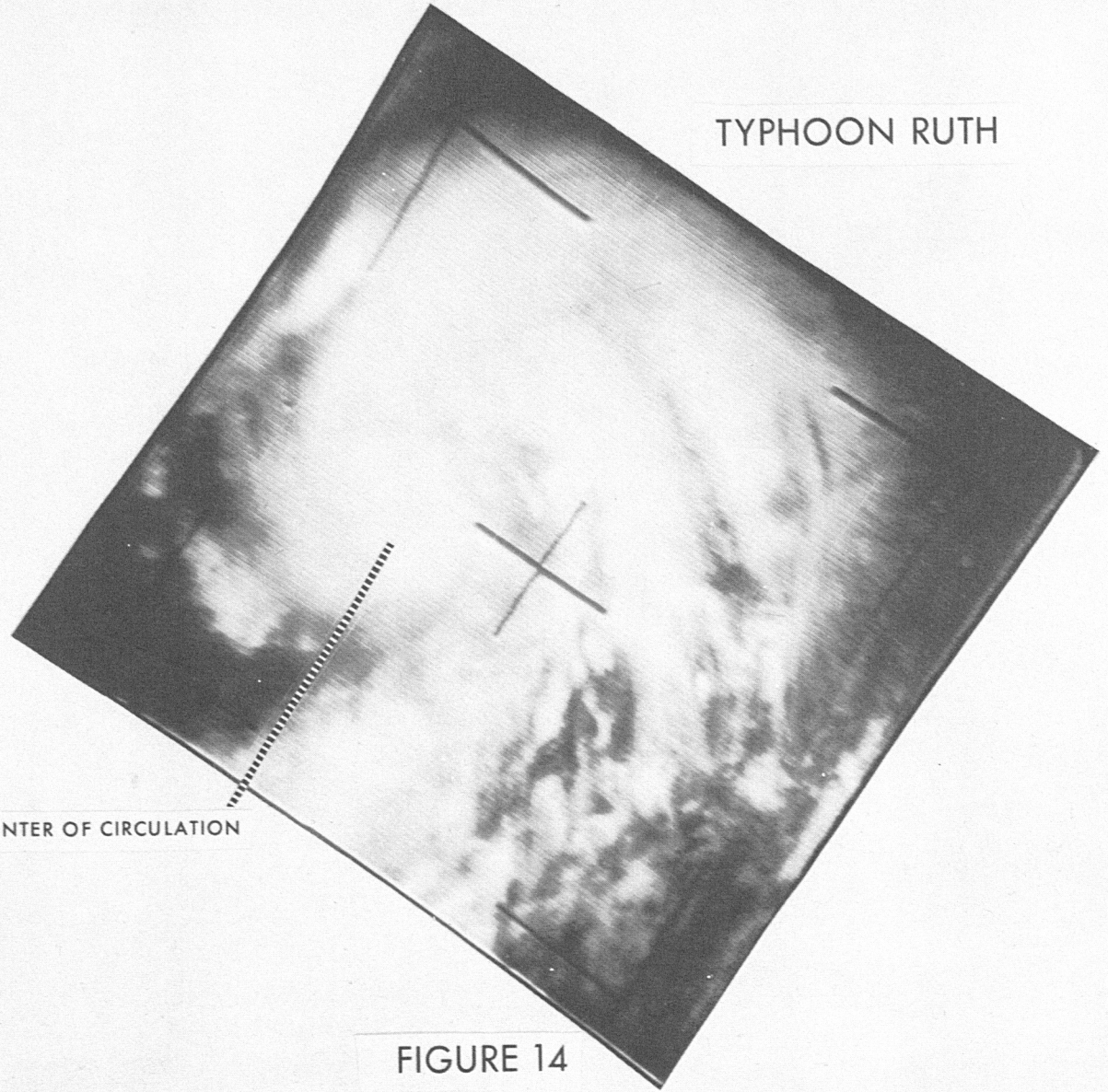


FIGURE 14

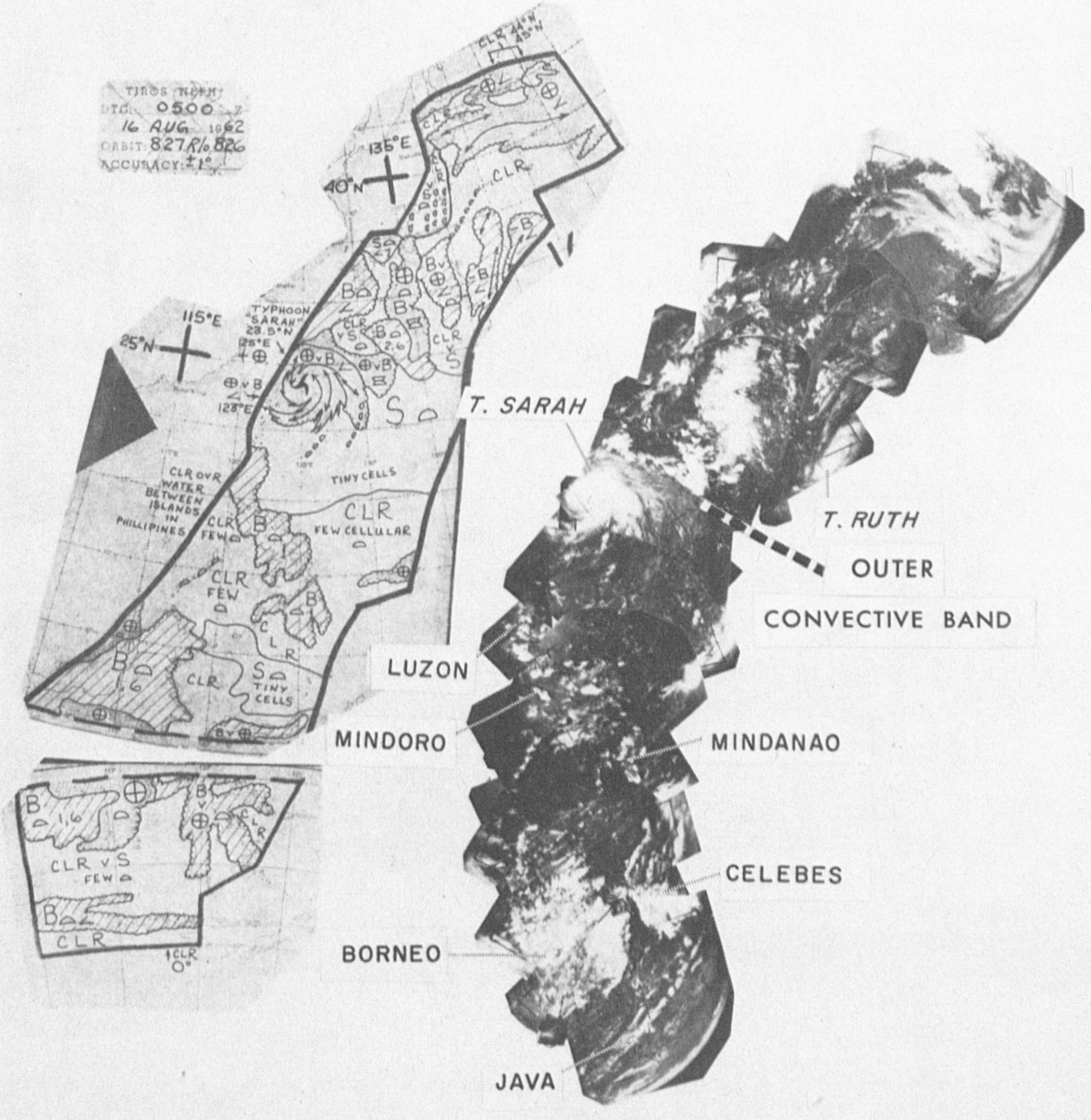
TIROS NOAA
DTG 0500 Z
16 AUG 1962
ORBIT 827R/826
ACCURACY ±1°
135°E
40°N
115°E
25°N
TYPHOON "SARAH"
23.5°N
125°E
123°E
CLR OVR WATER BETWEEN ISLANDS IN PHILLIPINES
TINY CELLS
CLR FEW CELLULAR
CLR FEW
CLR V S FEW
T. SARAH
T. RUTH
OUTER
CONVECTIVE BAND
LUZON
MINDORO
MINDANAO
CELEBES
BORNEO
JAVA

FIGURE 15

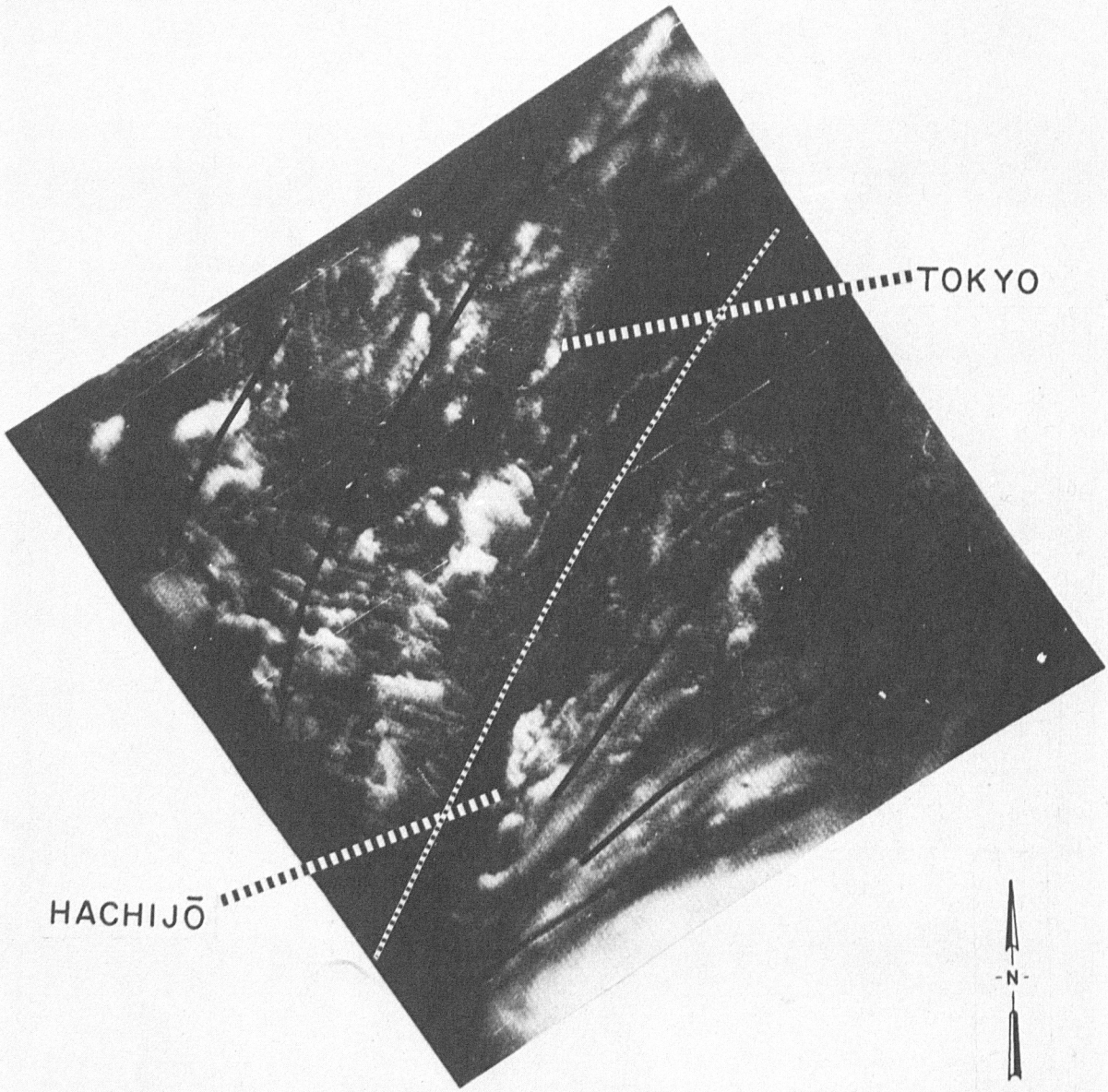


FIGURE 16

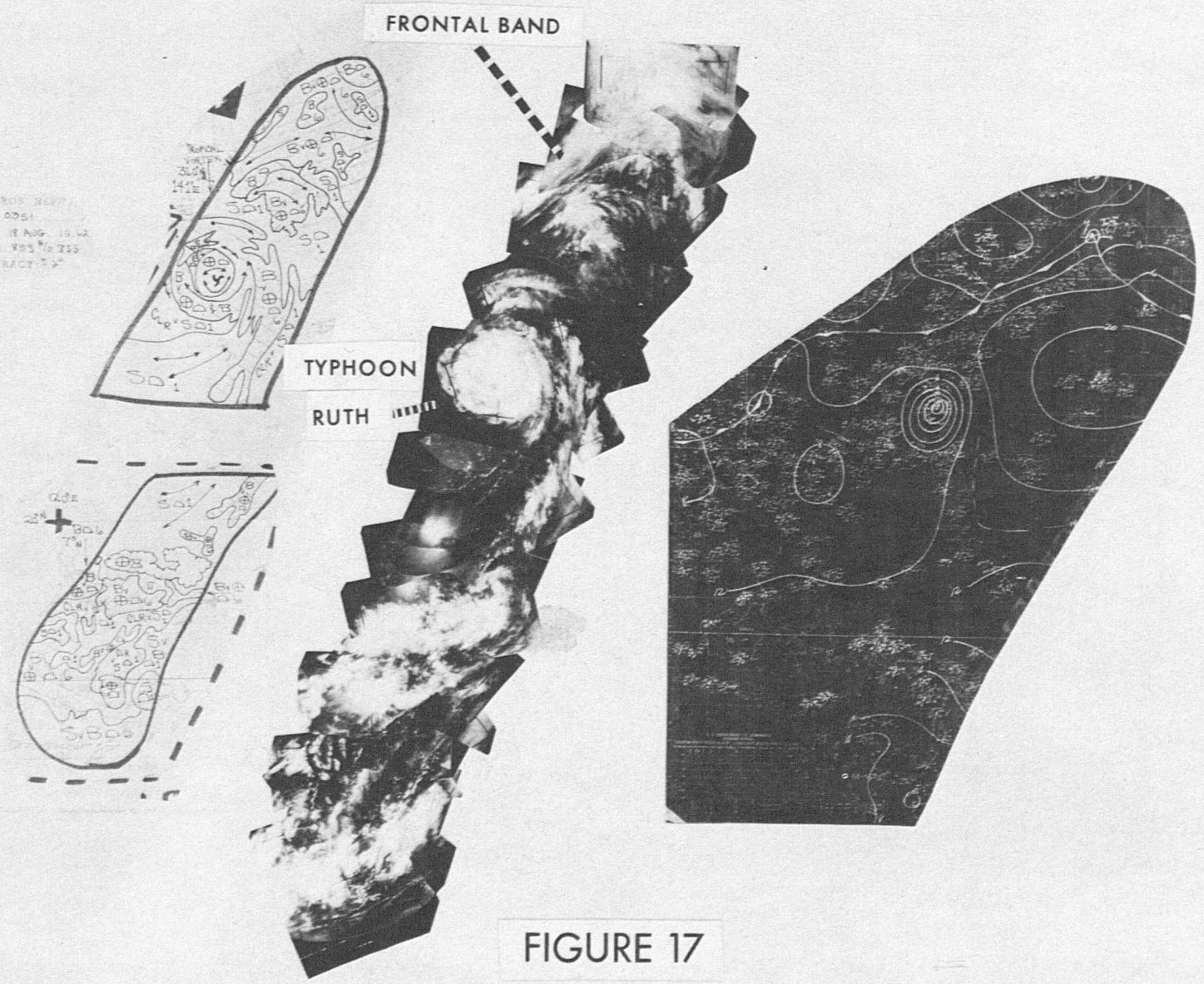


FIGURE 17

TYPHOON RUTH

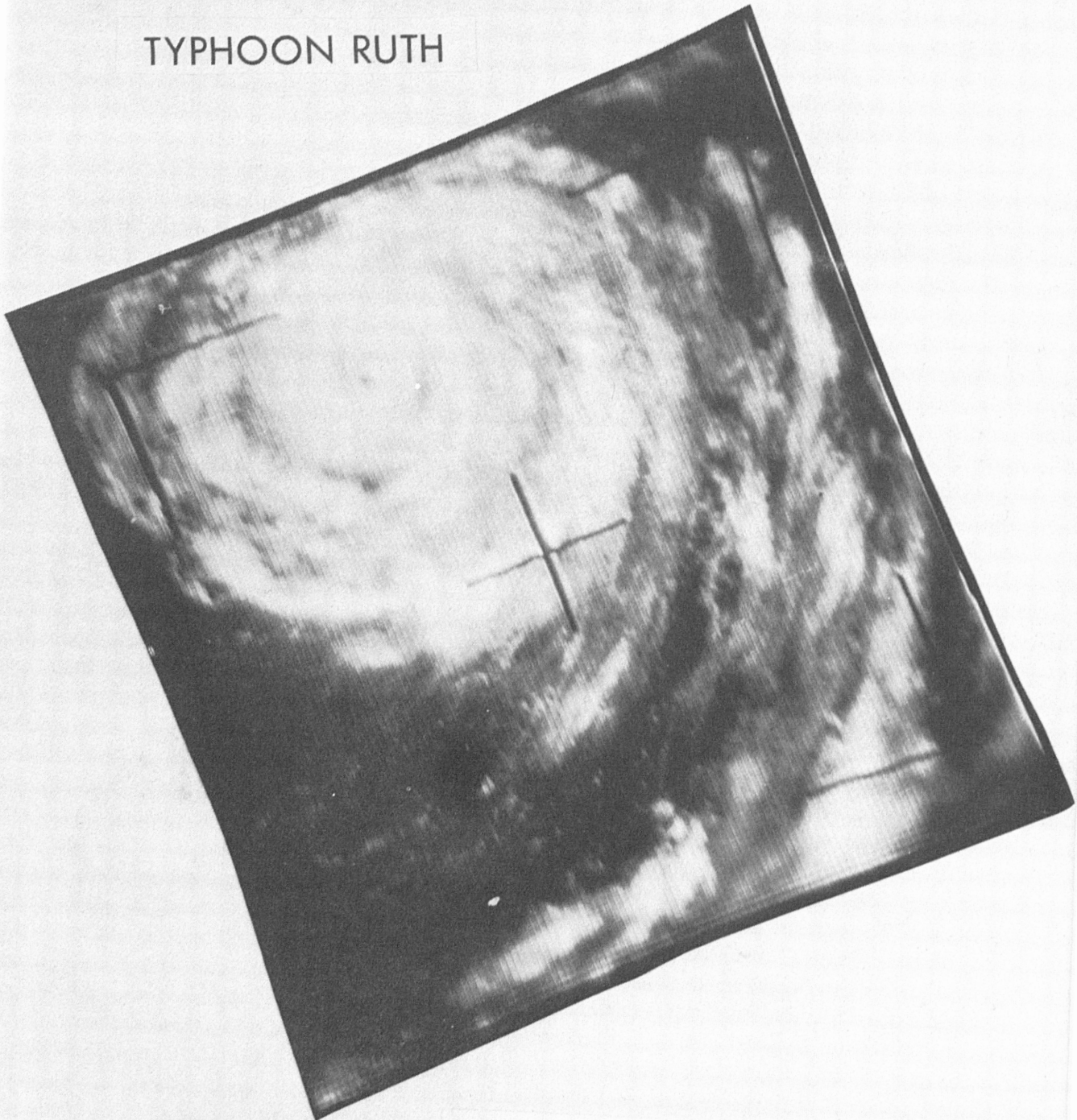

FIGURE 18

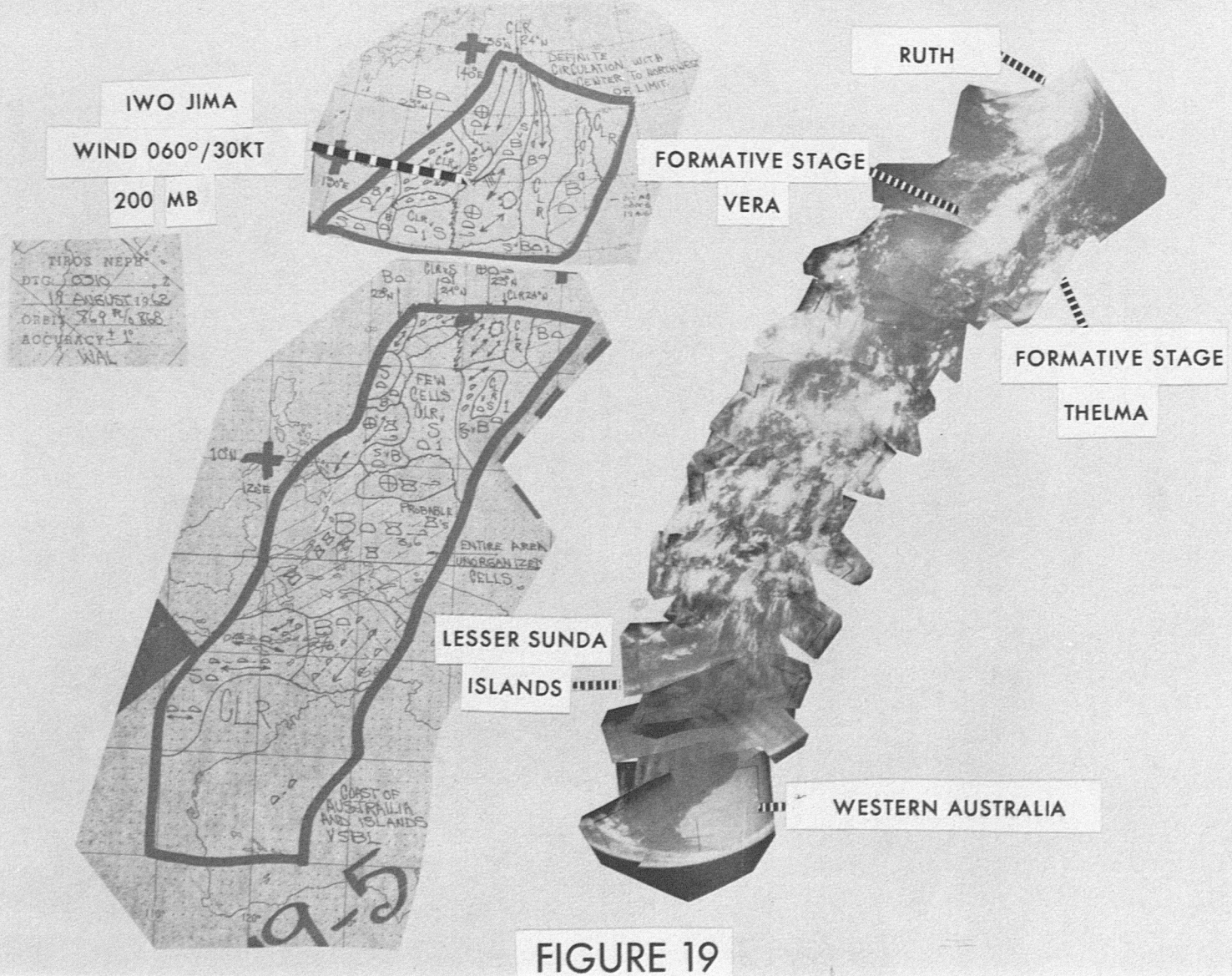
IWO JIMA
WIND 060°/30KT
200 MB
RUTH
FORMATIVE STAGE
VERA
FORMATIVE STAGE
THELMA
LESSER SUNDA
ISLANDS
WESTERN AUSTRALIA
TIROS NEPH
19 AUGUST 1962
ACCURACY ± 1°
WAL
CLR
DEFINITE CIRCULATION WITH CENTER TO NORTHWEST OF LIMIT
FEW CELLS
PROBABLE
ENTIRE AREA UNORGANIZED CELLS
COAST OF AUSTRALIA AND ISLANDS VSBL
a-5

FIGURE 19

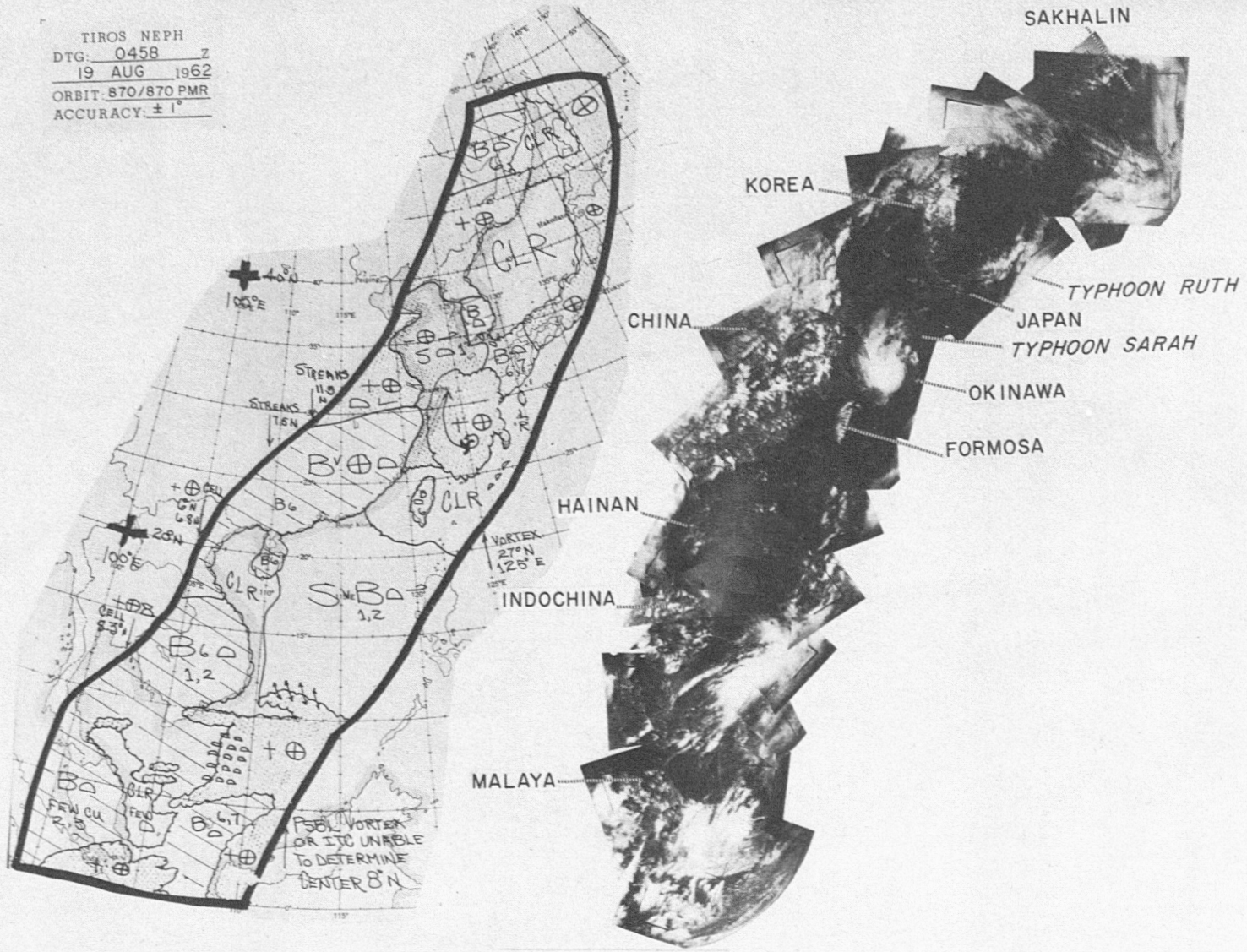
TIROS NEPH
DTG: 0458 Z
19 AUG 1962
ORBIT: 870/870 PMR
ACCURACY: ± 1°
SAKHALIN
KOREA
TYPHOON RUTH
CHINA
JAPAN
TYPHOON SARAH
OKINAWA
FORMOSA
HAINAN
INDOCHINA
MALAYA
CLR
STREAKS
VORTEX 27°N 125°E
FEW CU
P50L VORTEX OR ITC UNABLE TO DETERMINE CENTER 8°N

FIGURE 20

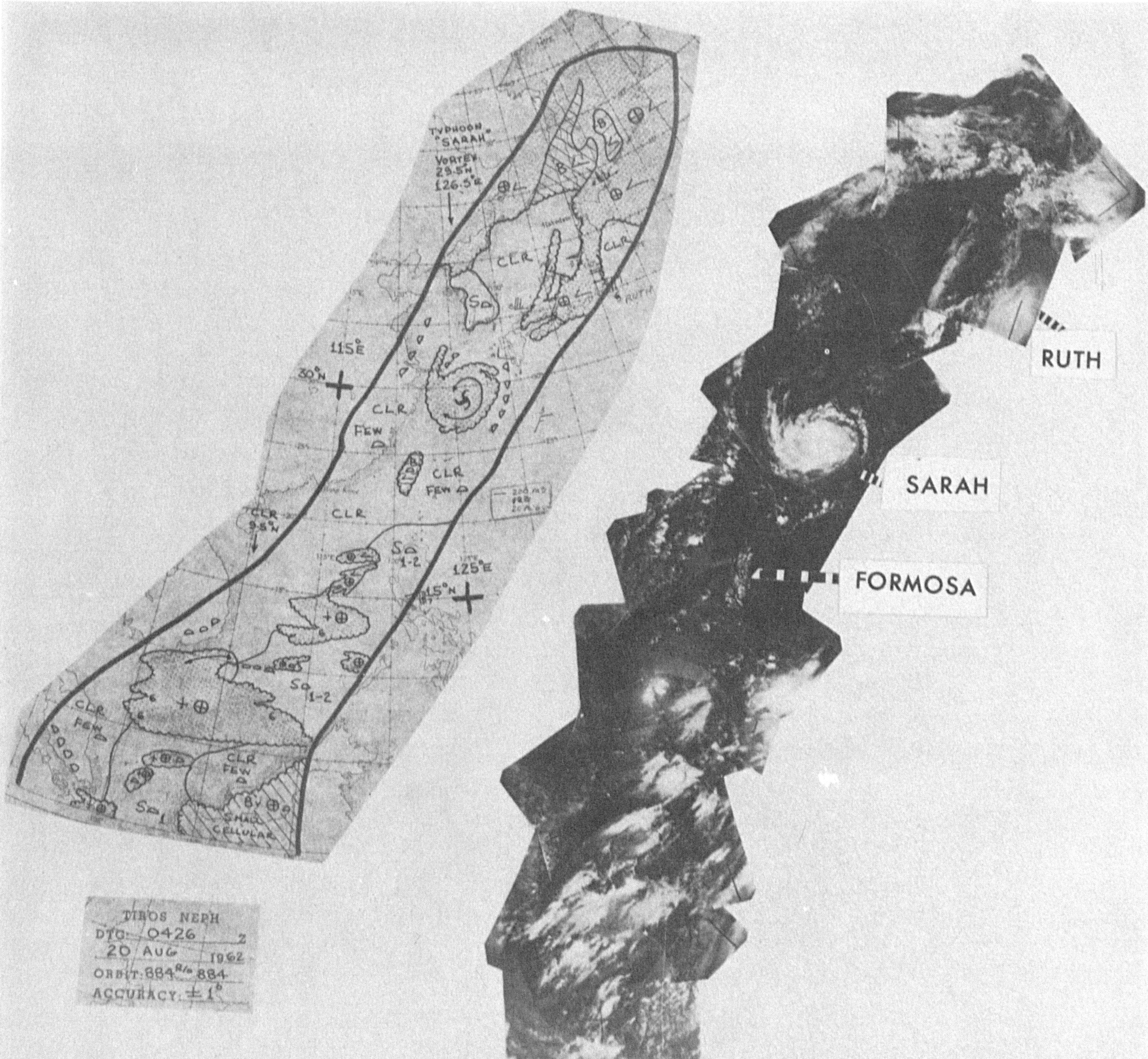

TYPHOON "SARAH" VORTEX 29.5°N 126.5°E
115°E
30°N
125°E
15°N
CLR
FEW
SMALL CELLULAR
TIROS NEPH
DTG: 0426 Z
20 AUG 1962
ORBIT: 884 R/O 884
ACCURACY: ± 1°
RUTH
SARAH
FORMOSA


FIGURE 21

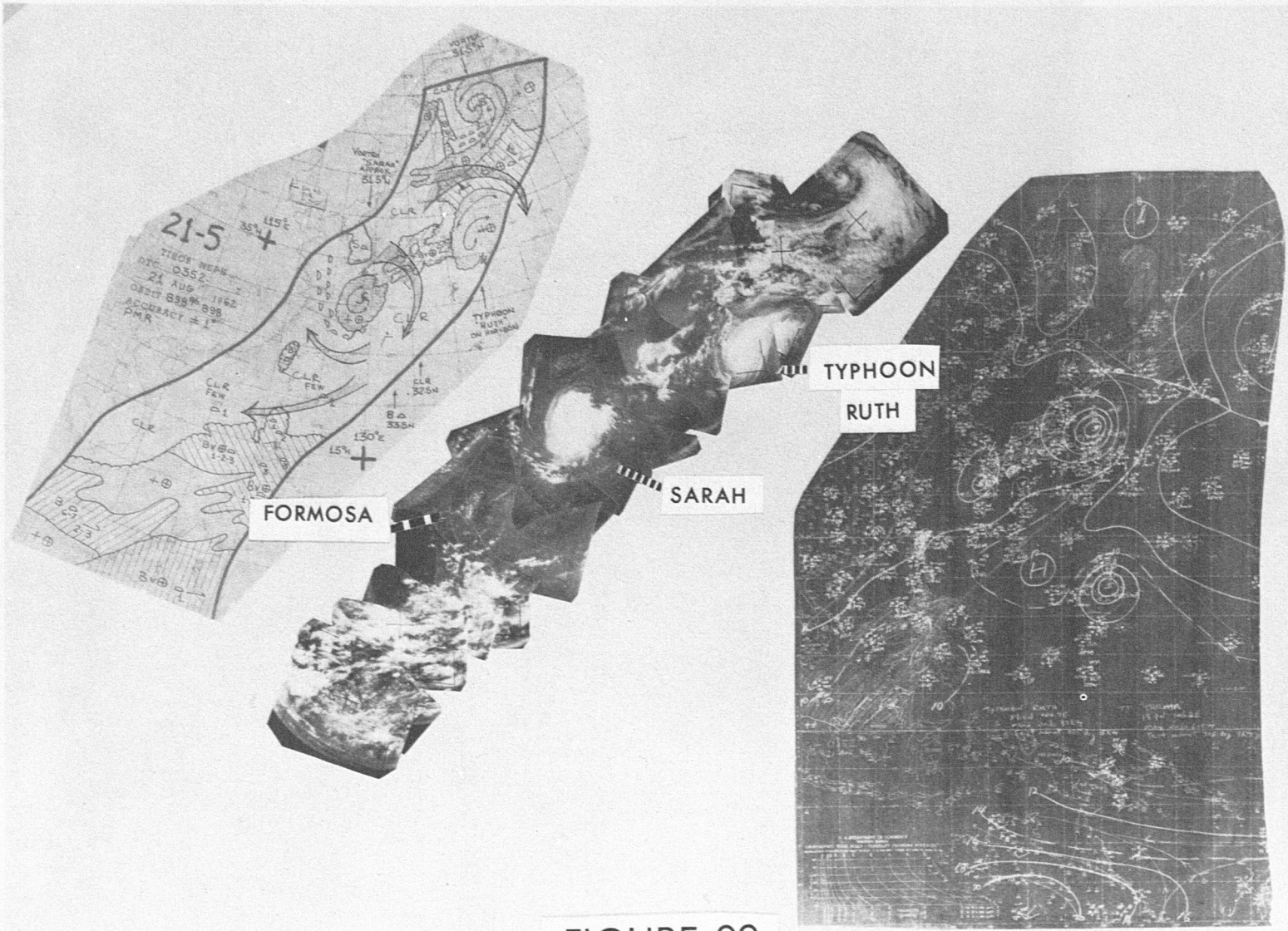


FIGURE 22

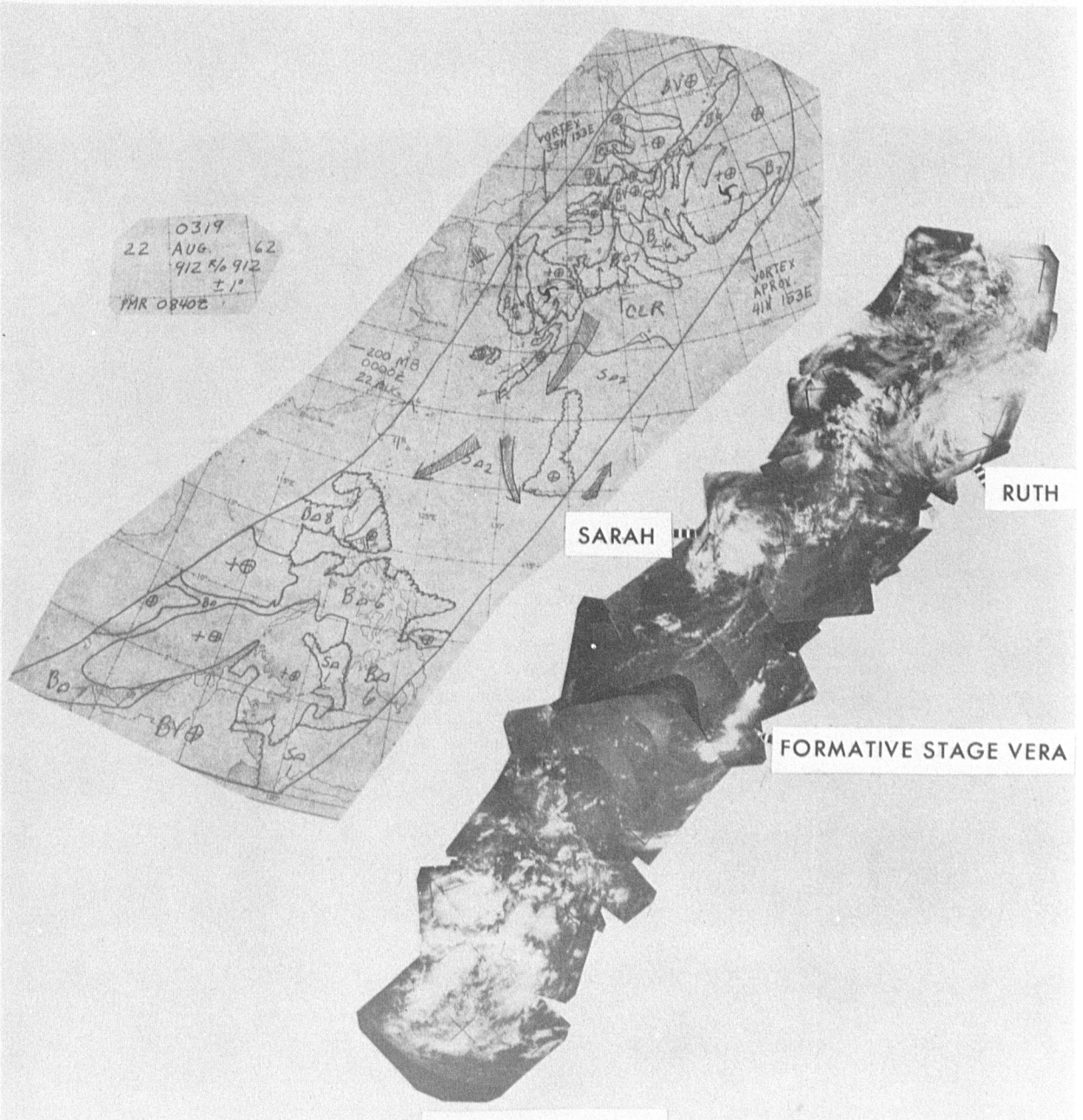
0319
22 AUG 62
912 R/O 912
± 1°
THR 0840Z
200 MB
0000Z
22 AUG
VORTEX
35N 153E
VORTEX
APROX
41N 153E
CLR
SARAH
RUTH
FORMATIVE STAGE VERA

FIGURE 23

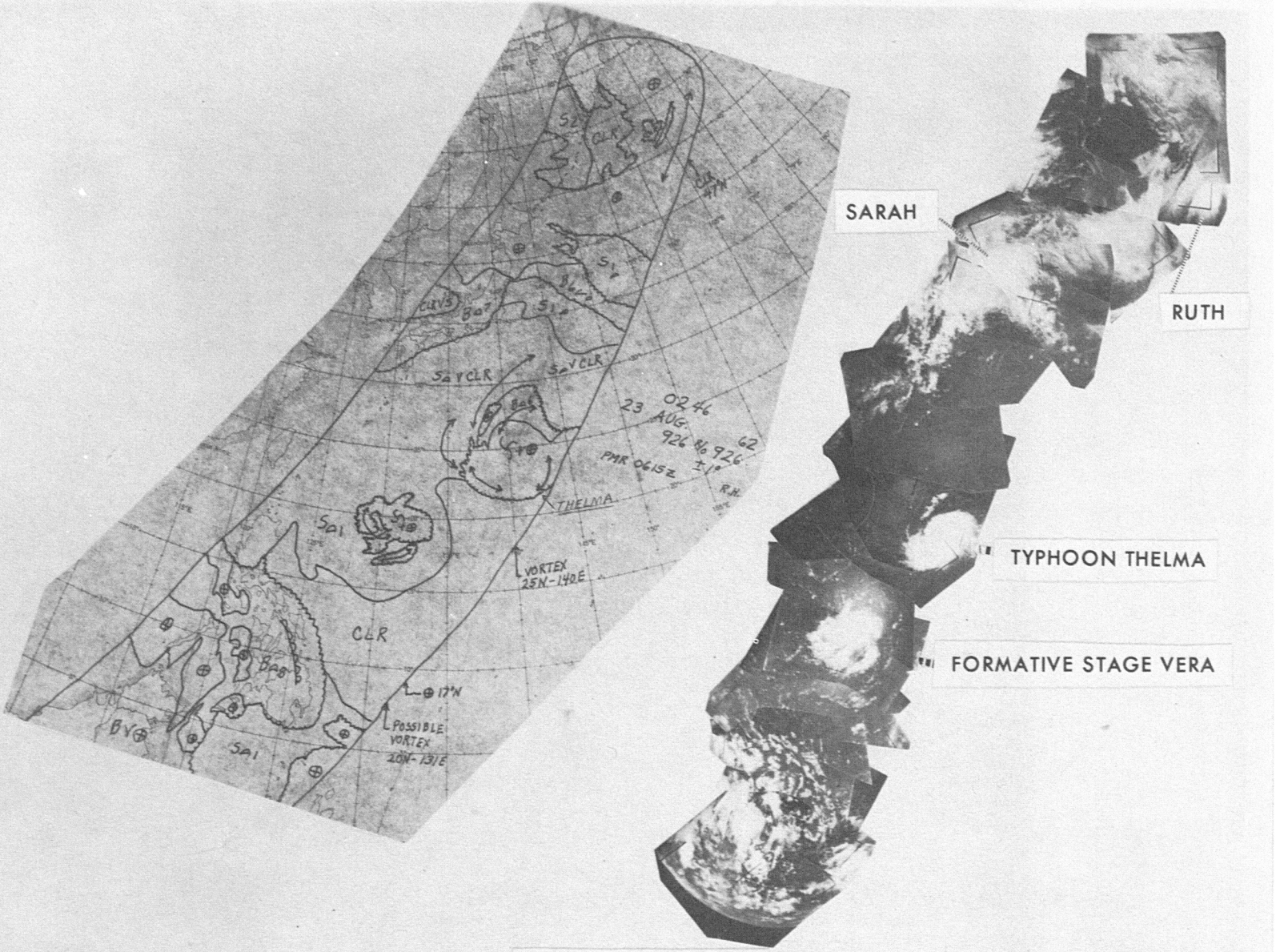
SARAH
RUTH
TYPHOON THELMA
FORMATIVE STAGE VERA
CLR
THELMA
VORTEX 25N-140E
POSSIBLE VORTEX 20N-131E
17°N
23 AUG
02 46
926
PMR 0615Z
R.H.

FIGURE 24

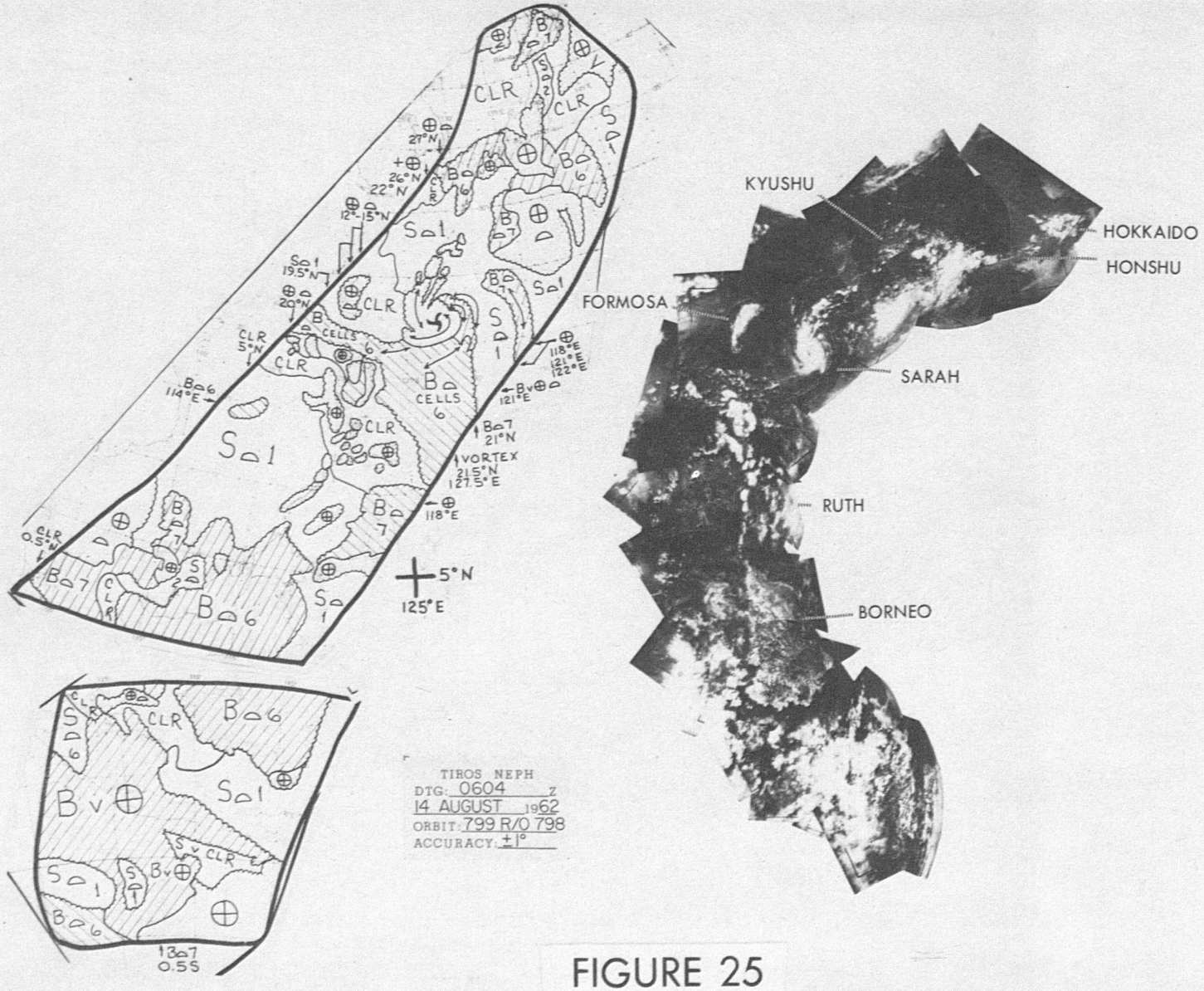
KYUSHU
HOKKAIDO
HONSHU
FORMOSA
SARAH
RUTH
BORNEO
CLR
Sa1
Ba6
Ba7
Bv
B CELLS 6
5°N
125°E
VORTEX 21.5°N 127.5°E
TIROS NEPH
DTG: 0604 Z
14 AUGUST 1962
ORBIT: 799 R/O 798
ACCURACY: ±1°

FIGURE 25

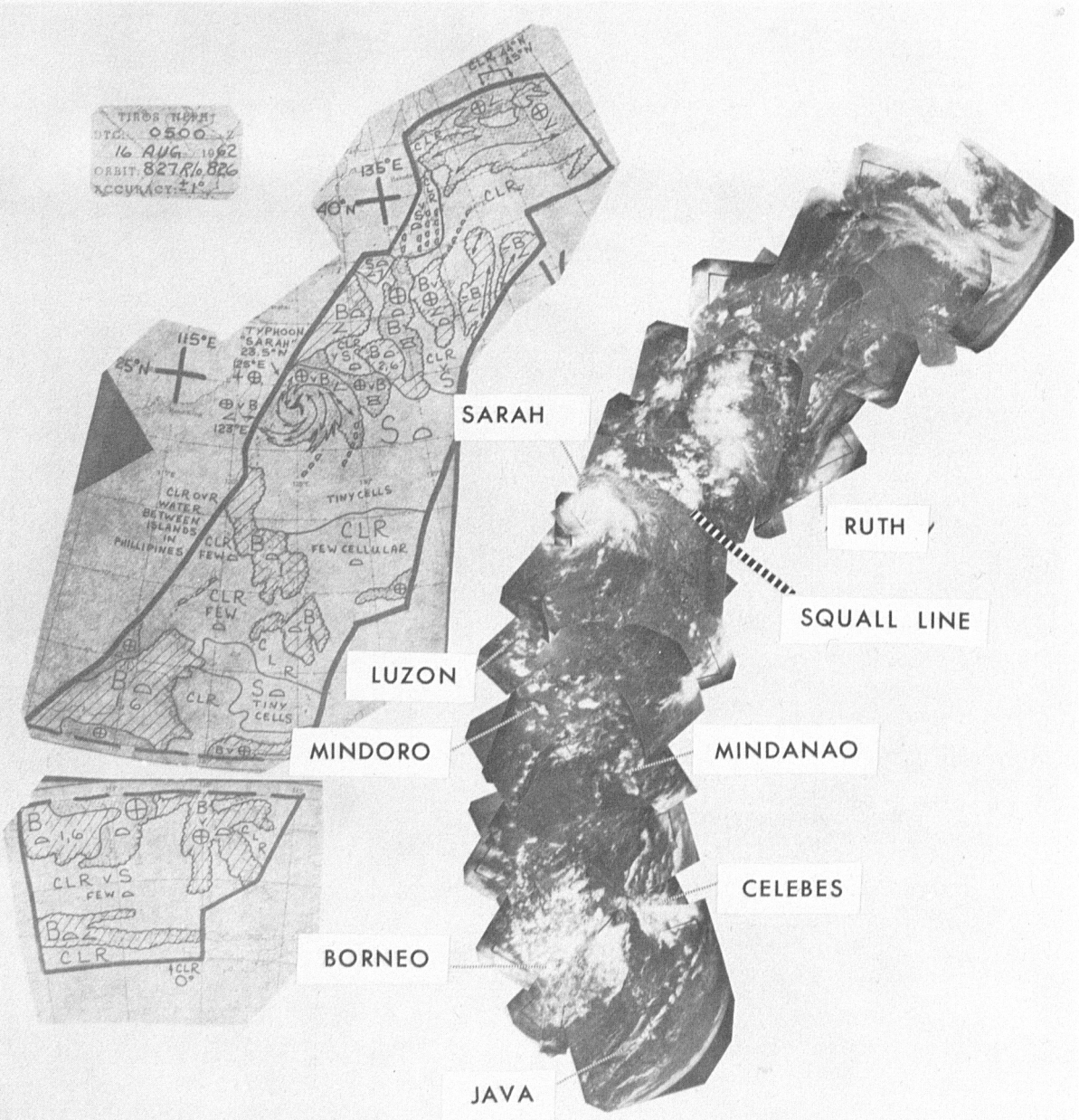
SARAH
RUTH
SQUALL LINE
LUZON
MINDORO
MINDANAO
CELEBES
BORNEO
JAVA

FIGURE 26

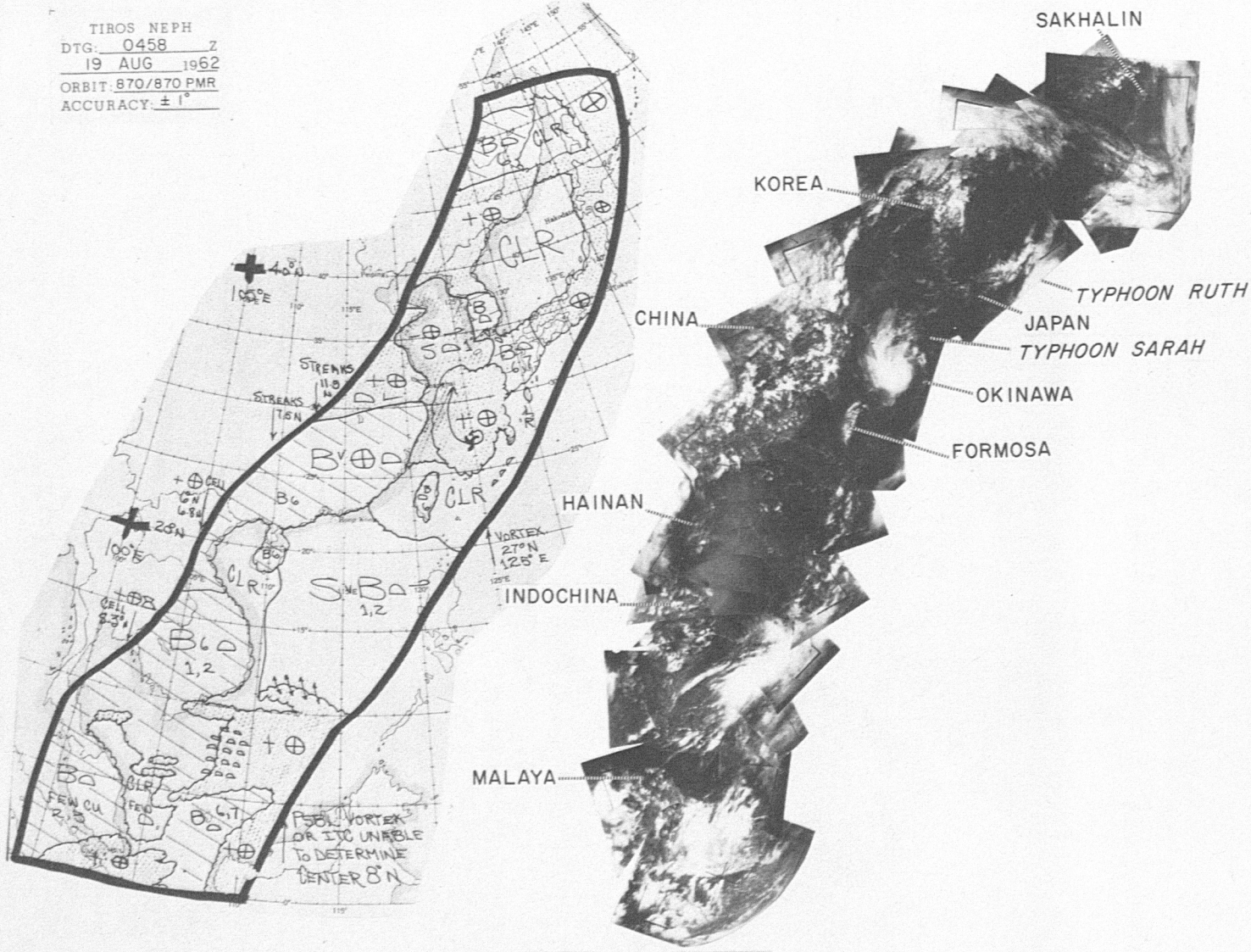
TIROS NEPH
DTG: 0458 Z
19 AUG 1962
ORBIT: 870/870 PMR
ACCURACY: ± 1°
SAKHALIN
KOREA
TYPHOON RUTH
CHINA
JAPAN
TYPHOON SARAH
OKINAWA
FORMOSA
HAINAN
INDOCHINA
MALAYA
STREAKS
VORTEX
27°N
125° E
POSS. VORTEX OR ITC UNABLE TO DETERMINE CENTER 8°N

FIGURE 27

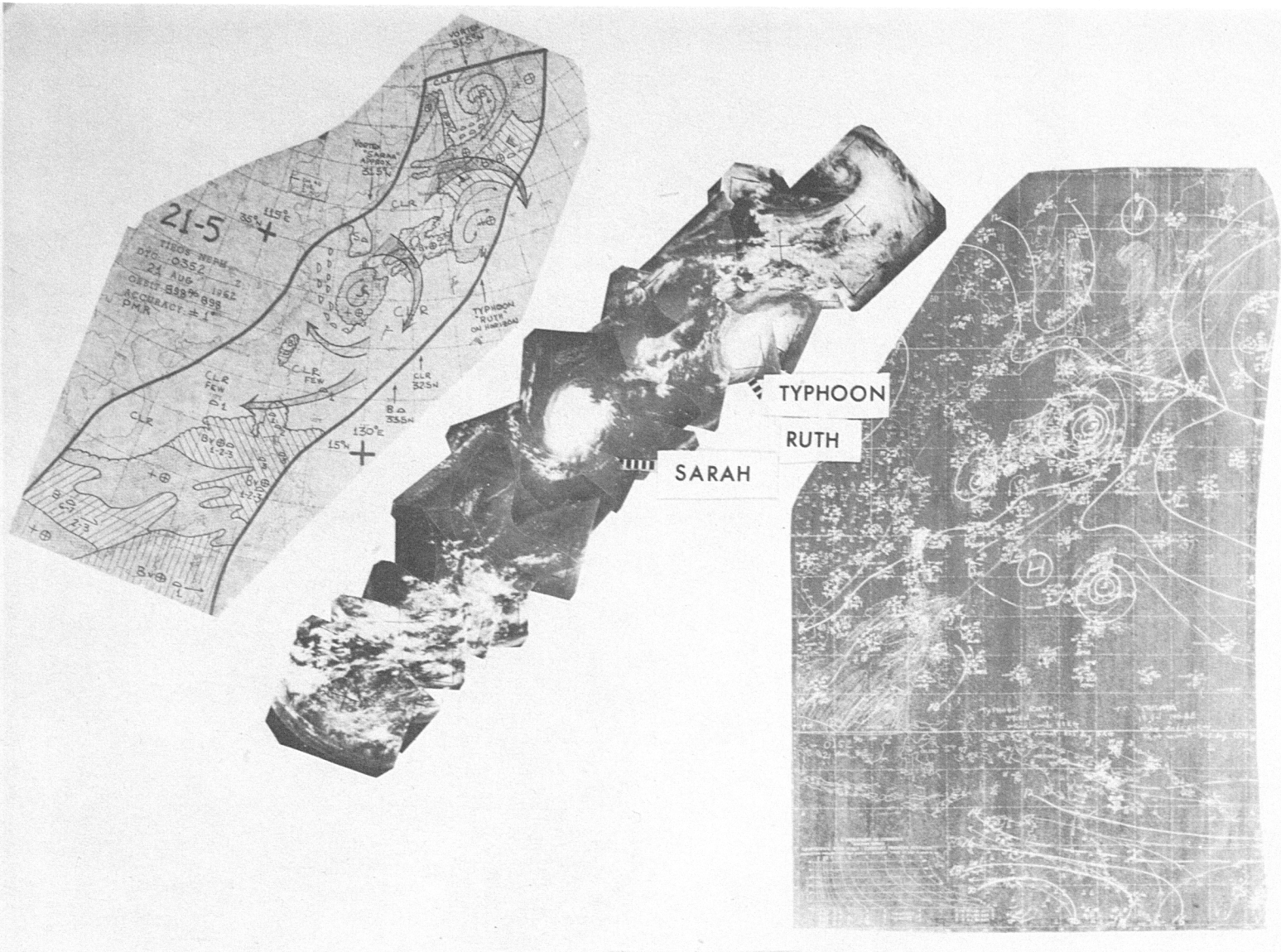


FIGURE 28

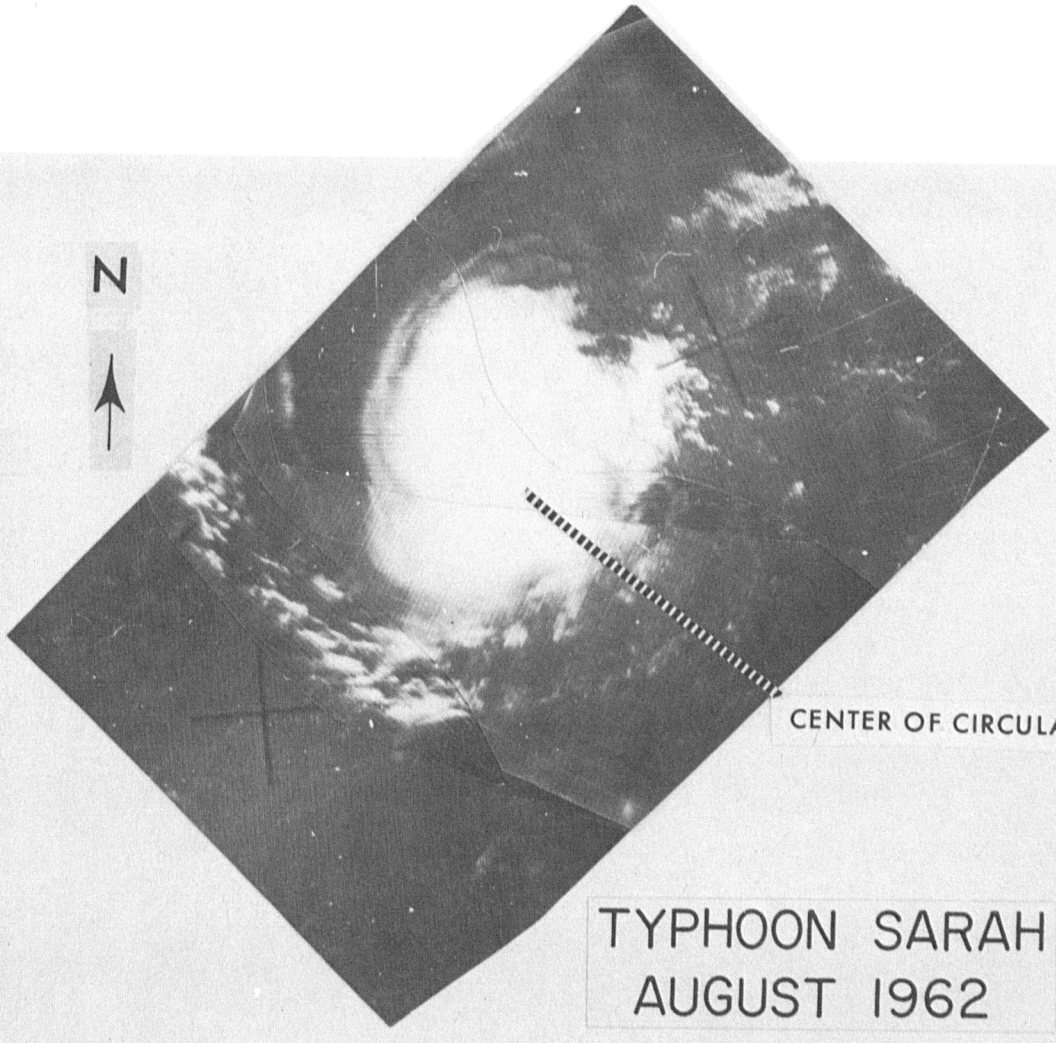


TYPHOON SARAH
AUGUST 1962

FIGURE 29

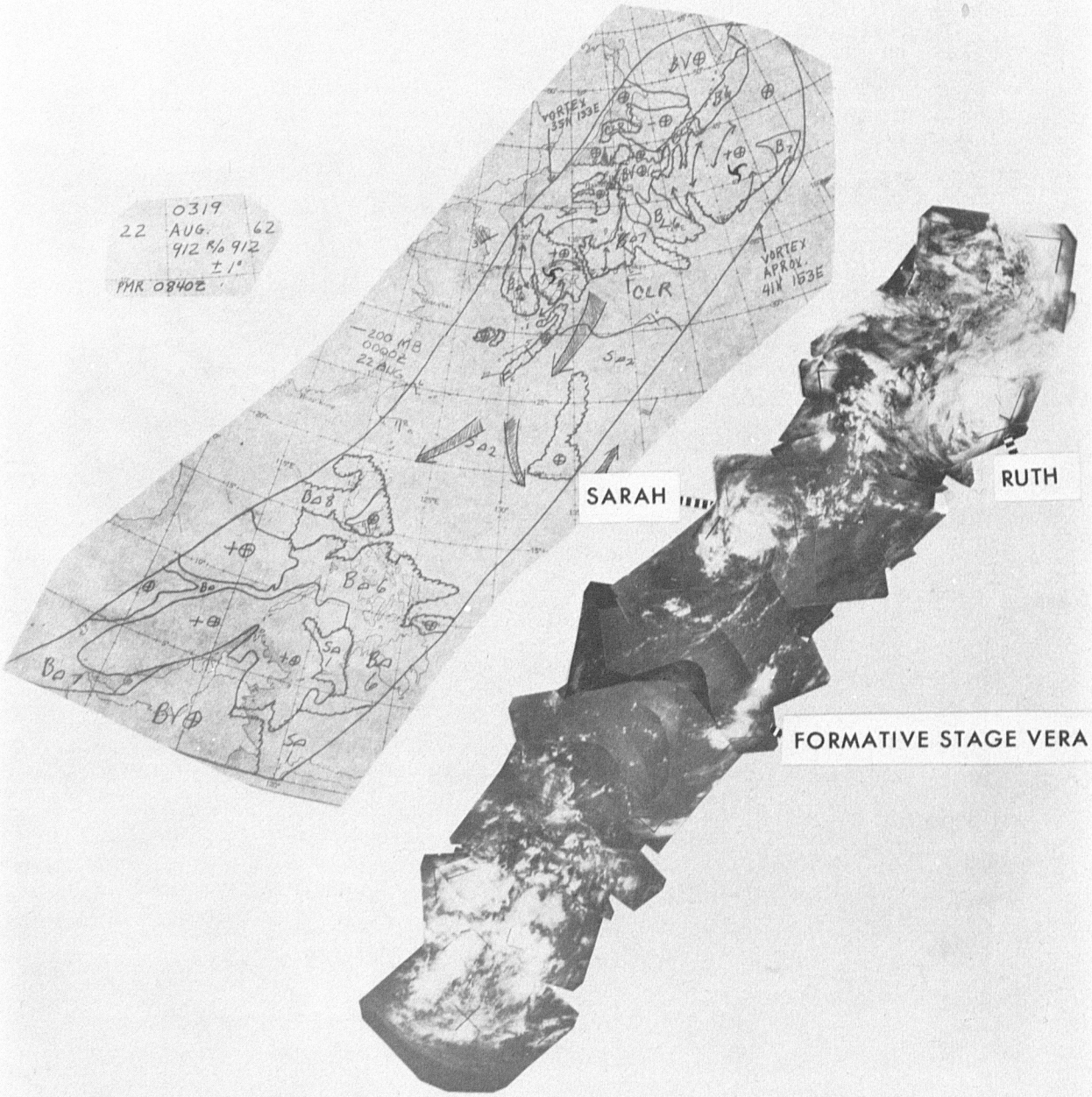
0319
22 AUG. 62
912 R/o 912
±1°
PMR 08402
VORTEX
35N 153E
VORTEX
APROX.
41N 153E
CLR
SARAH
RUTH
FORMATIVE STAGE VERA

FIGURE 30

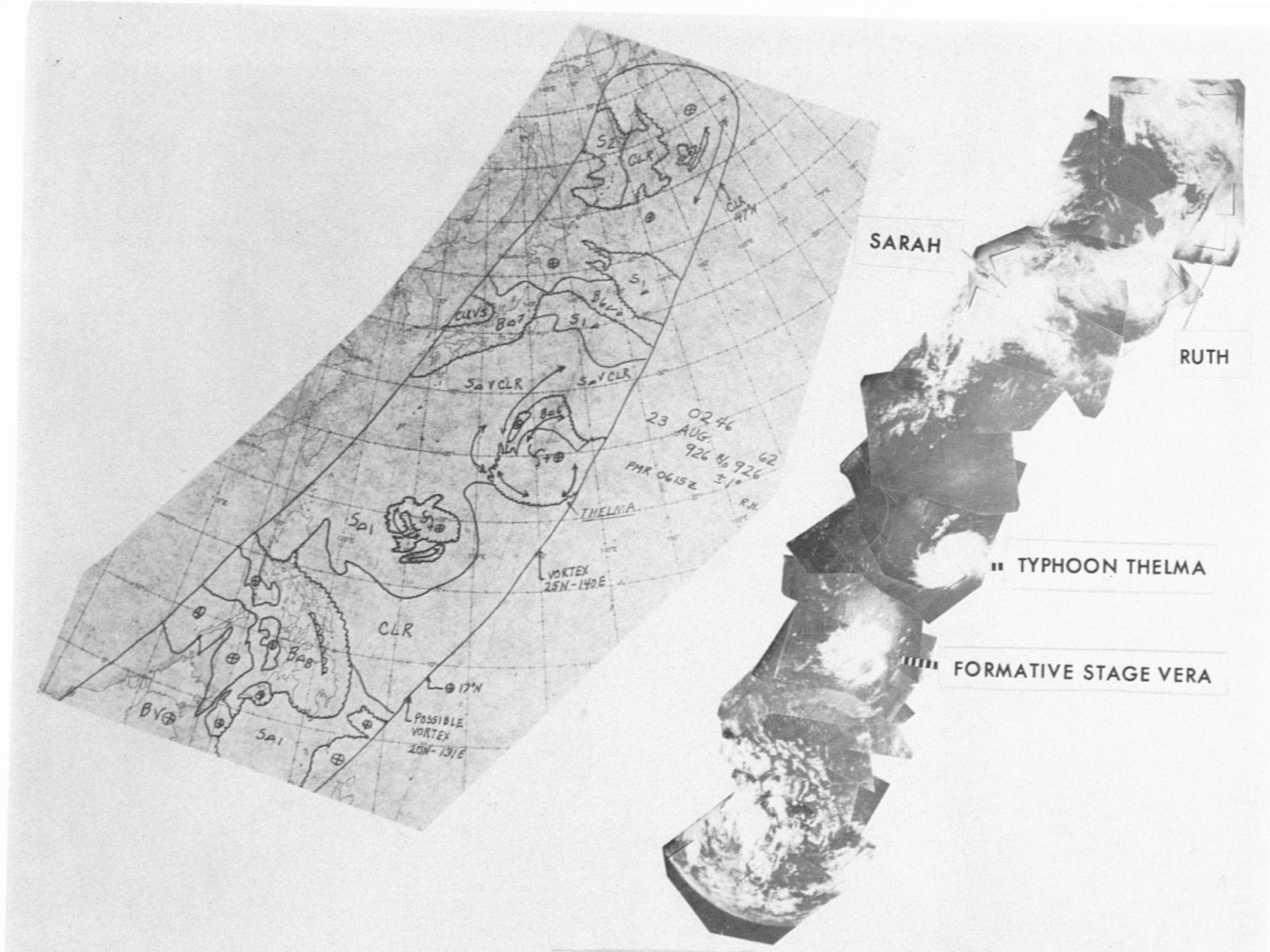
SARAH
RUTH
TYPHOON THELMA
FORMATIVE STAGE VERA
SZ
CLR
CLR 17°N
CLVS
Ba7
Sa VCLR
Sa VCLR
23 0246 AUG
926 mb 926 62
PMR 0615Z ±1°
R.H.
THELMA
Sa1
VORTEX 25N-140E
CLR
Ba8
BV
Sa1
17°N
POSSIBLE VORTEX 20N-131E

FIGURE 31

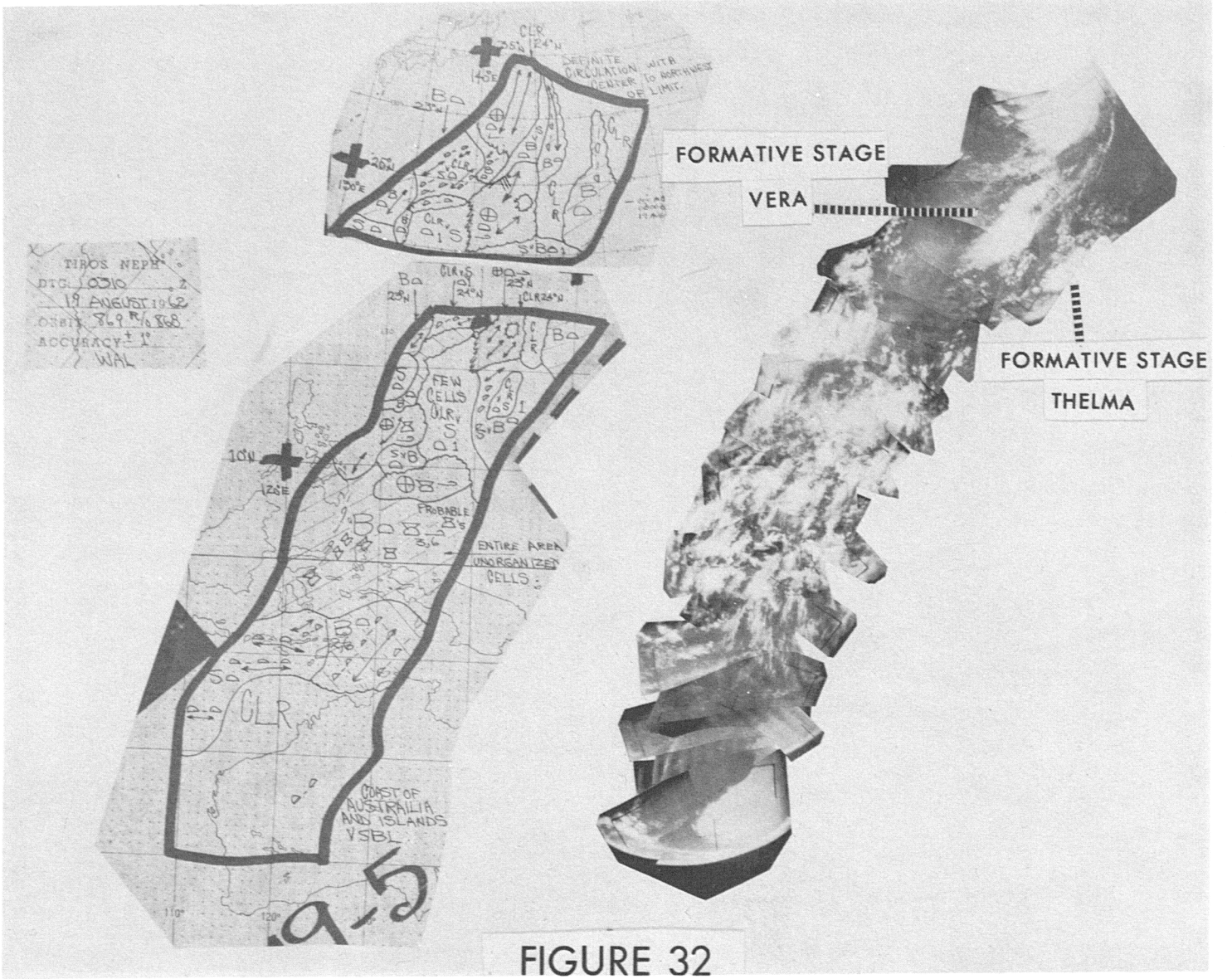
FORMATIVE STAGE
VERA
FORMATIVE STAGE
THELMA
TIROS NEPH
19 AUGUST 1962
ACCURACY ± 1°
WAL
DEFINITE CIRCULATION WITH CENTER TO NORTHWEST OF LIMIT.
FEW CELLS
ENTIRE AREA UNORGANIZED CELLS
PROBABLE
COAST OF AUSTRAILIA AND ISLANDS VSBL
CLR
9-5

FIGURE 32

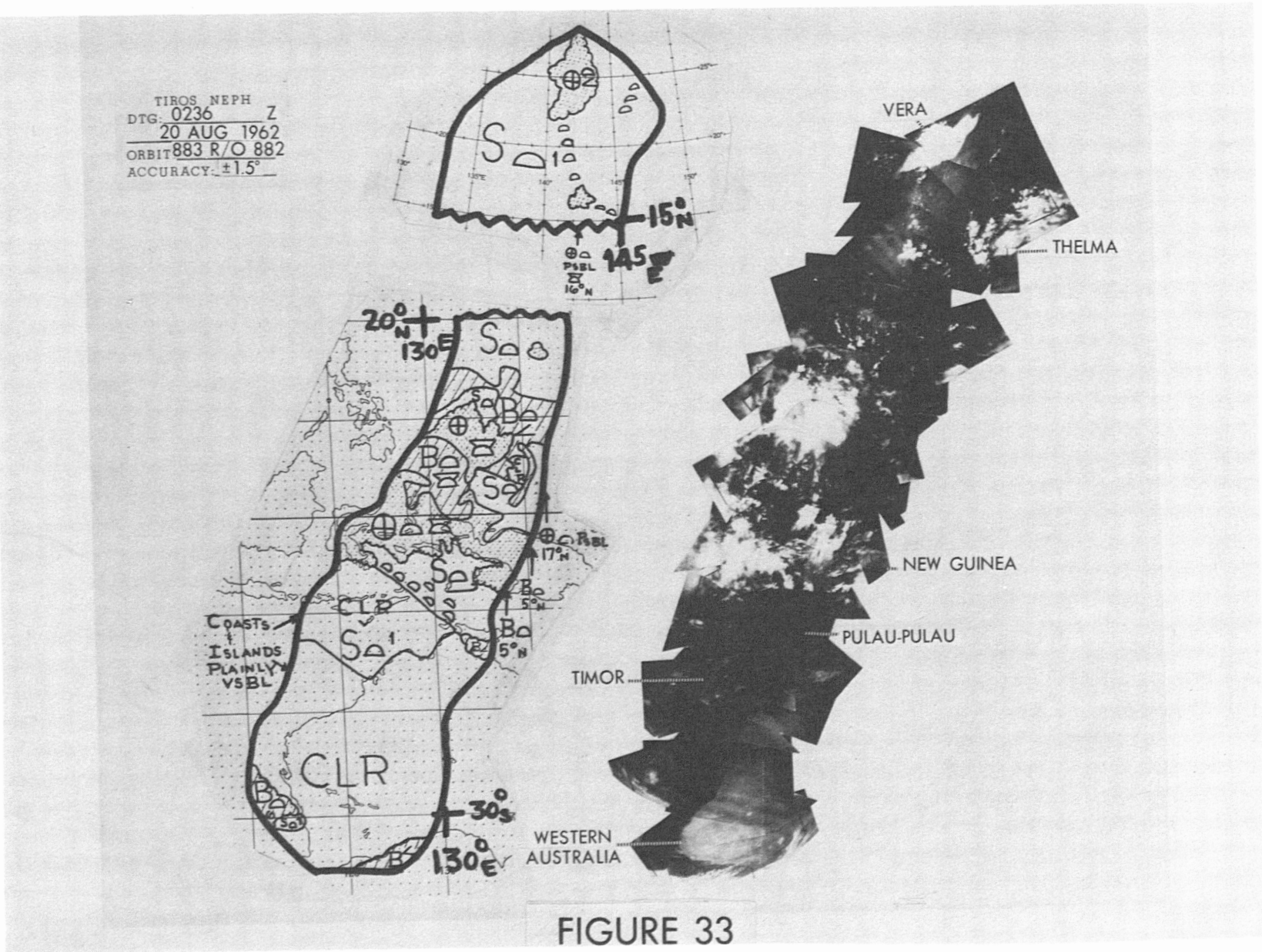
TIROS NEPH
DTG: 0236 Z
20 AUG 1962
ORBIT 883 R/O 882
ACCURACY: ±1.5°
15°N
145°E
20°N
130°E
30°S
130°E
CLR
COASTS & ISLANDS PLAINLY VSBL
VERA
THELMA
NEW GUINEA
PULAU-PULAU
TIMOR
WESTERN AUSTRALIA

FIGURE 33

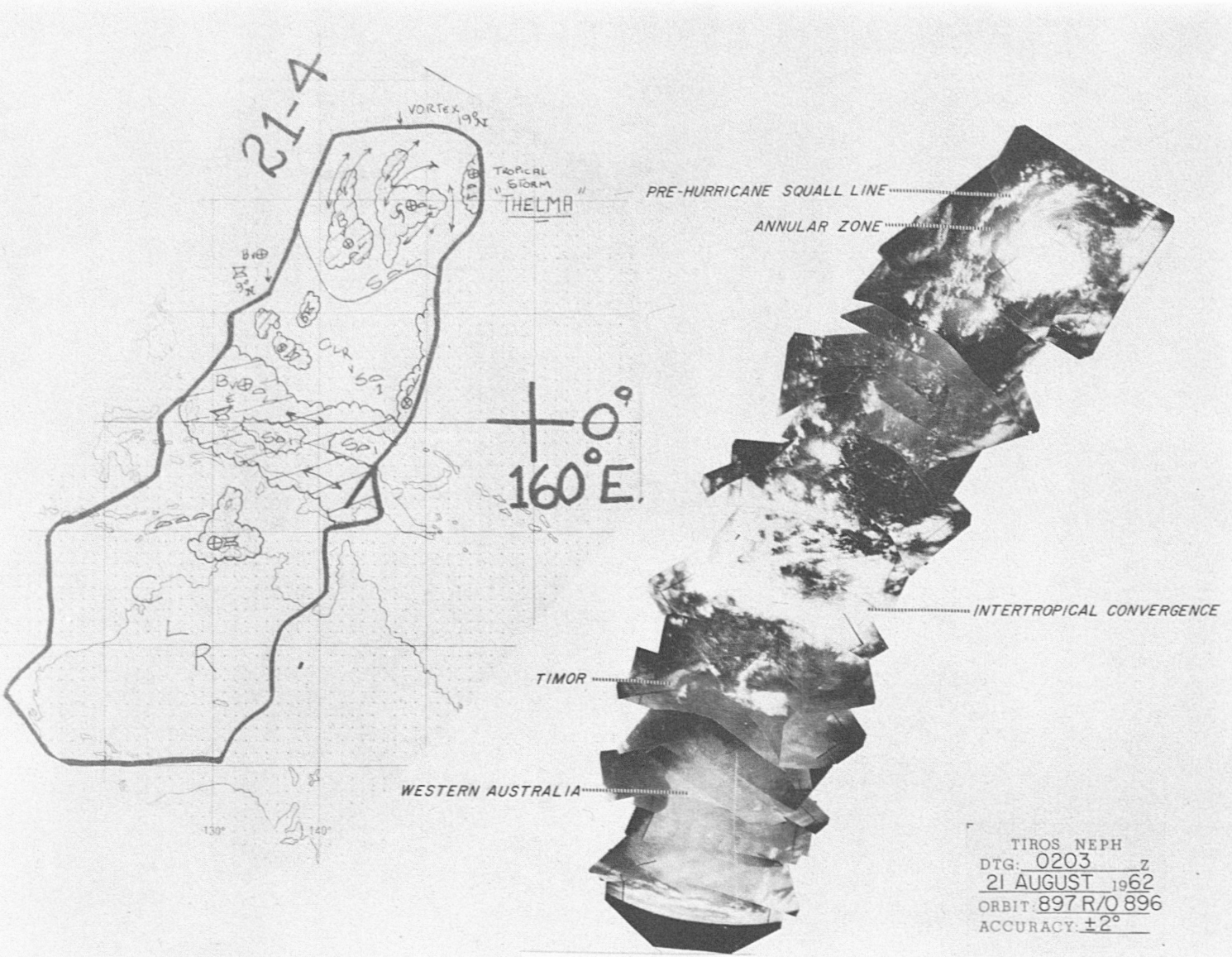
21-4
VORTEX 19 X
TROPICAL STORM "THELMA"
PRE-HURRICANE SQUALL LINE
ANNULAR ZONE
INTERTROPICAL CONVERGENCE
TIMOR
WESTERN AUSTRALIA
0°
160° E.
130°
140°
TIROS NEPH
DTG: 0203 Z
21 AUGUST 1962
ORBIT: 897 R/O 896
ACCURACY: ±2°

FIGURE 34

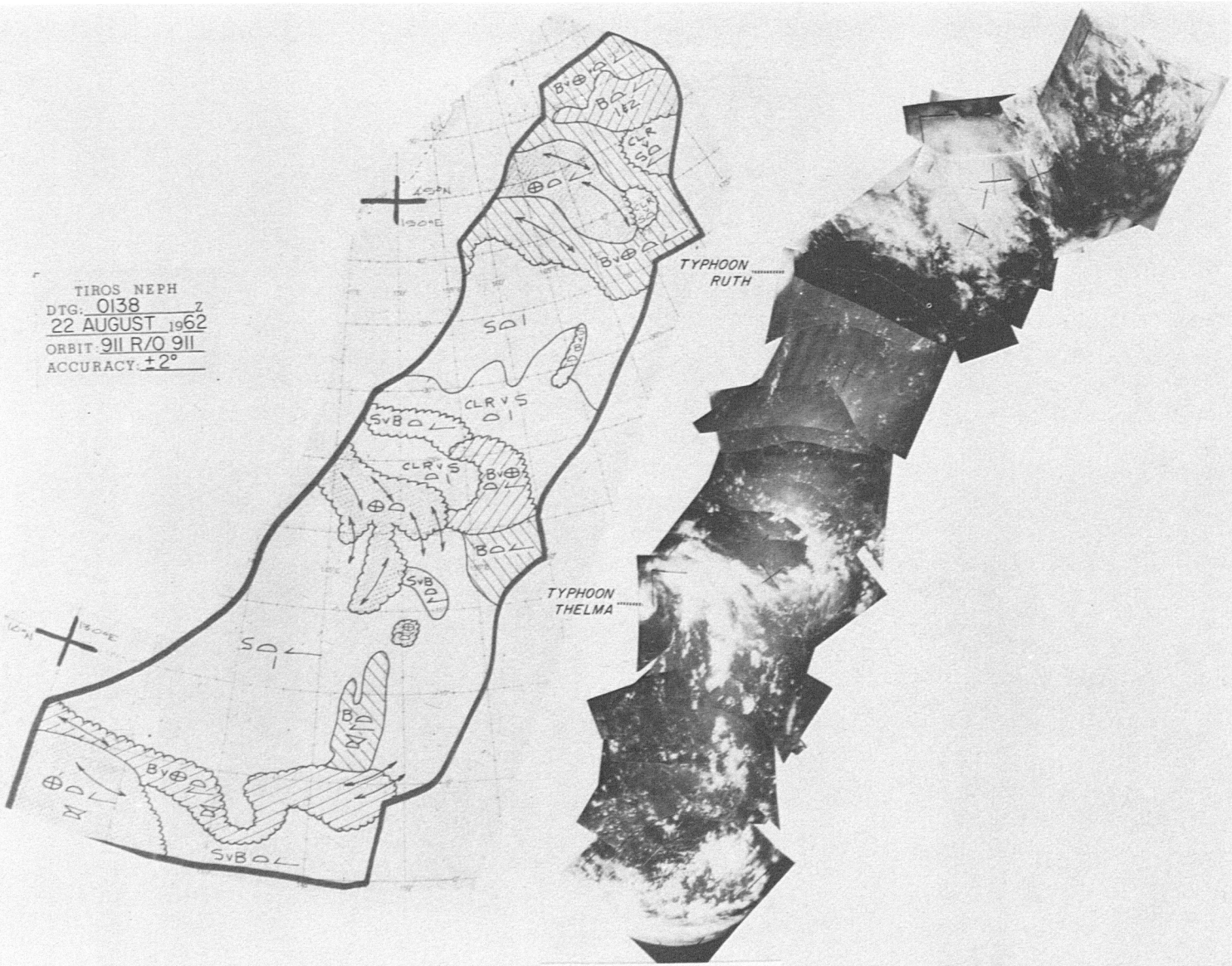
TIROS NEPH
DTG: 0138 Z
22 AUGUST 1962
ORBIT: 911 R/O 911
ACCURACY: ±2°
TYPHOON RUTH
TYPHOON THELMA

FIGURE 35

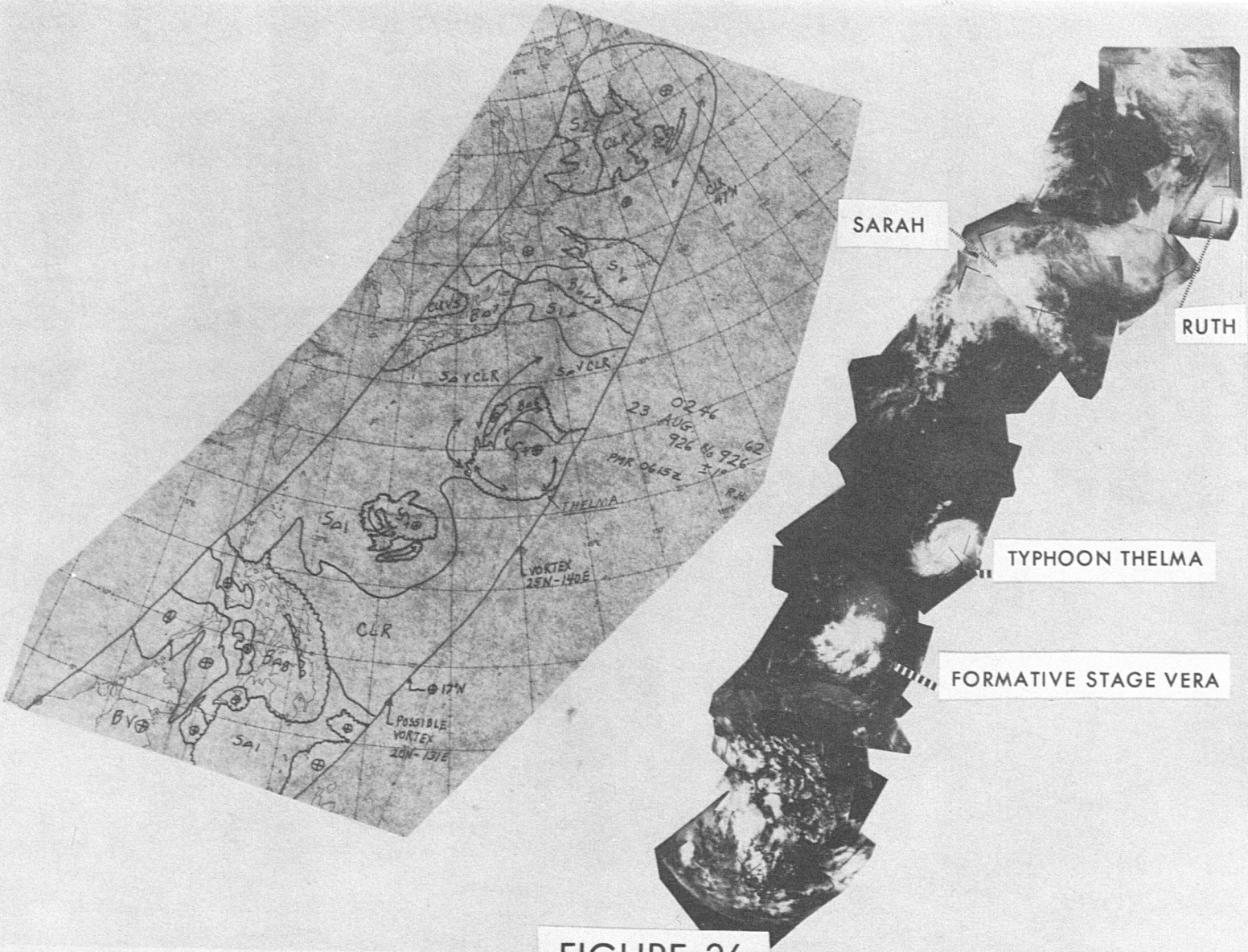
SARAH
RUTH
TYPHOON THELMA
FORMATIVE STAGE VERA
THELMA
VORTEX 25N-140E
POSSIBLE VORTEX 20N-131E
CLR
23 AUG
17°N

FIGURE 36

TIROS NEPH
DTG 0207 Z
24 AUGUST 1962
CLR FEW
CIRVS
BVBDL
BDL
FORMATIVE STAGE
VERA
TYPHOON
THELMA

FIGURE 37

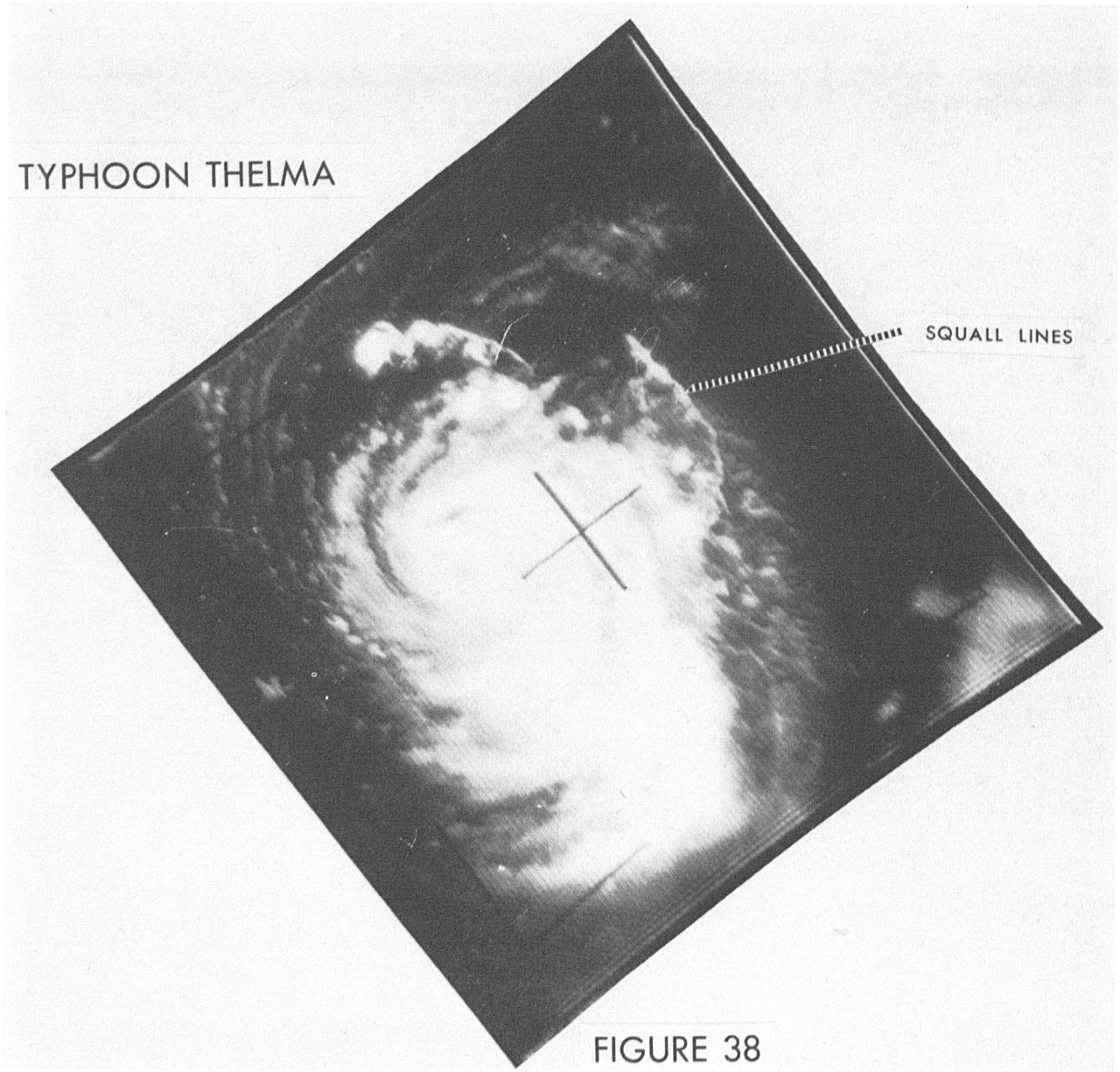


FIGURE 38

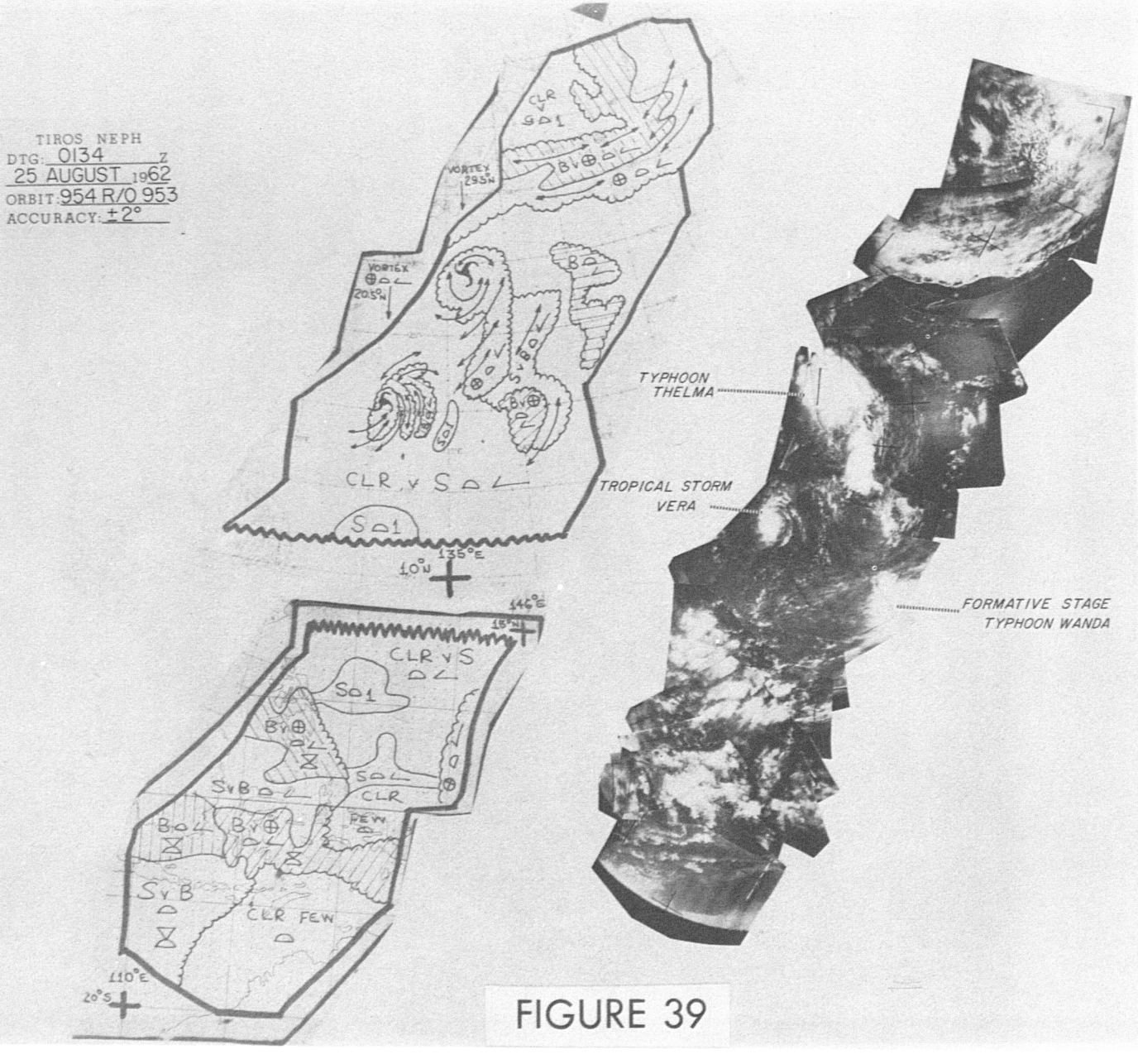
TIROS NEPH
DTG: 0134 Z
25 AUGUST 1962
ORBIT: 954 R/O 953
ACCURACY: ±2°
CLR v SC1
SC1
VORTEX 29.5°N
VORTEX 20.5°N
CLR v SC1
SC1
10°N 135°E
TYPHOON THELMA
TROPICAL STORM VERA
FORMATIVE STAGE TYPHOON WANDA
CLR v S
SC1
CLR
FEW
SvB
CLR FEW
20°S 110°E

FIGURE 39

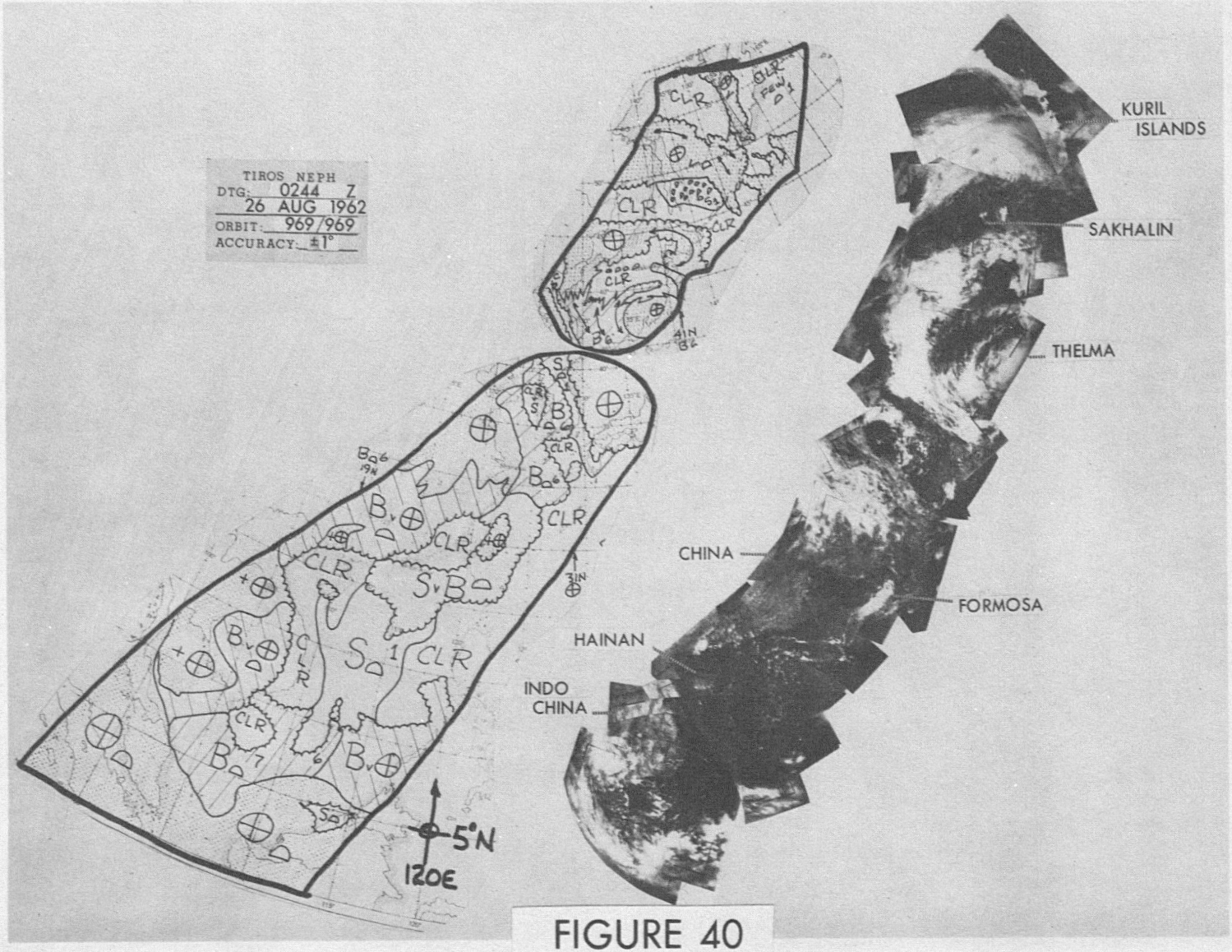
TIROS NEPH
DTG: 0244 Z
26 AUG 1962
ORBIT: 969/969
ACCURACY: ±1°
KURIL ISLANDS
SAKHALIN
THELMA
CHINA
FORMOSA
HAINAN
INDO CHINA
5°N
120E

FIGURE 40

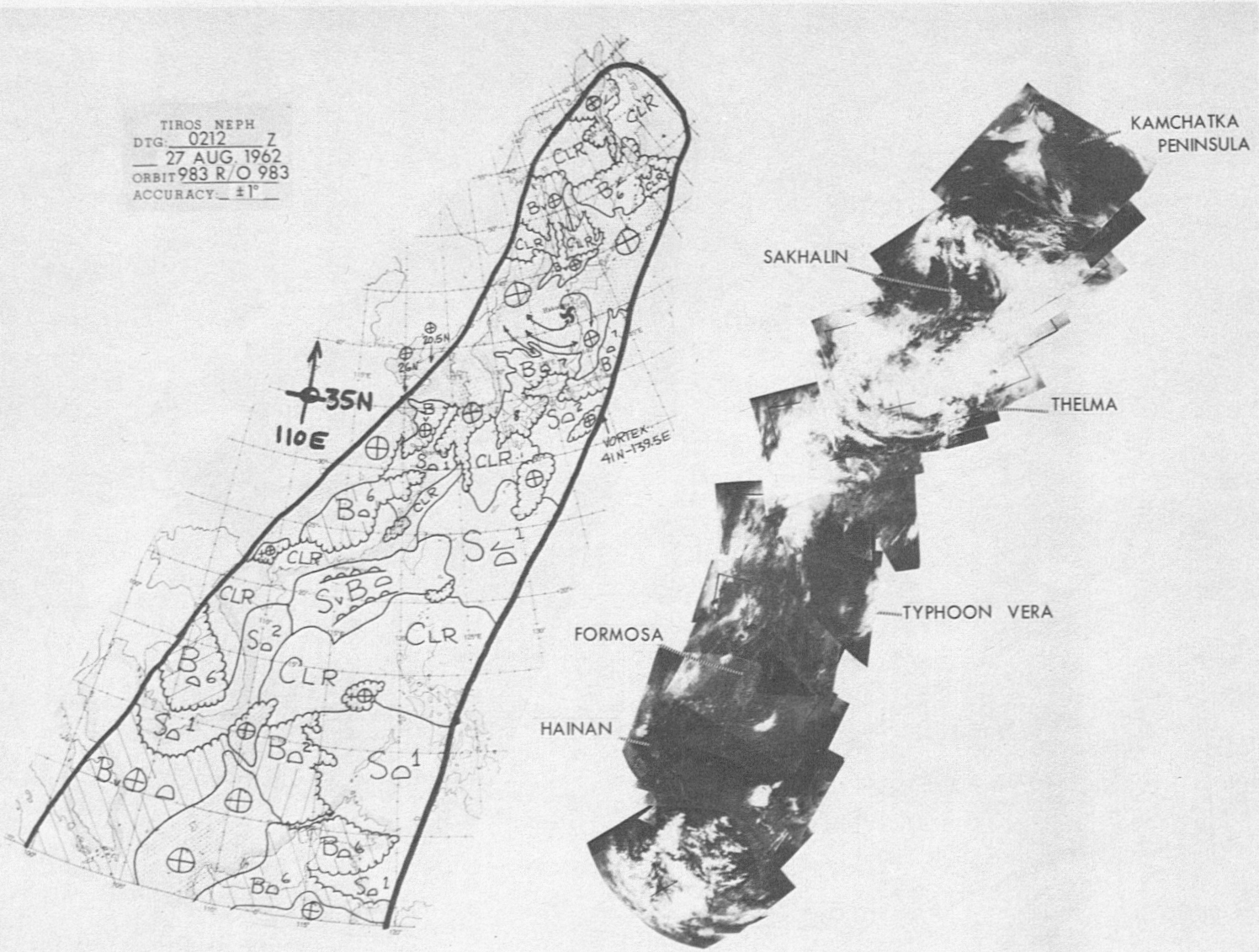
TIROS NEPH
DTG: 0212 Z
27 AUG. 1962
ORBIT 983 R/O 983
ACCURACY: ±1°
35N
110E
VORTEX
41N-139.5E
KAMCHATKA
PENINSULA
SAKHALIN
THELMA
TYPHOON VERA
FORMOSA
HAINAN

FIGURE 41

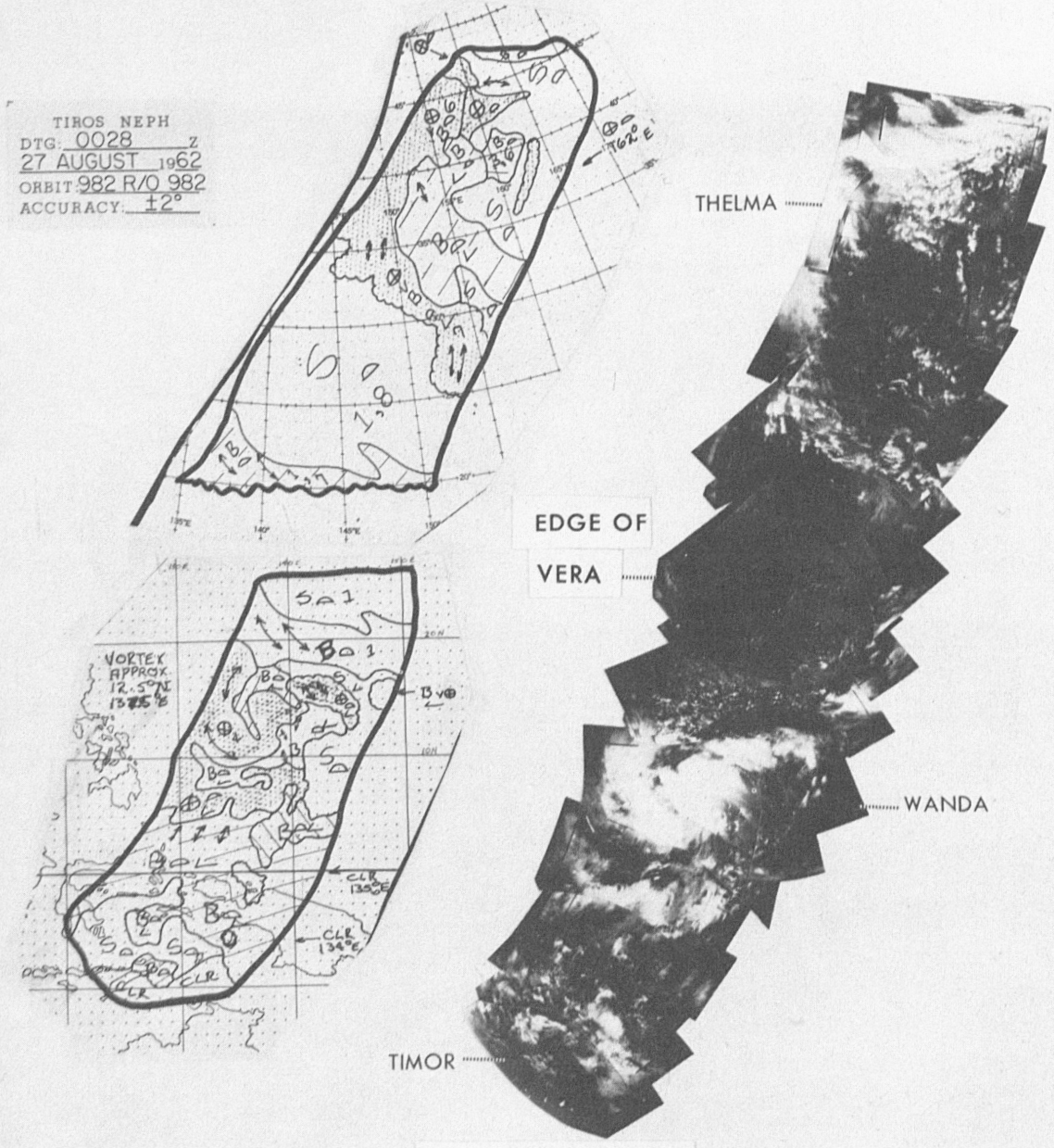
TIROS NEPH
DTG: 0028 Z
27 AUGUST 1962
ORBIT 982 R/O 982
ACCURACY: ±2°
VORTEX APPROX 12.5°N 135°E
CLR 135°E
CLR 134°E
THELMA
EDGE OF VERA
WANDA
TIMOR

FIGURE 42

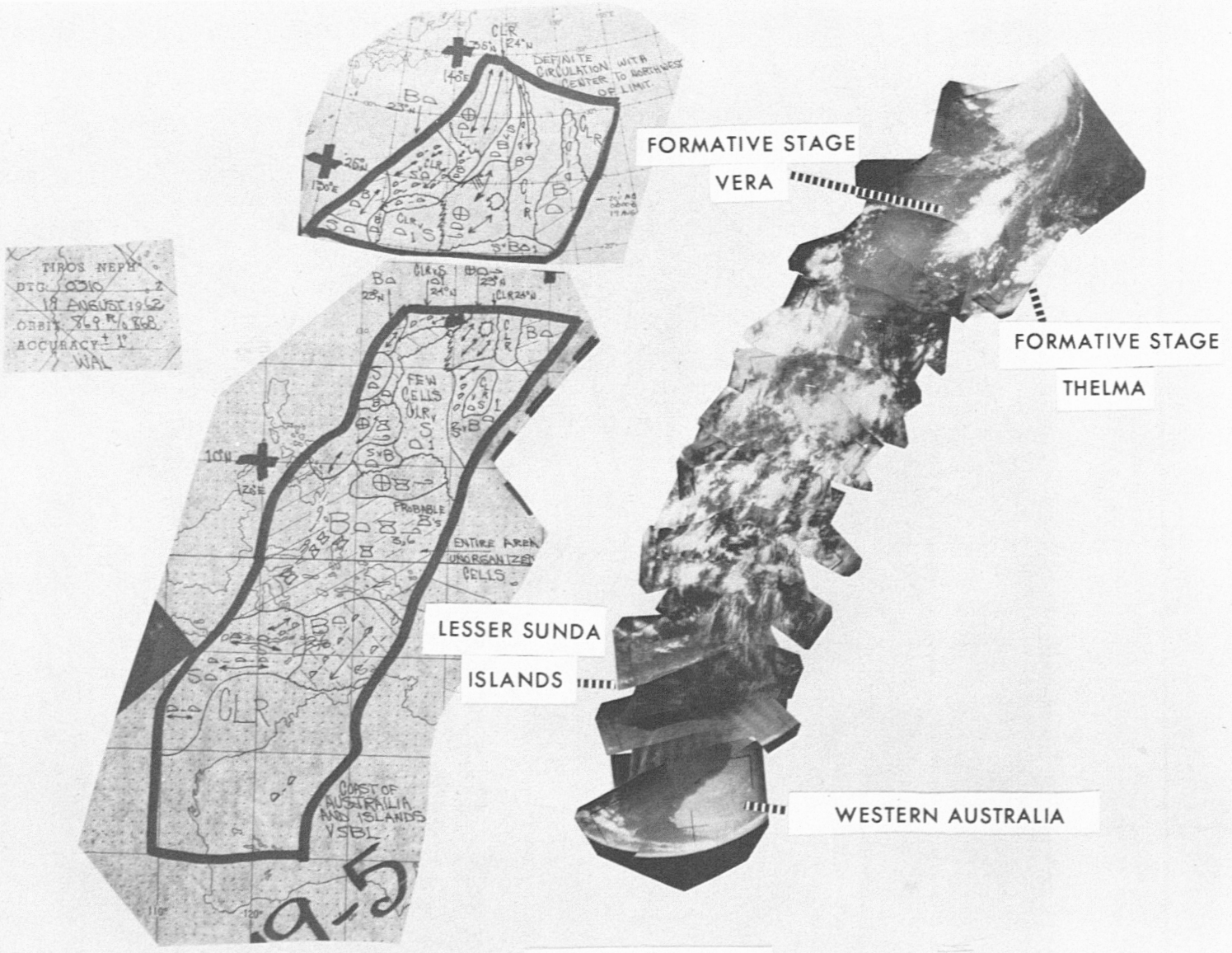
TIROS NEPH
DTG 0310 Z
18 AUGUST 1962
ORBIT 749 R/ 868
ACCURACY ± 1°
WAL
DEFINITE CIRCULATION WITH CENTER TO NORTHWEST OF LIMIT
FEW CELLS
ENTIRE AREA UNORGANIZED CELLS
PROBABLE
COAST OF AUSTRALIA AND ISLANDS VSBL
FORMATIVE STAGE
VERA
FORMATIVE STAGE
THELMA
LESSER SUNDA
ISLANDS
WESTERN AUSTRALIA

FIGURE 43

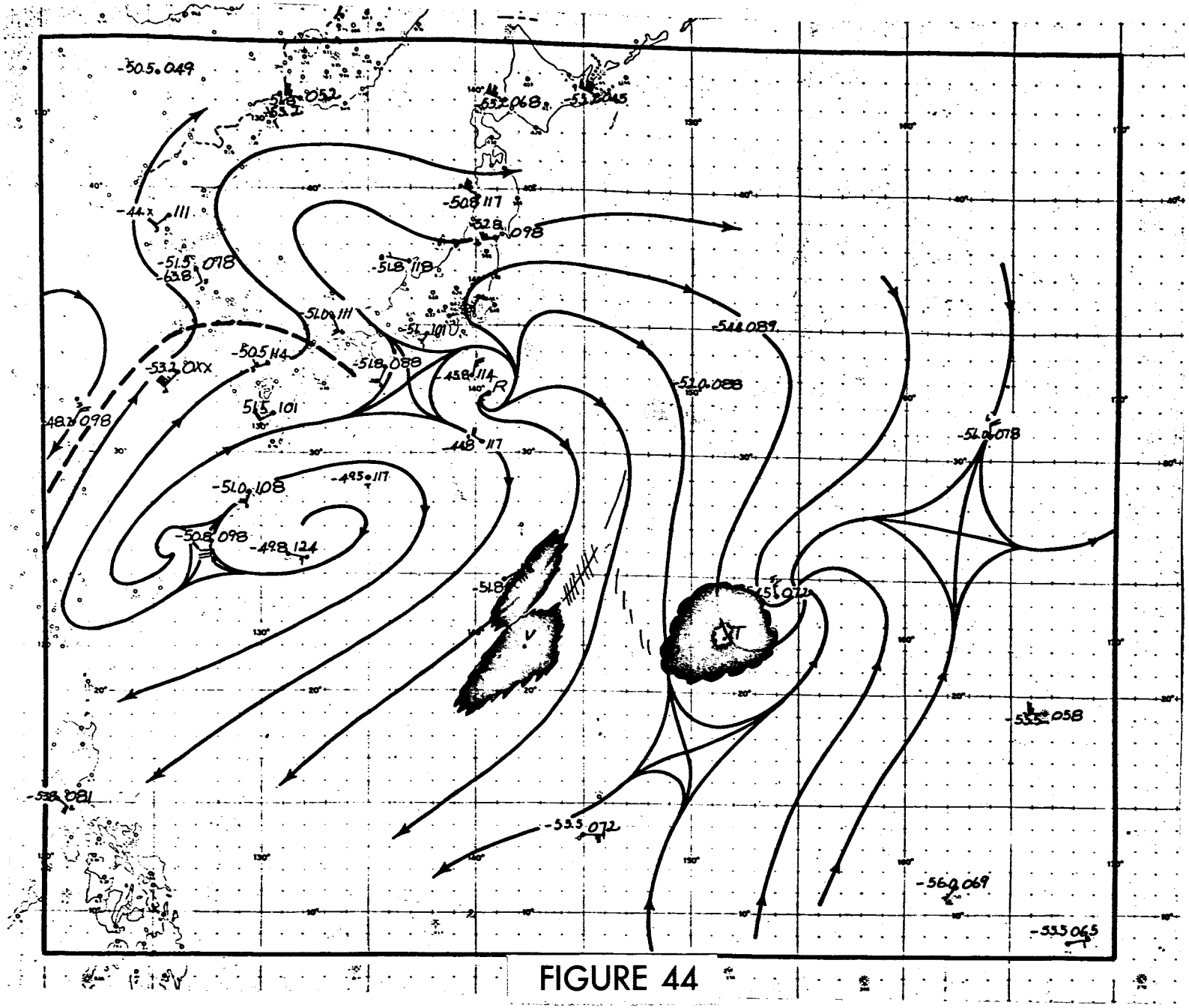
-505.049
-508 117
-515 078
-518 118
-510 111
-505 114
-518 088
-458 114
-515 101
-510 108
-495 117
-508 098
-498 124
-518
-515 072
-555 058
-538 081
-533 072
-560 069
-533 065

FIGURE 44

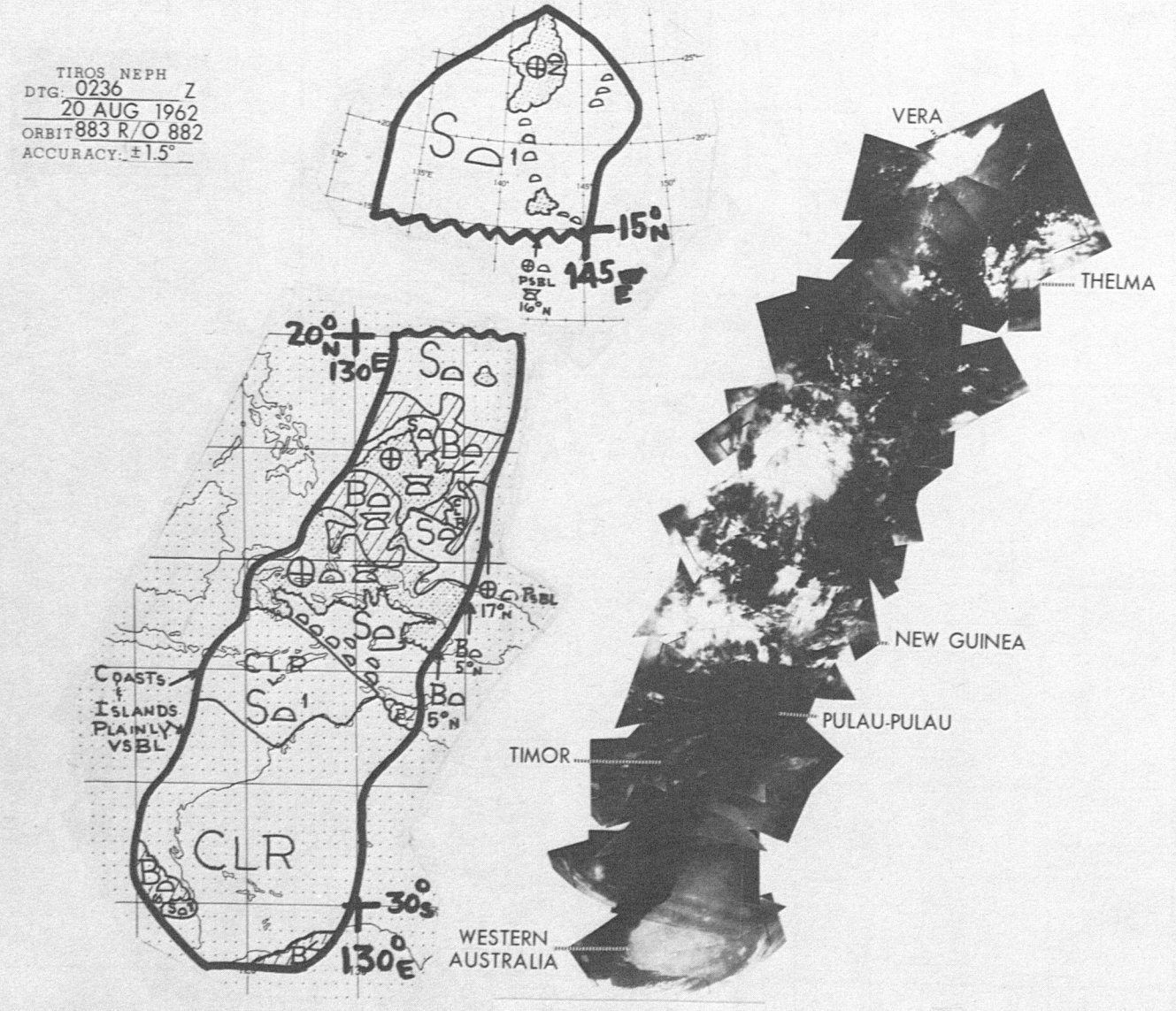
TIROS NEPH
DTG: 0236 Z
20 AUG 1962
ORBIT 883 R/O 882
ACCURACY: ±1.5°
S
1
15°N
145°E
PSBL
16°N
20°N
130°E
S
B
S
PSBL
17°N
Bo
5°N
CLR
COASTS & ISLANDS PLAINLY VSBL
S
1
Bo
5°N
CLR
Bo
VSO
30°S
130°E
VERA
THELMA
NEW GUINEA
PULAU-PULAU
TIMOR
WESTERN AUSTRALIA

FIGURE 45

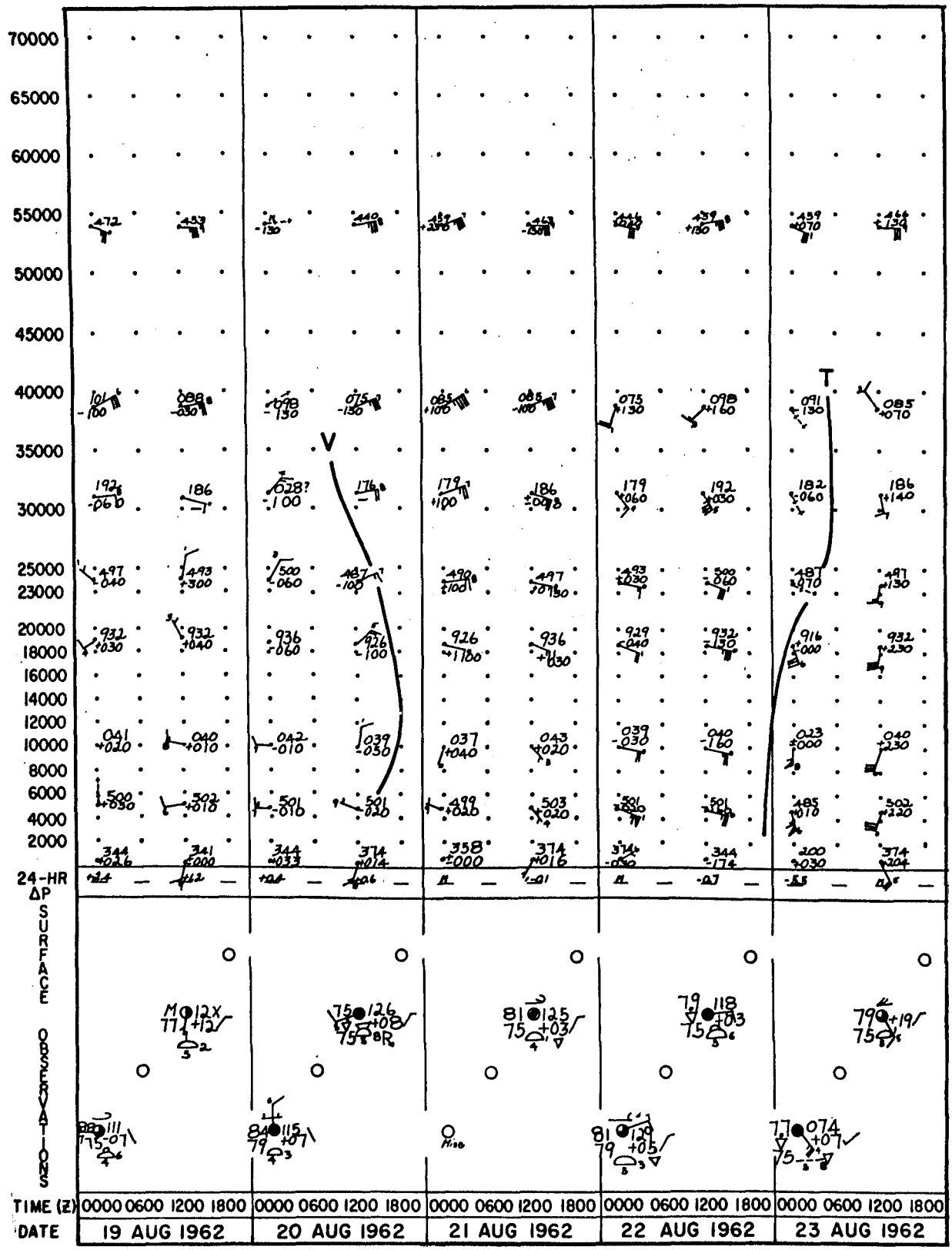
70000
65000
60000
55000
50000
45000
40000
35000
30000
25000
23000
20000
18000
16000
14000
12000
10000
8000
6000
4000
2000
24-HR ΔP
SURFACE OBSERVATIONS
TIME (Z)
0000 0600 1200 1800
DATE
19 AUG 1962
20 AUG 1962
21 AUG 1962
22 AUG 1962
23 AUG 1962

FIGURE 46

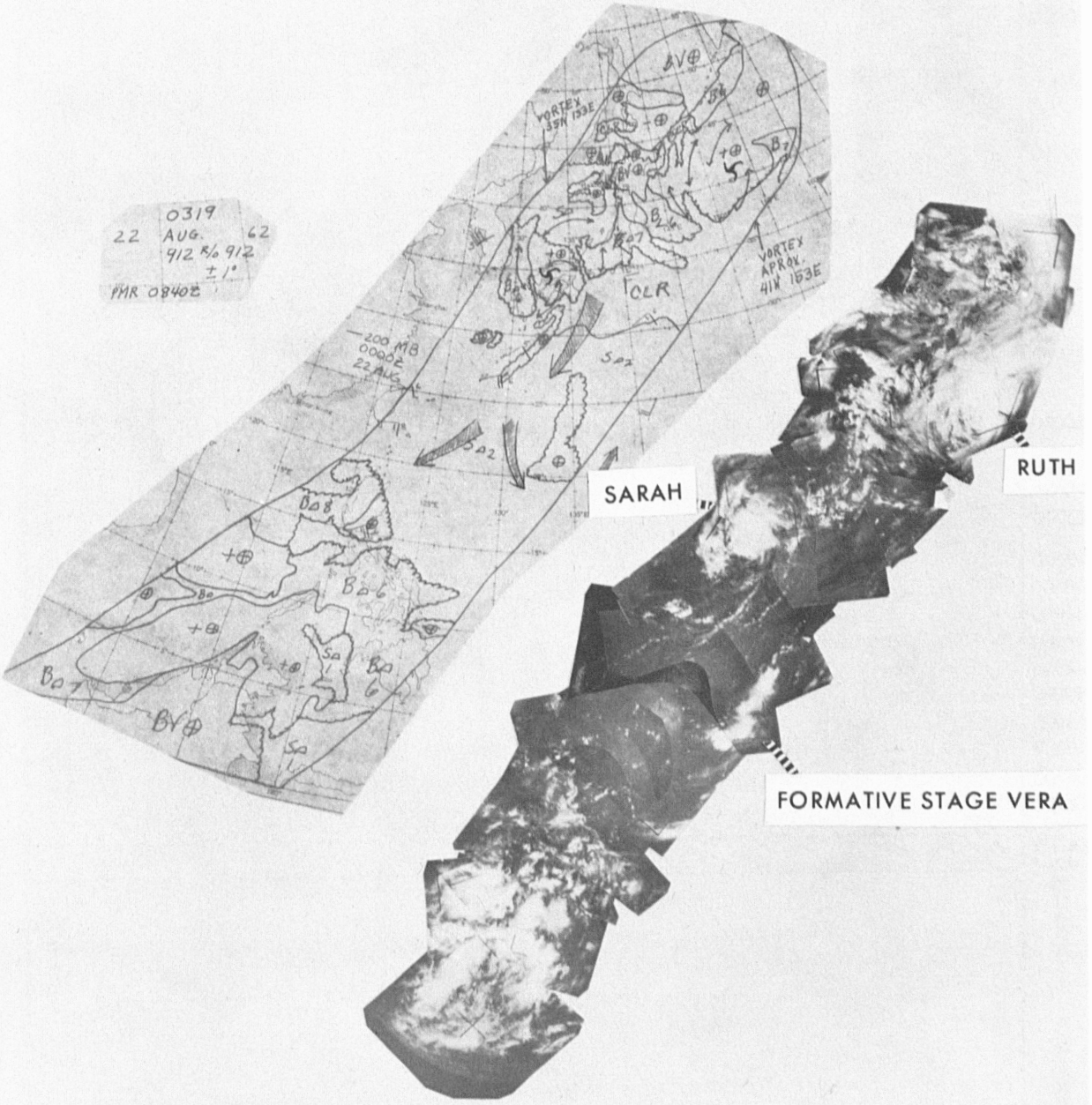
0319
22 AUG. 62
912 R/O 912
± 1°
PMR 08402
VORTEX
35N 153E
VORTEX
APROX.
41N 153E
CLR
200 MB
00002
22 AUG
SARAH
RUTH
FORMATIVE STAGE VERA

FIGURE 47

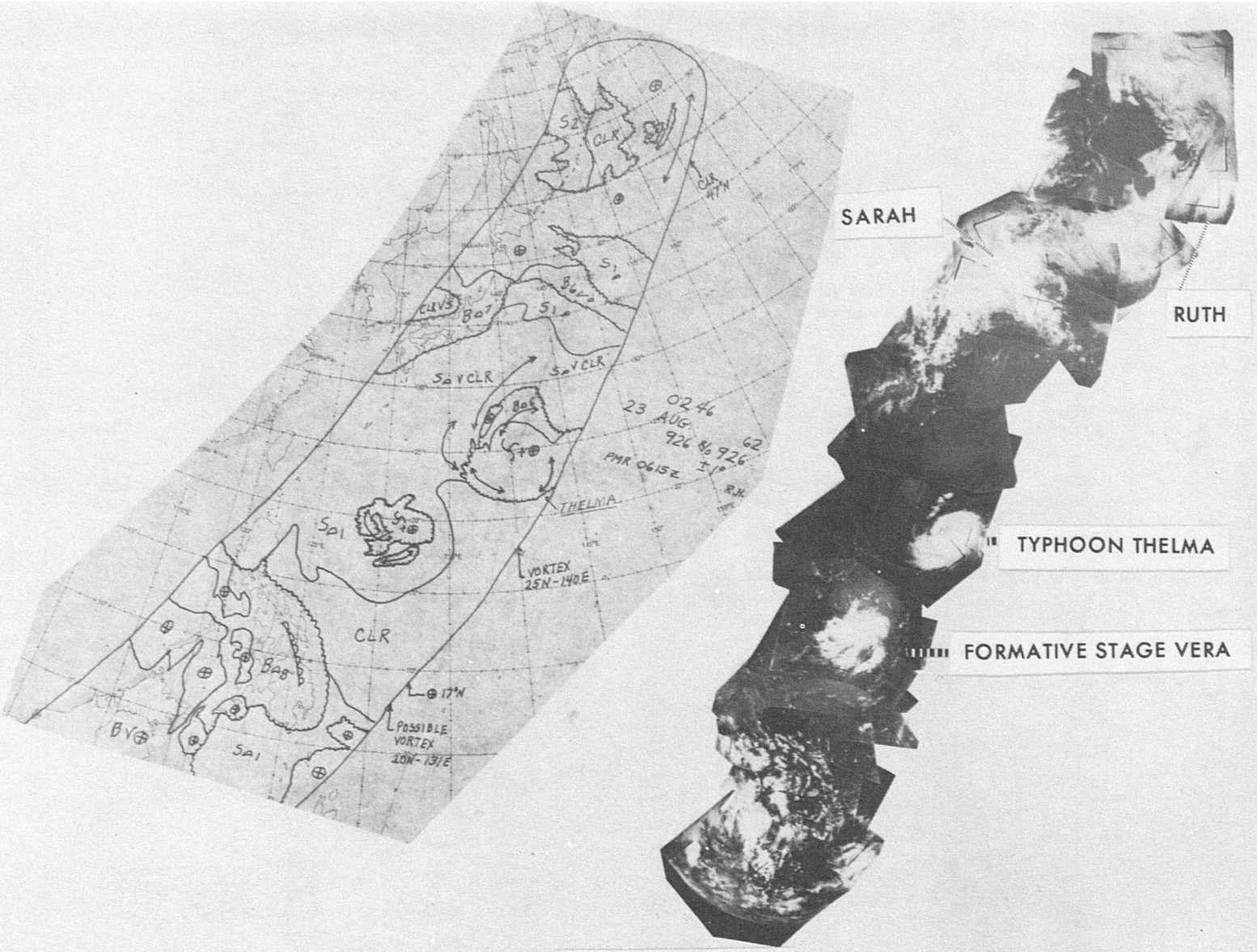
SARAH
RUTH
TYPHOON THELMA
FORMATIVE STAGE VERA
S2
CLR
CLR 17°N
S1
B6
B7
CLVS
S1
S2 V CLR
S2 V CLR
23 AUG
0246
926
926
62
PMR 0615Z
R.N.
THELMA
S2
VORTEX 25N-140E
CLR
B8
17°N
POSSIBLE VORTEX 20N-131E
S2

FIGURE 48

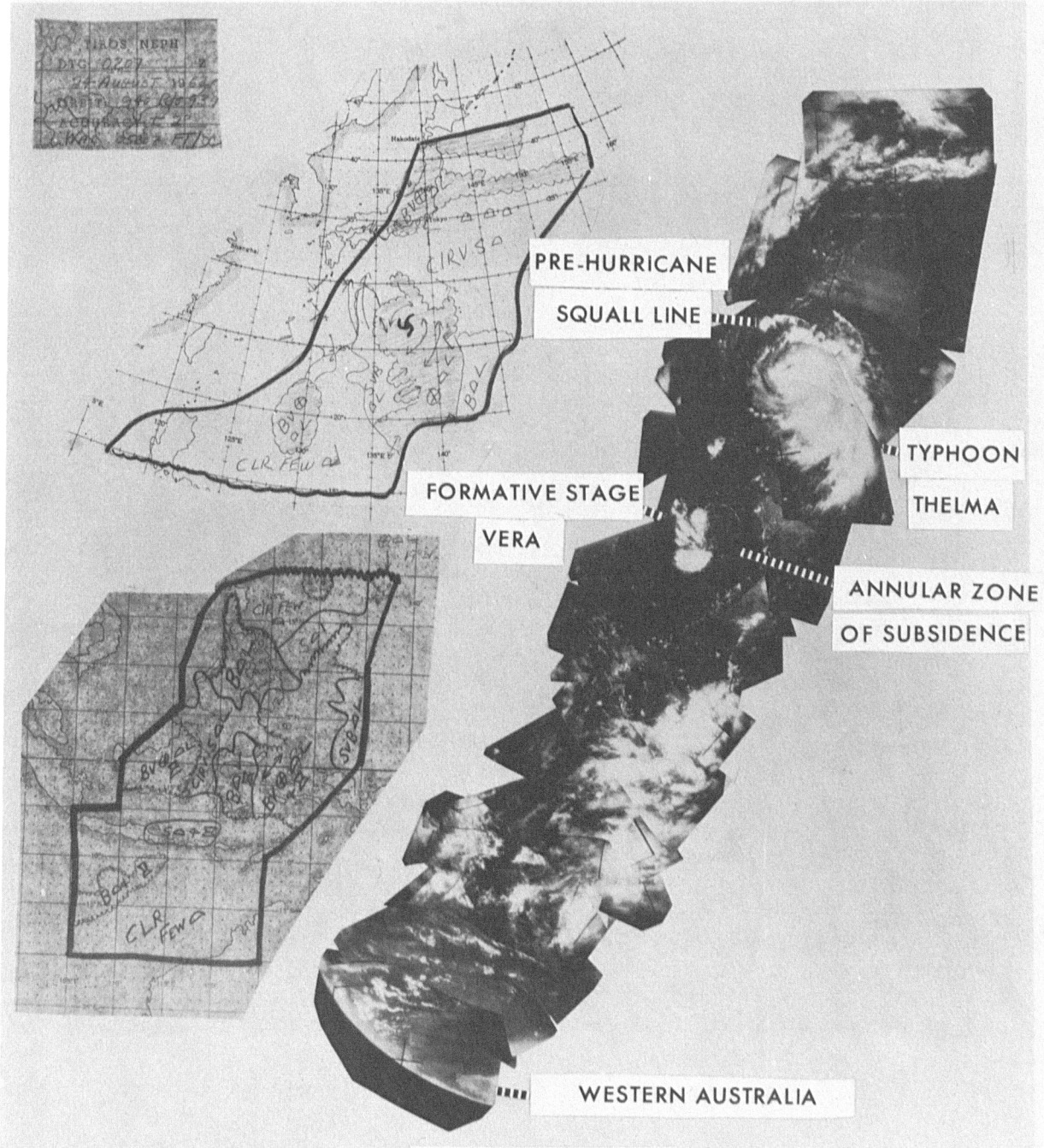
PRE-HURRICANE
SQUALL LINE
TYPHOON
THELMA
FORMATIVE STAGE
VERA
ANNULAR ZONE
OF SUBSIDENCE
WESTERN AUSTRALIA

FIGURE 49

# FORMATIVE STAGE VERA

FIGURE 50

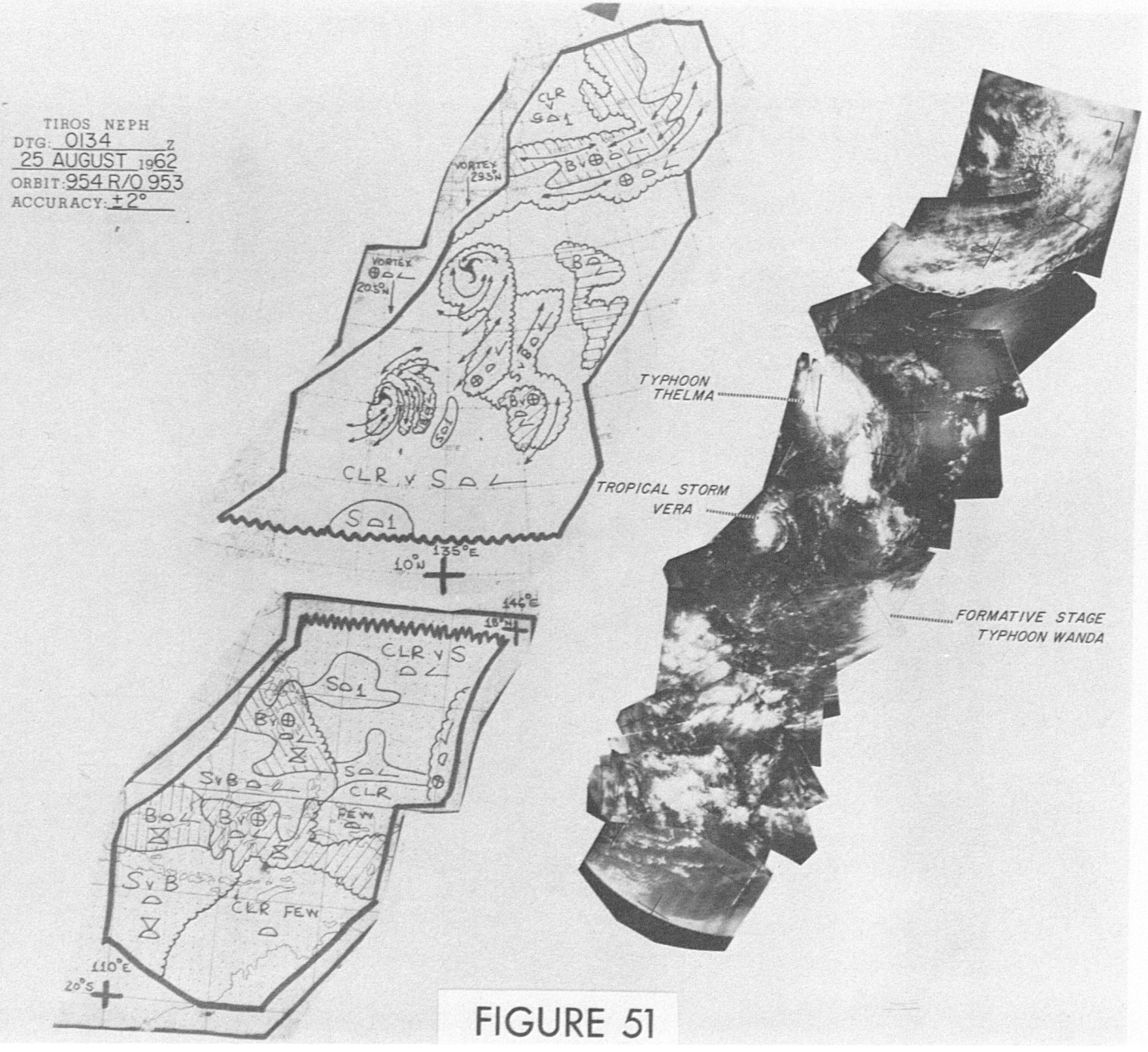
TIROS NEPH
DTG: 0134 Z
25 AUGUST 1962
ORBIT: 954 R/O 953
ACCURACY: ±2°
VORTEX 29.5°N
VORTEX 20.5°N
CLR V SC1
BV⊕
B
CLR V S
SC1
10°N 135°E
TYPHOON THELMA
TROPICAL STORM VERA
FORMATIVE STAGE TYPHOON WANDA
144°E
18°N
CLR V S
SC1
BV⊕
SC
CLR
SVB
BC
BV⊕
FEW
SVB
CLR FEW
110°E
20°S

FIGURE 51

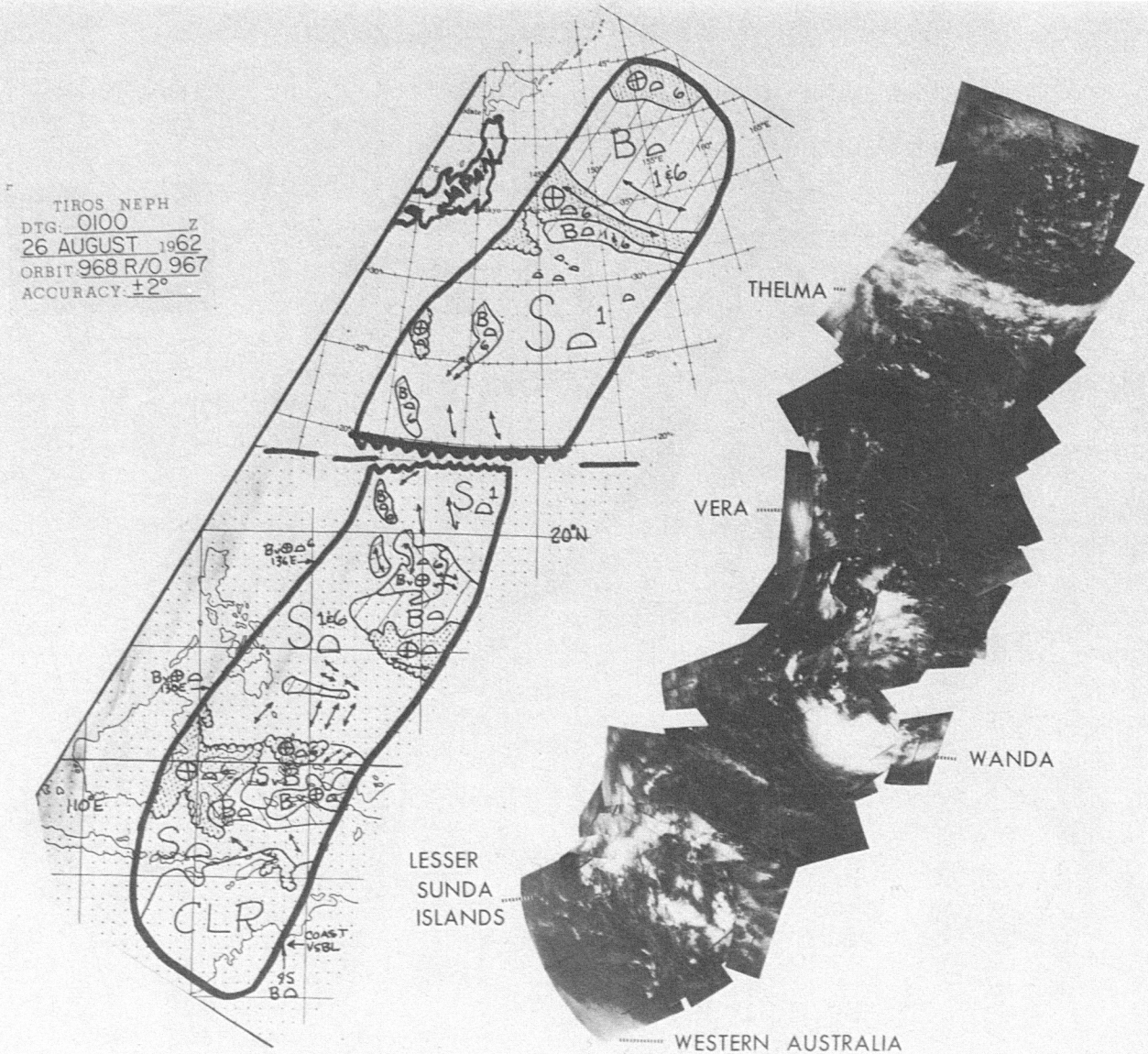
TIROS NEPH
DTG: 0100 Z
26 AUGUST 1962
ORBIT 968 R/O 967
ACCURACY ±2°
THELMA
VERA
WANDA
LESSER SUNDA ISLANDS
WESTERN AUSTRALIA
20°N
CLR
COAST VSBL

FIGURE 52

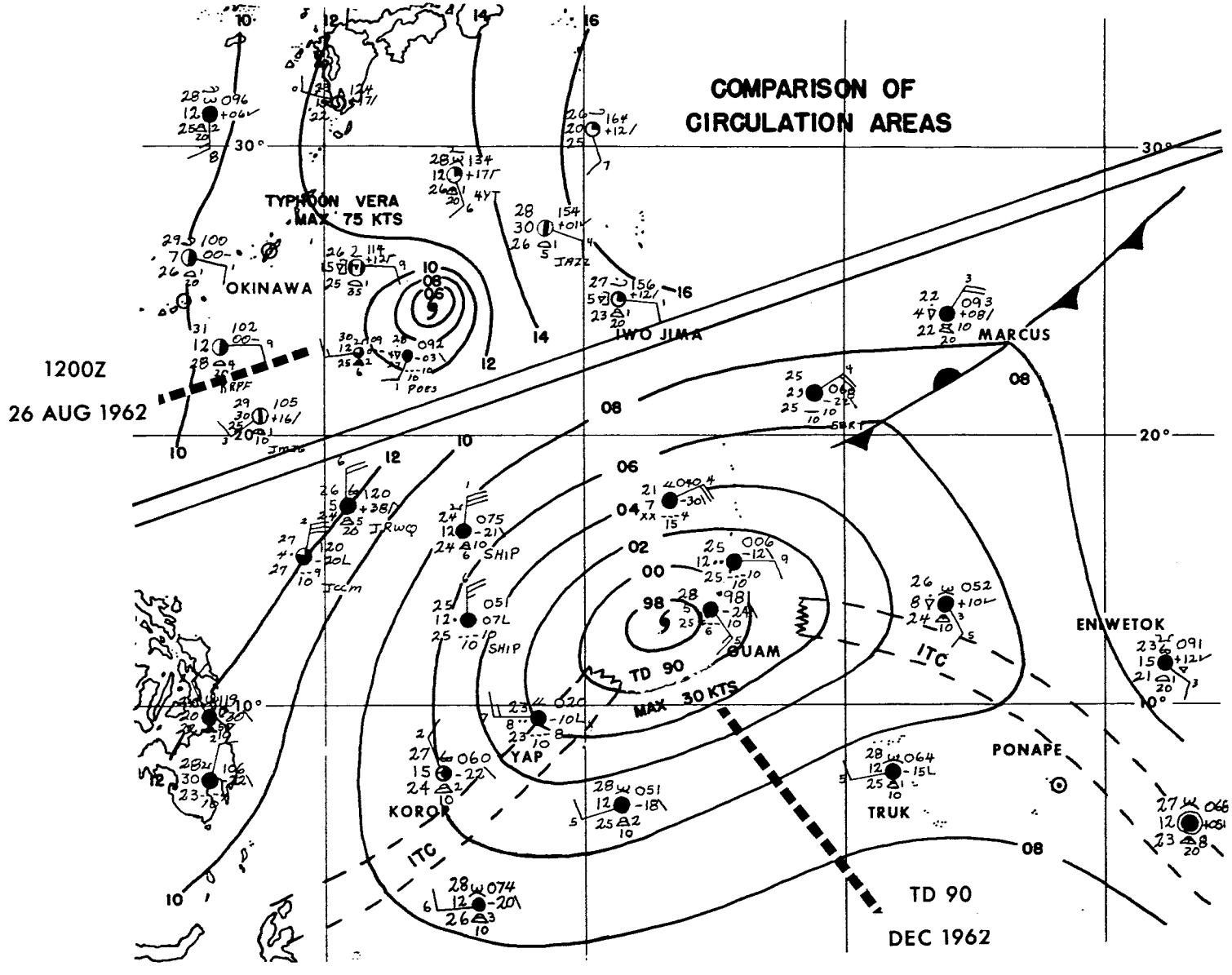
COMPARISON OF
CIRCULATION AREAS
1200Z
26 AUG 1962
TYPHOON VERA
MAX 75 KTS
OKINAWA
IWO JIMA
MARCUS
ENIWETOK
GUAM
TD 90
MAX 30 KTS
YAP
KOROR
TRUK
PONAPE
ITC
ITC
TD 90
DEC 1962

FIGURE 53

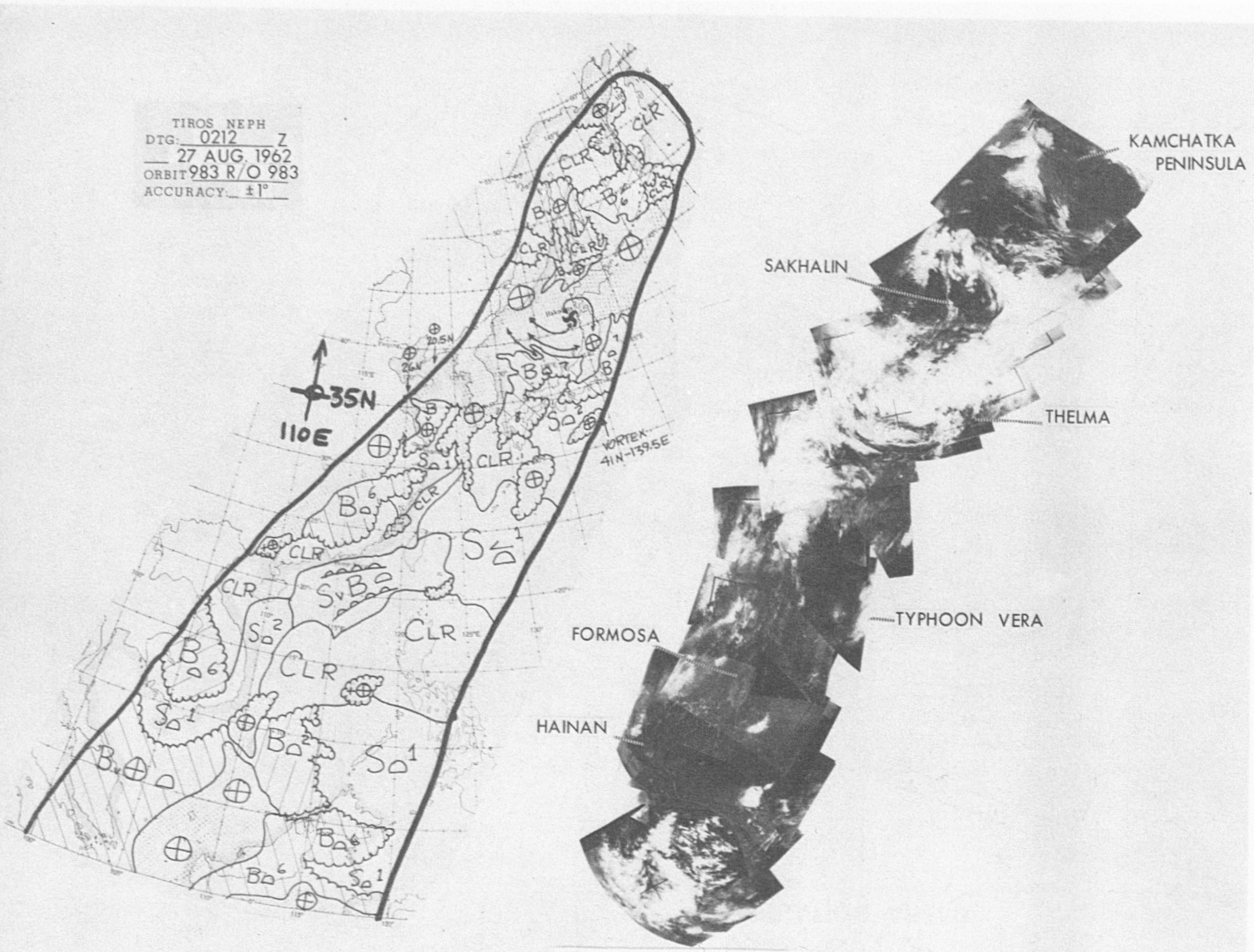
TIROS NEPH
DTG: 0212 Z
27 AUG 1962
ORBIT 983 R/O 983
ACCURACY: ±1°
35N
110E
KAMCHATKA PENINSULA
SAKHALIN
THELMA
TYPHOON VERA
FORMOSA
HAINAN
CLR

FIGURE 54

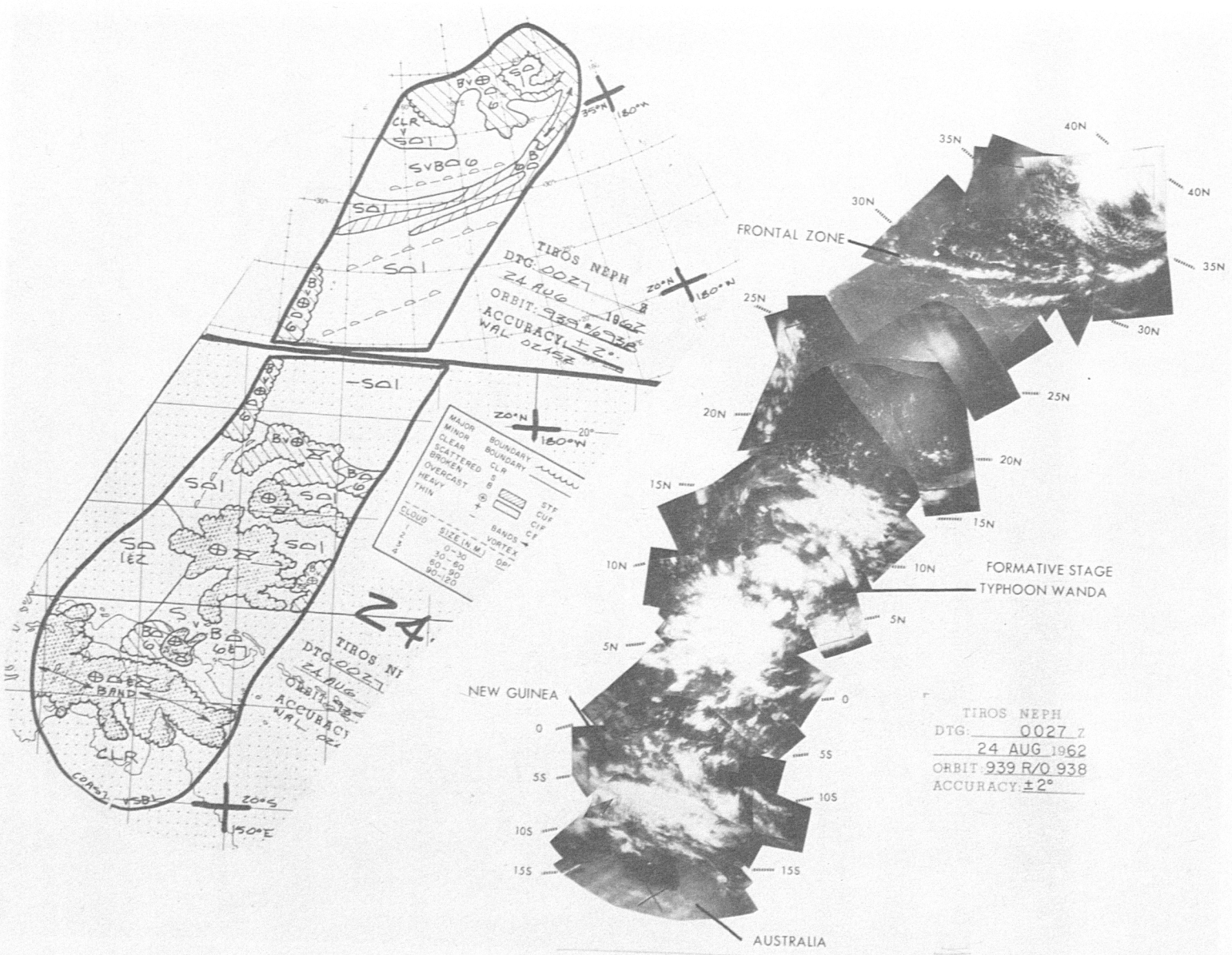
TIROS NEPH
DTG: 0027
24 AUG
ORBIT: 939 R/O 938
ACCURACY: ± 2°
FRONTAL ZONE
FORMATIVE STAGE
TYPHOON WANDA
NEW GUINEA
AUSTRALIA
40N
35N
30N
25N
20N
15N
10N
5N
0
5S
10S
15S

FIGURE 55

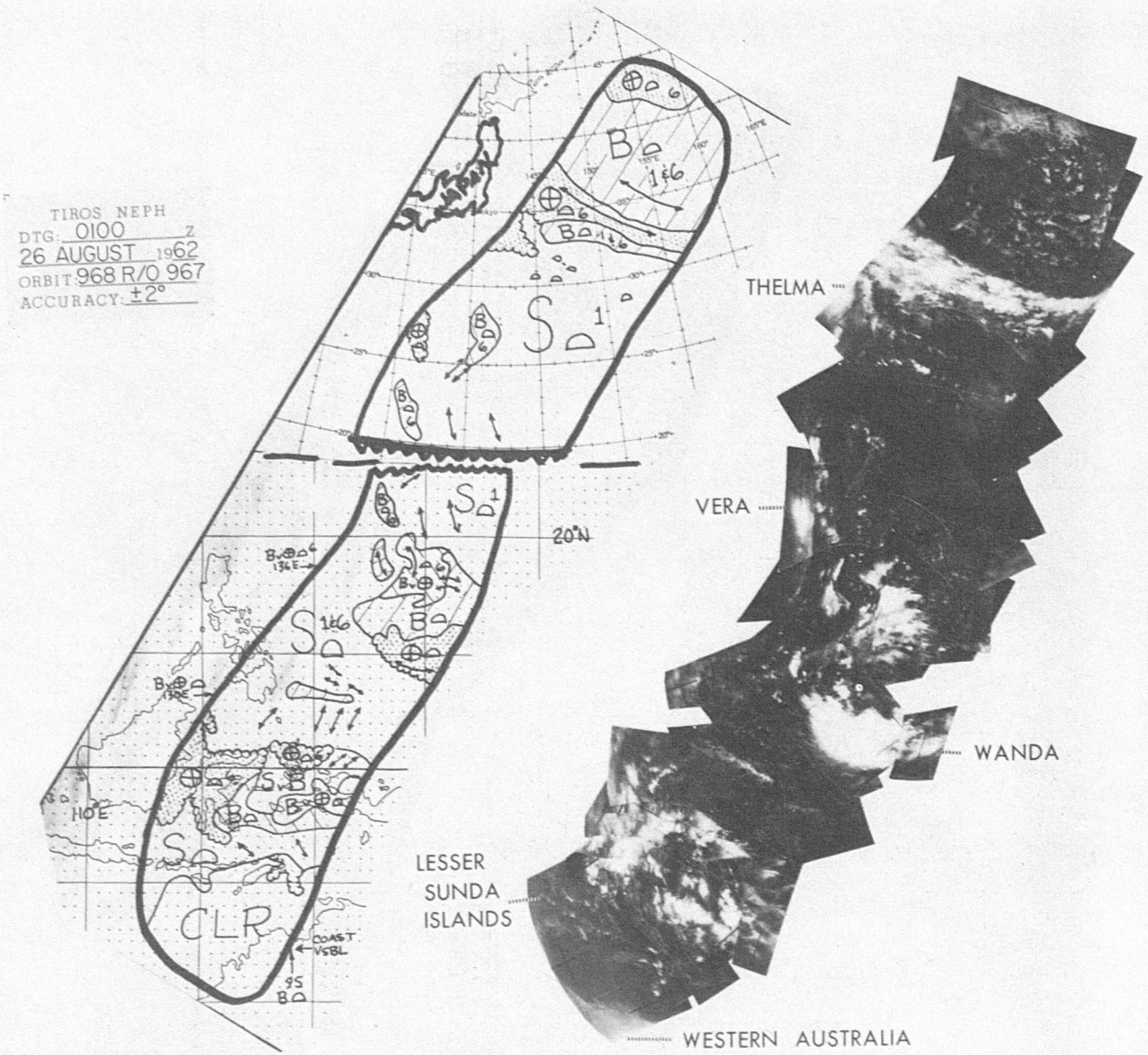
TIROS NEPH
DTG: 0100 Z
26 AUGUST 1962
ORBIT 968 R/O 967
ACCURACY: ±2°
THELMA
VERA
WANDA
LESSER SUNDA ISLANDS
WESTERN AUSTRALIA
20°N
CLR
COAST VSBL

FIGURE 56

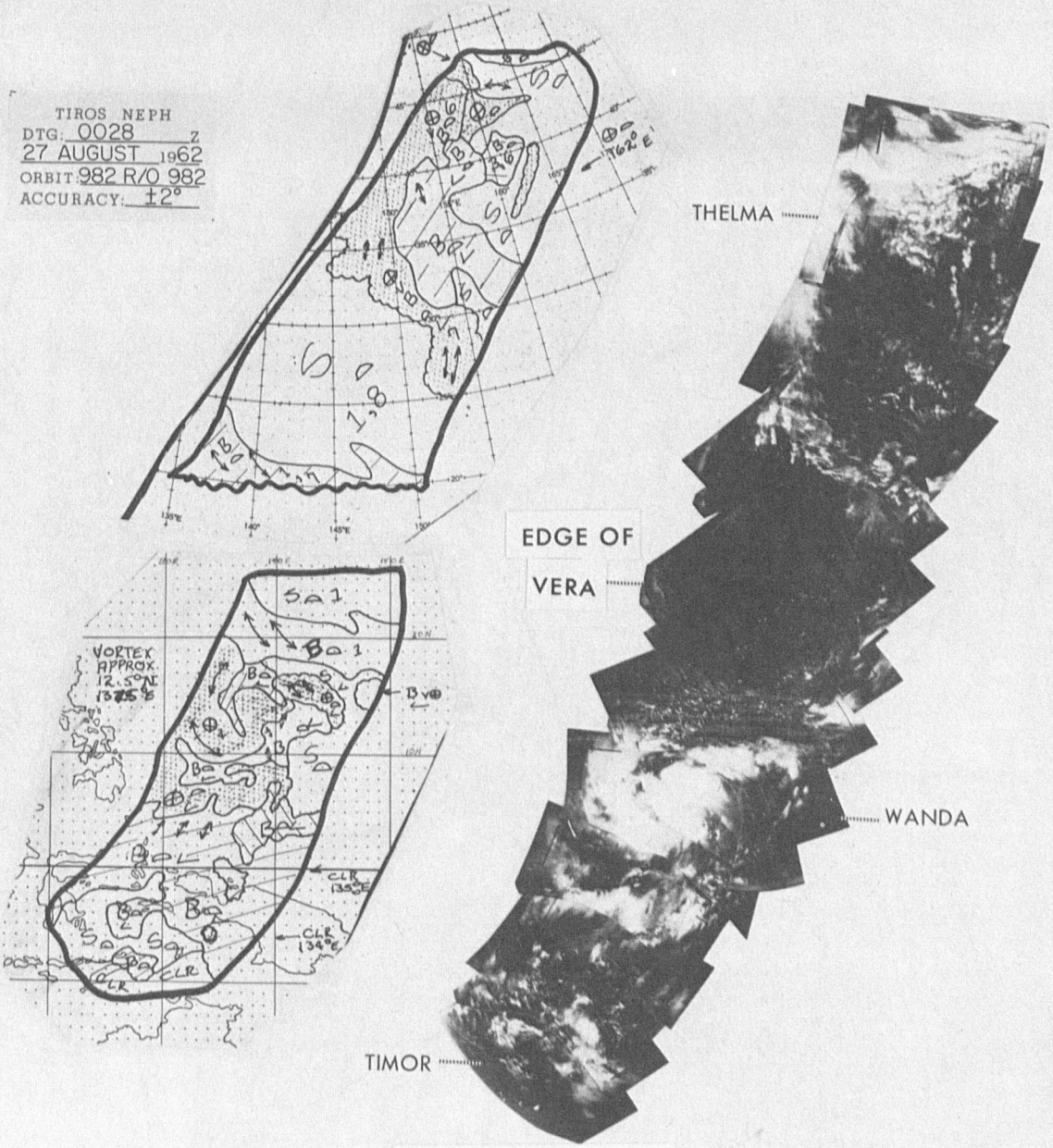
TIROS NEPH
DTG: 0028 Z
27 AUGUST 1962
ORBIT: 982 R/O 982
ACCURACY: ±2°
THELMA
EDGE OF
VERA
WANDA
TIMOR
VORTEX
APPROX.
12.5°N
135°E
CLR
135°E
CLR
134°E
CLR
CLR

FIGURE 57

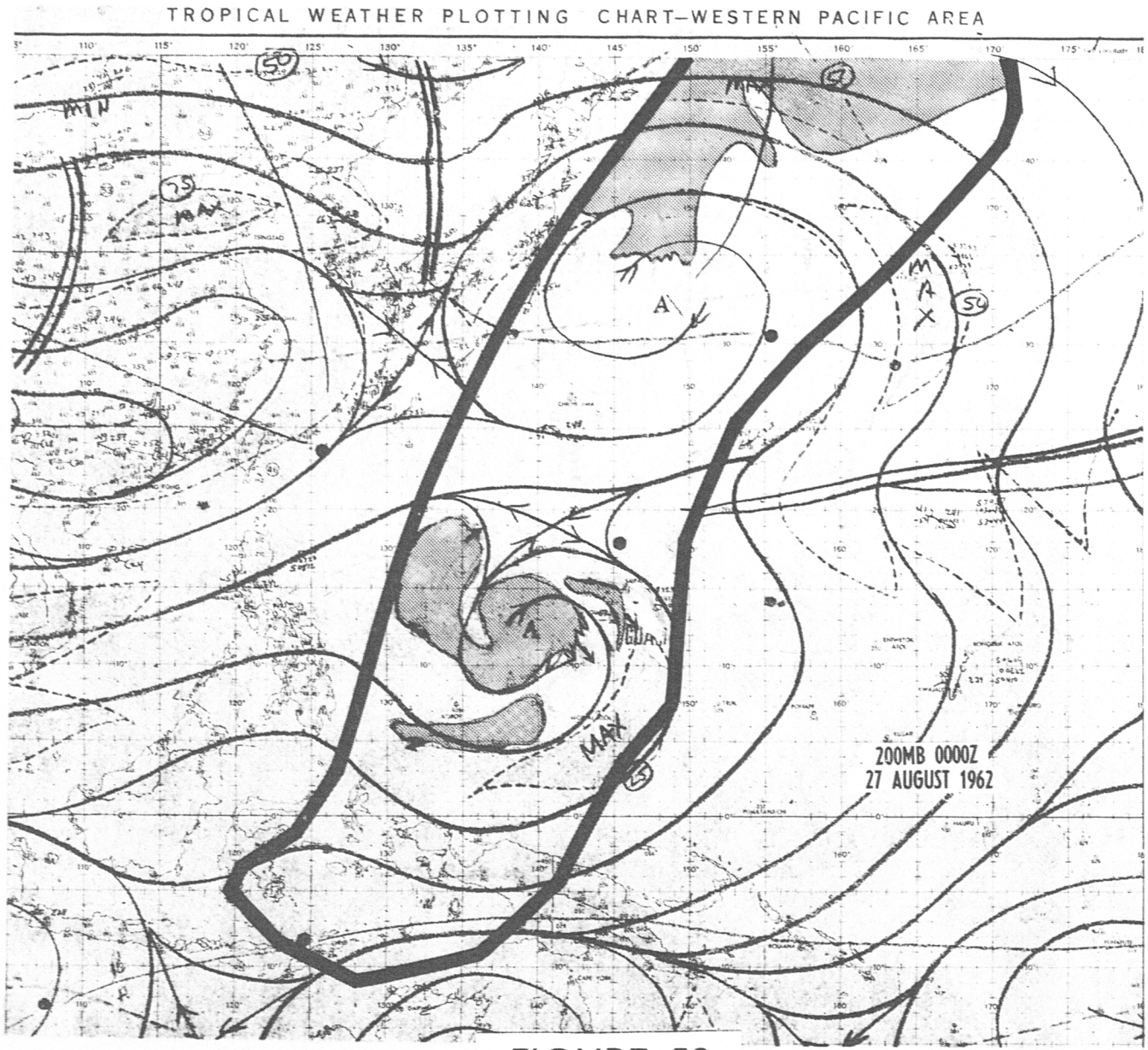
TROPICAL WEATHER PLOTTING CHART—WESTERN PACIFIC AREA
MIN
MAX
MAX
200MB 0000Z
27 AUGUST 1962

FIGURE 58

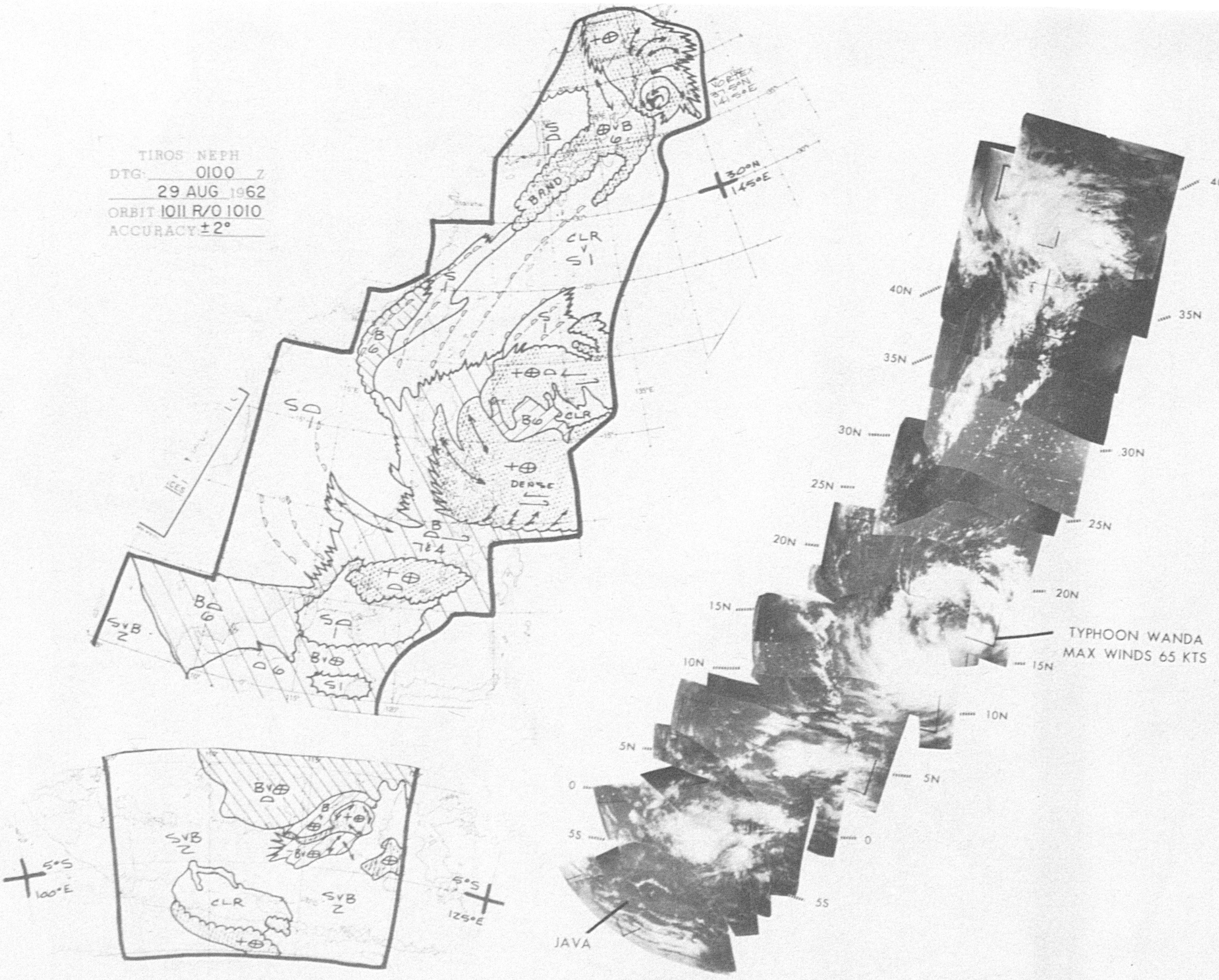
TIROS NEPH
DTG: 0100 Z
29 AUG 1962
ORBIT 1011 R/O 1010
ACCURACY: ±2°
30°N 145°E
5°S 100°E
5°S 125°E
BAND
CLR
DENSE
TYPHOON WANDA
MAX WINDS 65 KTS
JAVA
40N
35N
30N
25N
20N
15N
10N
5N
0
5S

FIGURE 59

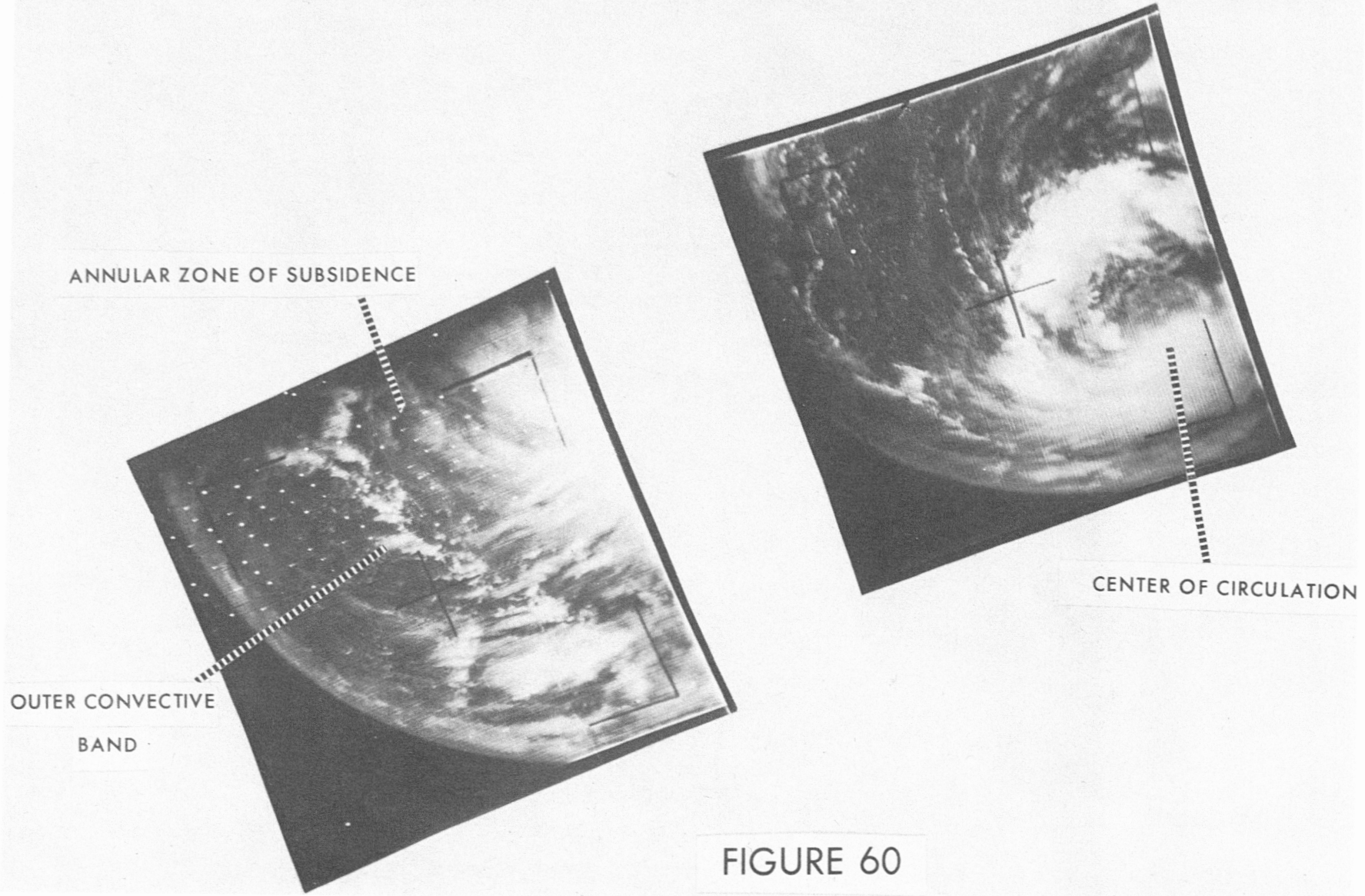
ANNULAR ZONE OF SUBSIDENCE
OUTER CONVECTIVE
BAND
CENTER OF CIRCULATION

FIGURE 60

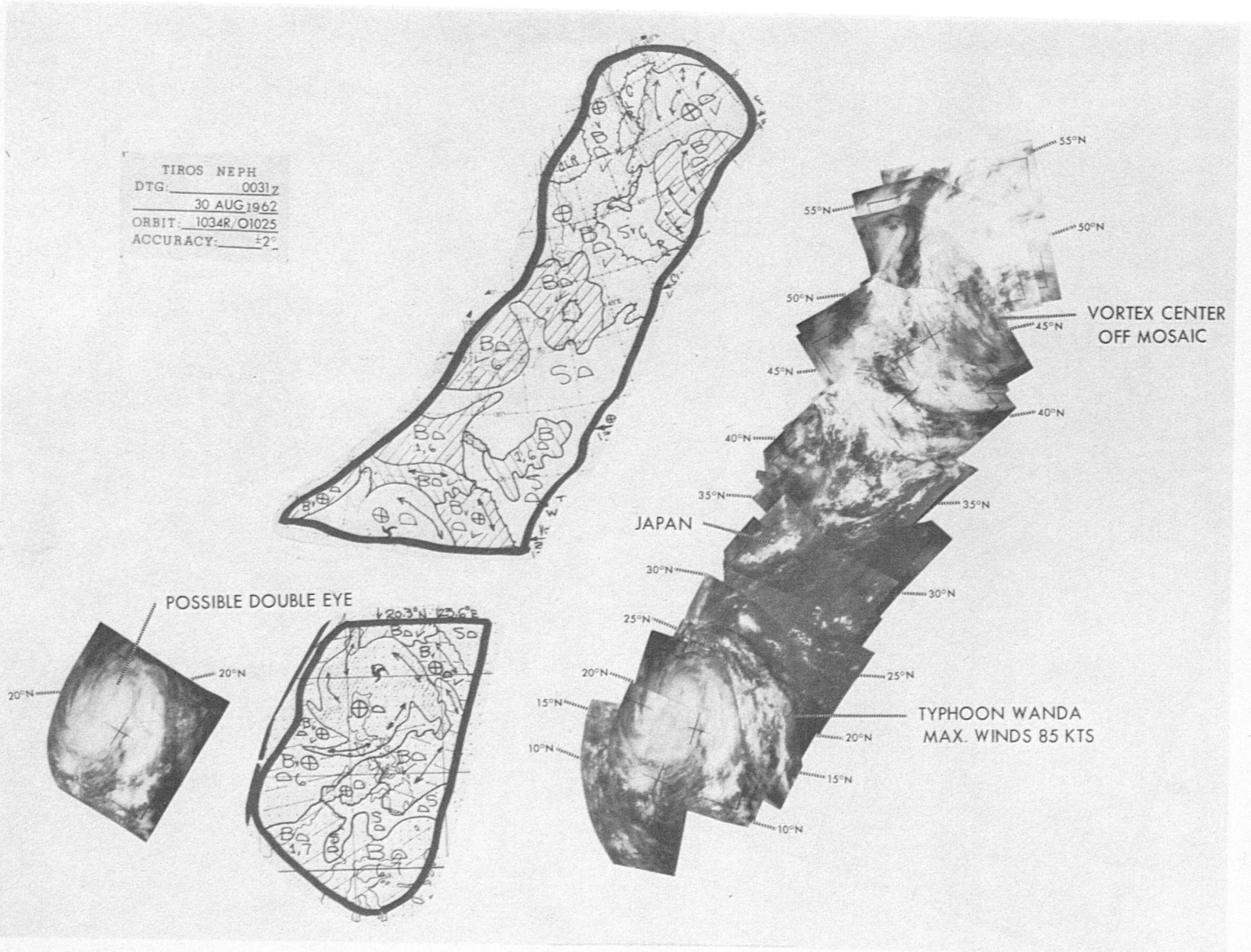
TIROS NEPH
DTG: 0031Z
30 AUG 1962
ORBIT: 1034R/01025
ACCURACY: ±2°
55°N
50°N
45°N
40°N
35°N
30°N
25°N
20°N
15°N
10°N
VORTEX CENTER
OFF MOSAIC
JAPAN
TYPHOON WANDA
MAX. WINDS 85 KTS
POSSIBLE DOUBLE EYE

FIGURE 61

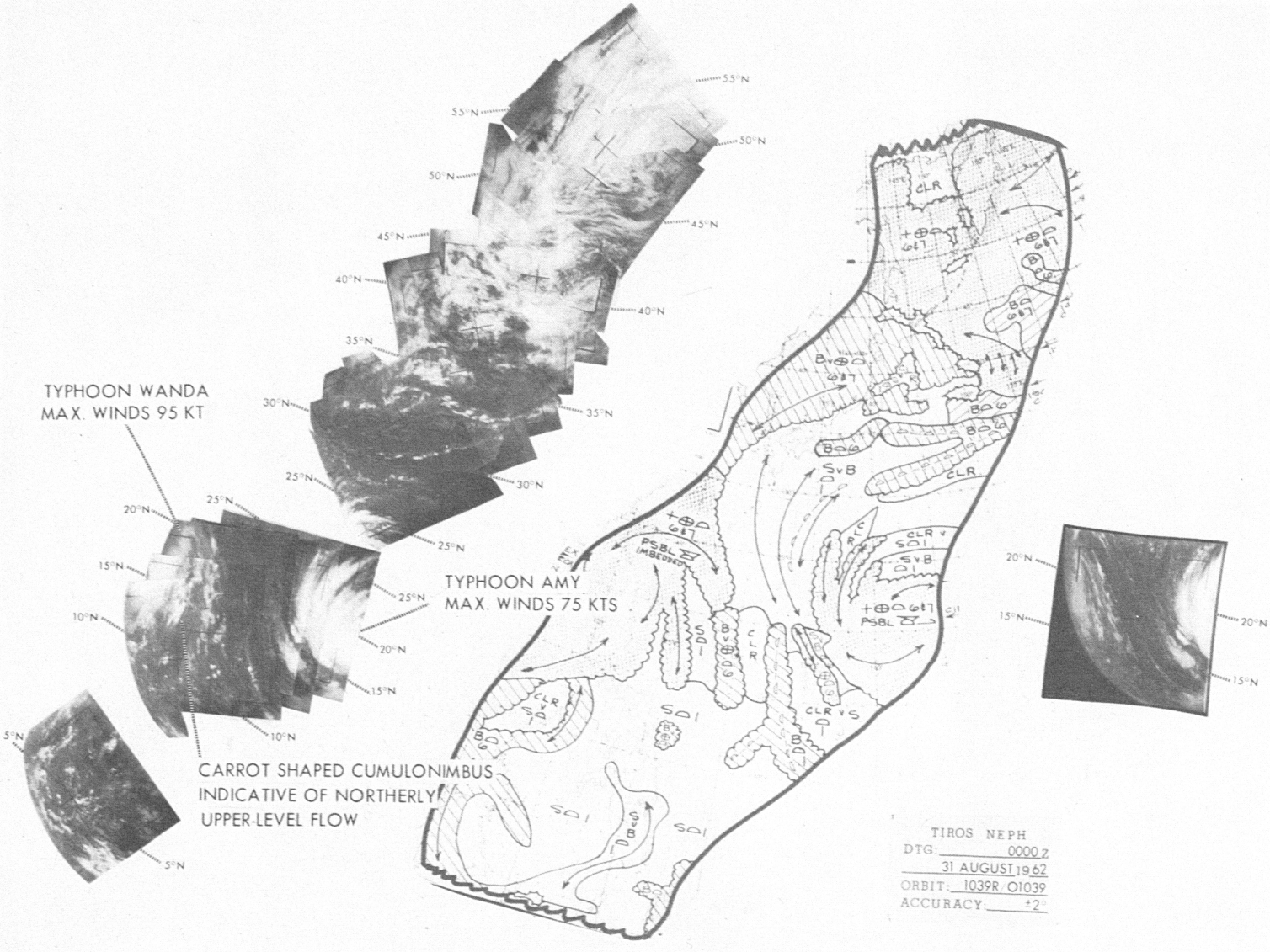
TYPHOON WANDA
MAX. WINDS 95 KT
TYPHOON AMY
MAX. WINDS 75 KTS
CARROT SHAPED CUMULONIMBUS
INDICATIVE OF NORTHERLY
UPPER-LEVEL FLOW
TIROS NEPH
DTG: 0000Z
31 AUGUST 1962
ORBIT: 1039R 01039
ACCURACY: ±2°

FIGURE 62

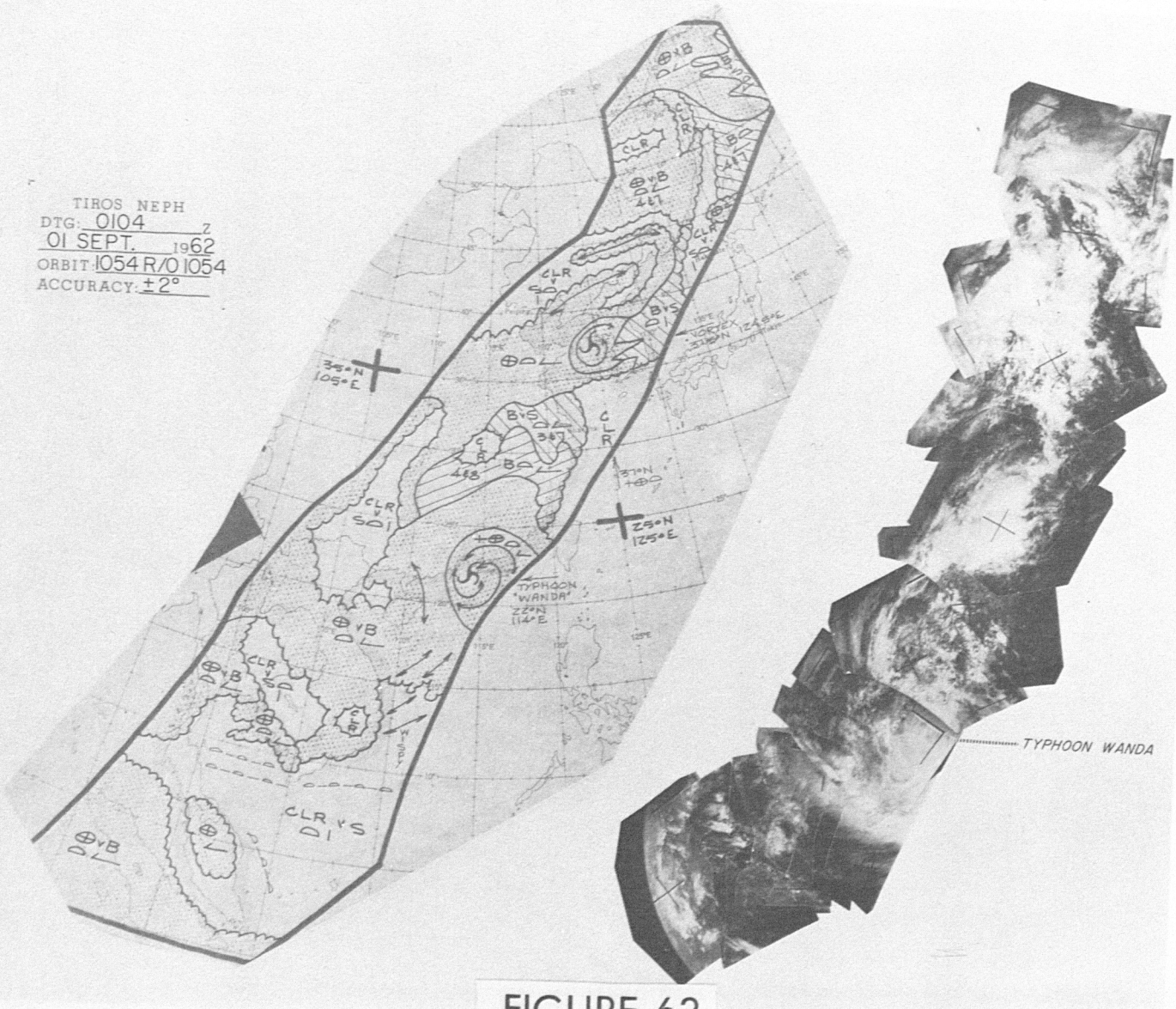
TIROS NEPH
DTG: 0104 Z
01 SEPT. 1962
ORBIT 1054 R/O 1054
ACCURACY: ± 2°
TYPHOON WANDA

FIGURE 63

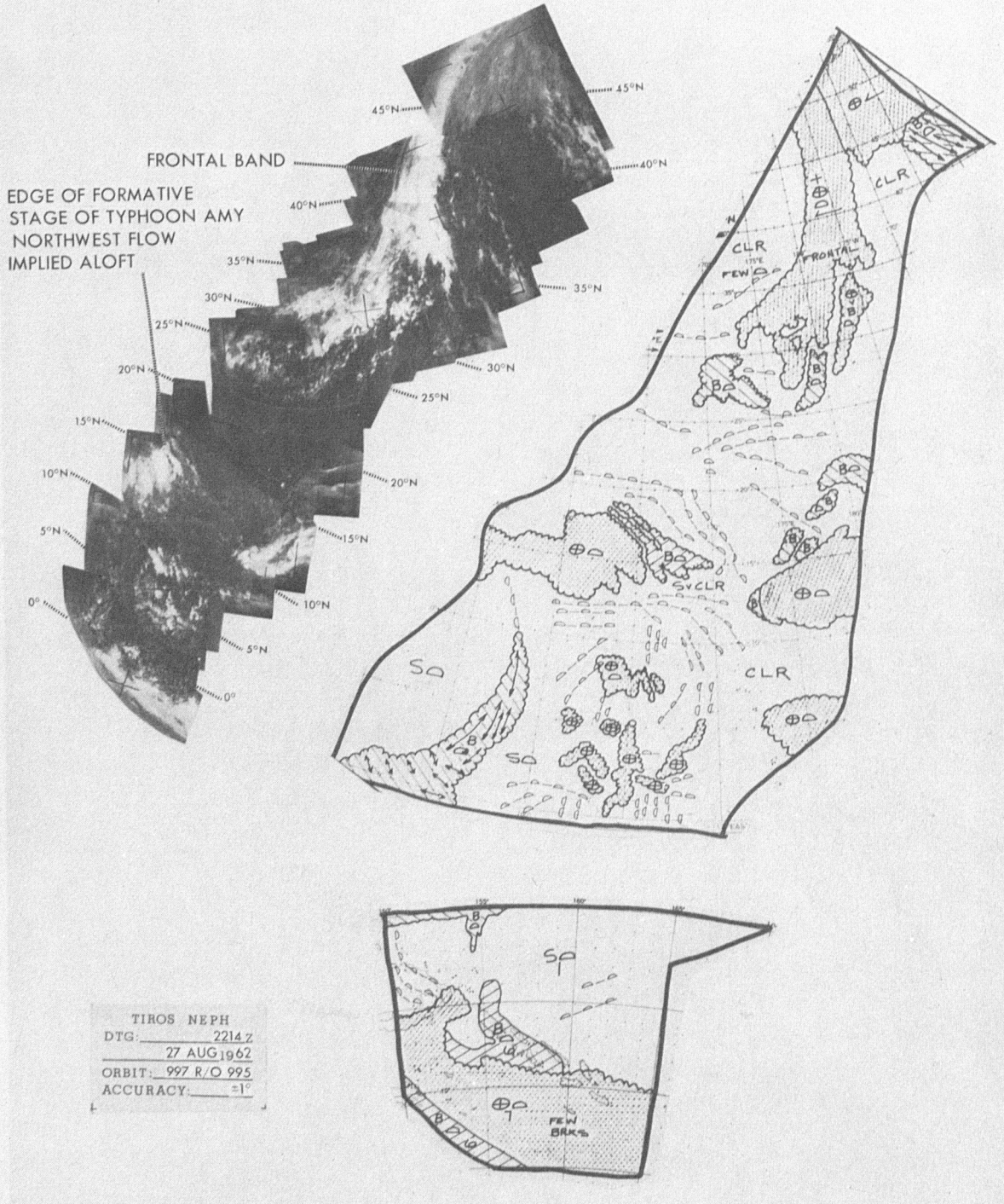


TIROS NEPH
DTG: 2214Z
27 AUG 1962
ORBIT: 997 R/O 995
ACCURACY: ±1°

FIGURE 64

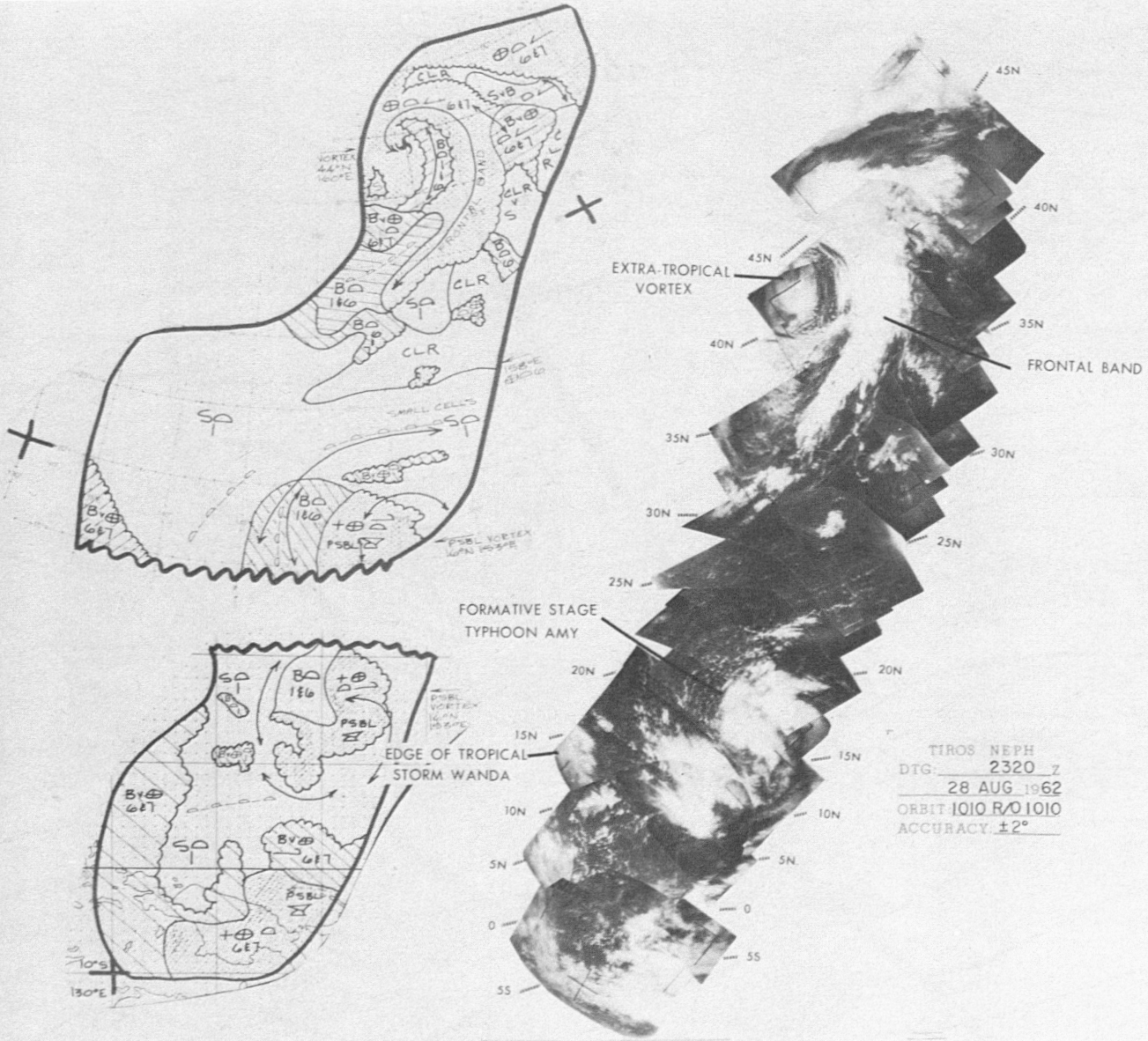
45N
40N
45N
EXTRA-TROPICAL VORTEX
40N
35N
FRONTAL BAND
35N
30N
30N
25N
25N
FORMATIVE STAGE TYPHOON AMY
20N
20N
15N
EDGE OF TROPICAL STORM WANDA
15N
10N
10N
5N
5N
0
0
5S
5S
TIROS NEPH
DTG: 2320 Z
28 AUG 1962
ORBIT 1010 R/O 1010
ACCURACY ±2°

FIGURE 65

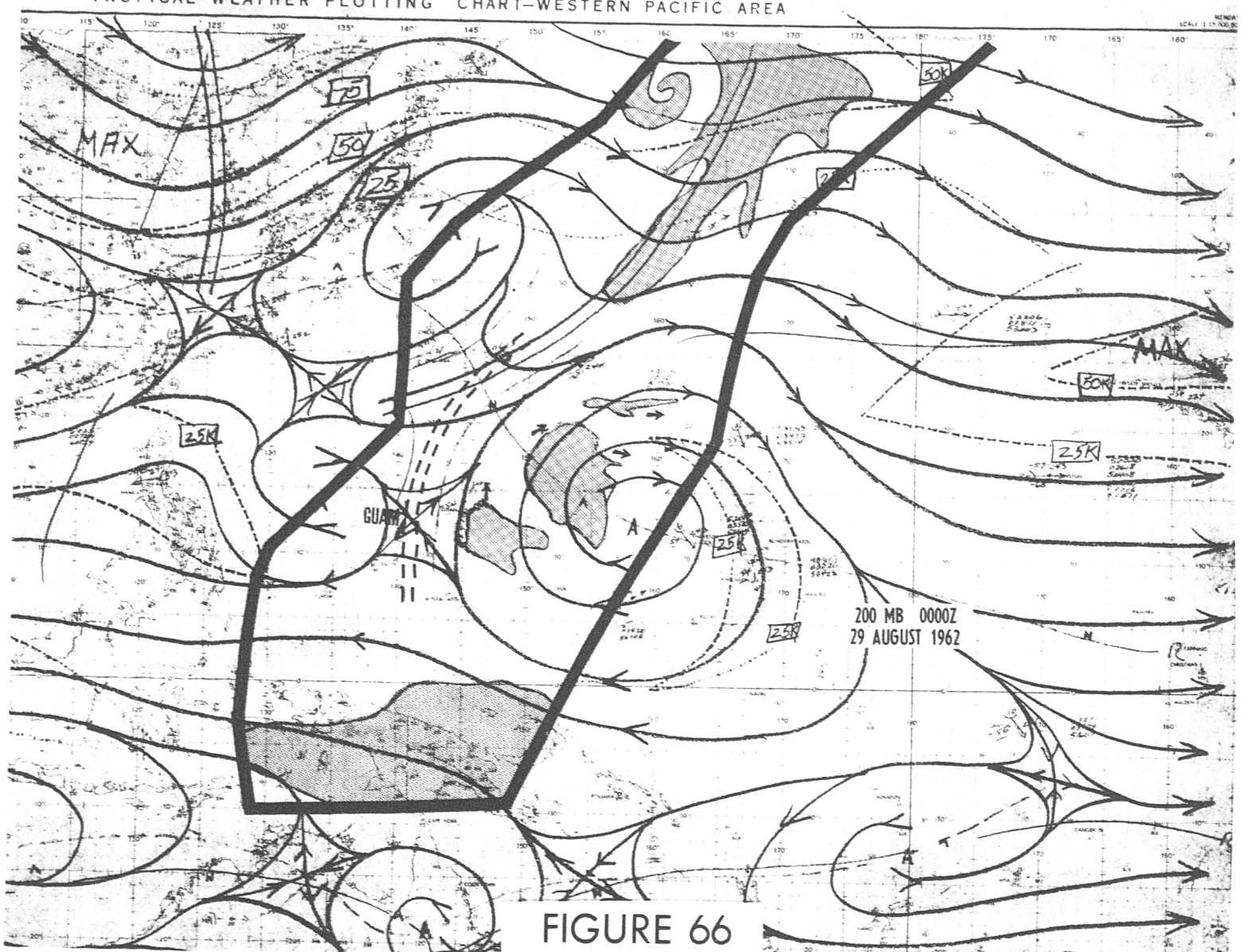
TROPICAL WEATHER PLOTTING CHART—WESTERN PACIFIC AREA
MAX
75
50
25
50K
MAX
50K
25K
25K
25K
25K
GUAM
200 MB 0000Z
29 AUGUST 1962

FIGURE 66

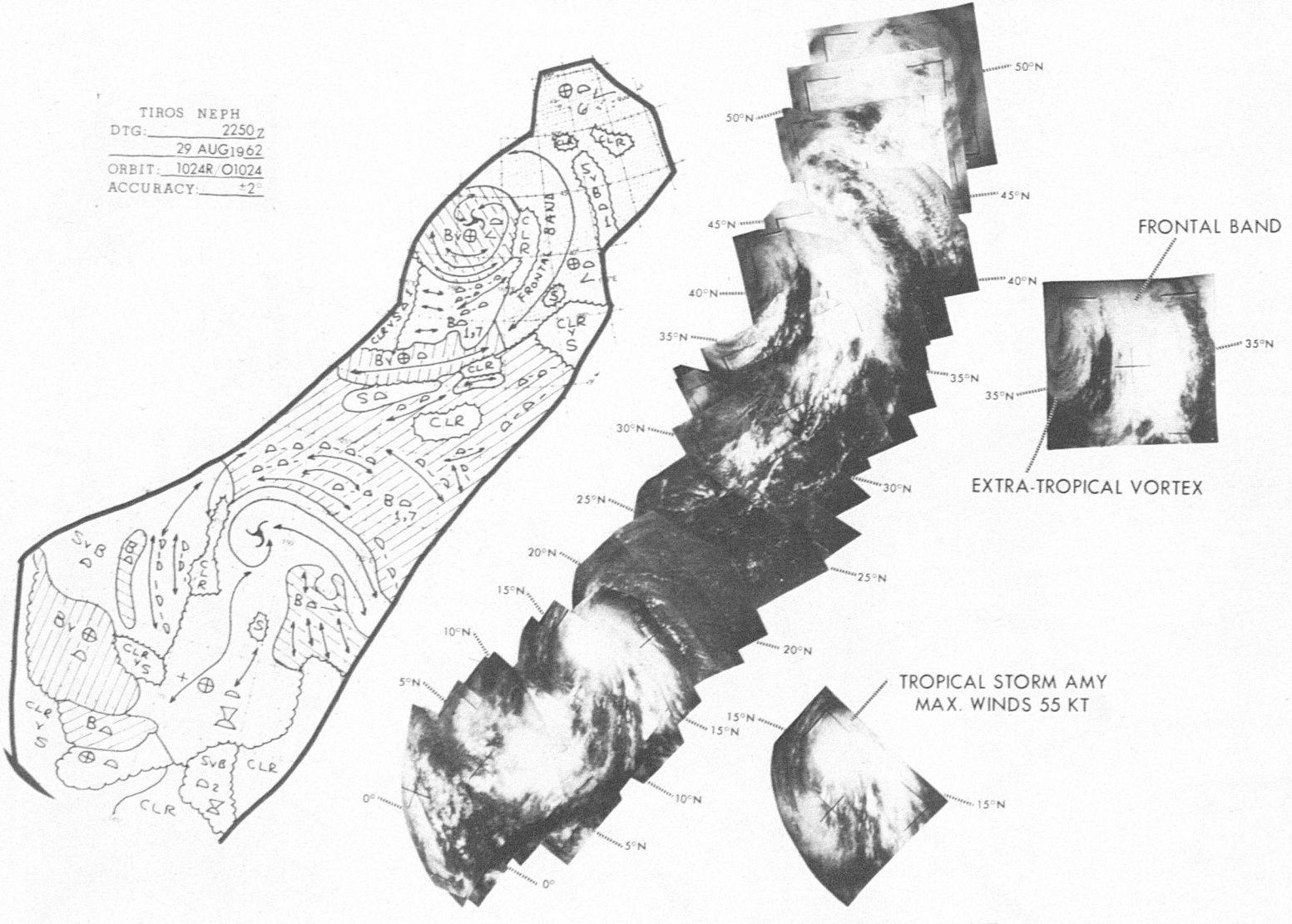
TIROS NEPH
DTG: 2250Z
29 AUG 1962
ORBIT: 1024R/01024
ACCURACY: ±2°
FRONTAL BAND
EXTRA-TROPICAL VORTEX
TROPICAL STORM AMY
MAX. WINDS 55 KT
50°N
45°N
40°N
35°N
30°N
25°N
20°N
15°N
10°N
5°N
0°

FIGURE 67

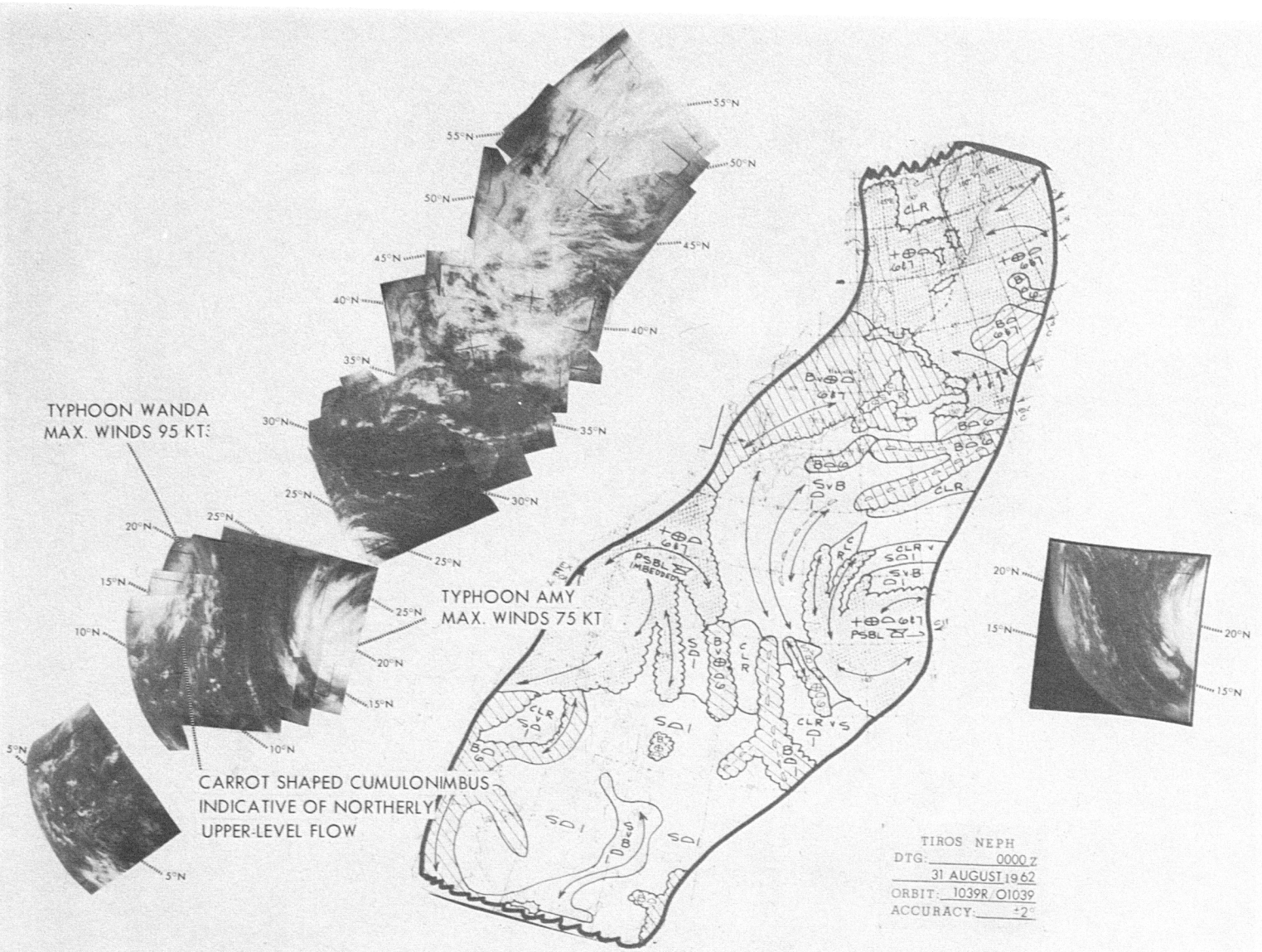
TYPHOON WANDA
MAX. WINDS 95 KTS
TYPHOON AMY
MAX. WINDS 75 KT
CARROT SHAPED CUMULONIMBUS
INDICATIVE OF NORTHERLY
UPPER-LEVEL FLOW
TIROS NEPH
DTG: 0000Z
31 AUGUST 1962
ORBIT: 1039R/O1039
ACCURACY: ±2°

FIGURE 68

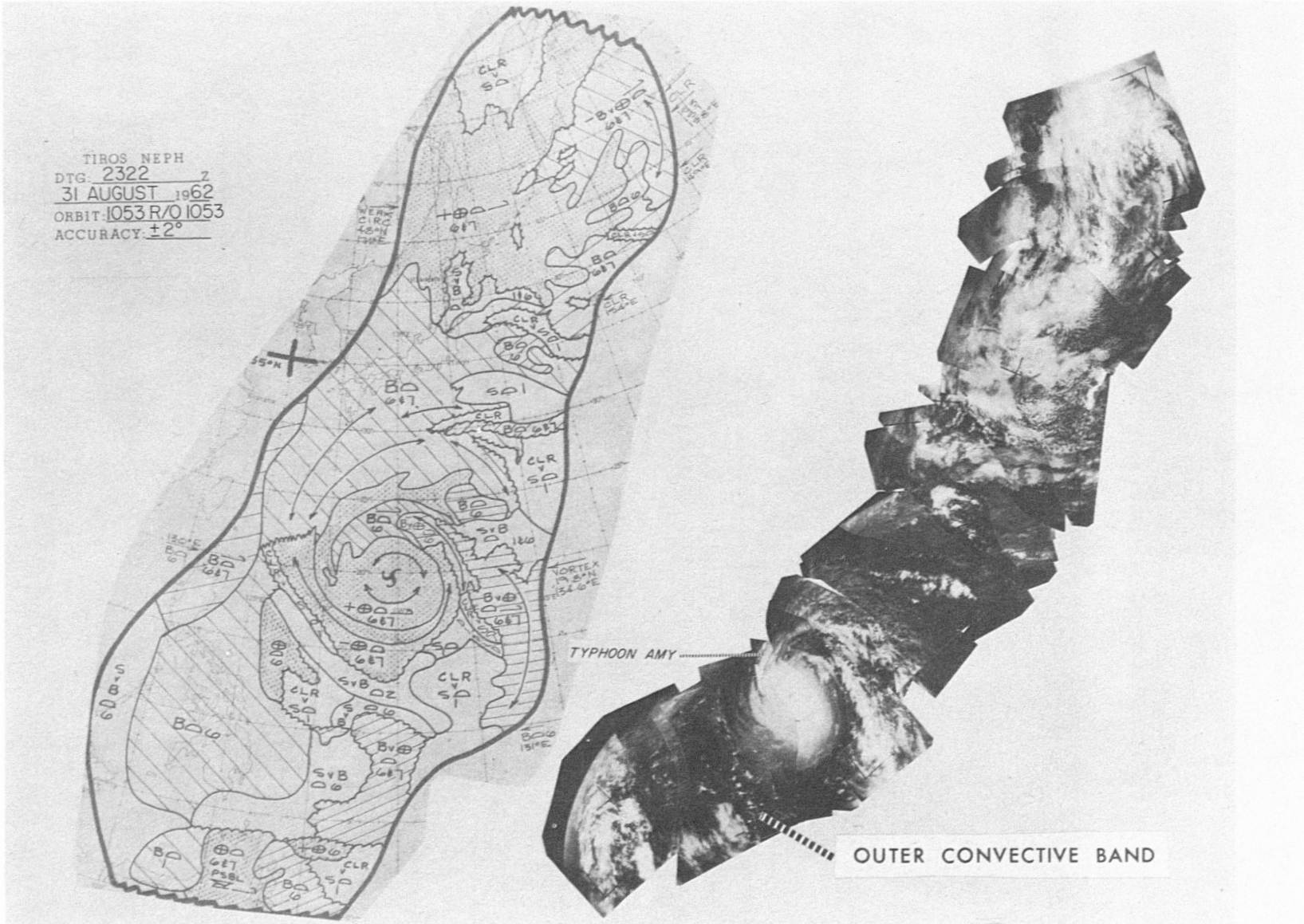
TIROS NEPH
DTG: 2322 Z
31 AUGUST 1962
ORBIT: 1053 R/O 1053
ACCURACY: ±2°
TYPHOON AMY
OUTER CONVECTIVE BAND

FIGURE 69

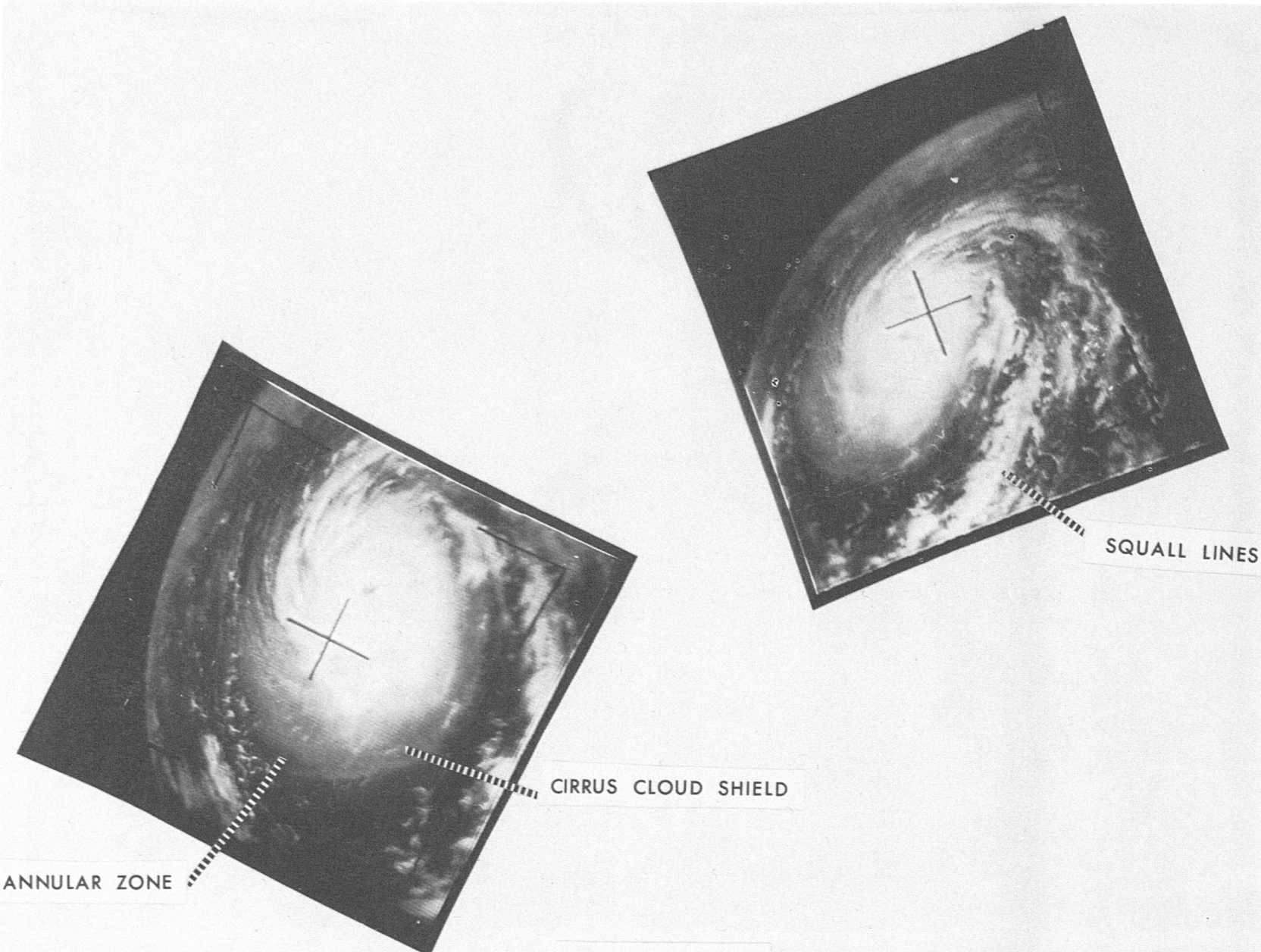


FIGURE 70

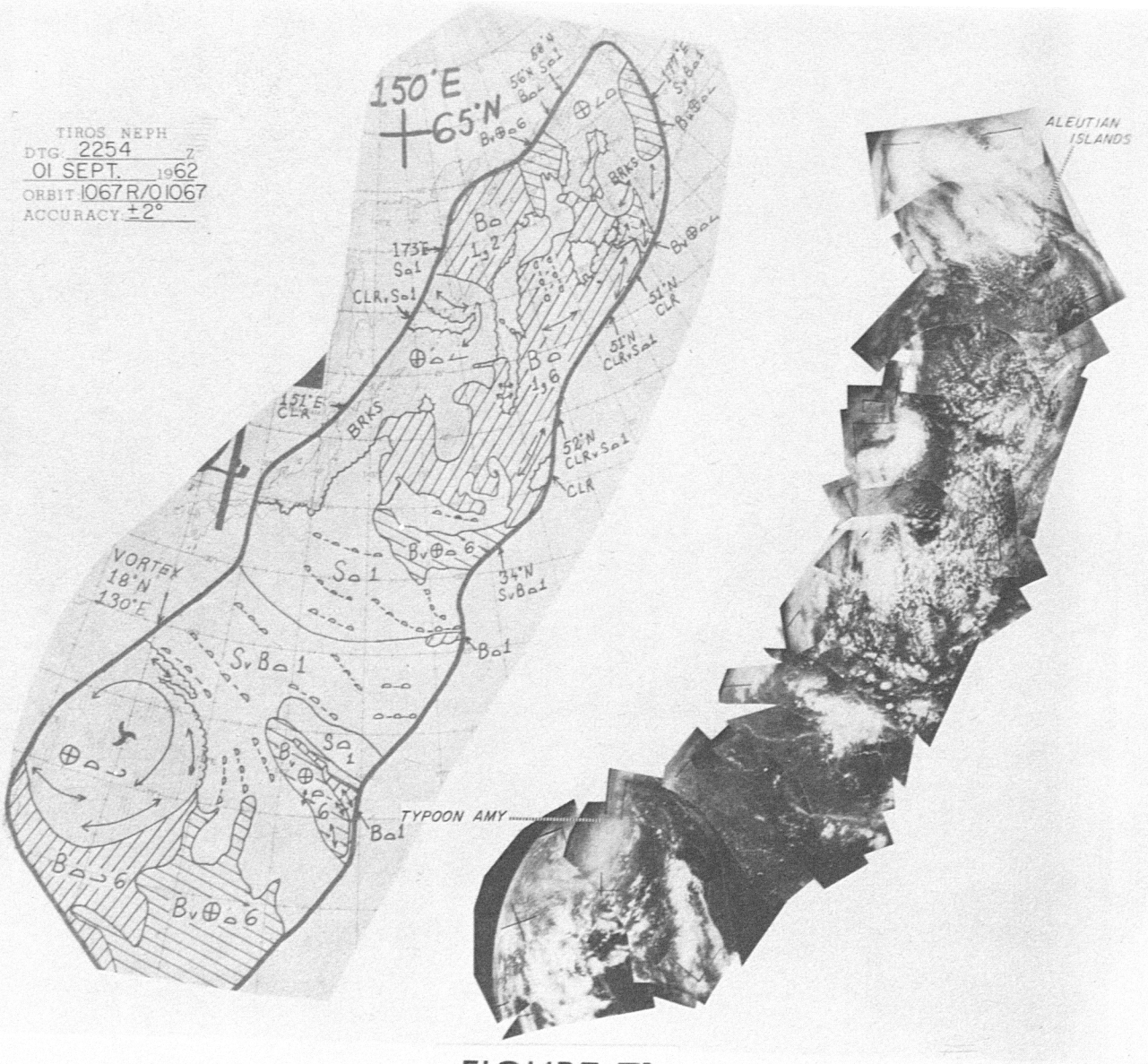
TIROS NEPH
DTG: 2254 Z
01 SEPT. 1962
ORBIT 1067 R/O 1067
ACCURACY ±2°
150°E
65°N
ALEUTIAN ISLANDS
TYPOON AMY
VORTEX
18°N
130°E
173°E
Sa1
CLR, Sa1
151°E
CLR
BRKS
Ba
1,2
Ba
1,6
51°N
CLR
51°N
CLR, Sa1
52°N
CLR, Sa1
CLR
34°N
SvBa1
Sa1
SvBa1
Ba1
Sa1
Ba1
Bv⊕a6
Ba6
Bv⊕a6

FIGURE 71

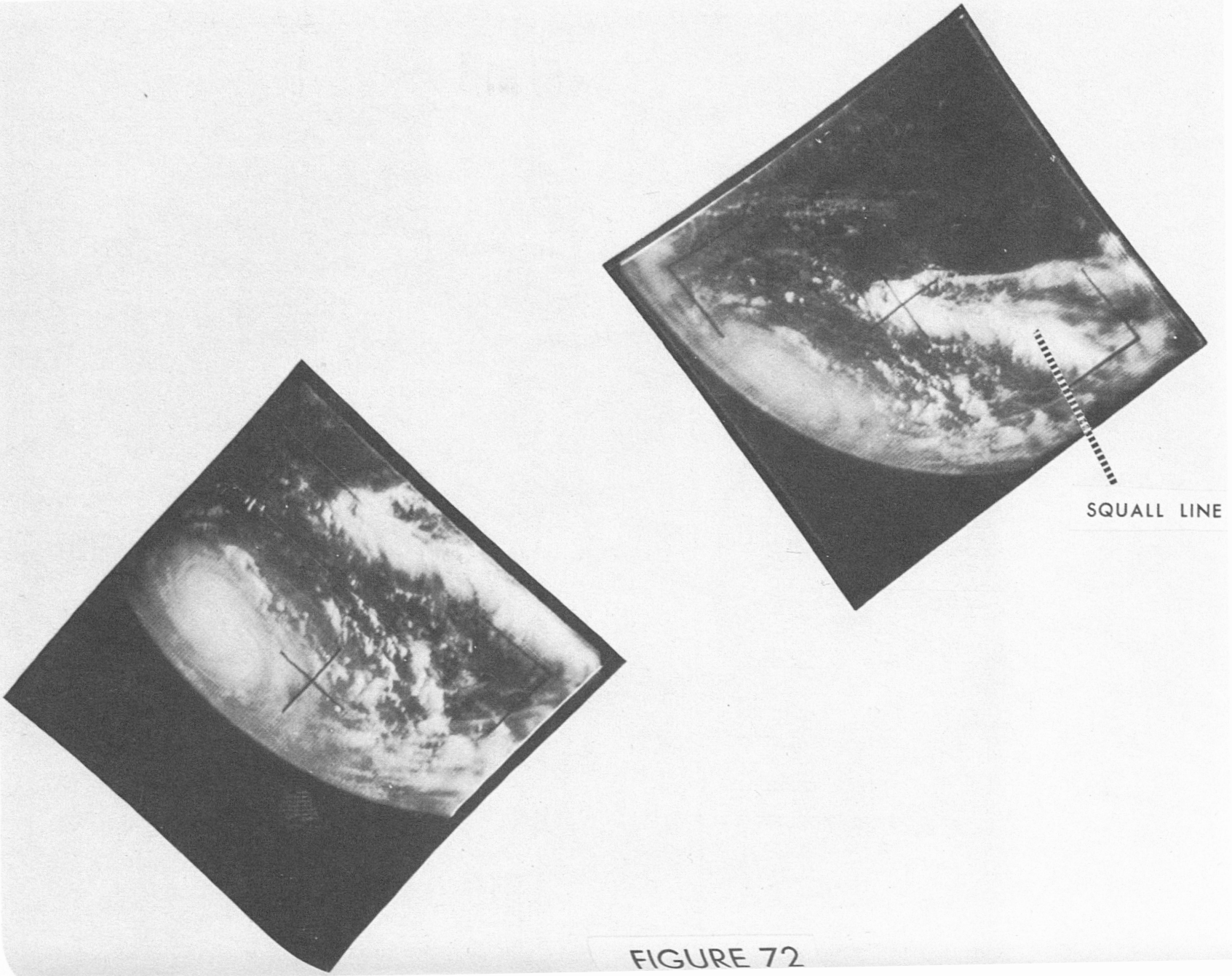


FIGURE 72

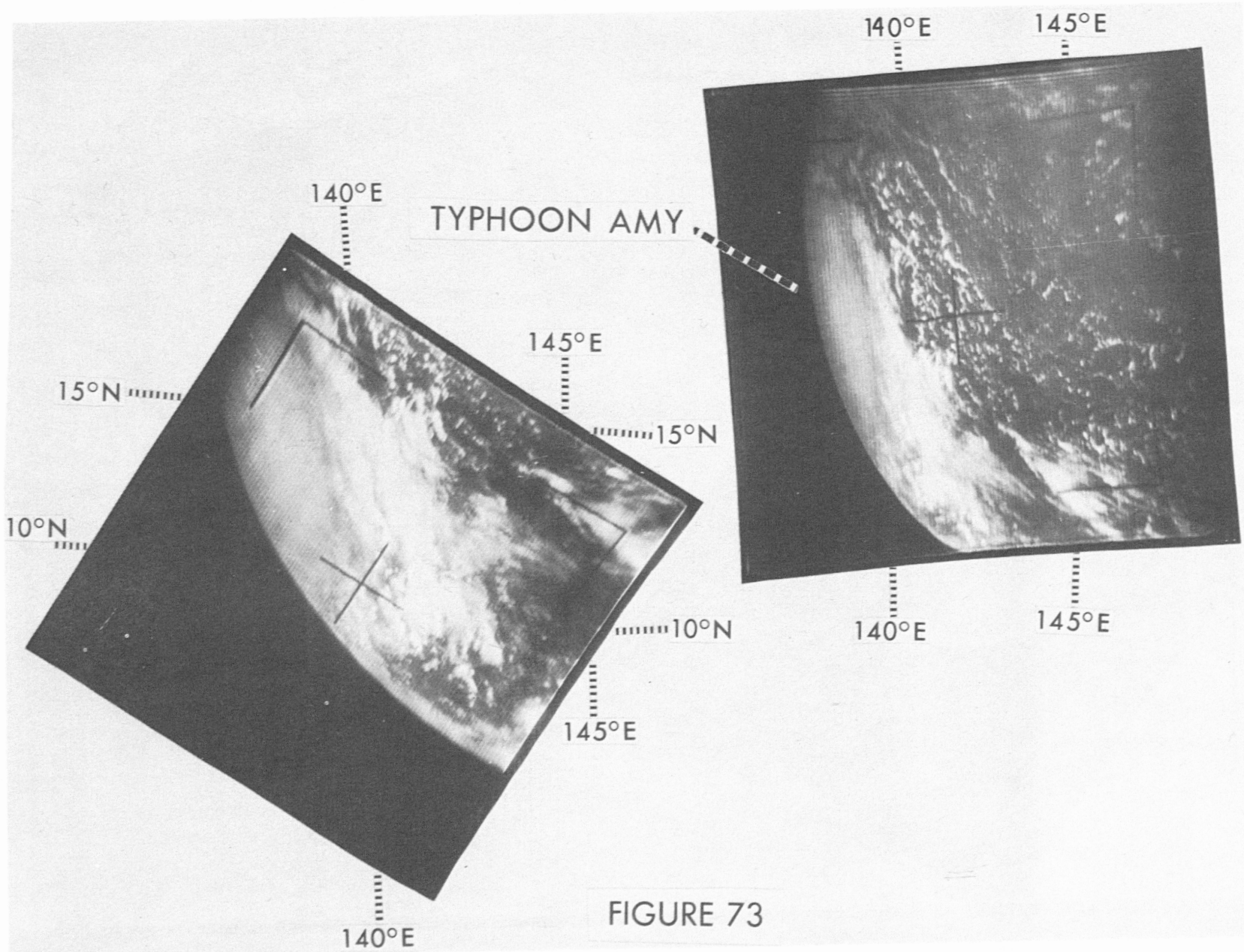
140°E
145°E
TYPHOON AMY
140°E
145°E
15°N
15°N
10°N
10°N
140°E
145°E
145°E
140°E

FIGURE 73

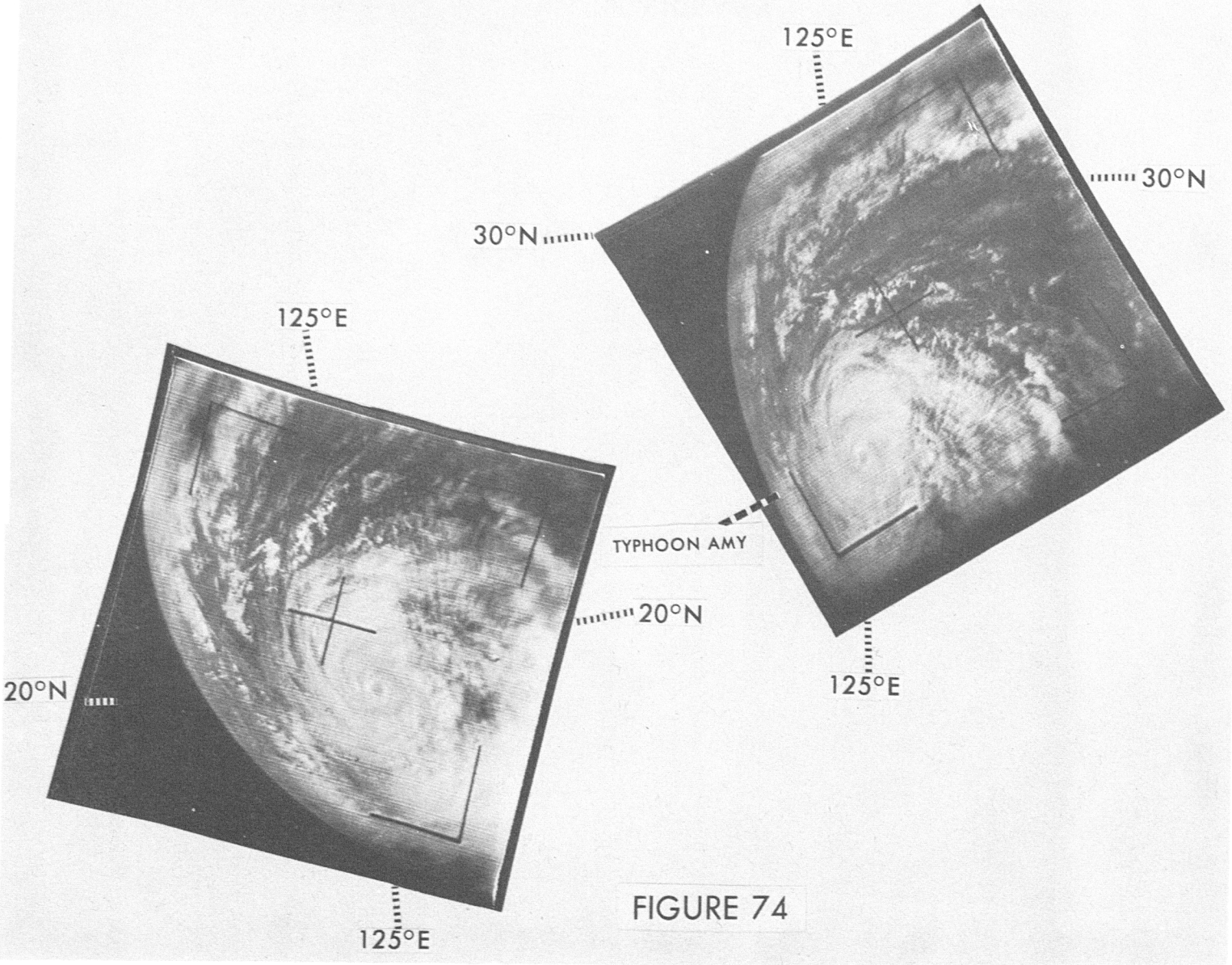


FIGURE 74

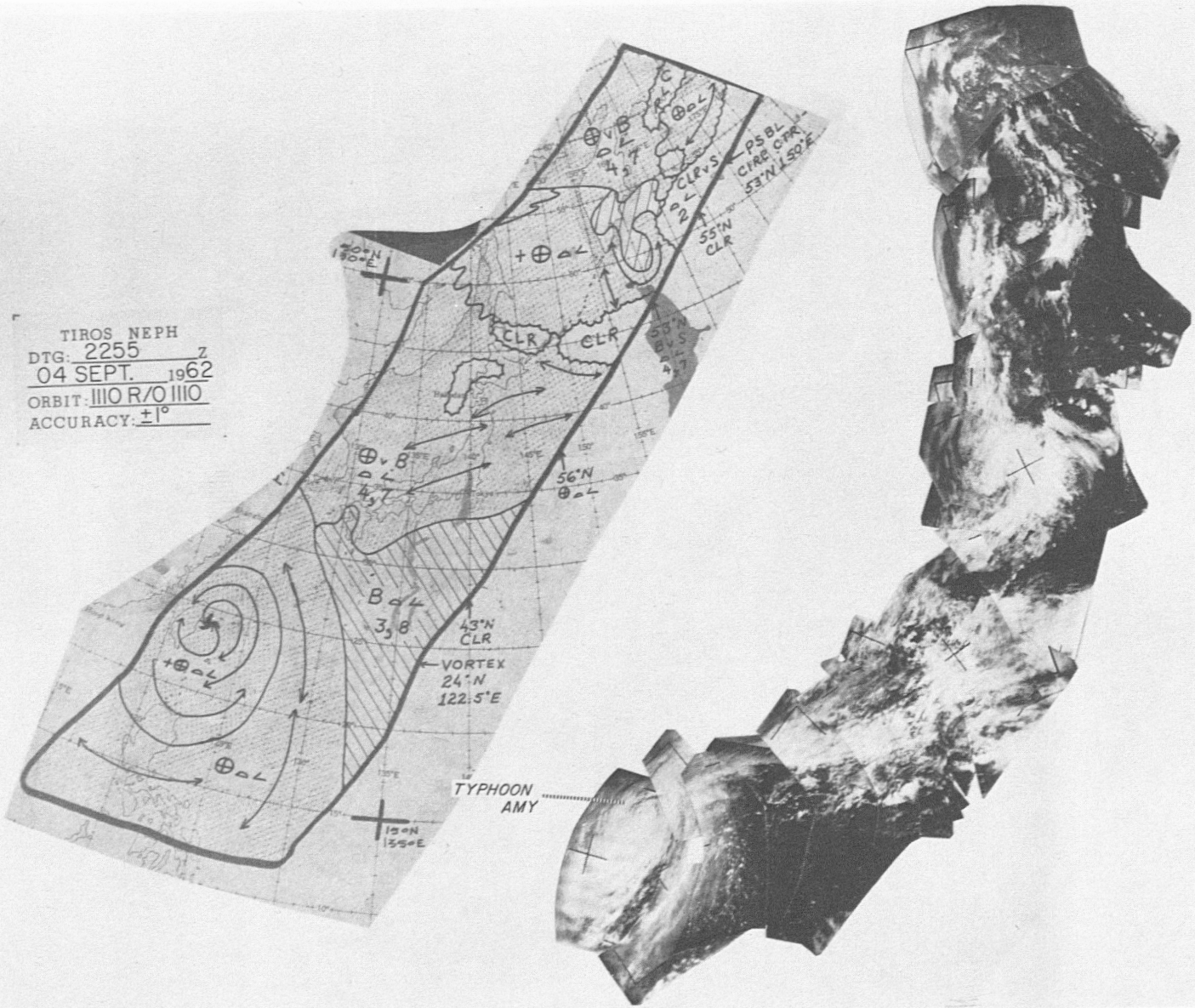
TIROS NEPH
DTG: 2255 Z
04 SEPT. 1962
ORBIT: 1110 R/O 1110
ACCURACY: ±1°
CLR
CLR
CLR
CLR
43°N
CLR
56°N
VORTEX
24°N
122.5°E
TYPHOON
AMY

FIGURE 75

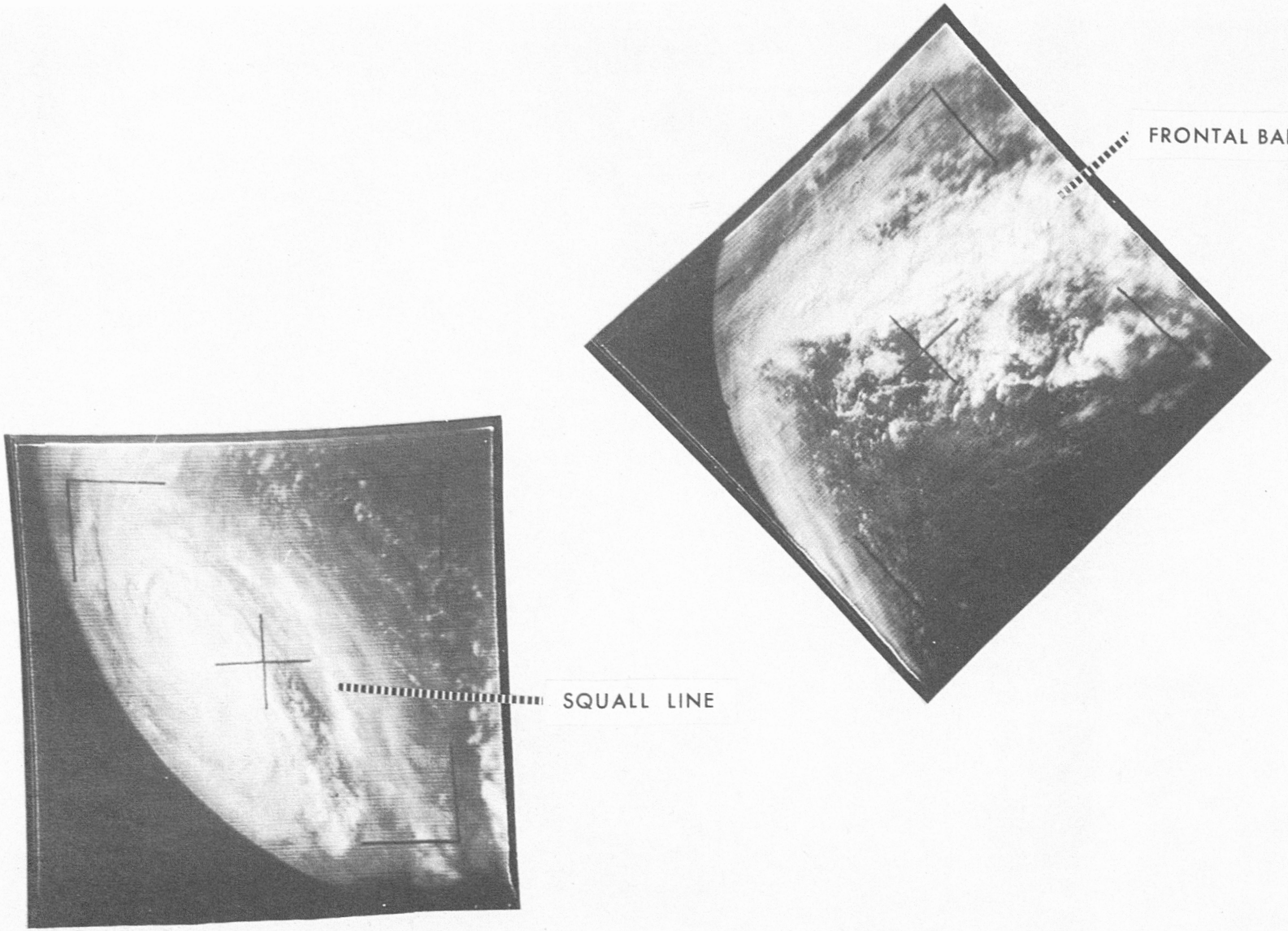


FIGURE 76

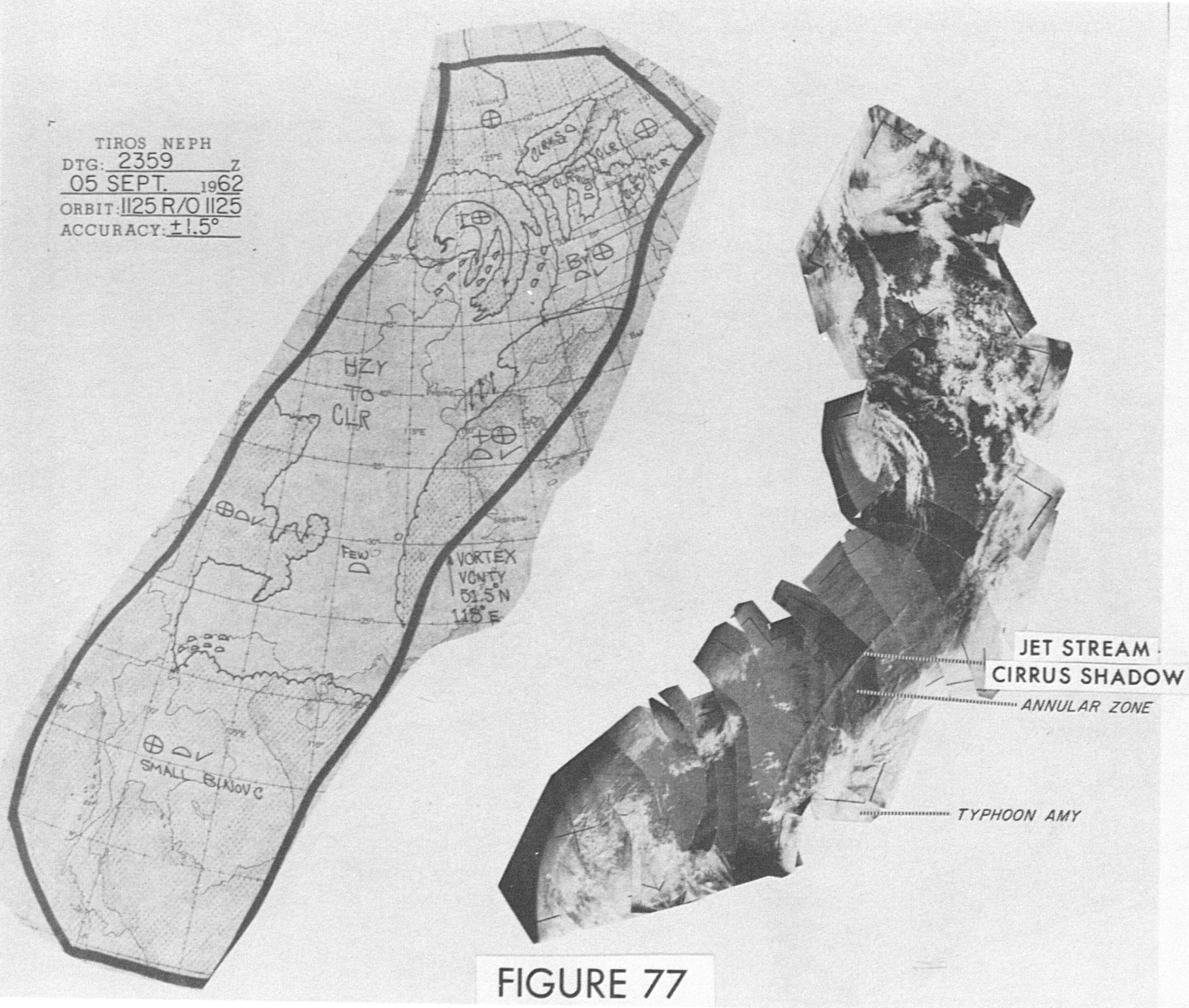
TIROS NEPH
DTG: 2359 Z
05 SEPT. 1962
ORBIT: 1125 R/O 1125
ACCURACY: ±1.5°
HZY
TO
CLR
VORTEX
VCNTY
51.5 N
118° E
SMALL BKN OVC
JET STREAM
CIRRUS SHADOW
ANNULAR ZONE
TYPHOON AMY

FIGURE 77

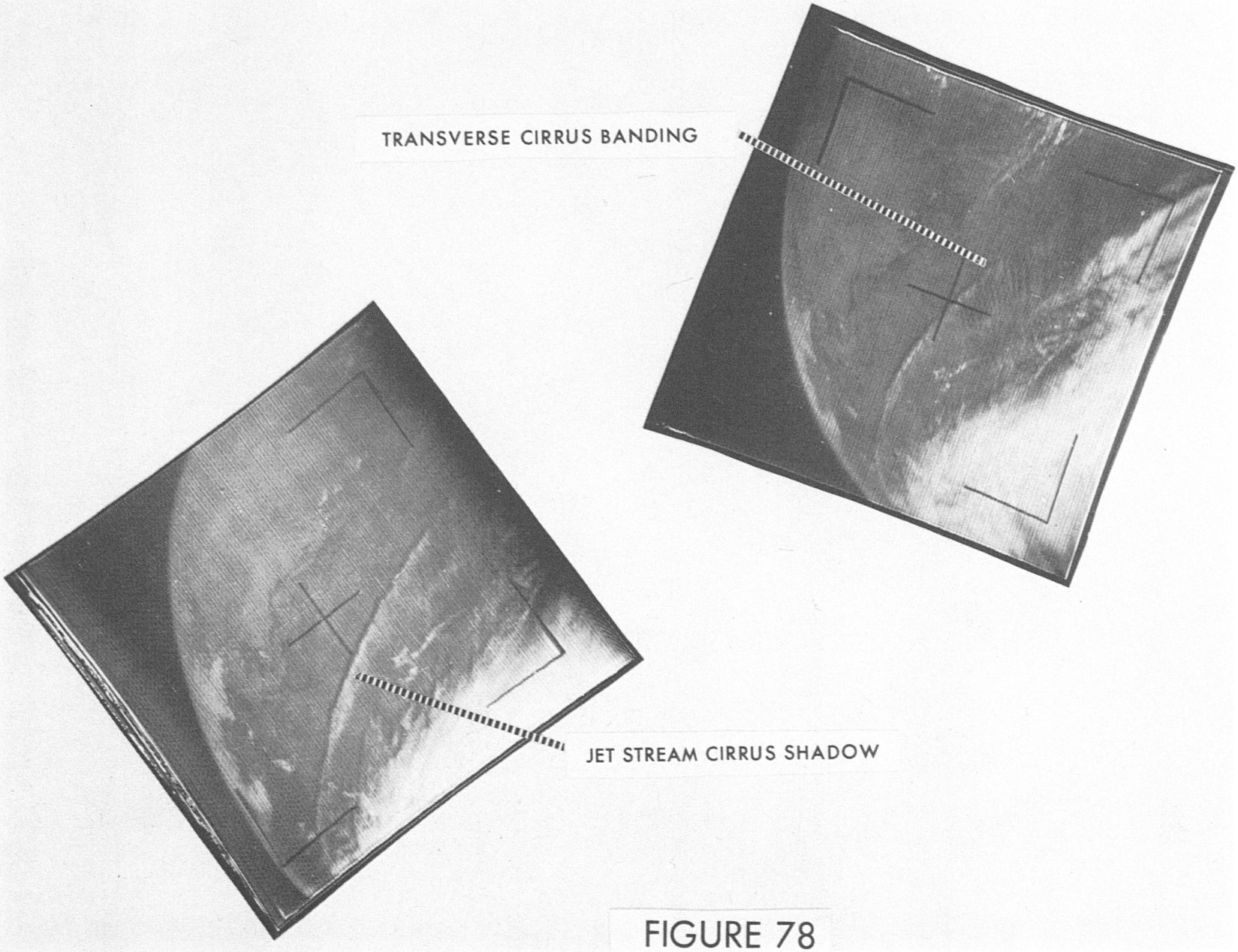


FIGURE 78

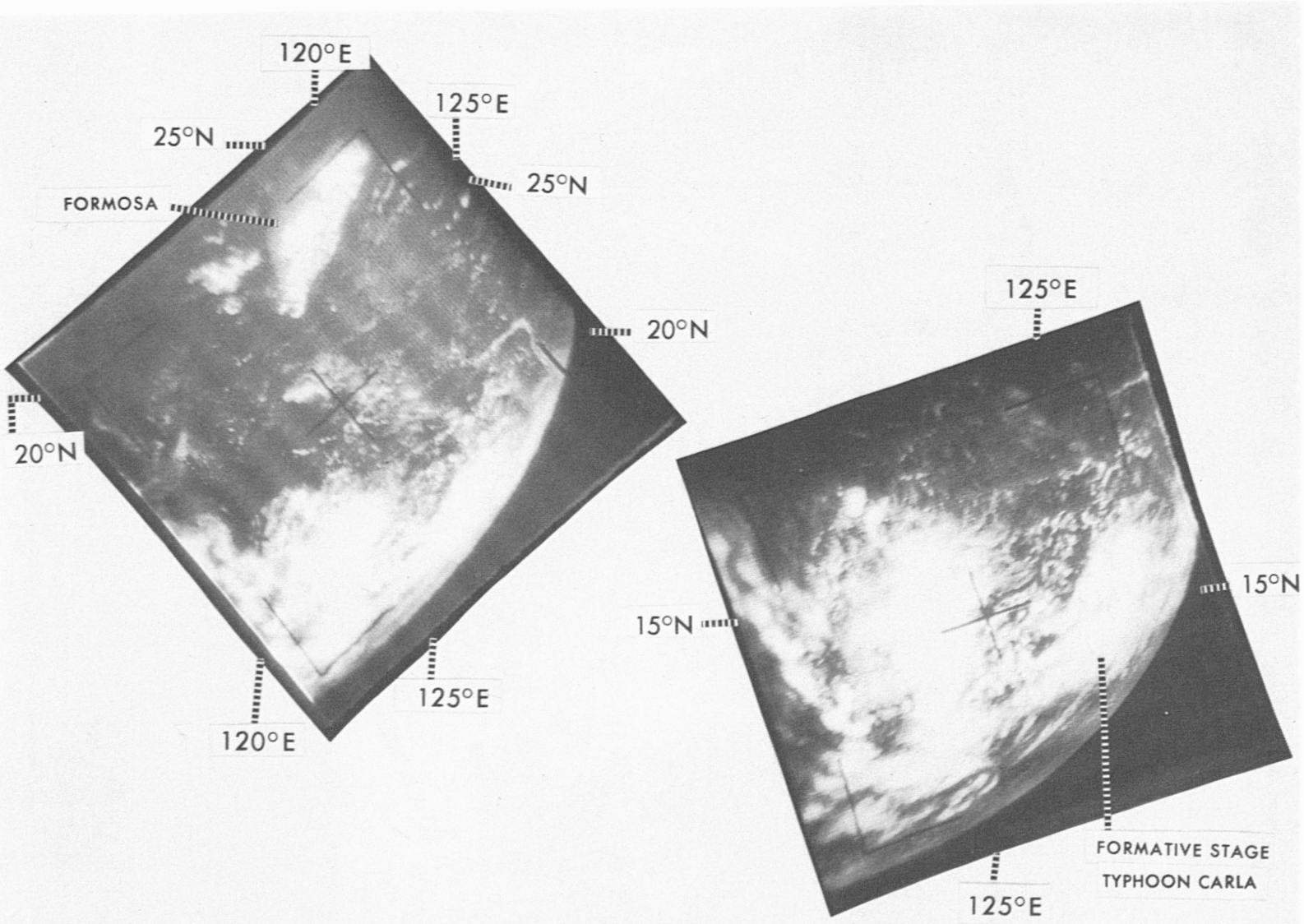
120°E
125°E
25°N
25°N
FORMOSA
20°N
20°N
125°E
120°E
125°E
15°N
15°N
FORMATIVE STAGE
TYPHOON CARLA
125°E

FIGURE 79

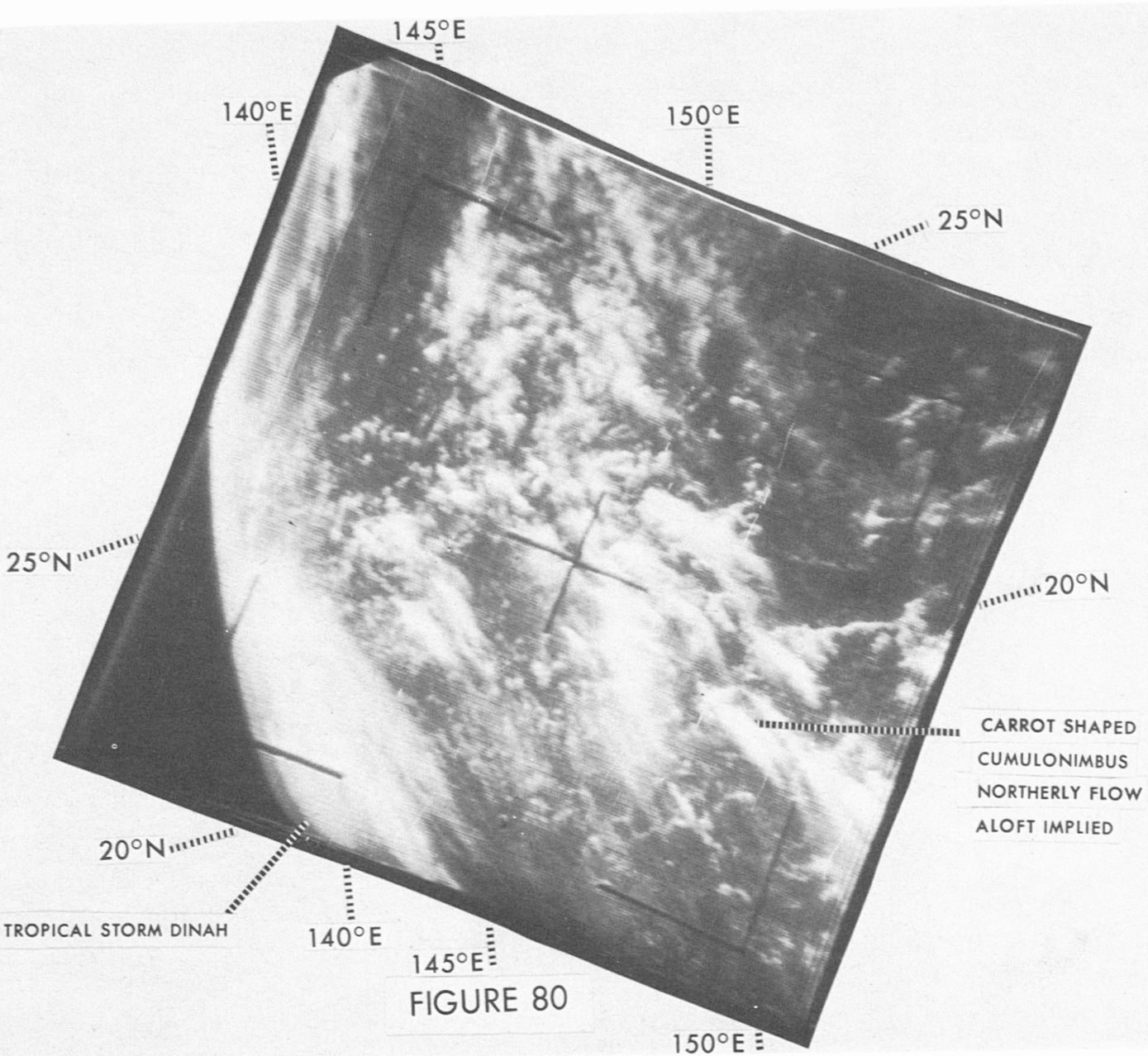
145°E
140°E
150°E
25°N
25°N
20°N
CARROT SHAPED
CUMULONIMBUS
NORTHERLY FLOW
ALOFT IMPLIED
20°N
TROPICAL STORM DINAH
140°E
145°E
150°E

FIGURE 80

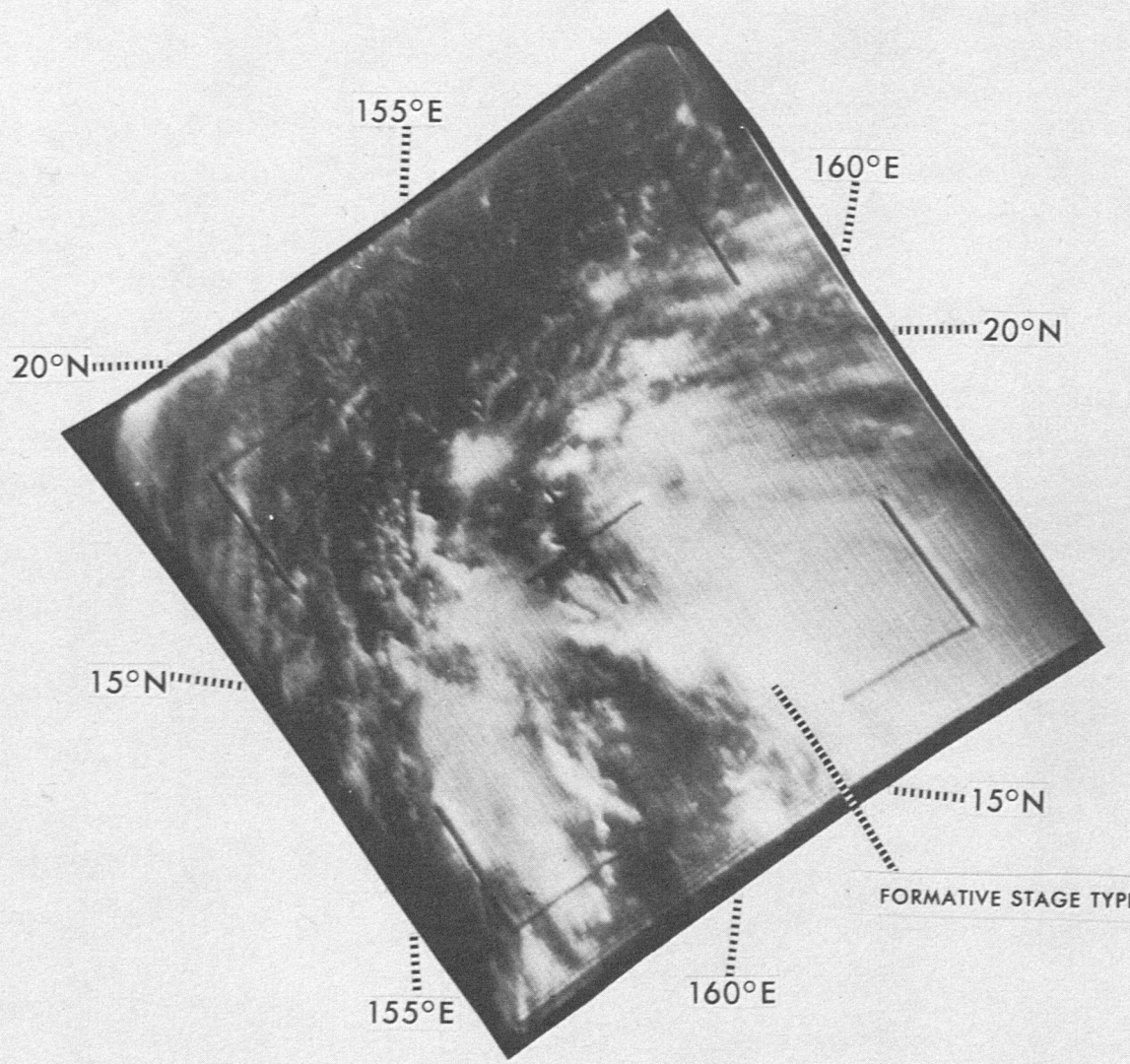


FORMATIVE STAGE TYPHOON EMMA

FIGURE 81

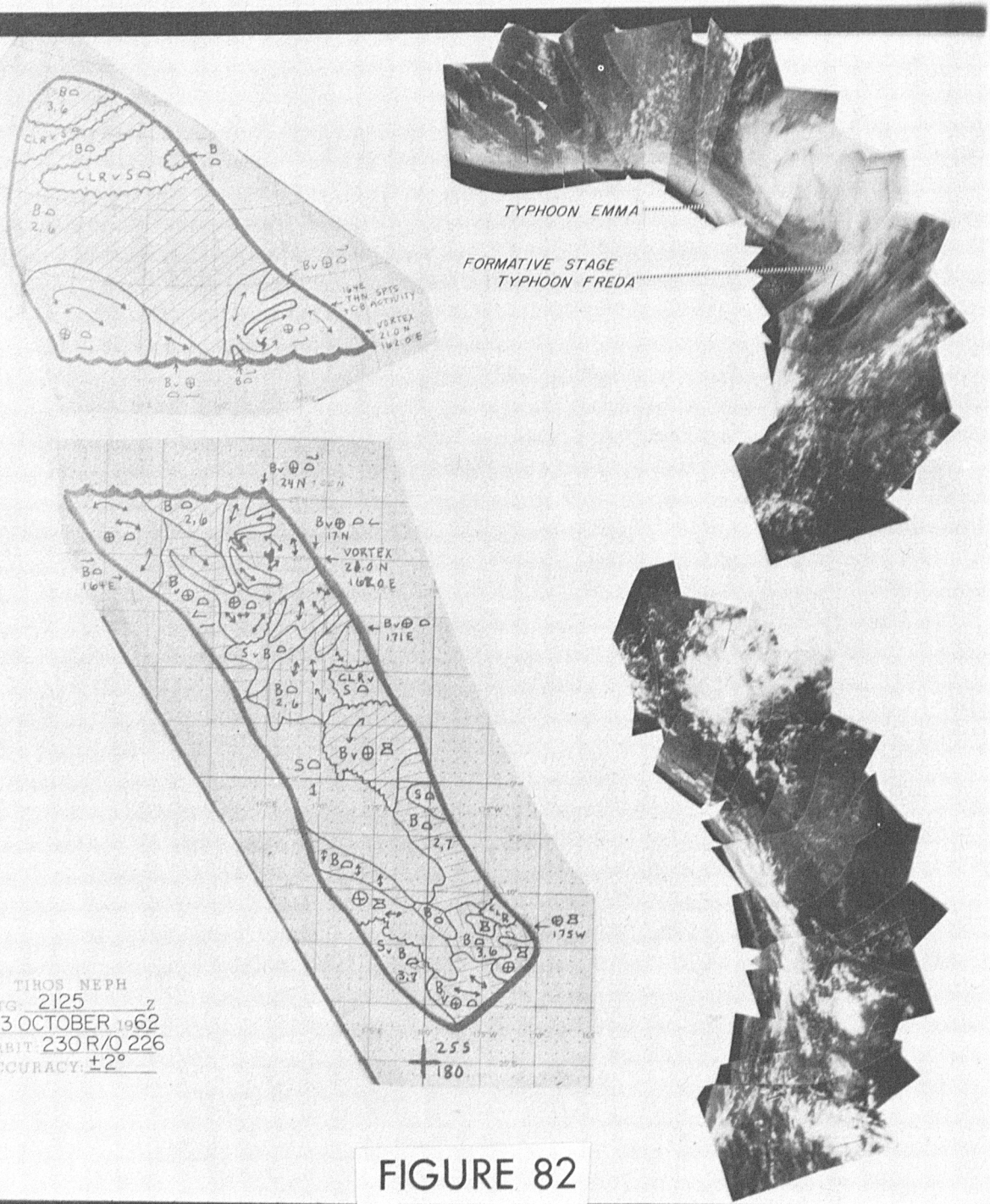
TYPHOON EMMA
FORMATIVE STAGE
TYPHOON FREDA
VORTEX
28.0 N
166.0 E
VORTEX
21.0 N
162.0 E
TIROS NEPH
DTG 2125 Z
03 OCTOBER 1962
ORBIT 230 R/O 226
ACCURACY: ±2°

FIGURE 82

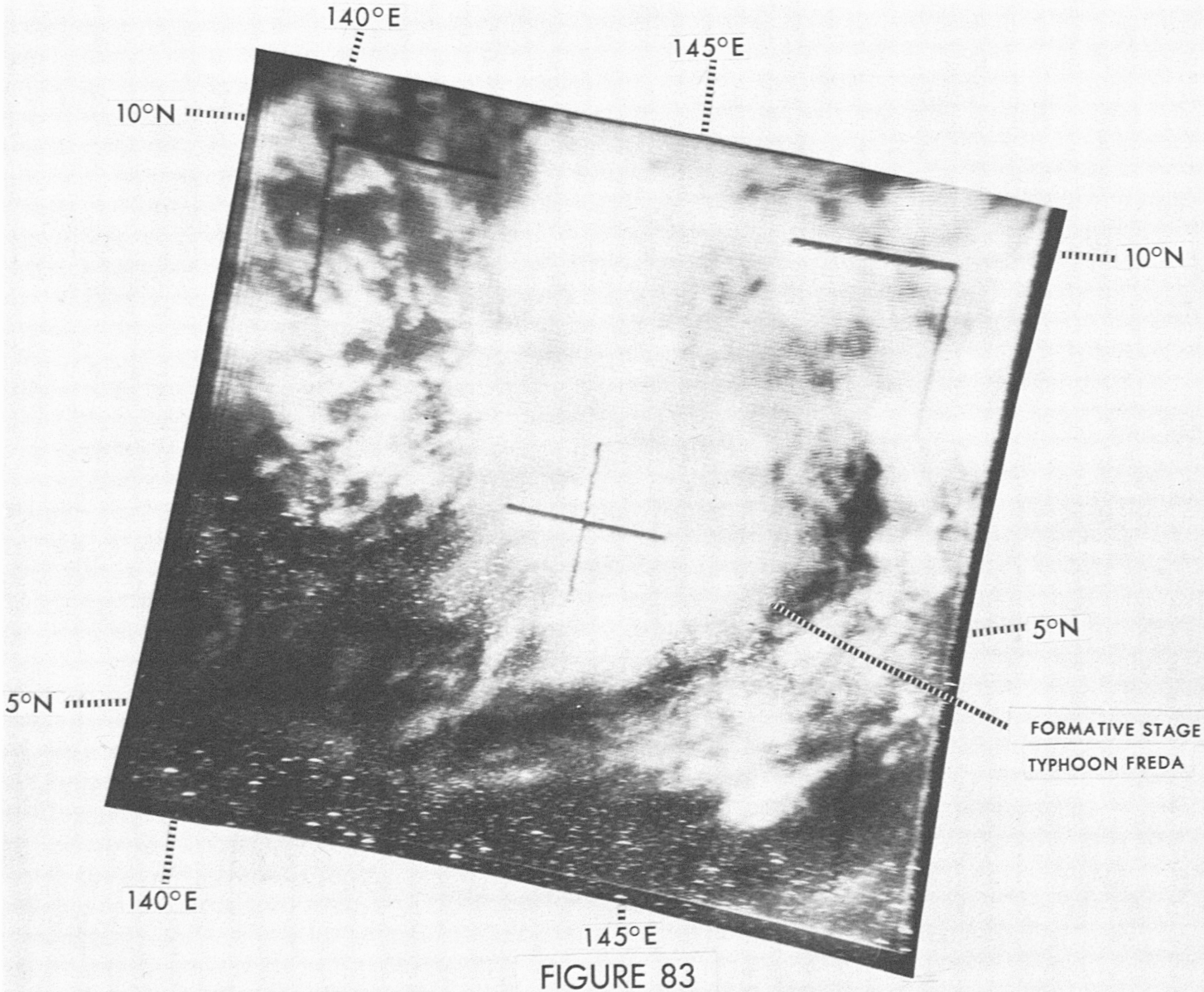
140°E
145°E
10°N
10°N
5°N
5°N
FORMATIVE STAGE
TYPHOON FREDA
140°E
145°E

FIGURE 83

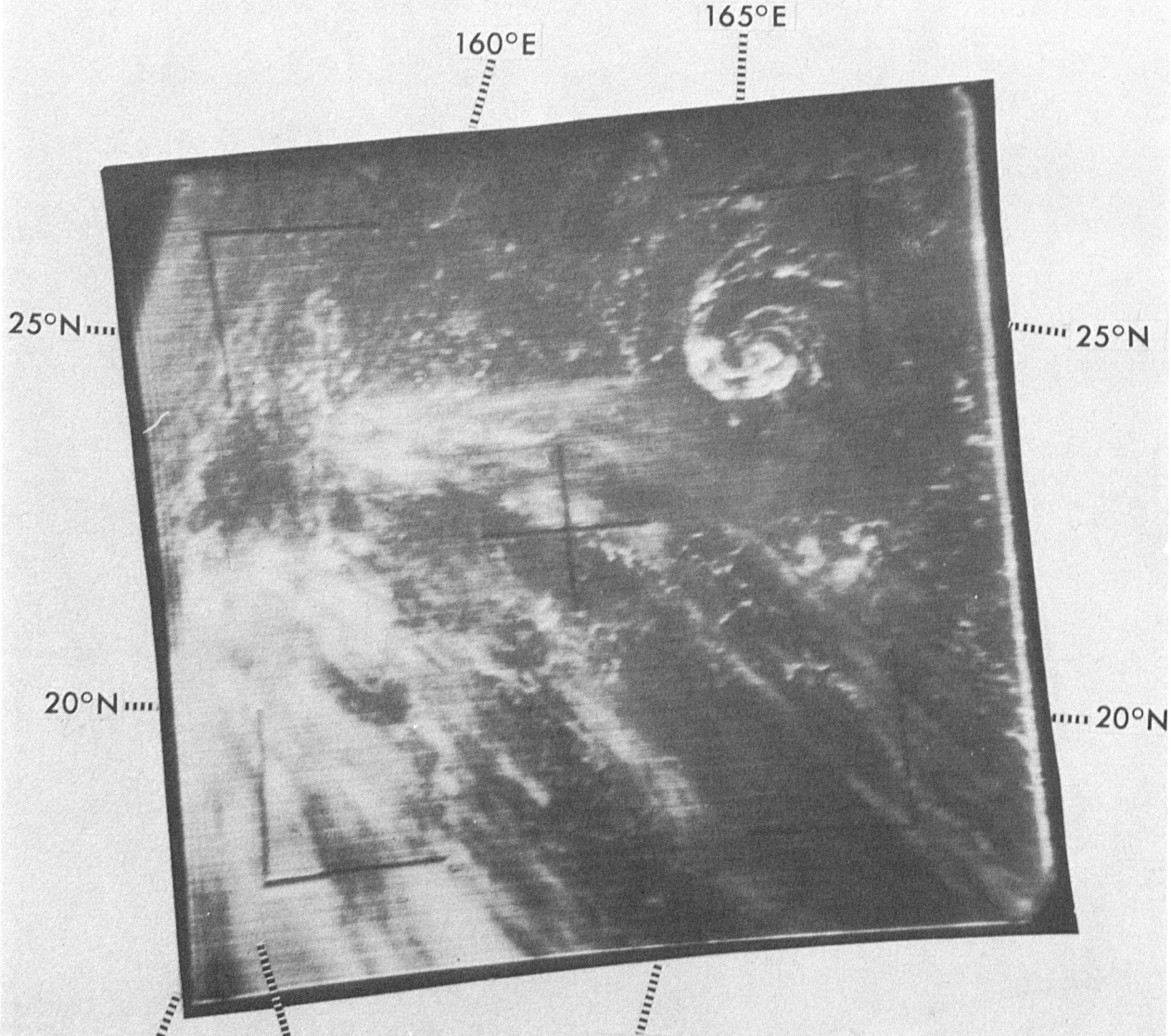


FORMATIVE STAGE TYPHOON FREDA

FIGURE 84

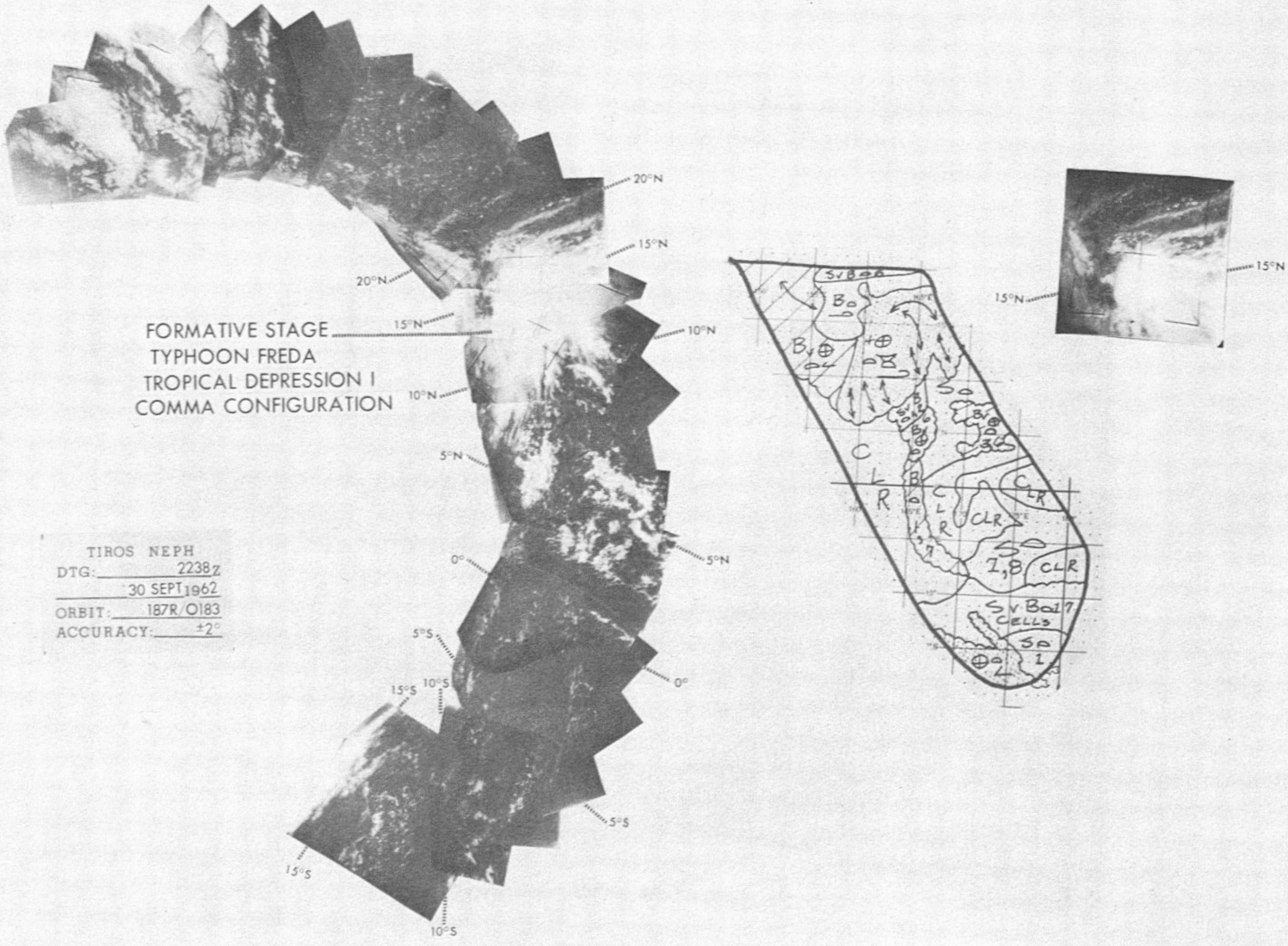
FORMATIVE STAGE
TYPHOON FREDA
TROPICAL DEPRESSION I
COMMA CONFIGURATION
TIROS NEPH
DTG: 2238Z
30 SEPT 1962
ORBIT: 187R/0183
ACCURACY: ±2°
20°N
15°N
10°N
5°N
0°
5°S
10°S
15°S
CLR
SV BAS CELLS

FIGURE 85

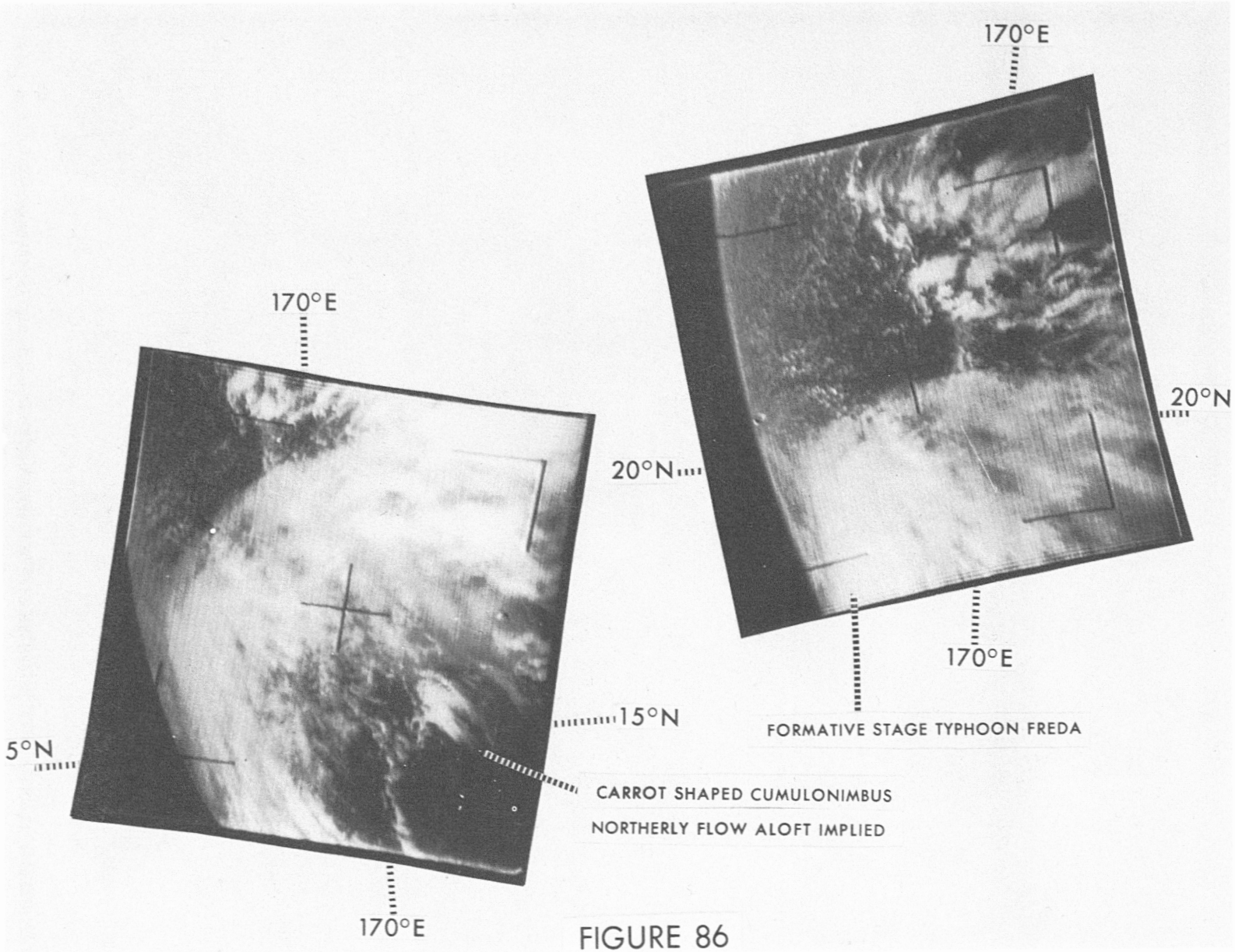
170°E
20°N
170°E
FORMATIVE STAGE TYPHOON FREDA
170°E
15°N
5°N
CARROT SHAPED CUMULONIMBUS
NORTHERLY FLOW ALOFT IMPLIED
170°E

FIGURE 86

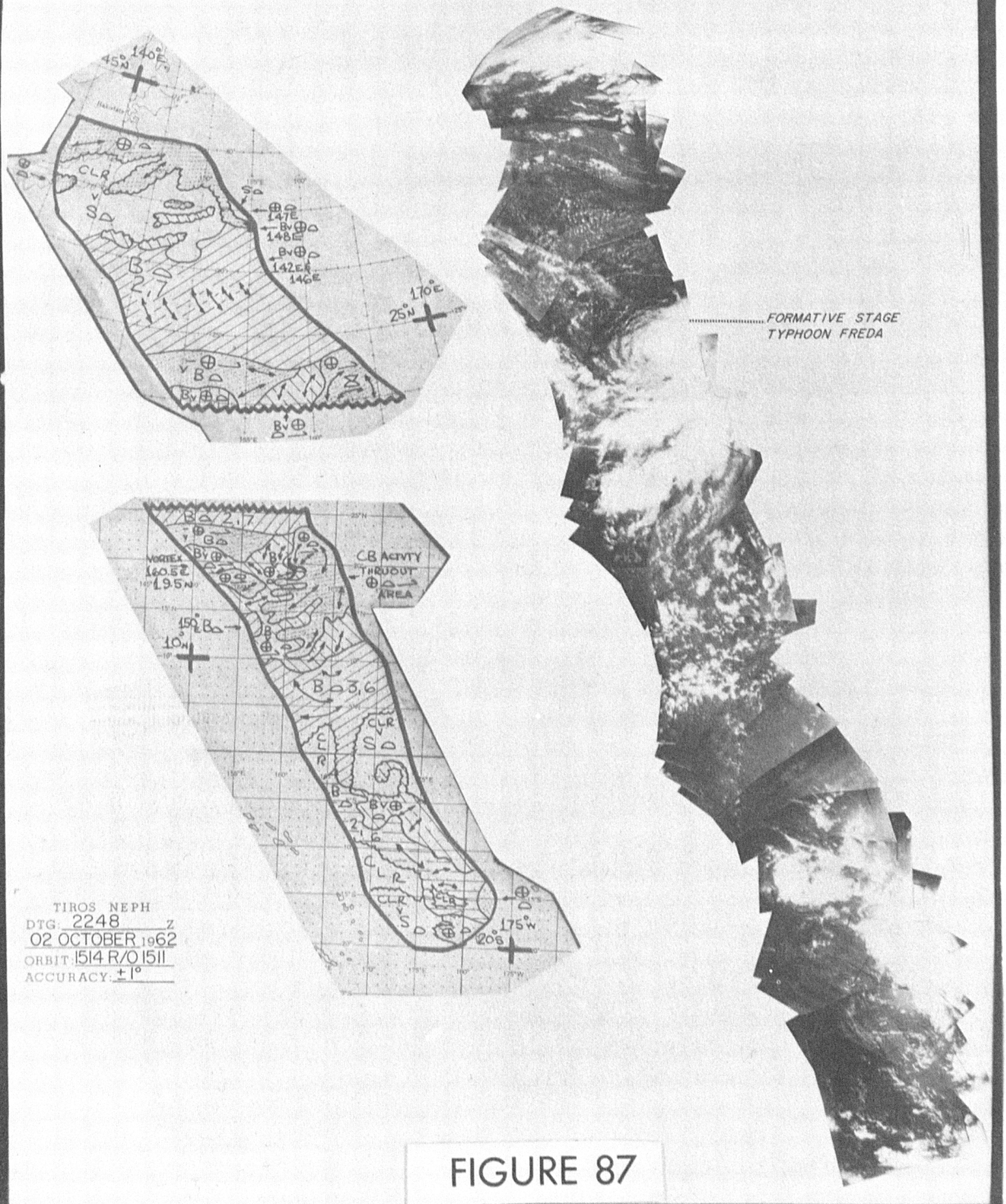
45°N 140°E
CLR
V
S
B
147E
148E
BV
142E
146E
170°E
25°N
V
B
BV
FORMATIVE STAGE
TYPHOON FREDA
B 2,7
VORTEX
160.5E
19.5N
C.B ACTVTY
THRUOUT
AREA
150°E
10°N
B 3,6
CLR
S
BV
2,6
175°W
20°S
TIROS NEPH
DTG: 2248 Z
02 OCTOBER 1962
ORBIT: 1514 R/O 1511
ACCURACY: ±1°

FIGURE 87

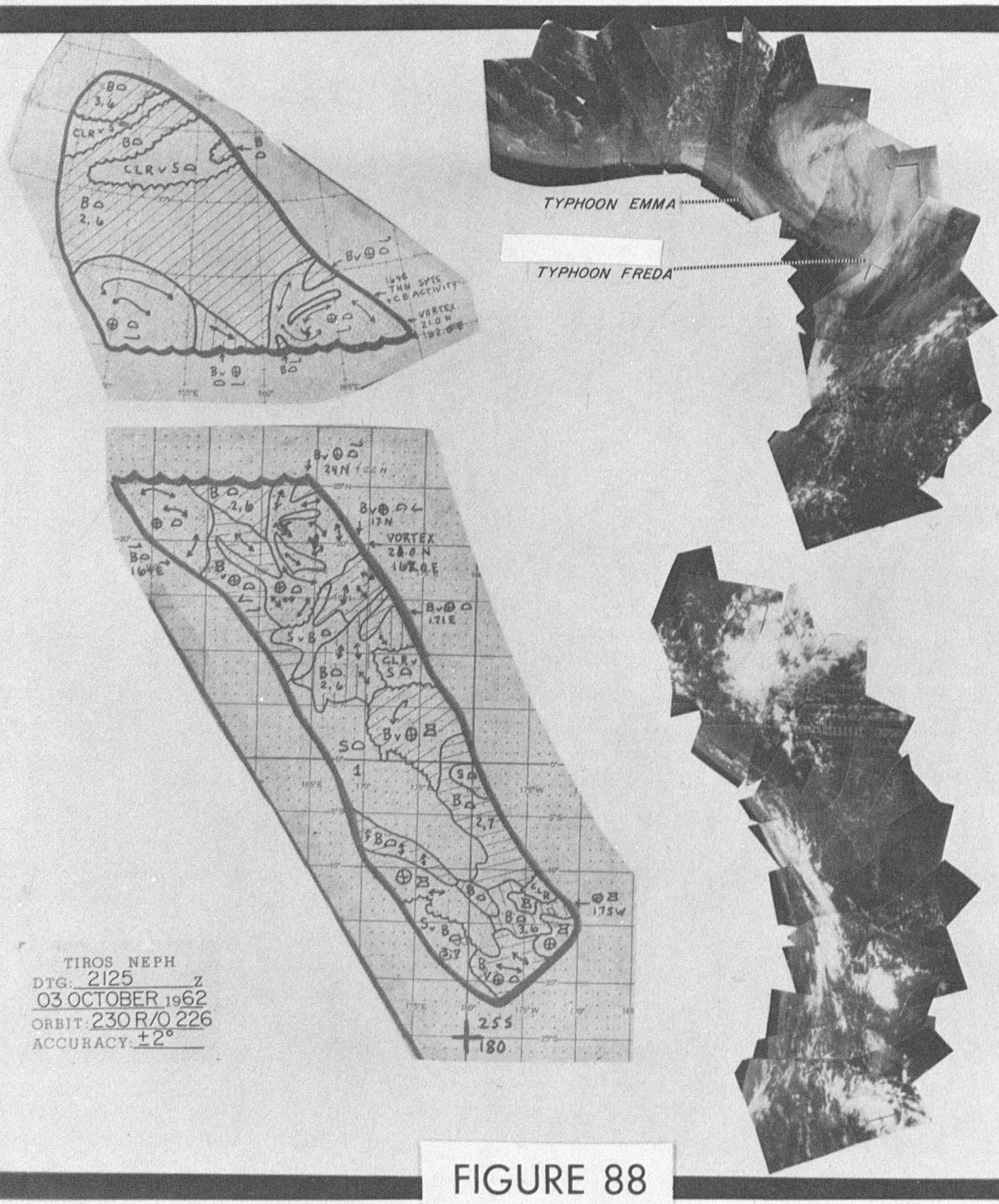
TYPHOON EMMA
TYPHOON FREDA
TIROS NEPH
DTG: 2125 Z
03 OCTOBER 1962
ORBIT: 230 R/O 226
ACCURACY: ±2°

FIGURE 88

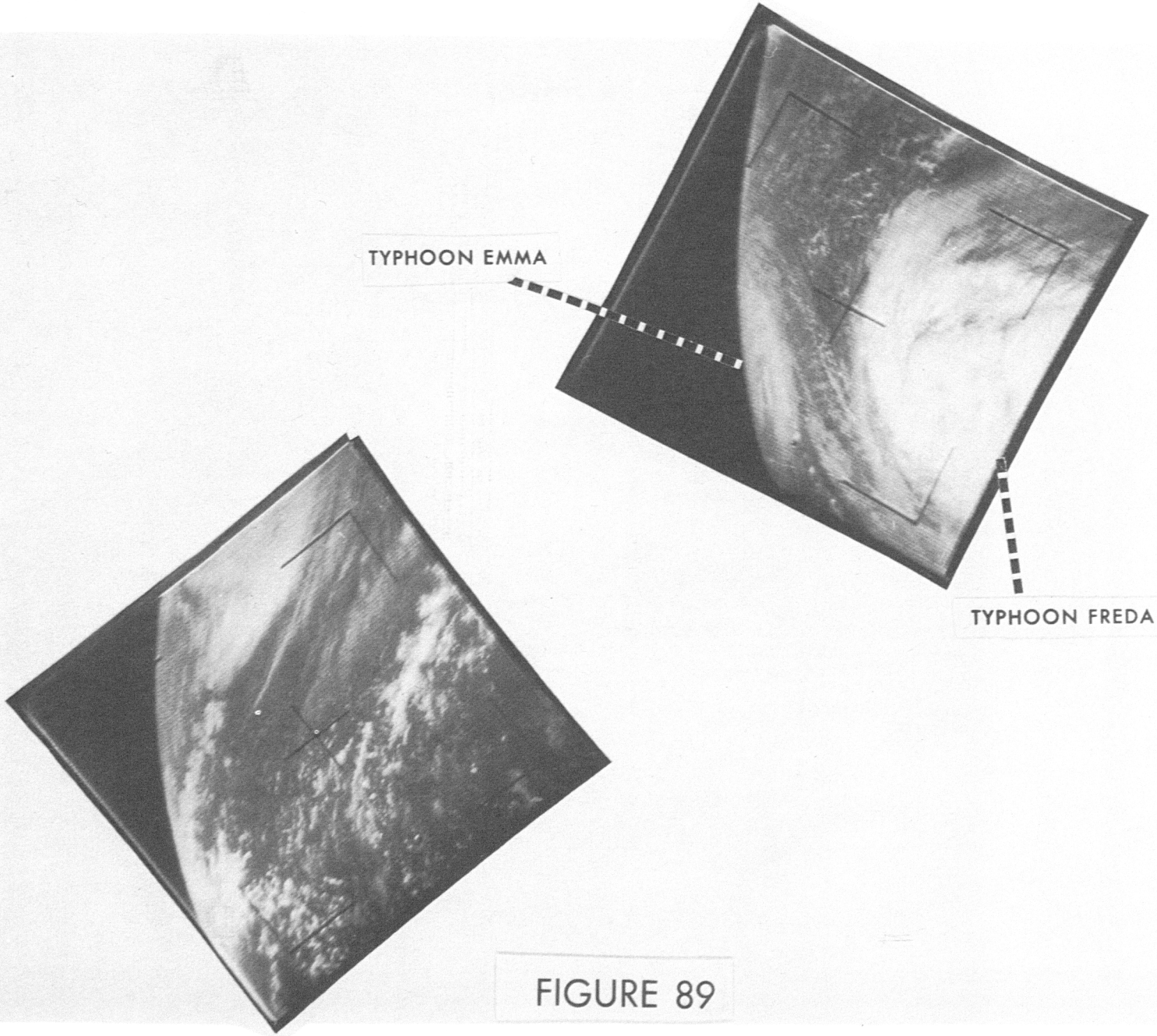


FIGURE 89

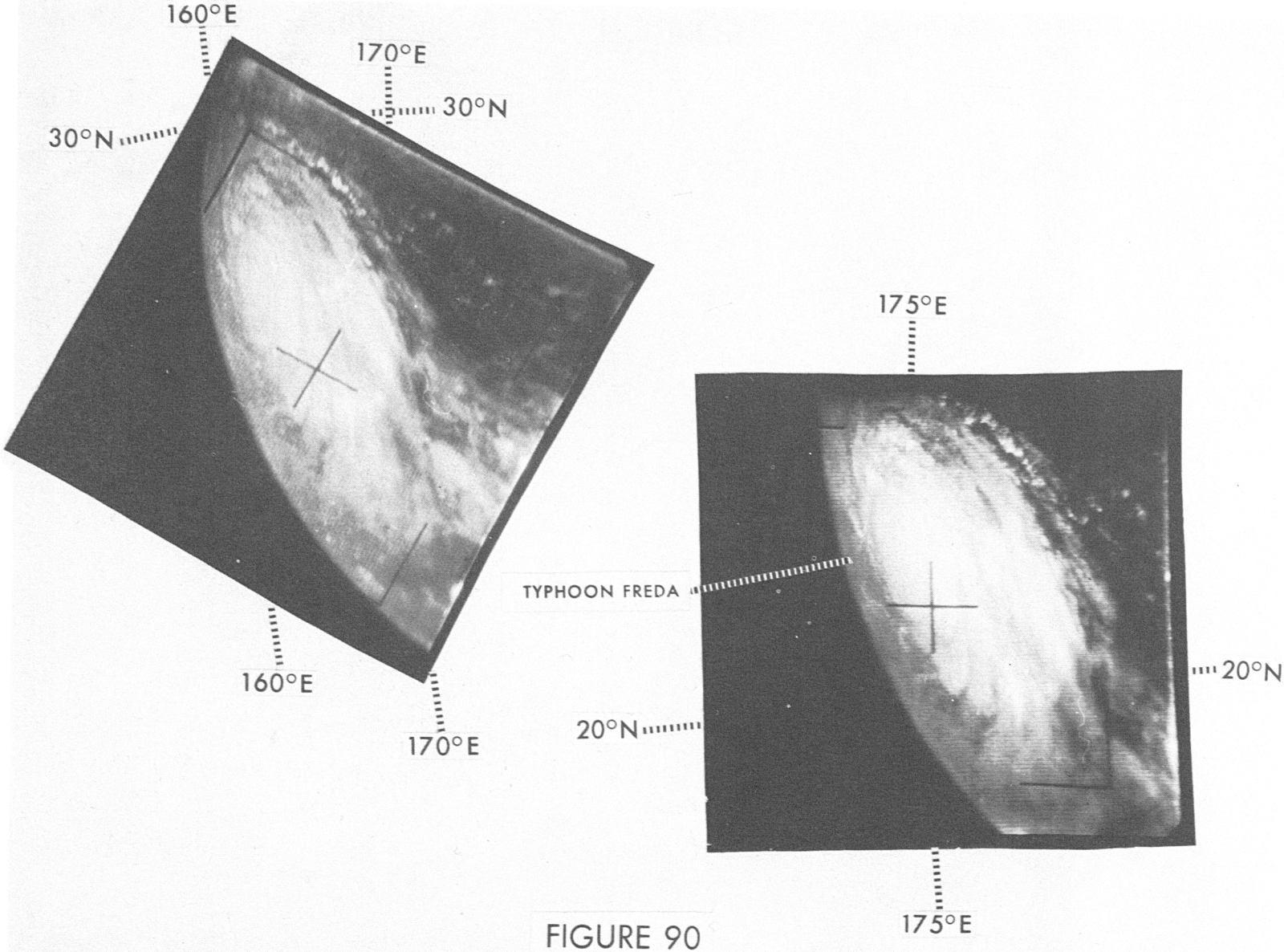


FIGURE 90

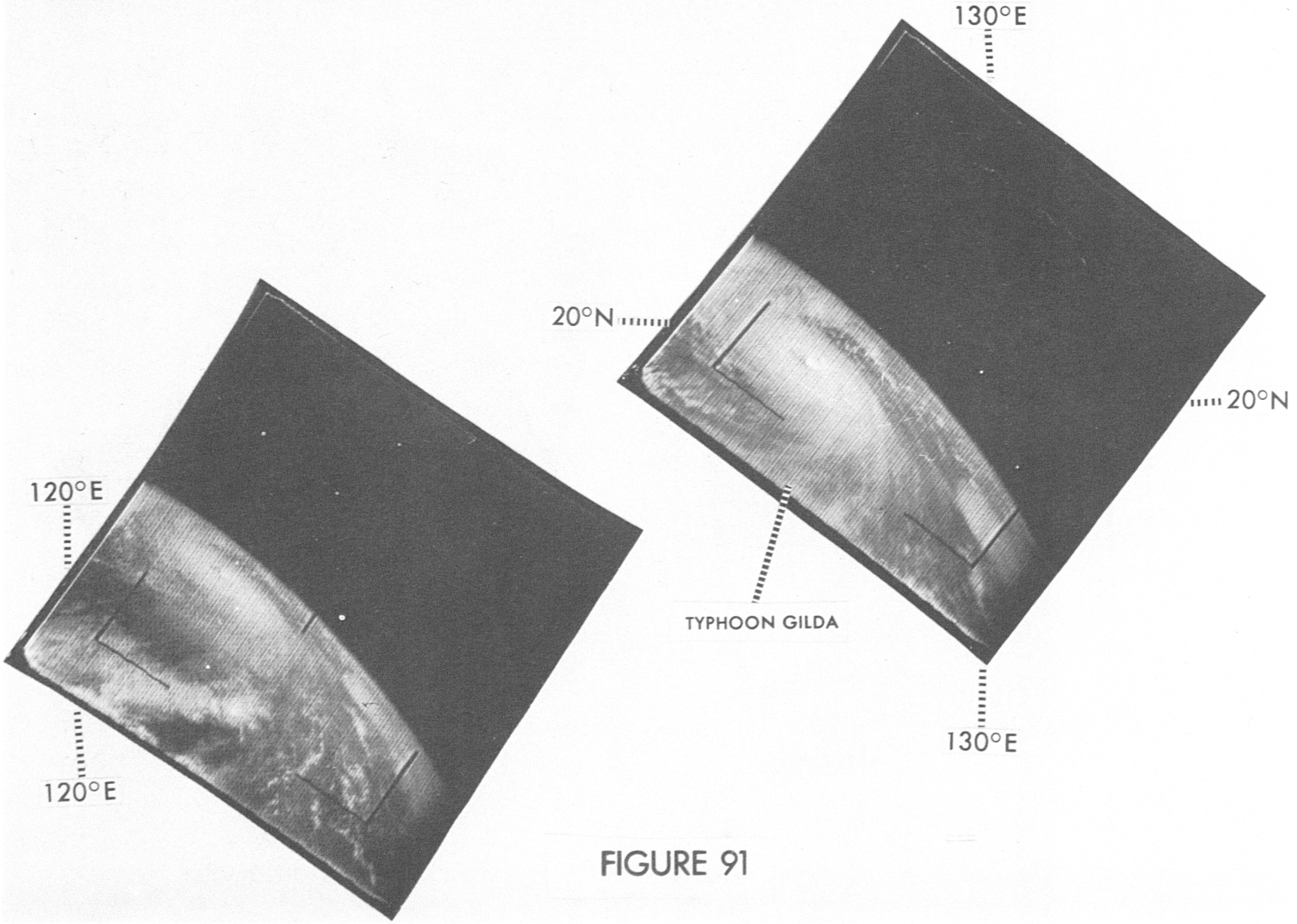


FIGURE 91

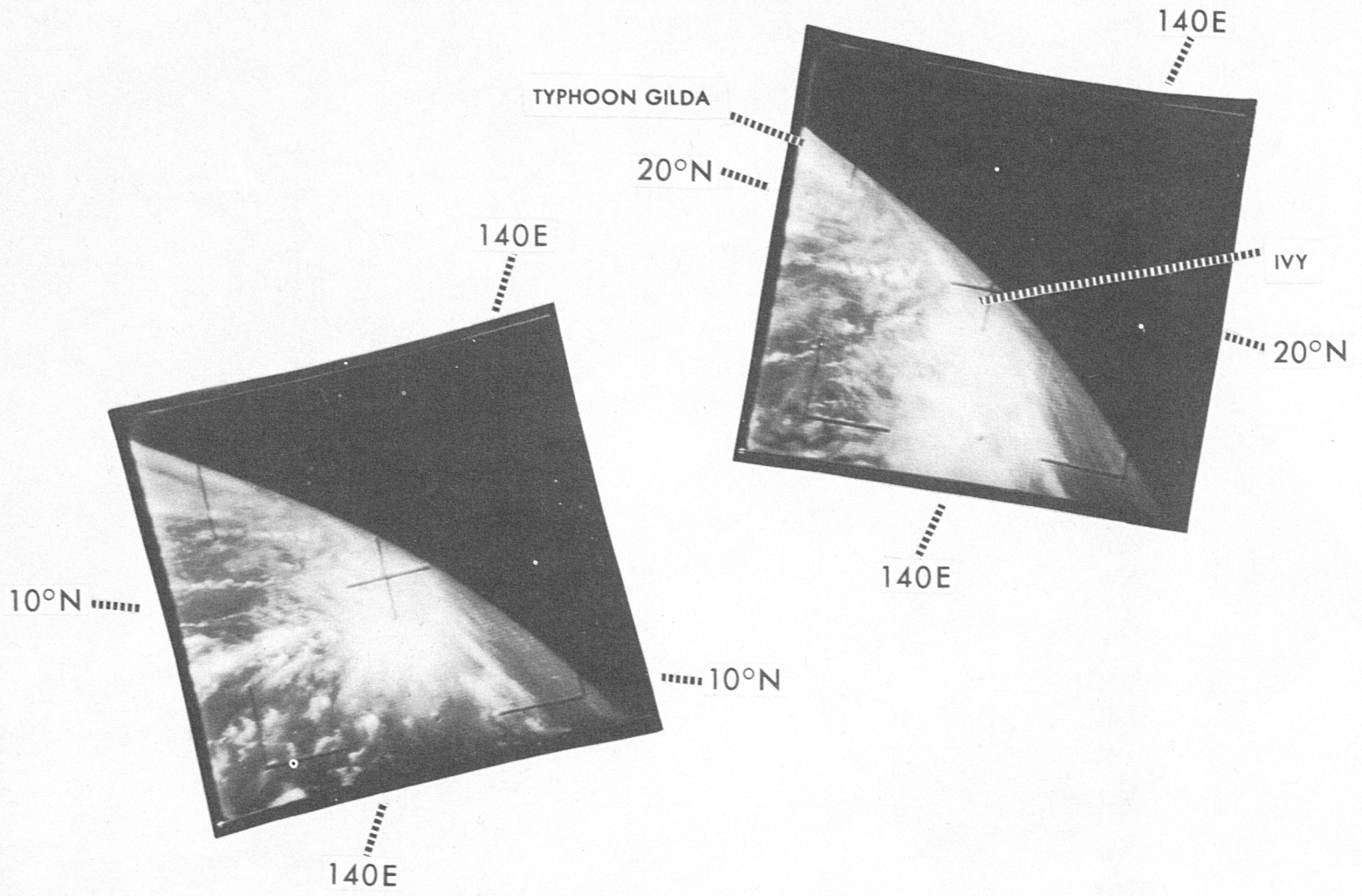


FIGURE 92

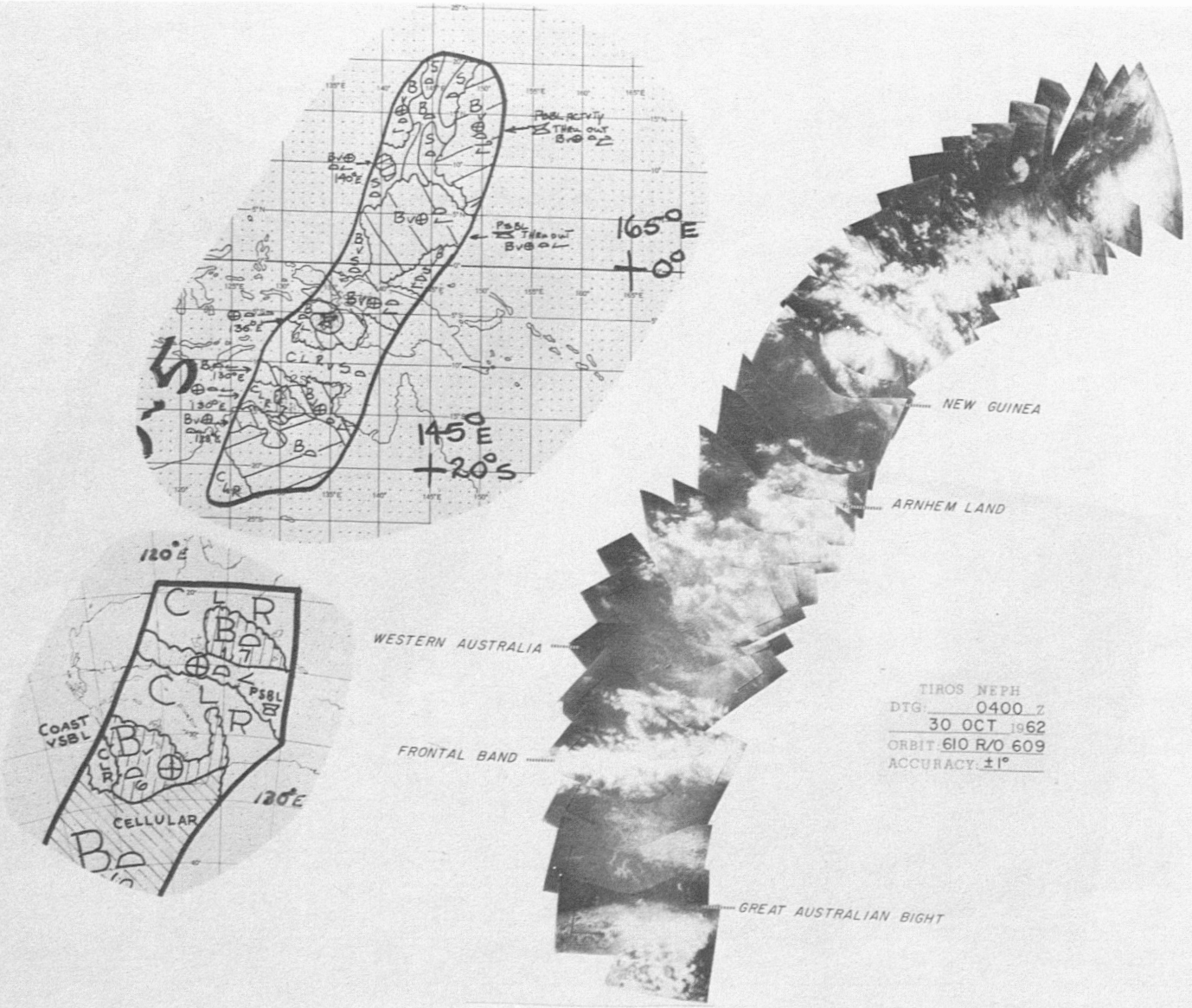
165°E
+00
145°E
+20°S
120°E
120°E
COAST
VSBL
PSBL
CELLULAR
NEW GUINEA
ARNHEM LAND
WESTERN AUSTRALIA
FRONTAL BAND
GREAT AUSTRALIAN BIGHT
TIROS NEPH
DTG: 0400 Z
30 OCT 1962
ORBIT 610 R/O 609
ACCURACY: ±1°

FIGURE 93

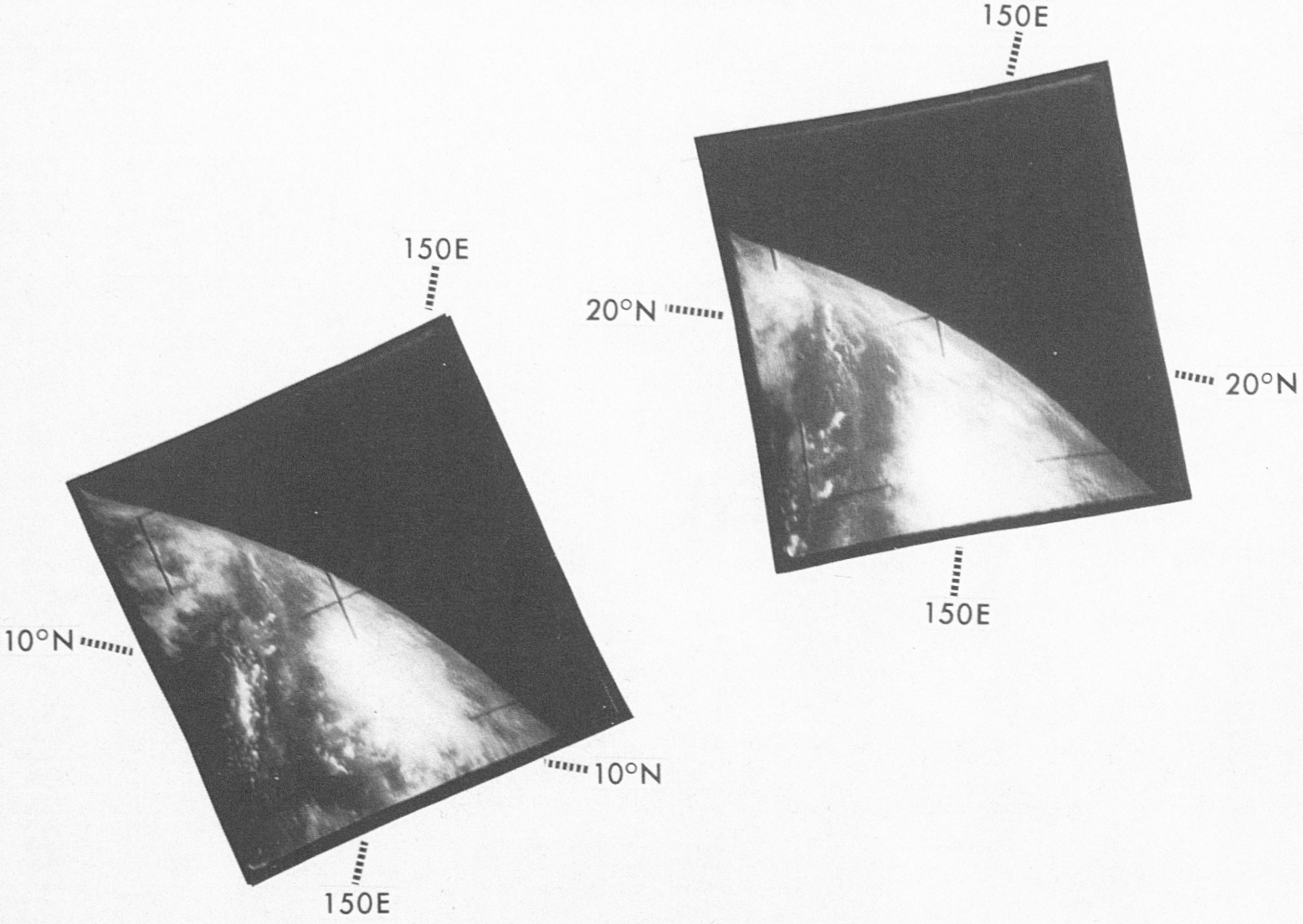


FIGURE 94

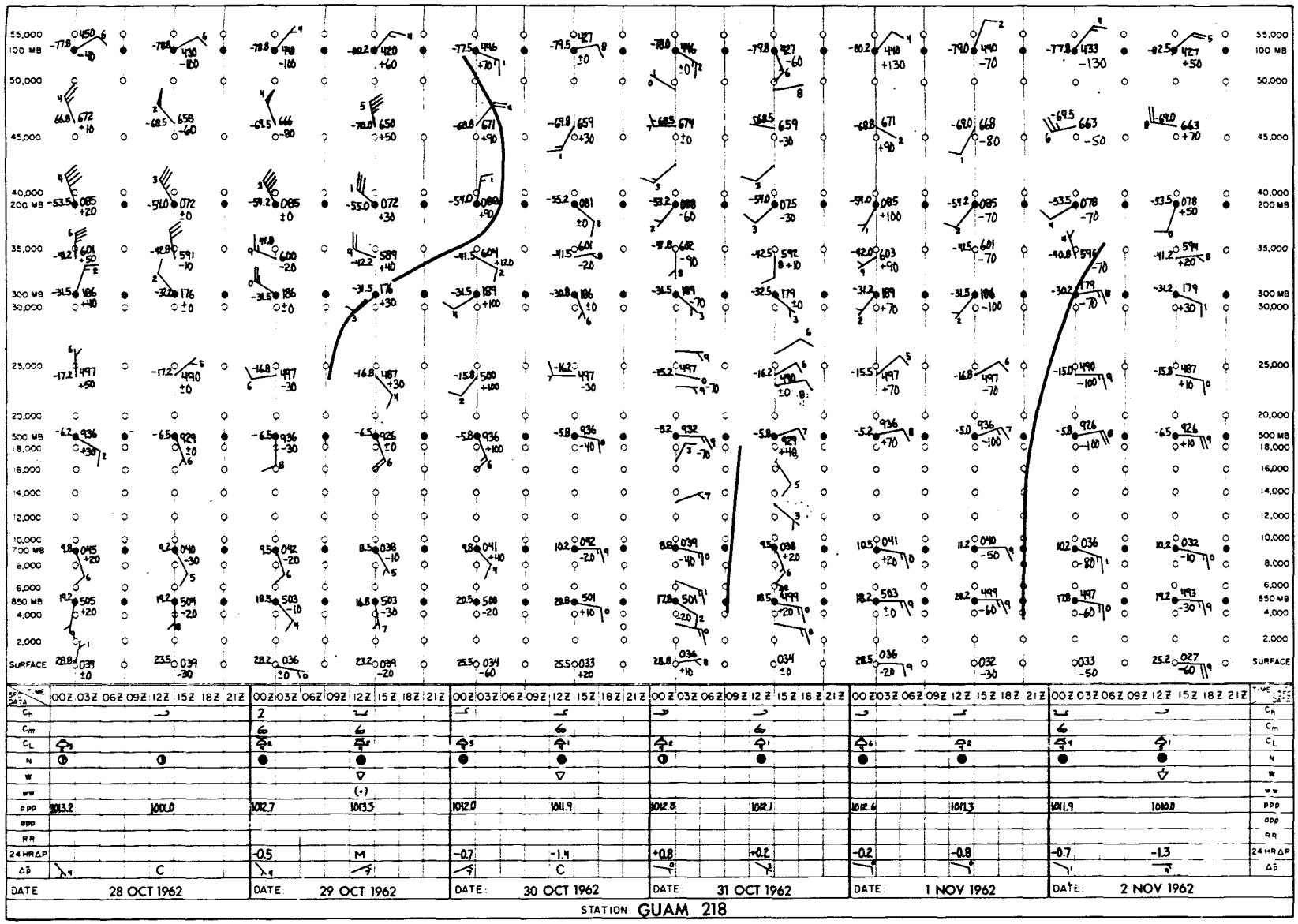
55,000
100 MB
50,000
45,000
40,000
200 MB
35,000
300 MB
30,000
25,000
20,000
500 MB
18,000
16,000
14,000
12,000
10,000
700 MB
8,000
6,000
850 MB
4,000
2,000
SURFACE
00Z 03Z 06Z 09Z 12Z 15Z 18Z 21Z
Cn
Cm
CL
N
W
ww
PPP
ppp
RR
24 HR ΔP
Δp̄
DATE 28 OCT 1962
DATE 29 OCT 1962
DATE 30 OCT 1962
DATE 31 OCT 1962
DATE 1 NOV 1962
DATE 2 NOV 1962
STATION GUAM 218

FIGURE 95

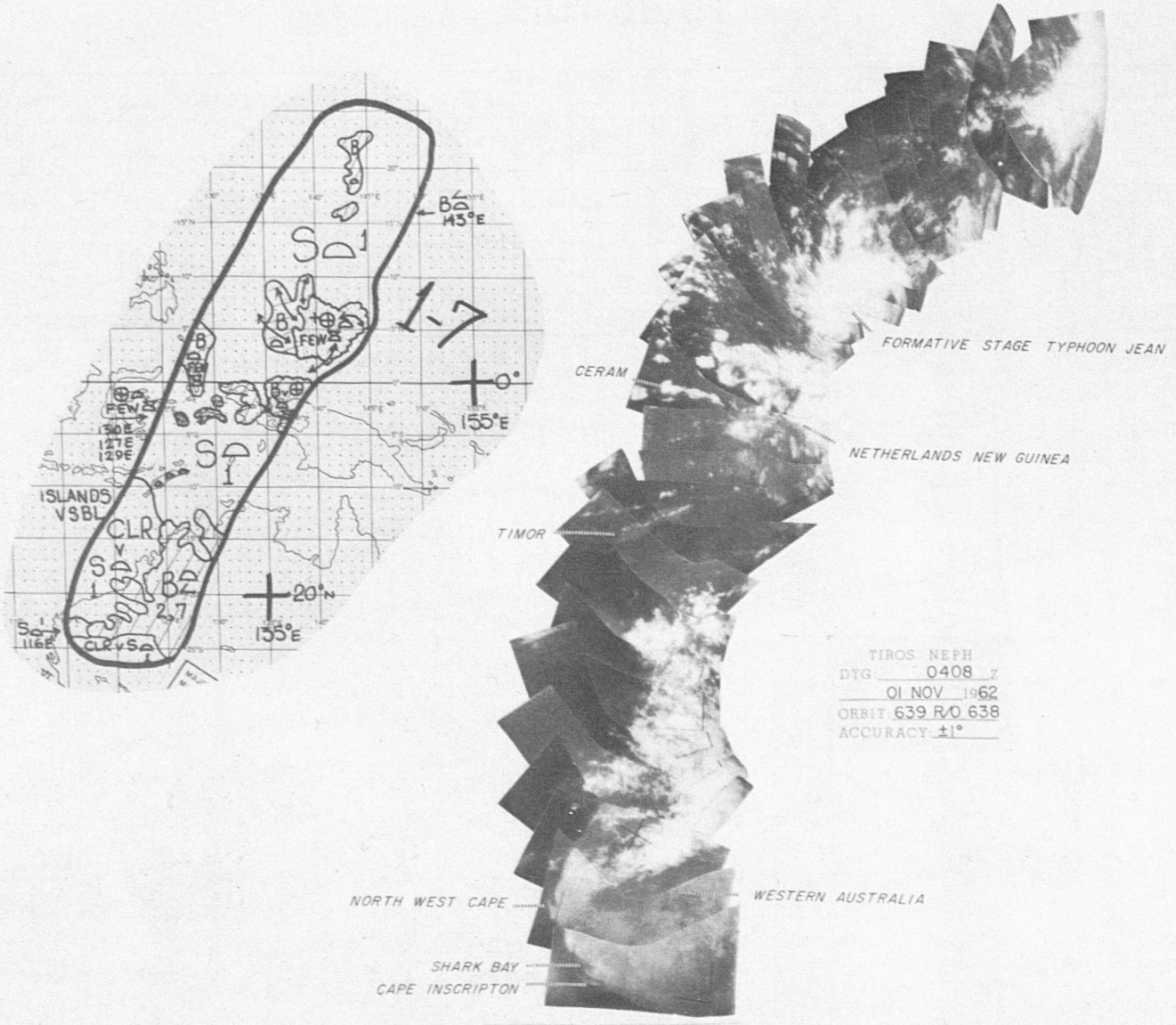
FORMATIVE STAGE TYPHOON JEAN
CERAM
NETHERLANDS NEW GUINEA
TIMOR
NORTH WEST CAPE
WESTERN AUSTRALIA
SHARK BAY
CAPE INSCRIPTON
TIROS NEPH
DTG 0408 Z
01 NOV 1962
ORBIT 639 R/O 638
ACCURACY ±1°
ISLANDS VSBL
CLR
FEW
SD 1
1-7
155°E
20°N
143°E
116E

FIGURE 96

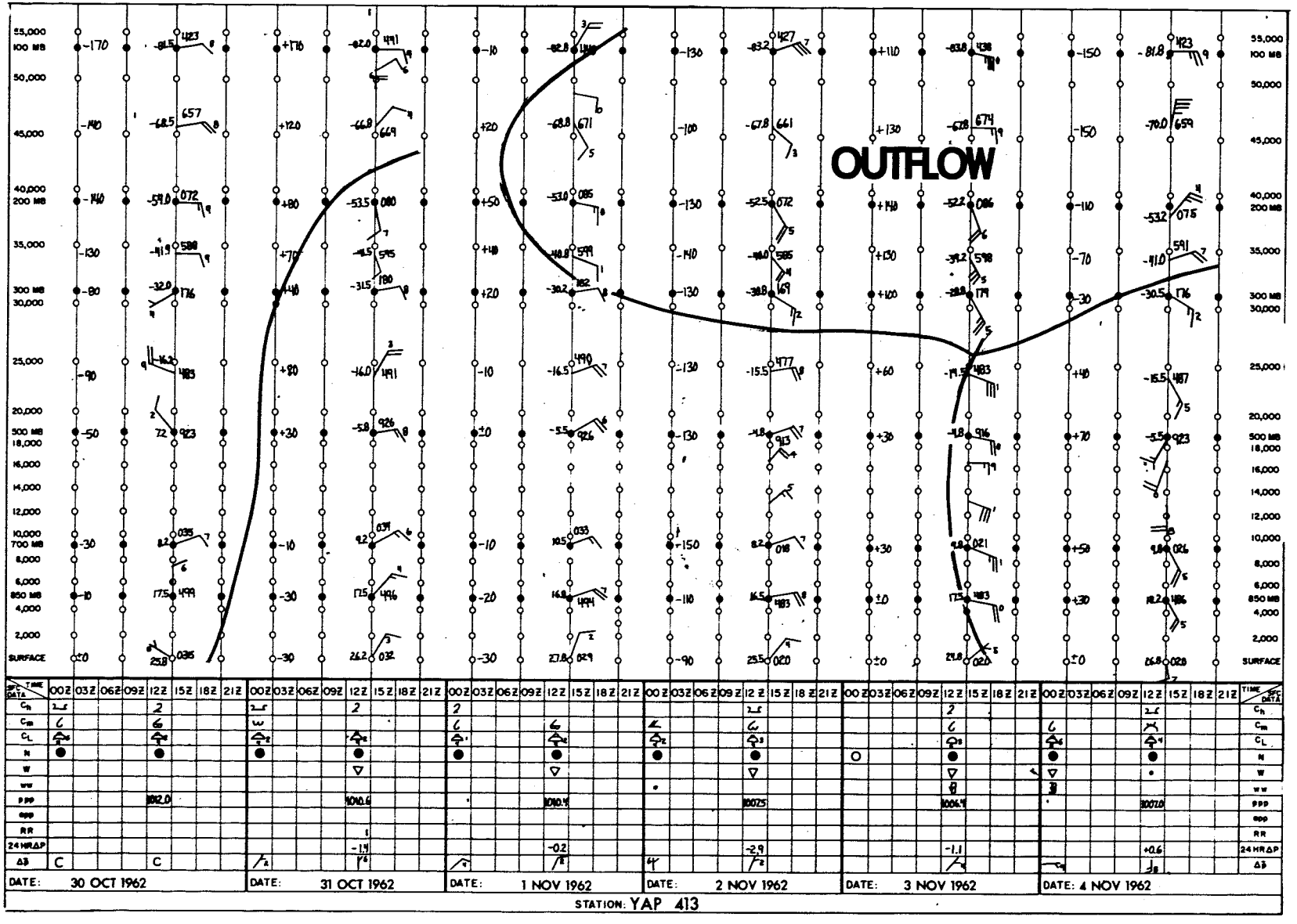
OUTFLOW
55,000
100 MB
50,000
45,000
40,000
200 MB
35,000
300 MB
30,000
25,000
20,000
500 MB
18,000
16,000
14,000
12,000
10,000
700 MB
8,000
6,000
850 MB
4,000
2,000
SURFACE
TIME
SFC DATA
00Z 03Z 06Z 09Z 12Z 15Z 18Z 21Z
Ch
Cm
CL
N
W
ww
PPP
ppp
RR
24 HR ΔP
Δ3
DATE: 30 OCT 1962
DATE: 31 OCT 1962
DATE: 1 NOV 1962
DATE: 2 NOV 1962
DATE: 3 NOV 1962
DATE: 4 NOV 1962
STATION: YAP 413

FIGURE 97

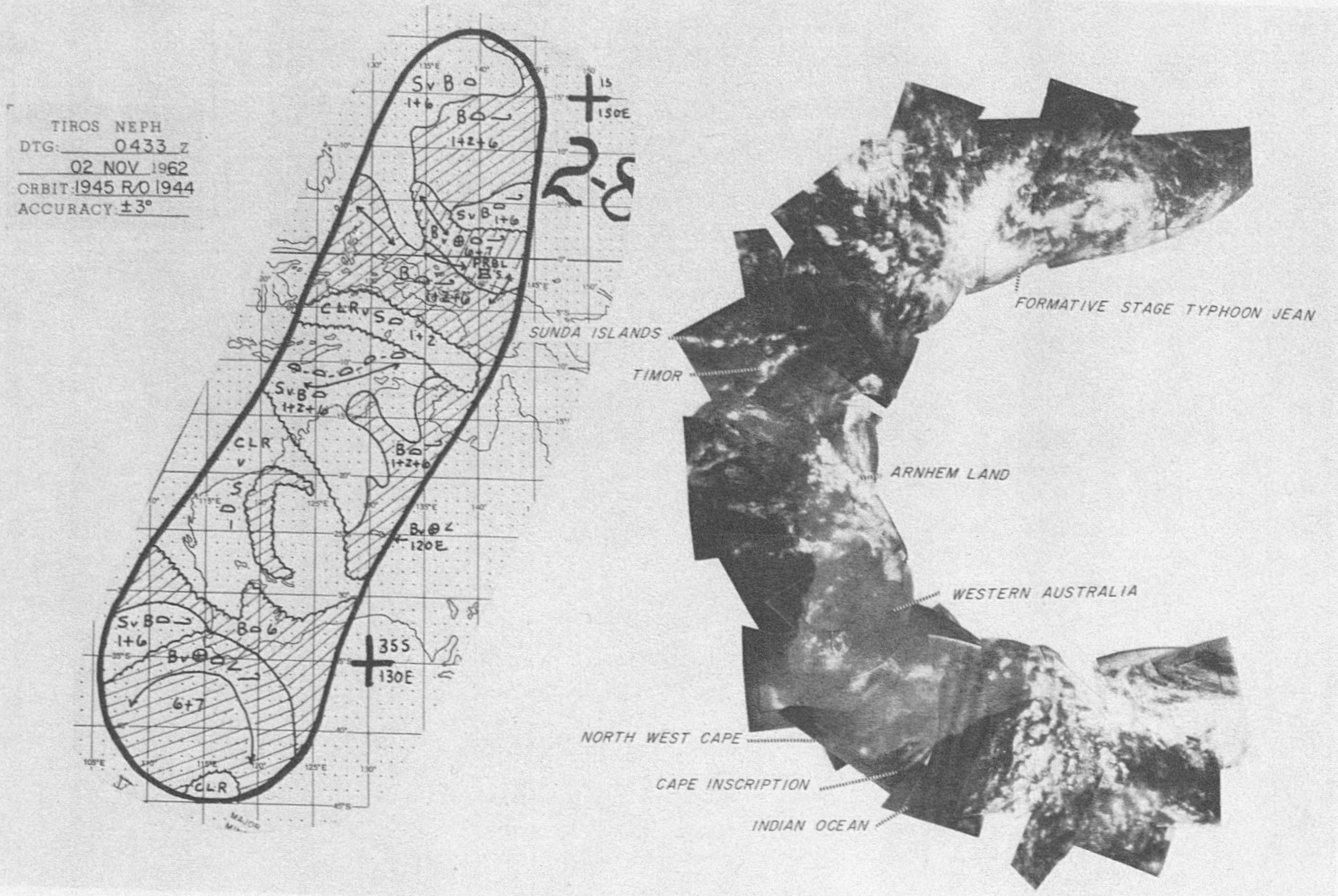
TIROS NEPH
DTG: 0433 Z
02 NOV 1962
ORBIT 1945 R/O 1944
ACCURACY ±3°
SUNDA ISLANDS
TIMOR
ARNHEM LAND
WESTERN AUSTRALIA
NORTH WEST CAPE
CAPE INSCRIPTION
INDIAN OCEAN
FORMATIVE STAGE TYPHOON JEAN

FIGURE 98

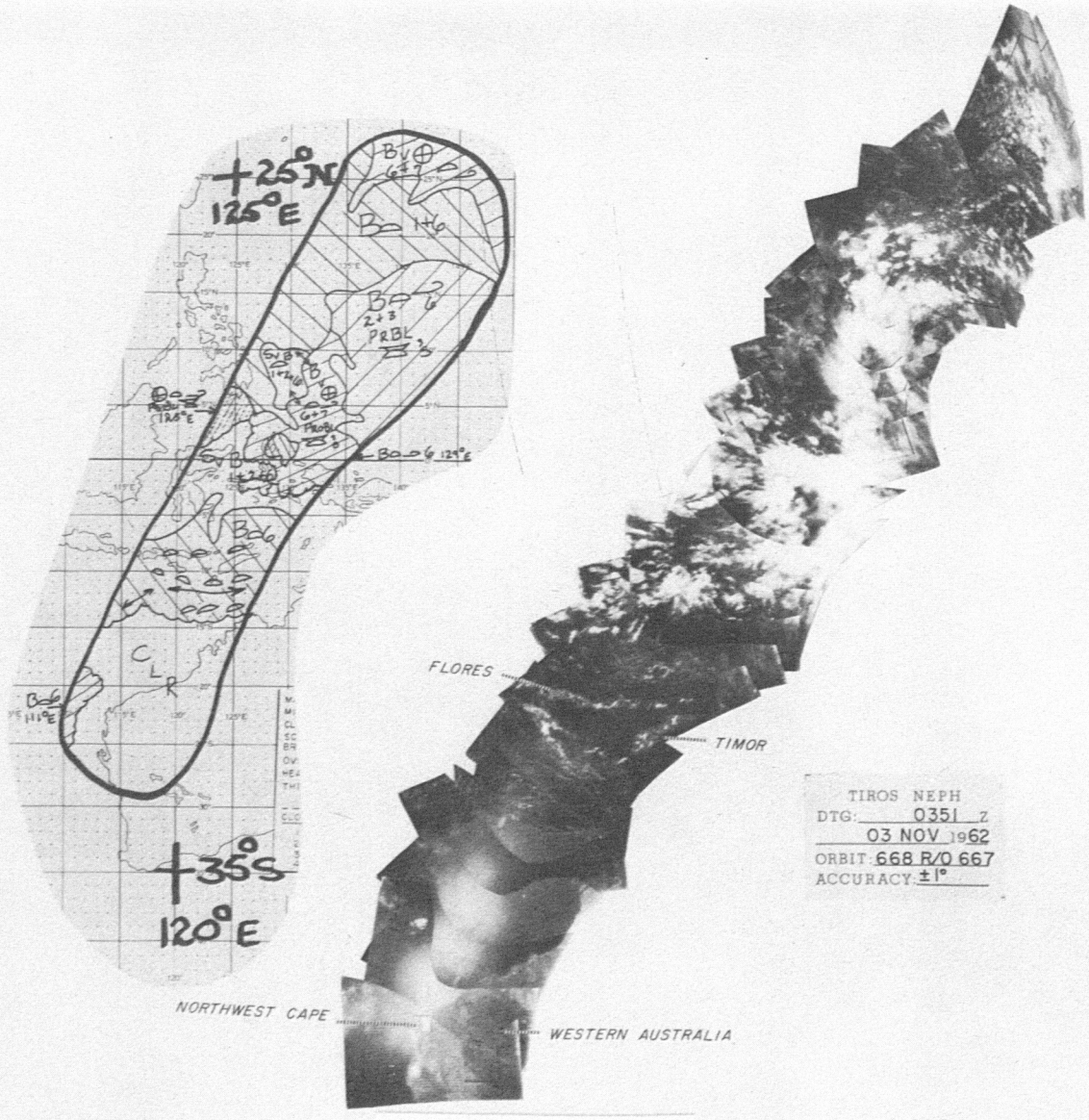
+25°N
125°E
+35°S
120°E
FLORES
TIMOR
NORTHWEST CAPE
WESTERN AUSTRALIA
TIROS NEPH
DTG: 0351 Z
03 NOV 1962
ORBIT: 668 R/O 667
ACCURACY: ±1°

FIGURE 99

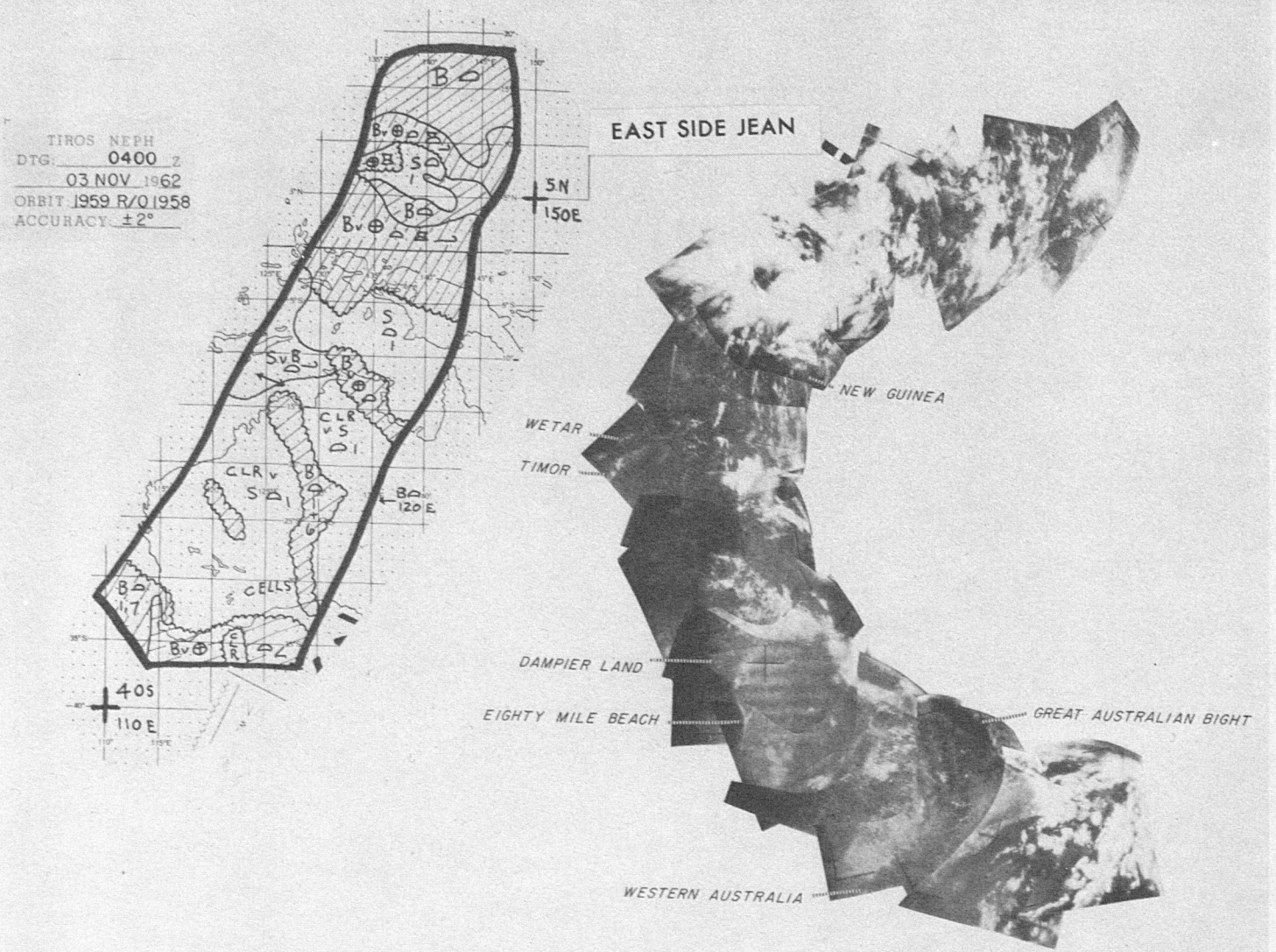
TIROS NEPH
DTG: 0400 Z
03 NOV 1962
ORBIT 1959 R/O 1958
ACCURACY ±2°
EAST SIDE JEAN
5N
150E
40S
110E
120E
CELLS
NEW GUINEA
WETAR
TIMOR
DAMPIER LAND
EIGHTY MILE BEACH
GREAT AUSTRALIAN BIGHT
WESTERN AUSTRALIA

FIGURE 100

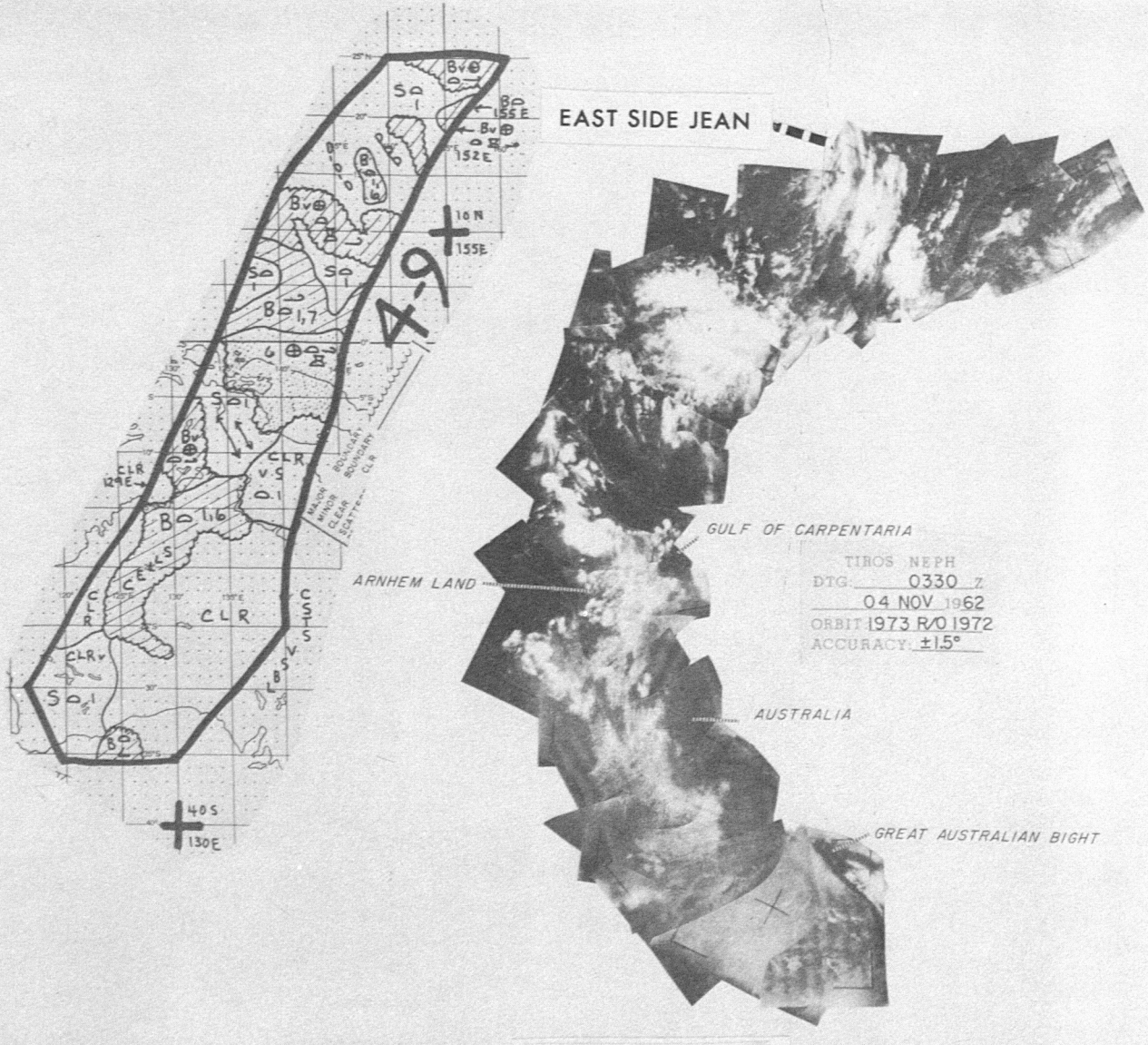
EAST SIDE JEAN
GULF OF CARPENTARIA
ARNHEM LAND
AUSTRALIA
GREAT AUSTRALIAN BIGHT
TIROS NEPH
DTG: 0330 Z
04 NOV 1962
ORBIT 1973 R/O 1972
ACCURACY: ±1.5°
4-9
10 N
155E
40 S
130E

FIGURE 101

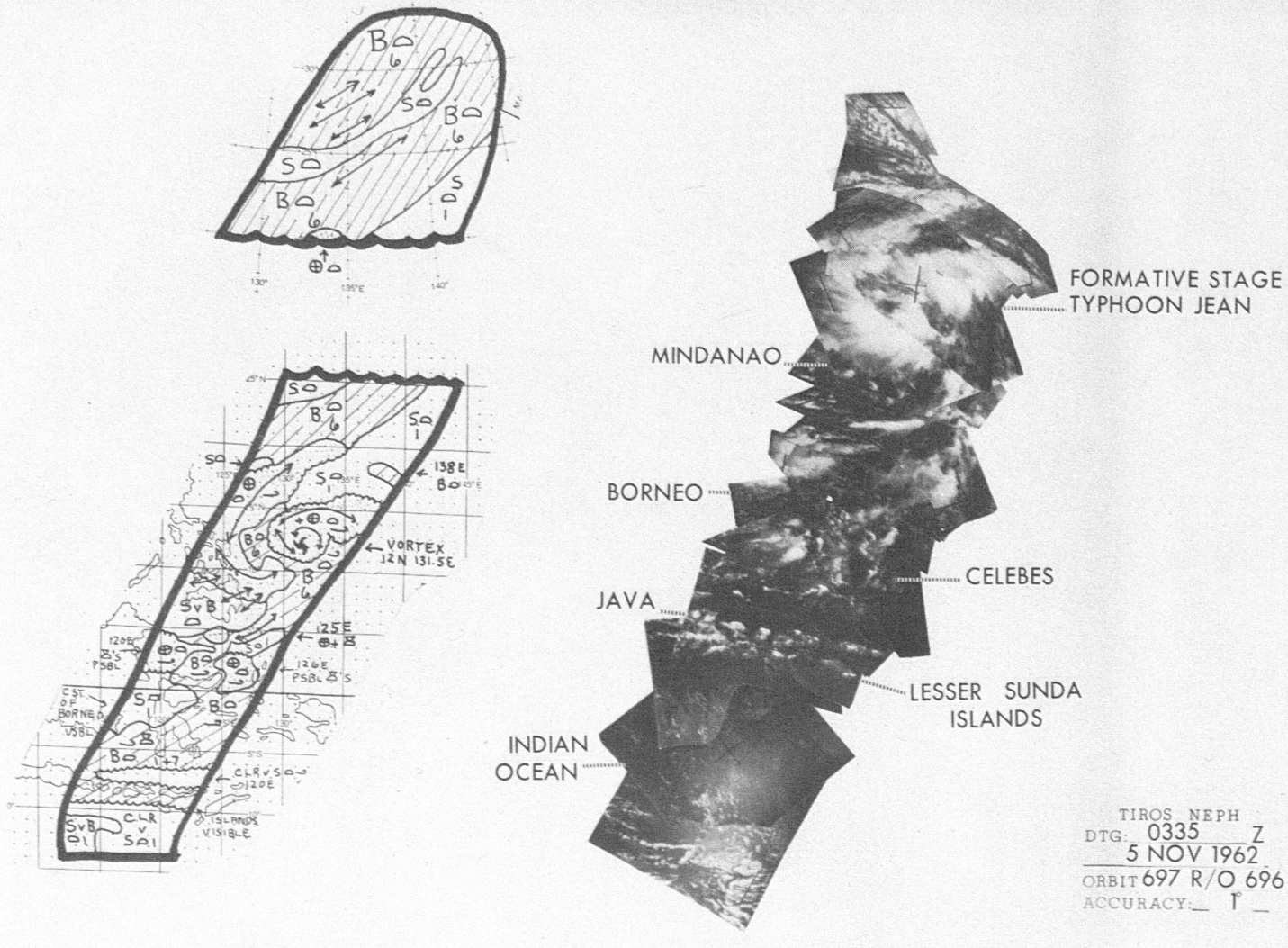
FORMATIVE STAGE
TYPHOON JEAN
MINDANAO
BORNEO
CELEBES
JAVA
LESSER SUNDA
ISLANDS
INDIAN
OCEAN
VORTEX
12N 131.5E
TIROS NEPH
DTG: 0335 Z
5 NOV 1962
ORBIT 697 R/O 696
ACCURACY: 1°

FIGURE 102

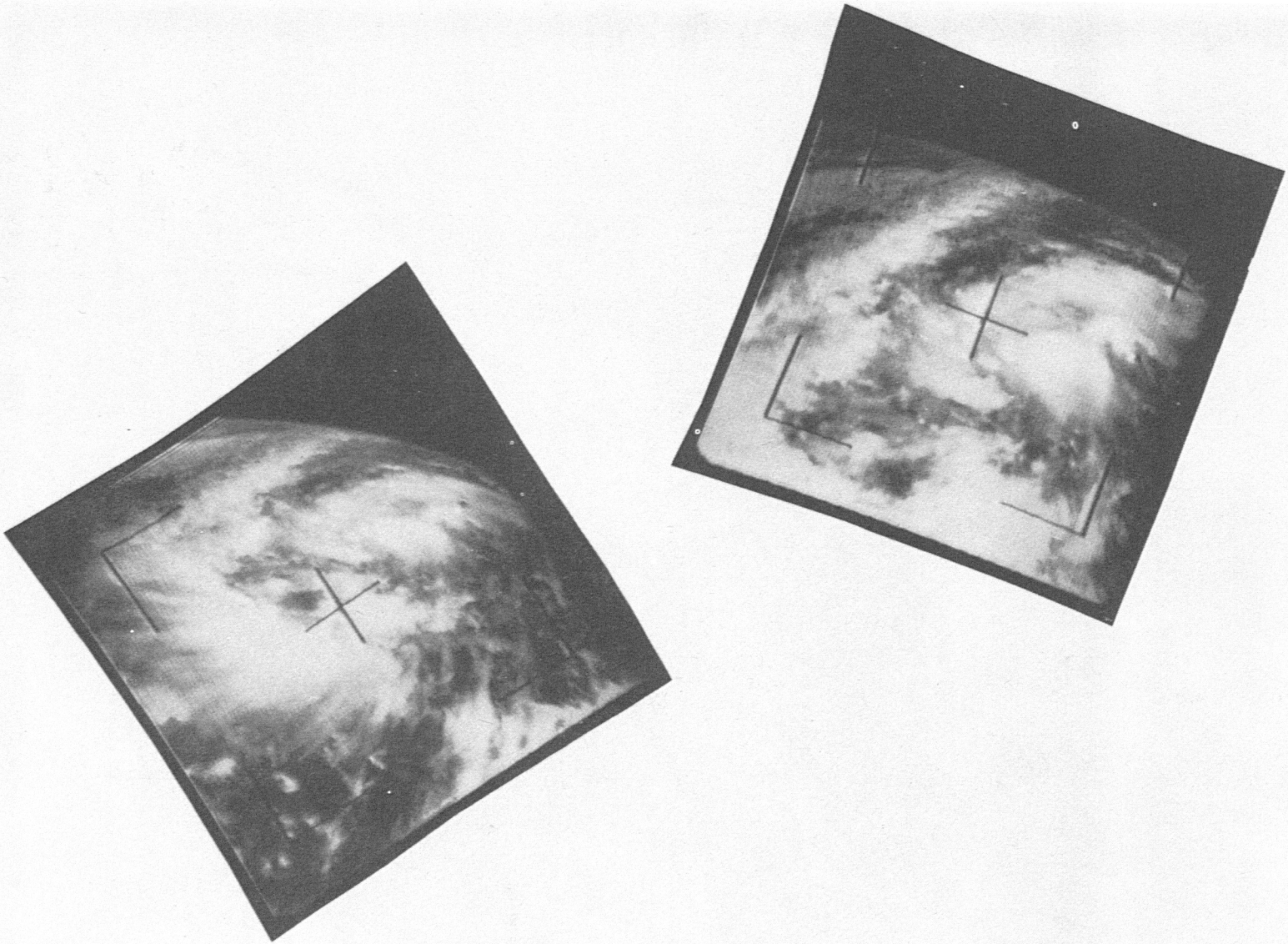

FIGURE 103

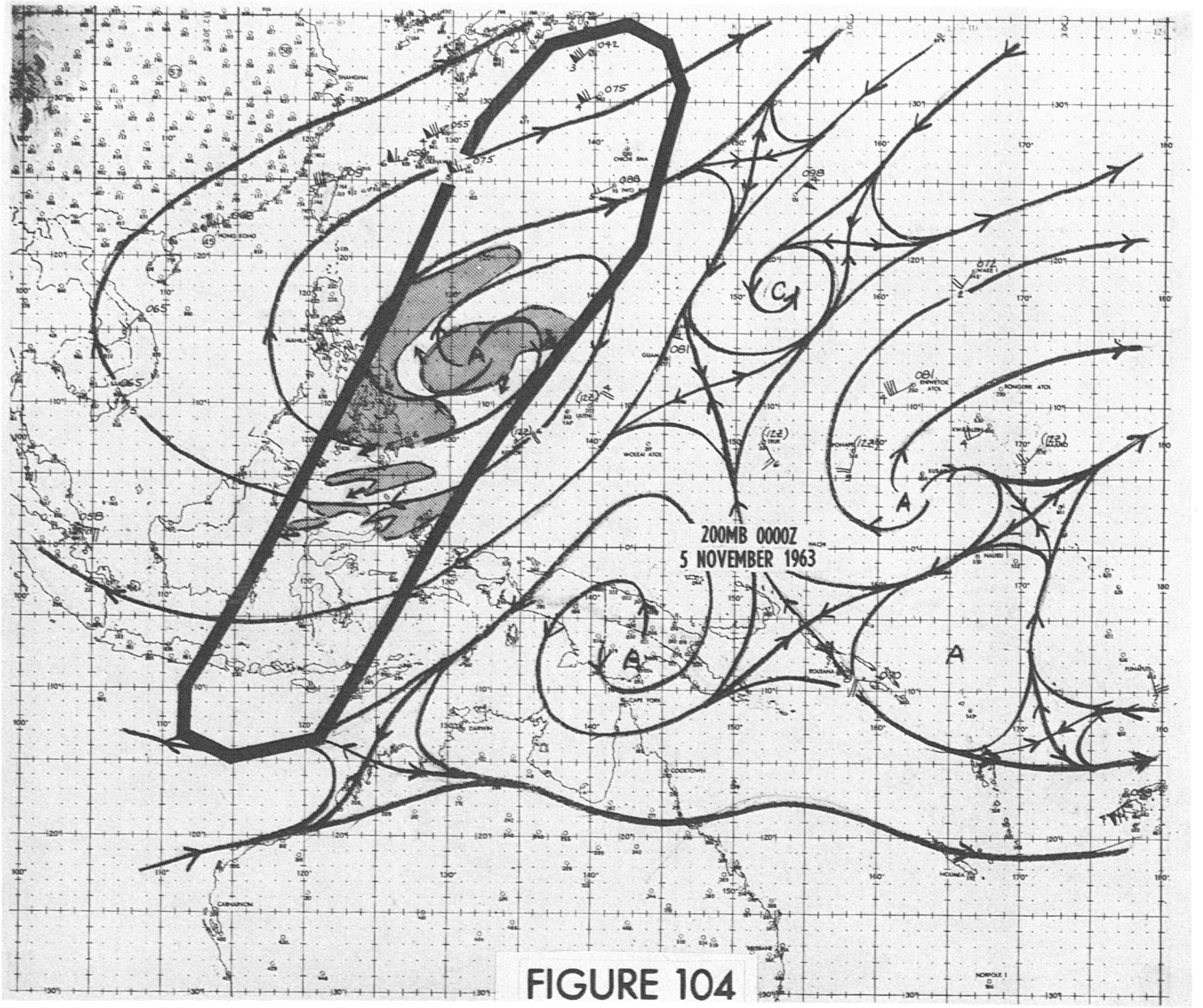


FIGURE 104

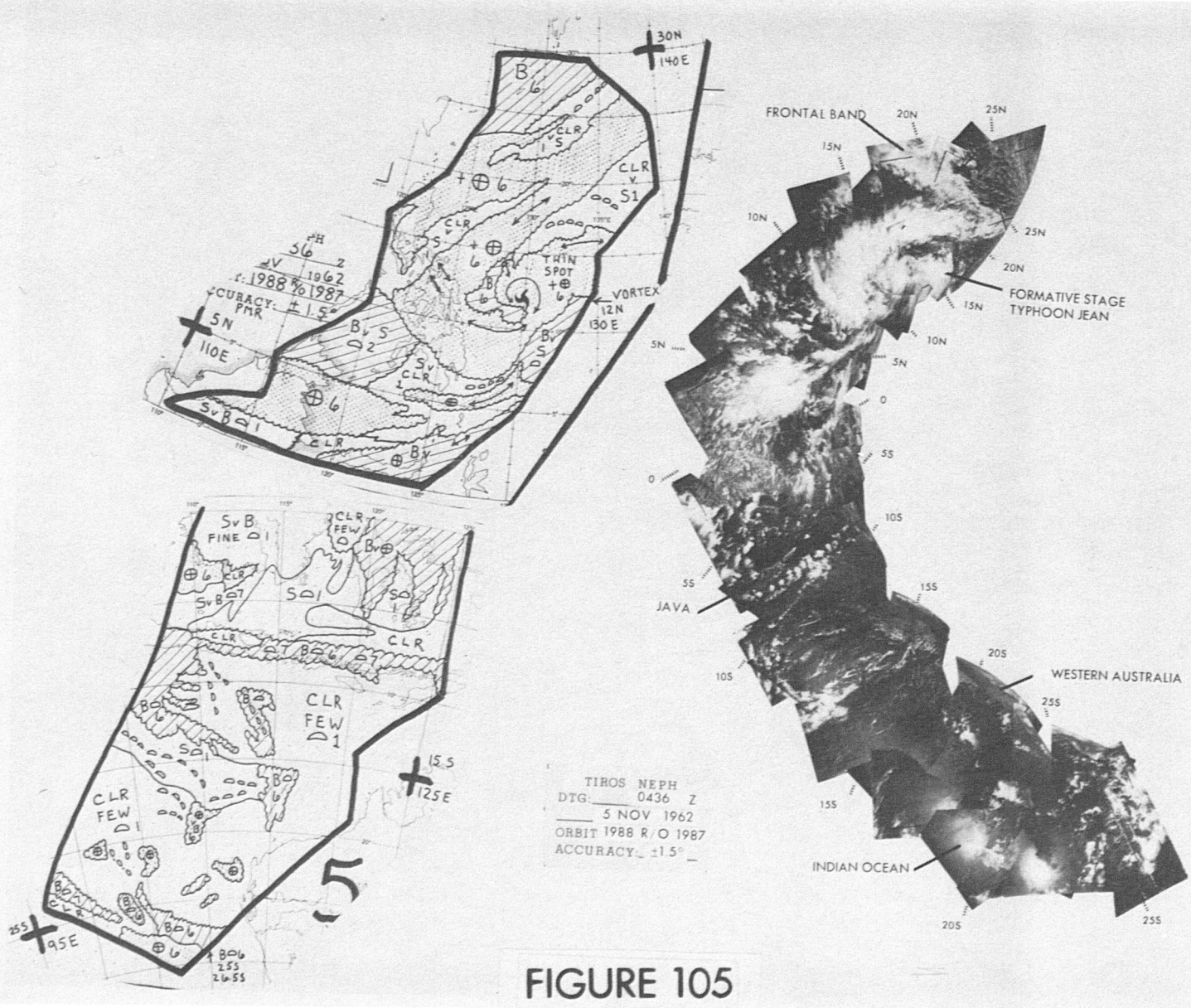
30N
140E
FRONTAL BAND
FORMATIVE STAGE
TYPHOON JEAN
VORTEX
12N
130E
THIN
SPOT
5N
110E
JAVA
WESTERN AUSTRALIA
INDIAN OCEAN
15S
125E
25S
95E
TIROS NEPH
DTG: 0436 Z
5 NOV 1962
ORBIT 1988 R/O 1987
ACCURACY: ±1.5°

FIGURE 105

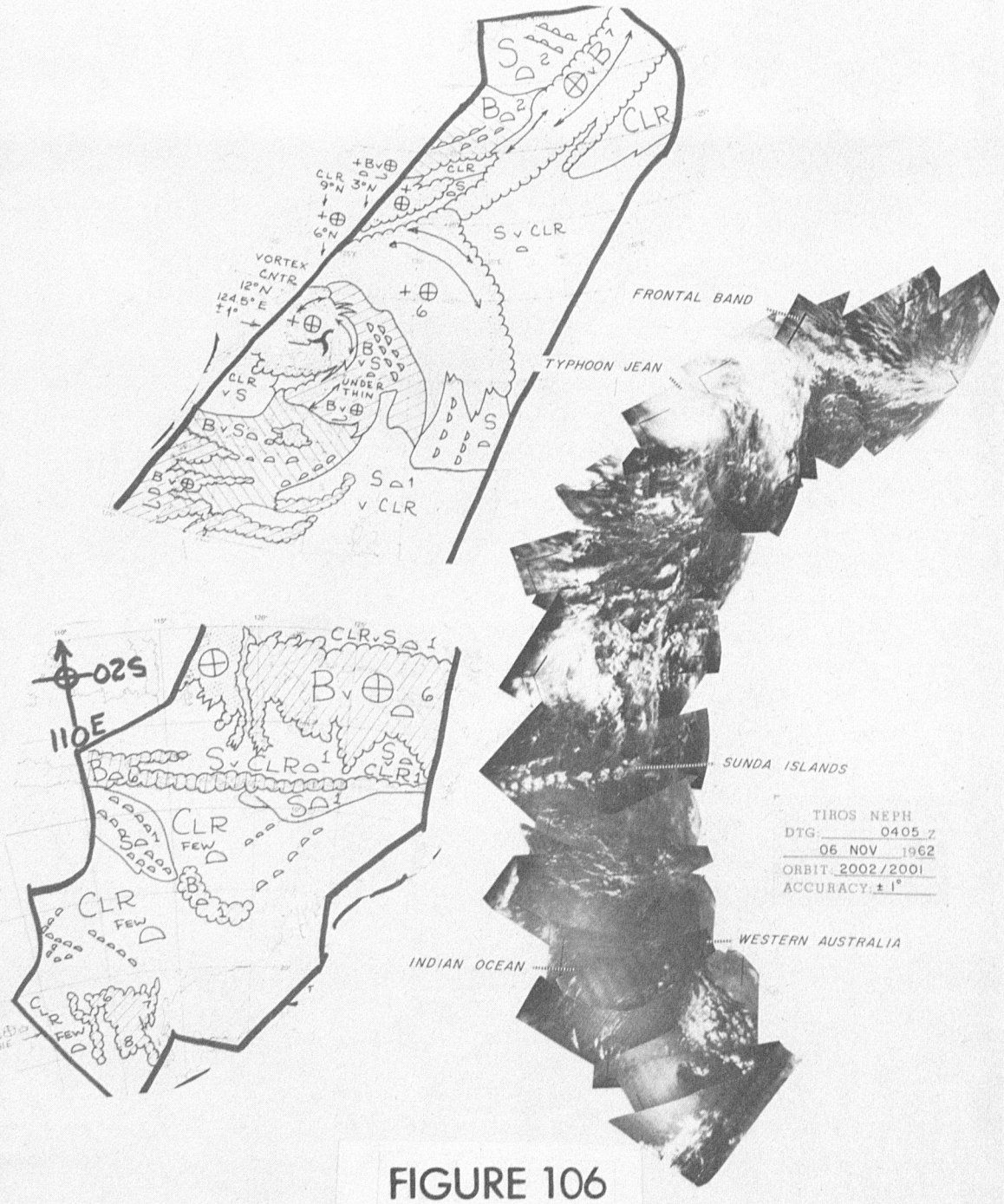
FRONTAL BAND
TYPHOON JEAN
SUNDA ISLANDS
WESTERN AUSTRALIA
INDIAN OCEAN
TIROS NEPH
DTG: 0405 Z
06 NOV 1962
ORBIT 2002/2001
ACCURACY ± 1°
VORTEX CNTR
12°N
124.5°E
±1°
CLR
FEW
UNDER THIN
025
110E

FIGURE 106

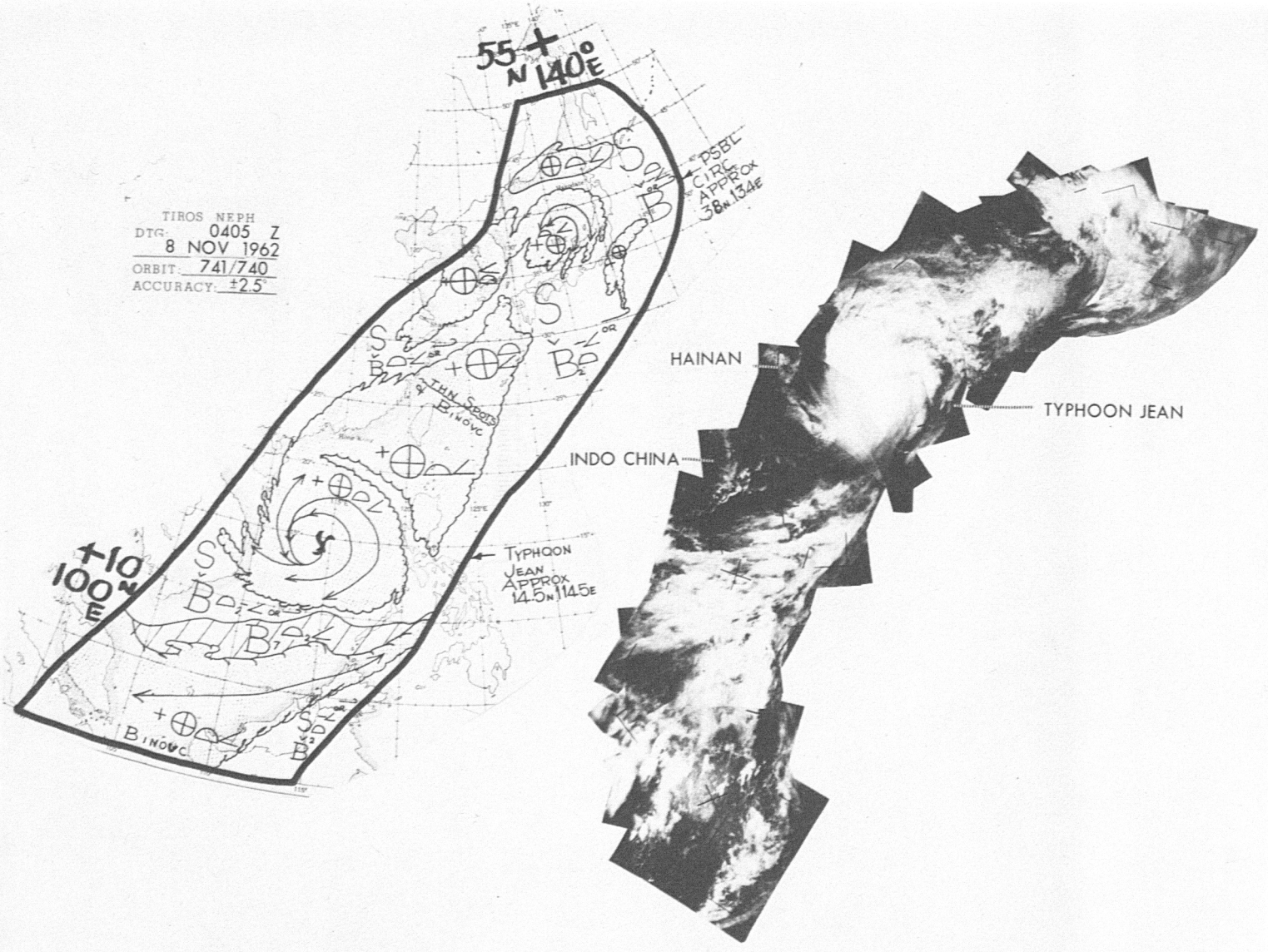
55+
N 140°E
TIROS NEPH
DTG: 0405 Z
8 NOV 1962
ORBIT: 741/740
ACCURACY: ±2.5°
PSBL CIRC APPROX 38N 134E
HAINAN
TYPHOON JEAN
INDO CHINA
THN Spots Binovc
Typhoon Jean Approx 14.5N 114.5E
+10
100
E
Binovc

FIGURE 107

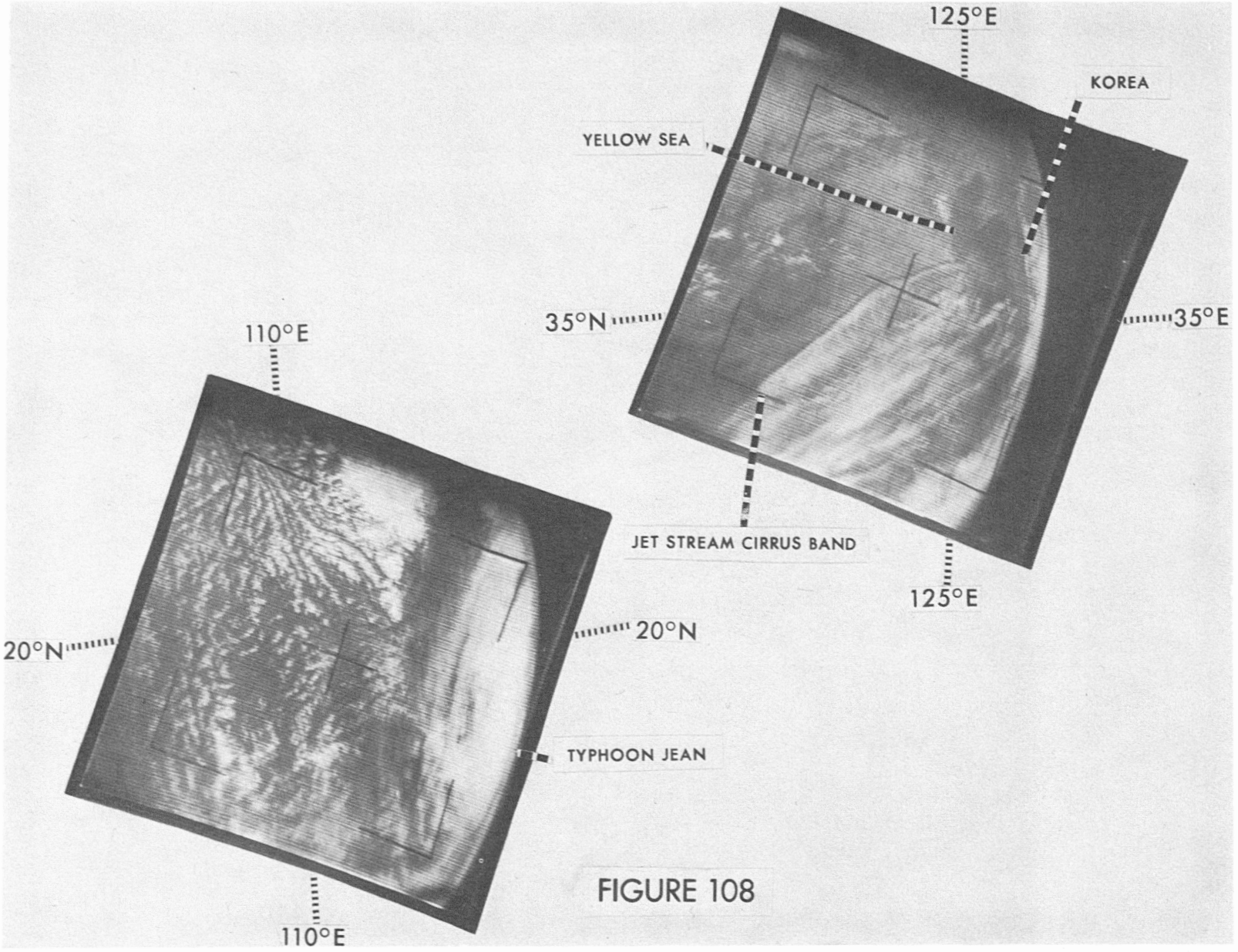
125°E
KOREA
YELLOW SEA
35°N
35°E
JET STREAM CIRRUS BAND
125°E
110°E
20°N
20°N
TYPHOON JEAN
110°E

FIGURE 108

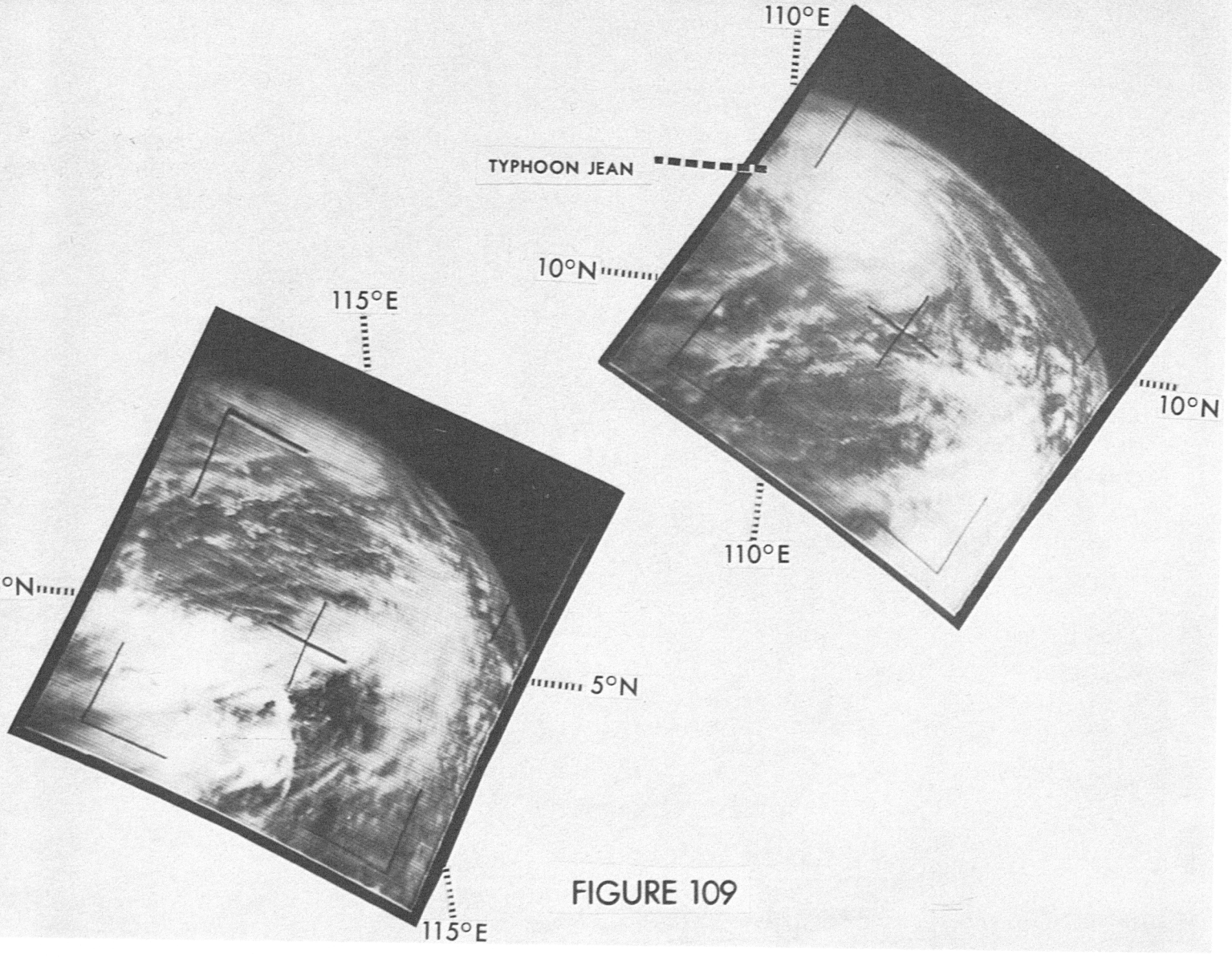


FIGURE 109

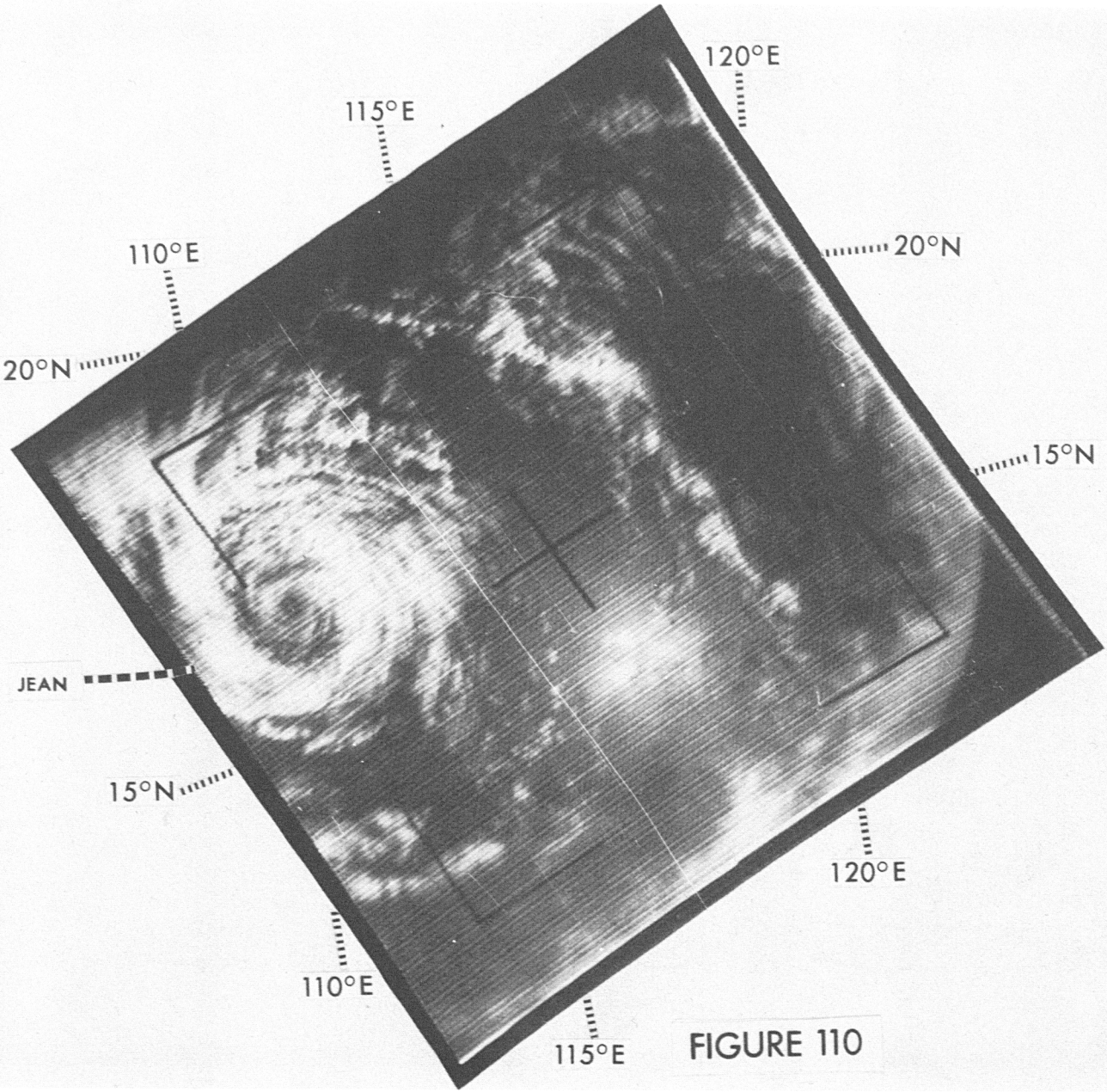


FIGURE 110

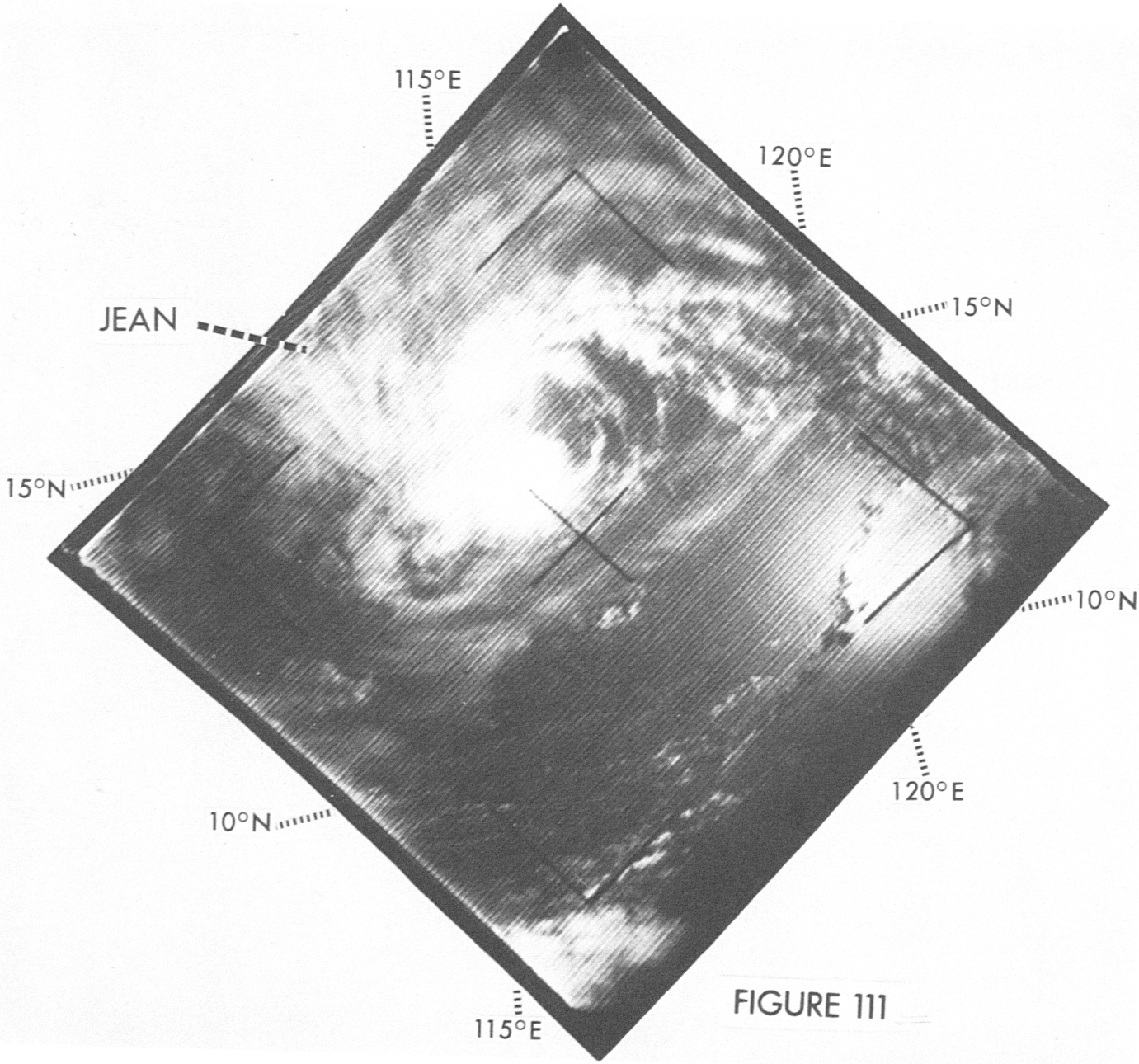


FIGURE 111

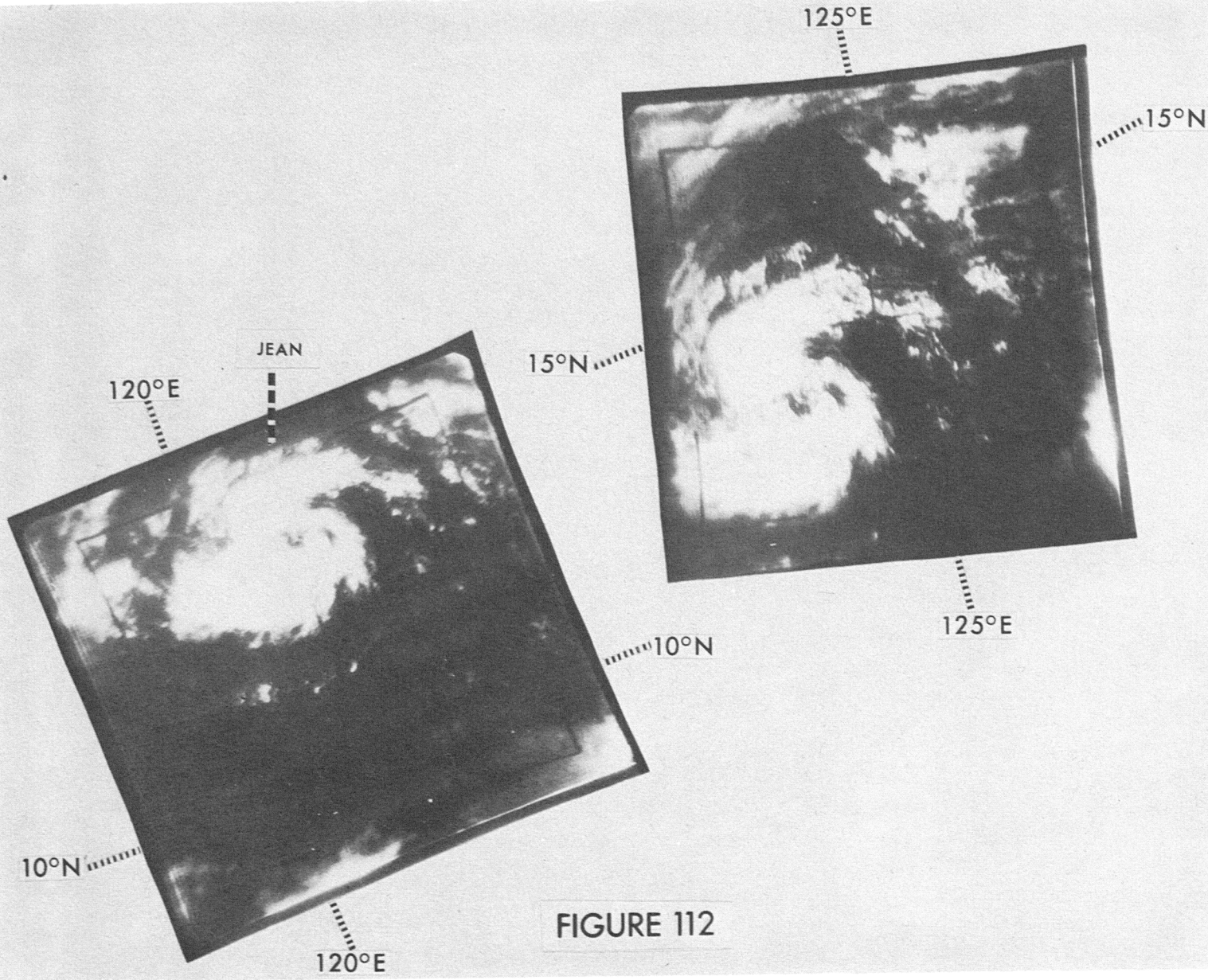


FIGURE 112

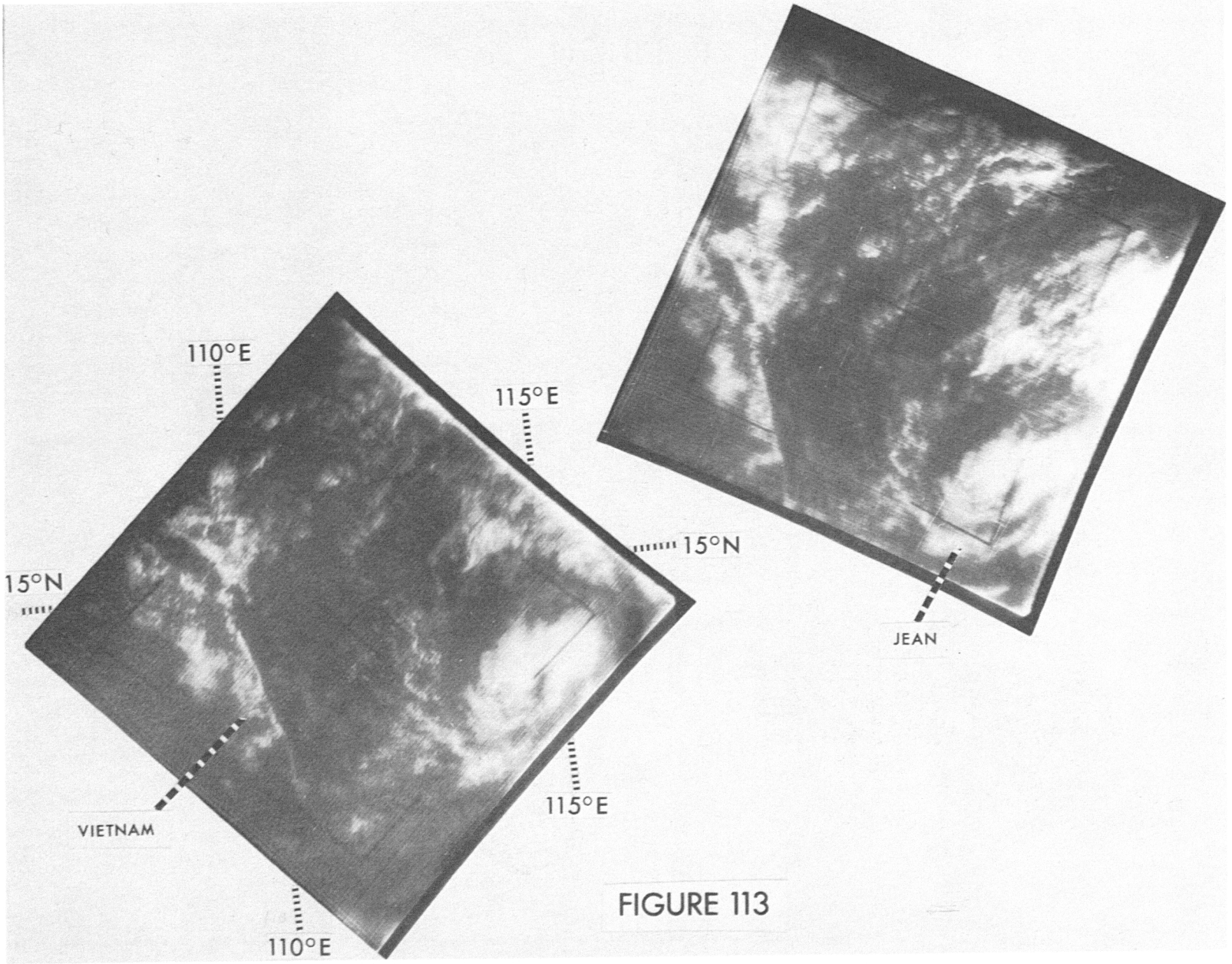


FIGURE 113

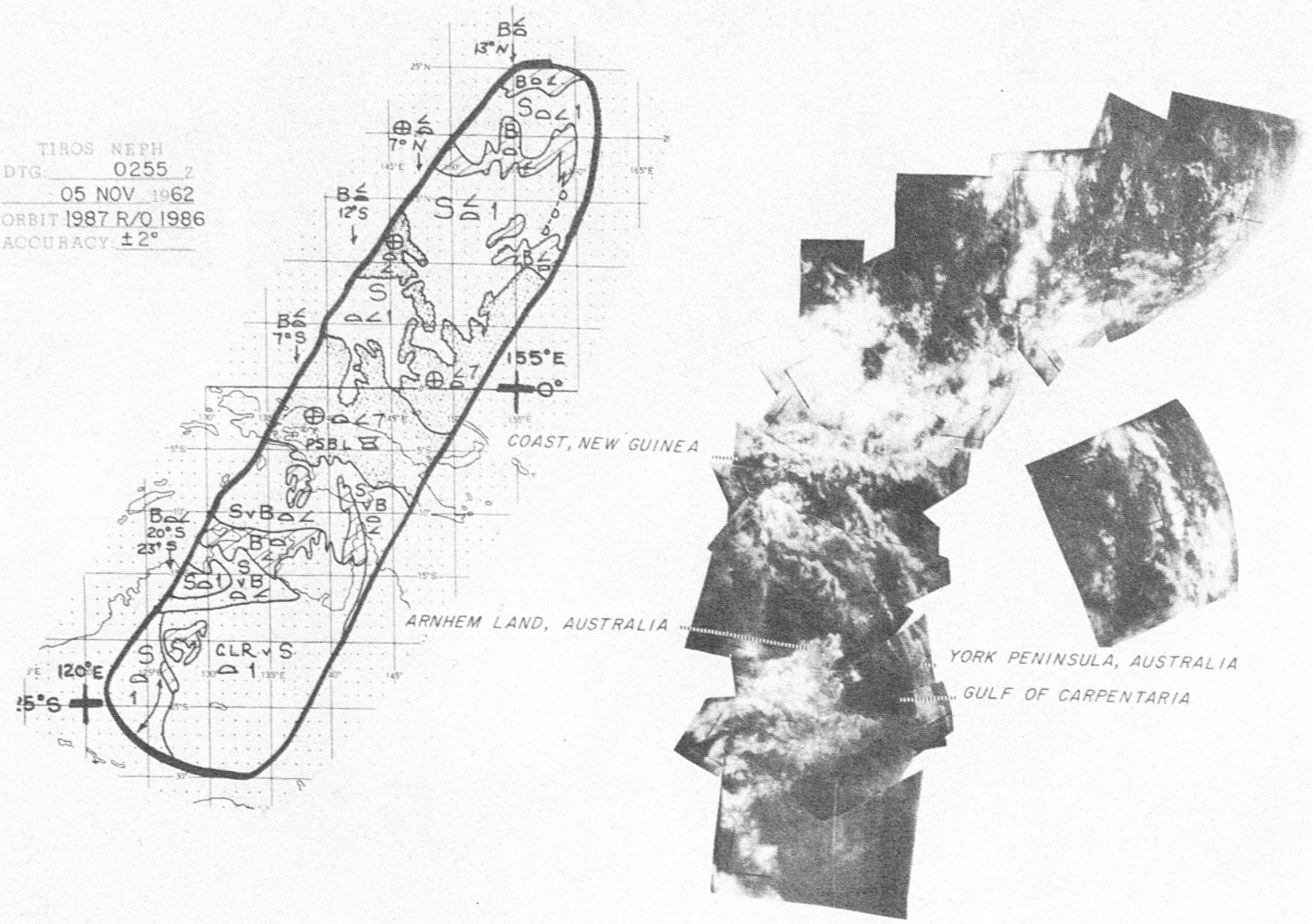
TIROS NEPH
DTG: 0255 Z
05 NOV 1962
ORBIT 1987 R/O 1986
ACCURACY: ±2°
13°N
7°N
12°S
7°S
20°S
23°S
155°E
0°
120°E
25°S
PSBL
CLR v S
COAST, NEW GUINEA
ARNHEM LAND, AUSTRALIA
YORK PENINSULA, AUSTRALIA
GULF OF CARPENTARIA

FIGURE 114

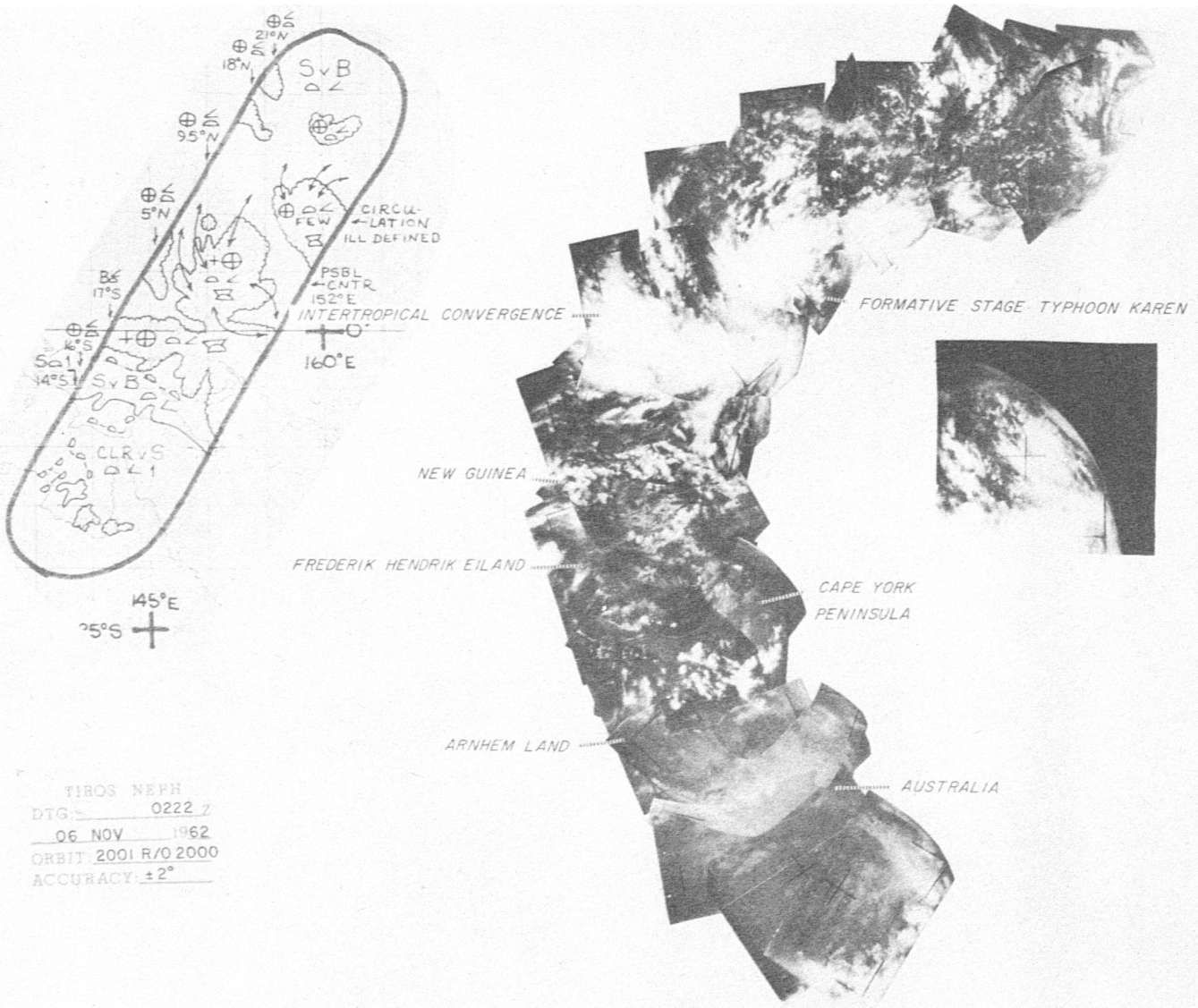
21°N
18°N
S v B
9.5°N
5°N
CIRCU-
LATION
ILL DEFINED
FEW
PSBL
CNTR
152°E
17°S
INTERTROPICAL CONVERGENCE
160°E
14°S
S v B
CLR v S
145°E
FORMATIVE STAGE TYPHOON KAREN
NEW GUINEA
FREDERIK HENDRIK EILAND
CAPE YORK
PENINSULA
ARNHEM LAND
AUSTRALIA
TIROS NEPH
DTG: 0222 Z
06 NOV 1962
ORBIT: 2001 R/O 2000
ACCURACY: ±2°

FIGURE 115

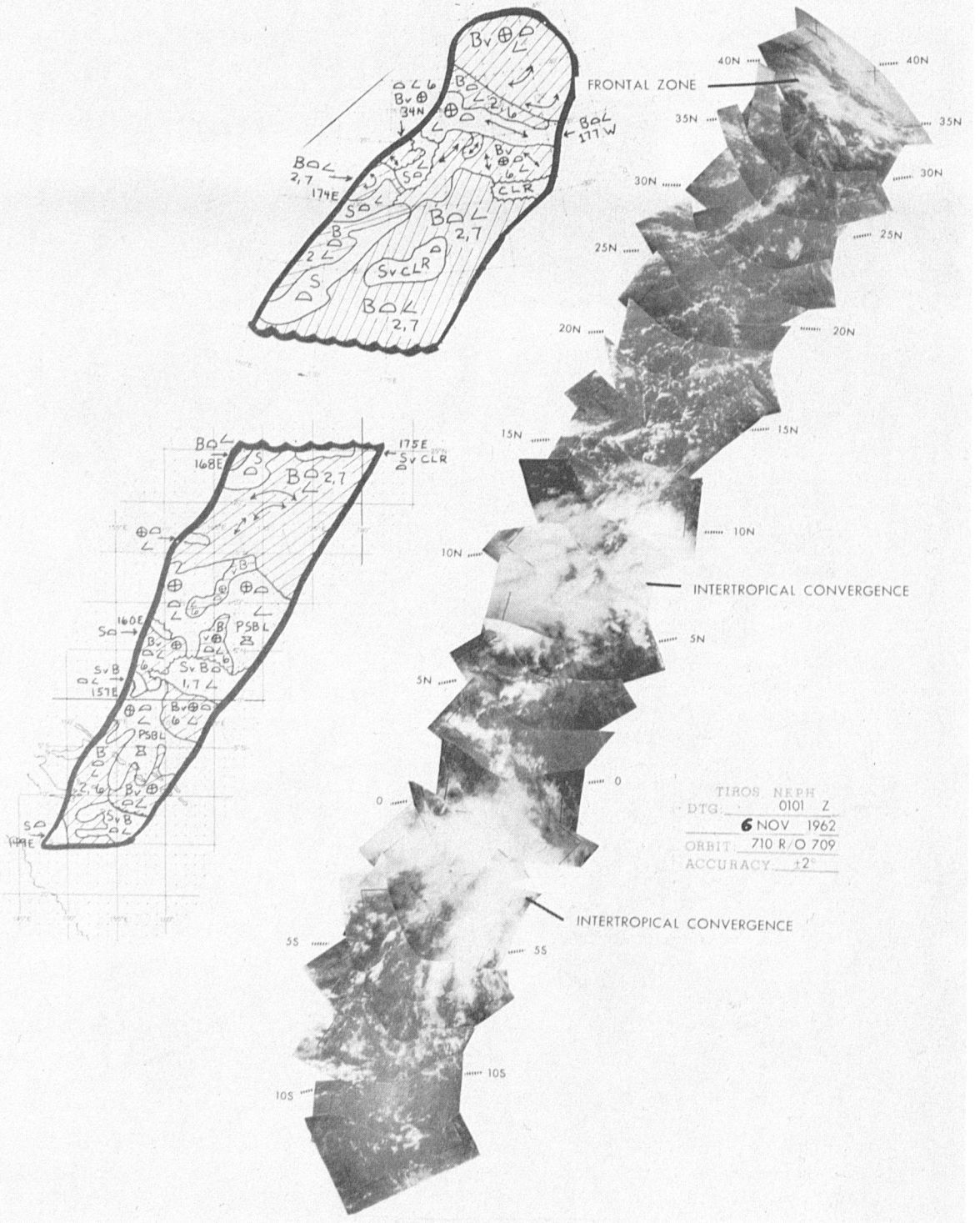
FRONTAL ZONE
INTERTROPICAL CONVERGENCE
INTERTROPICAL CONVERGENCE
40N
35N
30N
25N
20N
15N
10N
5N
0
5S
10S
TIROS NEPH
DTG 0101 Z
6 NOV 1962
ORBIT 710 R/O 709
ACCURACY ±2°

FIGURE 116

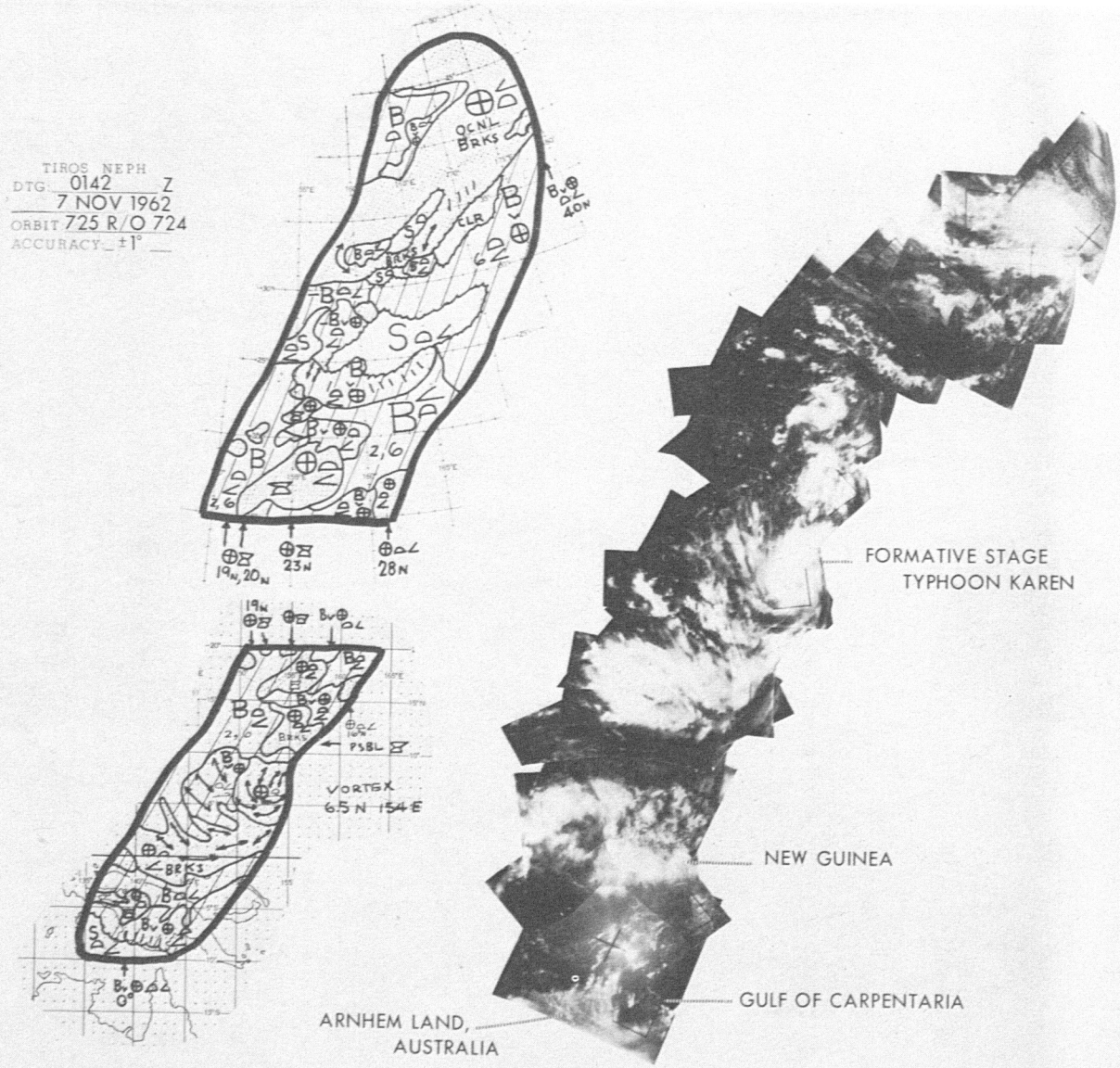
TIROS NEPH
DTG: 0142 Z
7 NOV 1962
ORBIT 725 R/O 724
ACCURACY: ±1°
OCNL BRKS
CLR
19N, 20N
23N
28N
40N
VORTEX
6.5 N 154 E
PSBL
BRKS
FORMATIVE STAGE
TYPHOON KAREN
NEW GUINEA
GULF OF CARPENTARIA
ARNHEM LAND,
AUSTRALIA

FIGURE 117

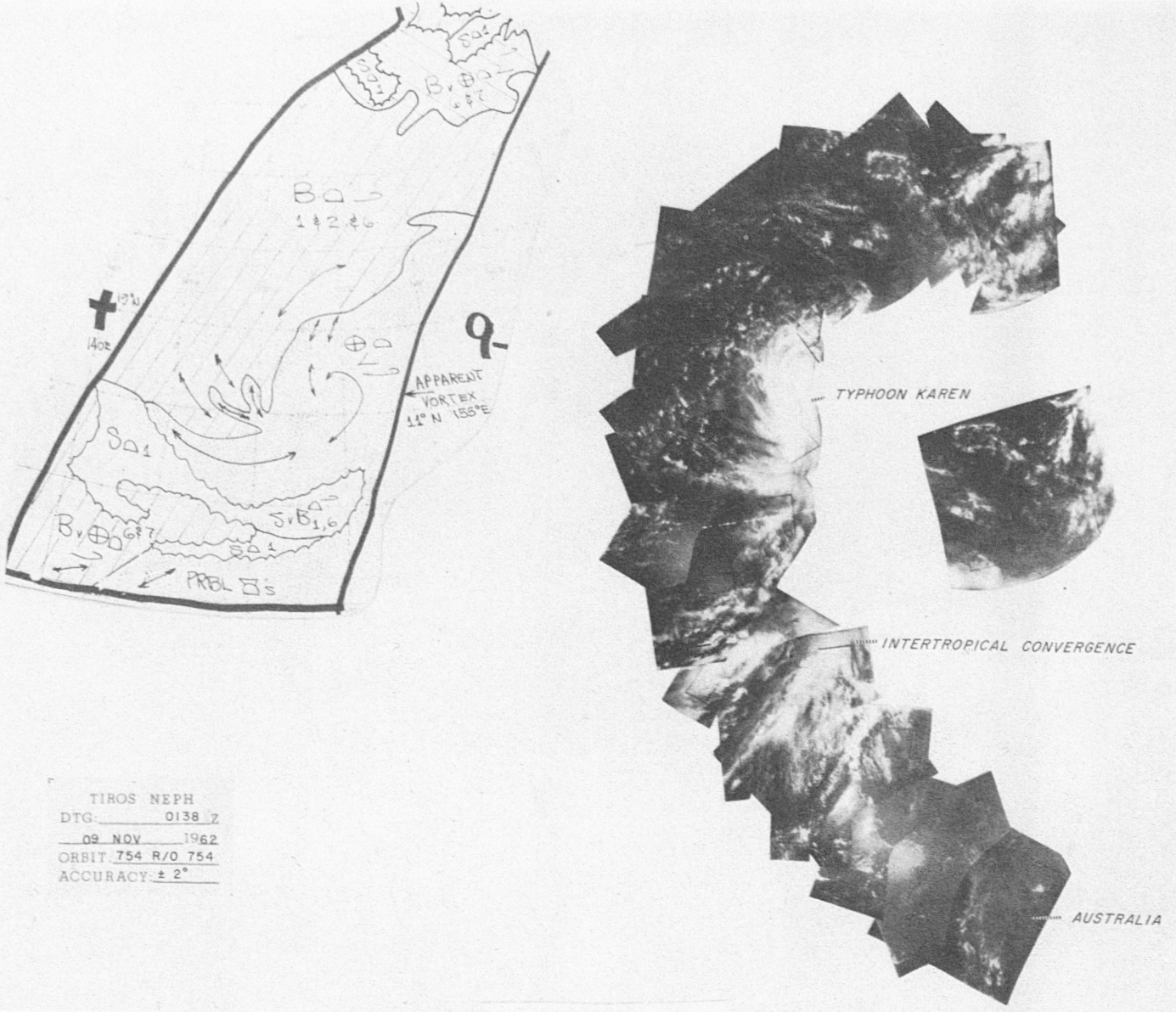
APPARENT VORTEX 11° N 156° E
TYPHOON KAREN
INTERTROPICAL CONVERGENCE
AUSTRALIA
TIROS NEPH
DTG: 0138 Z
09 NOV 1962
ORBIT 754 R/O 754
ACCURACY ± 2°

FIGURE 118

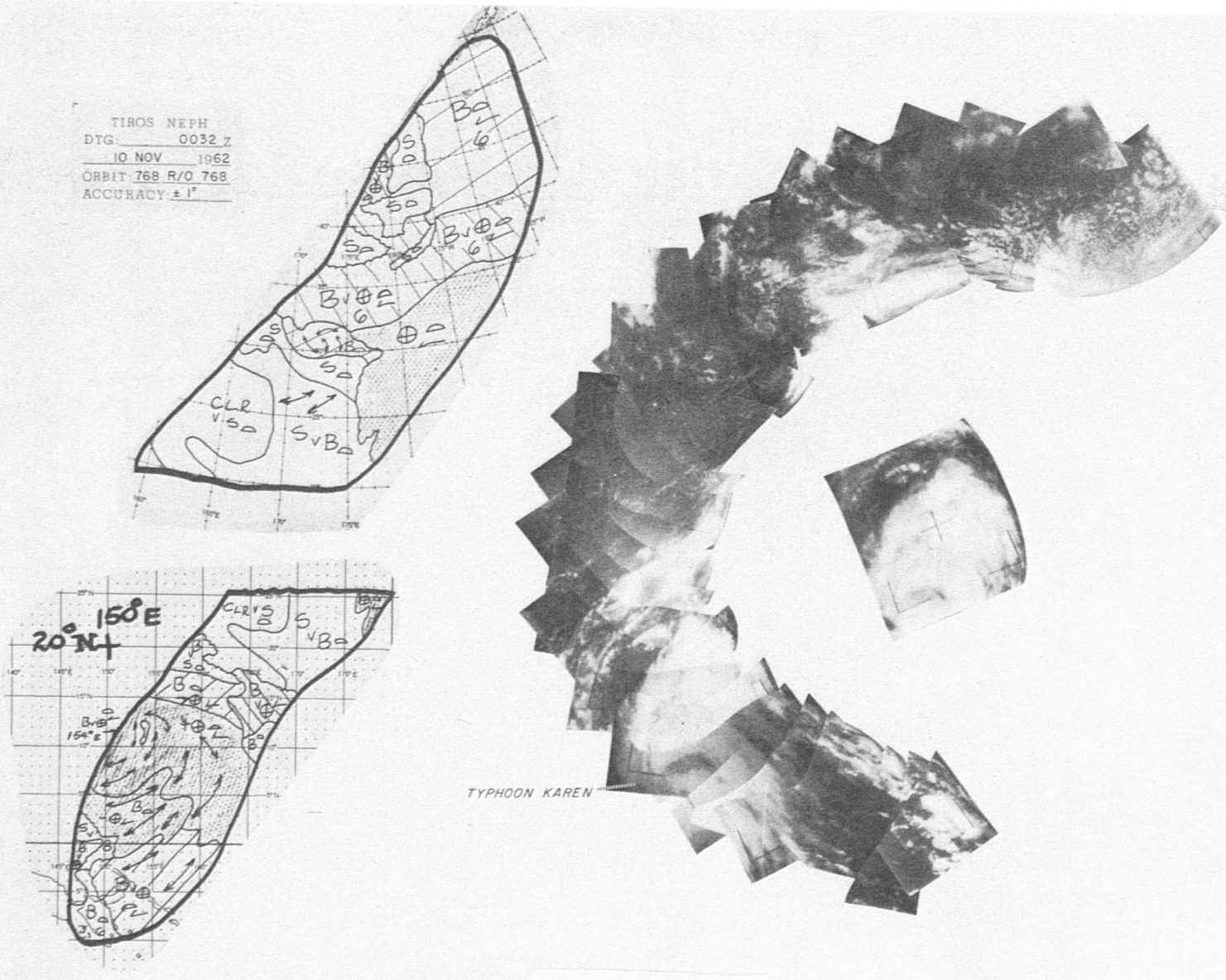
TIROS NEPH
DTG: 0032 Z
10 NOV 1962
ORBIT 768 R/O 768
ACCURACY ± 1°
150°E
20°N
TYPHOON KAREN

FIGURE 119

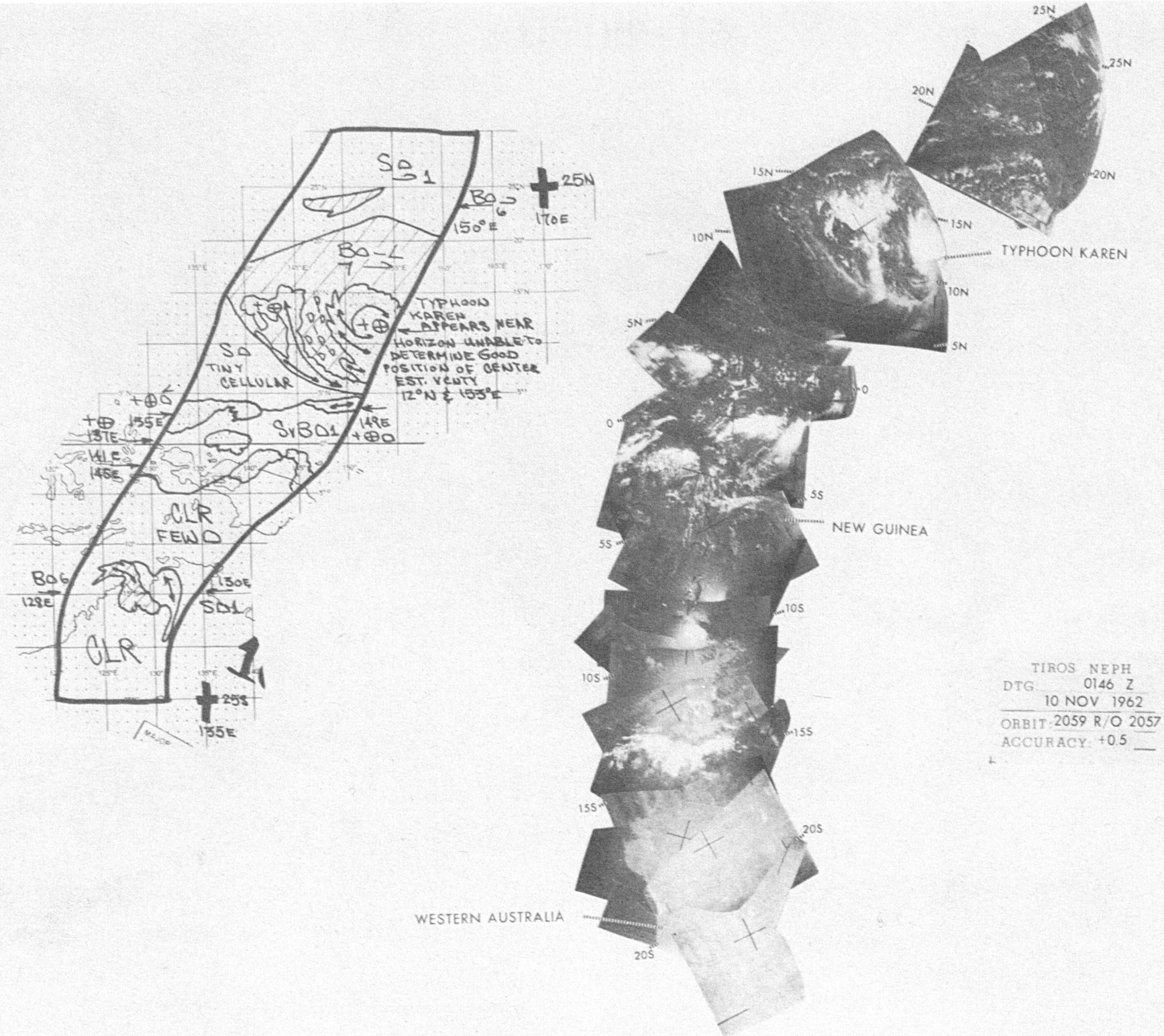
25N
170E
150°E
TYPHOON KAREN APPEARS NEAR HORIZON UNABLE TO DETERMINE GOOD POSITION OF CENTER EST. VCNTY 12°N & 153°E
TINY CELLULAR
CLR
FEWO
CLR
128E
130E
25S
135E
TYPHOON KAREN
NEW GUINEA
WESTERN AUSTRALIA
TIROS NEPH
DTG: 0146 Z
10 NOV 1962
ORBIT: 2059 R/O 2057
ACCURACY: ±0.5

# FIGURE 120

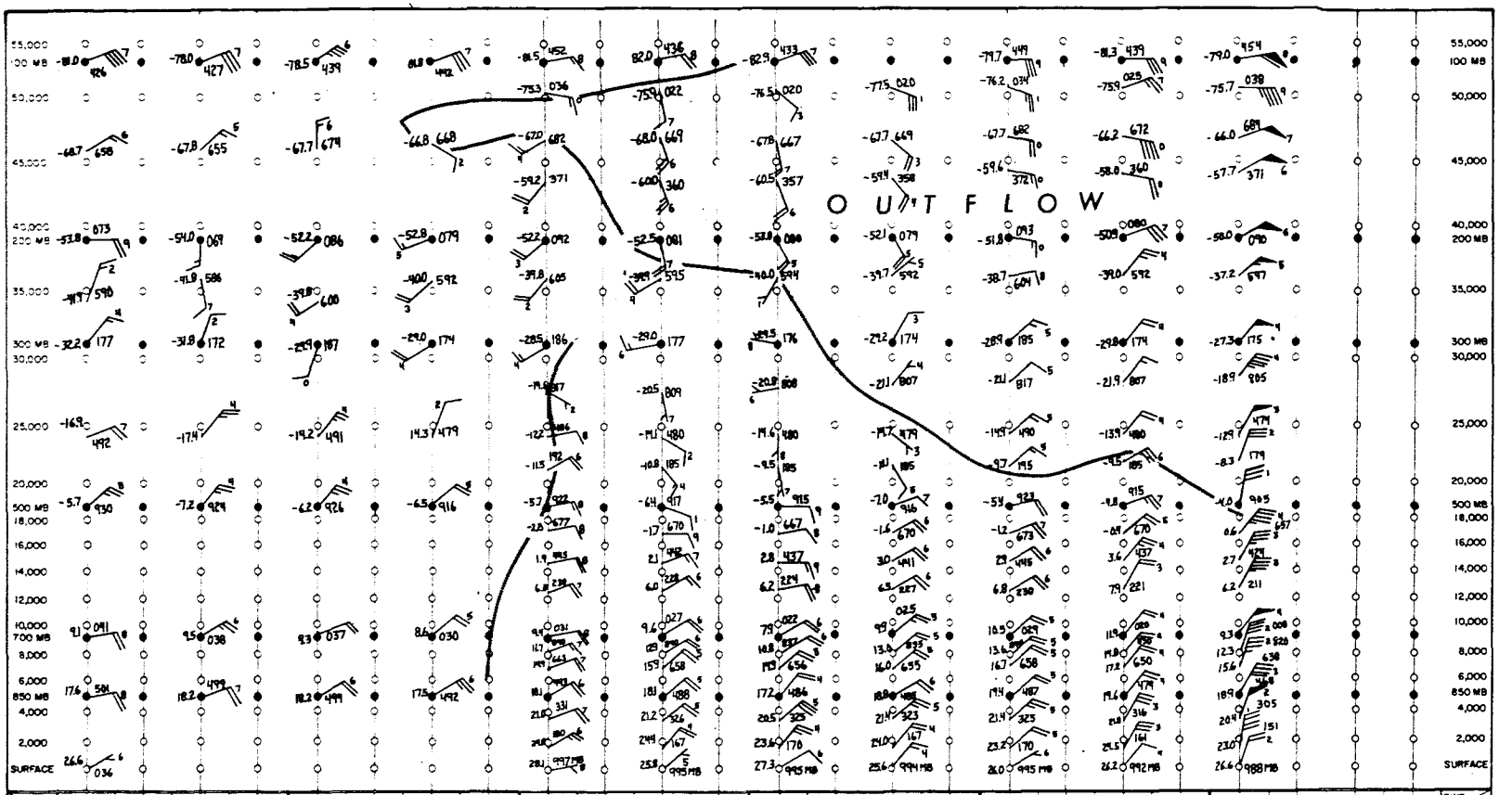
OUTFLOW
55,000
100 MB
50,000
45,000
40,000
200 MB
35,000
300 MB
30,000
25,000
20,000
500 MB
18,000
16,000
14,000
12,000
10,000
700 MB
8,000
6,000
850 MB
4,000
2,000
SURFACE
TIME
SFC DATA
Ch
Cm
CL
N
W
PPP
OPAQUE SKY USAF
OPAQUE SKY NAVY
RR
24 HR ΔP
SFC WIND
DATE 6 NOV 1962
DATE 7 NOV 1962
DATE 8 NOV 1962
DATE 9 NOV 1962
DATE 10 NOV 1962
DATE 11 NOV 1962
STATION GUAM (218)

FIGURE 121

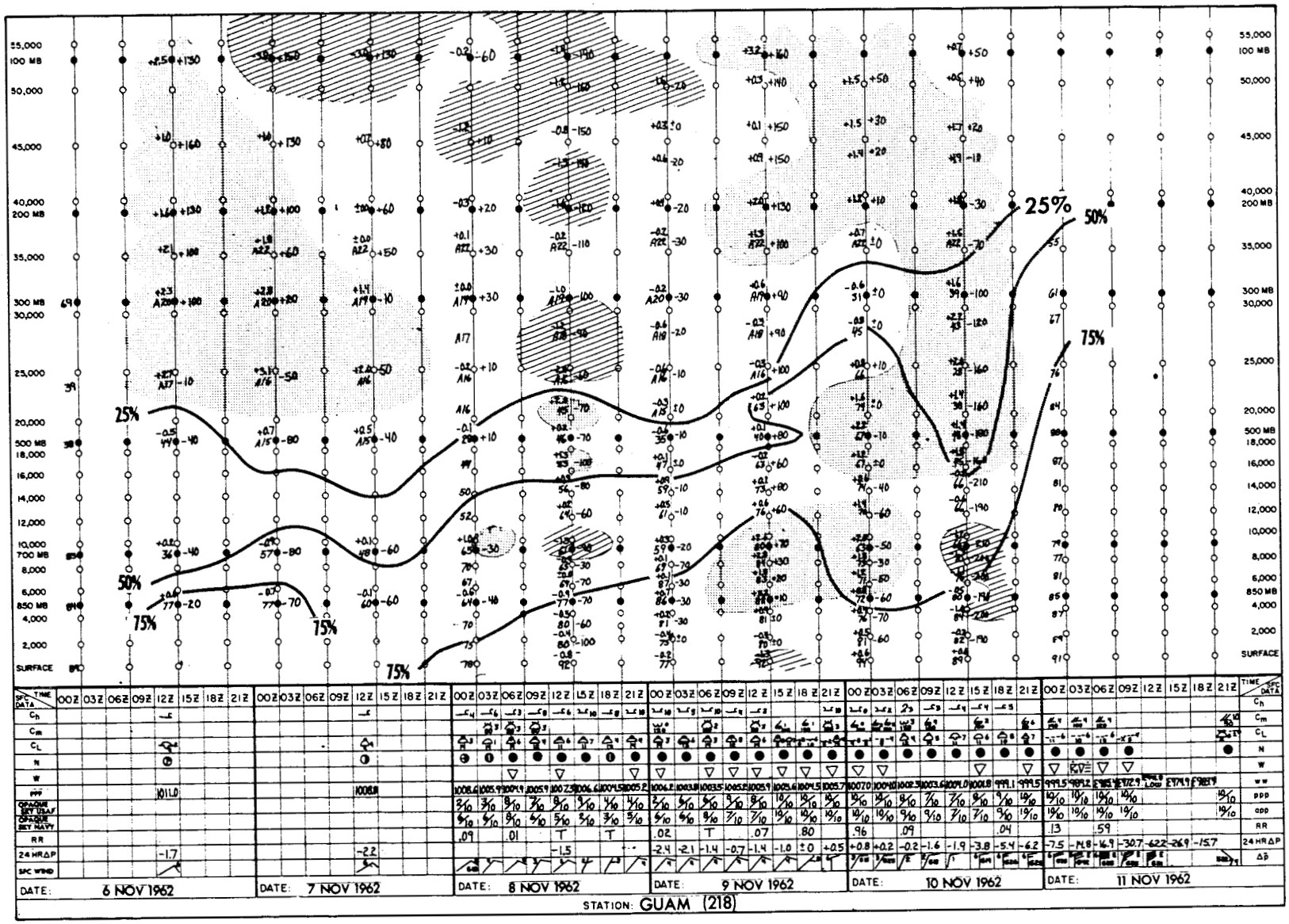
55,000
100 MB
50,000
45,000
40,000
200 MB
35,000
300 MB
30,000
25,000
20,000
500 MB
18,000
16,000
14,000
12,000
10,000
700 MB
8,000
6,000
850 MB
4,000
2,000
SURFACE
25%
50%
75%
25%
50%
75%
75%
75%
DATE: 6 NOV 1962
DATE: 7 NOV 1962
DATE: 8 NOV 1962
DATE: 9 NOV 1962
DATE: 10 NOV 1962
DATE: 11 NOV 1962
STATION: GUAM (218)

FIGURE 122

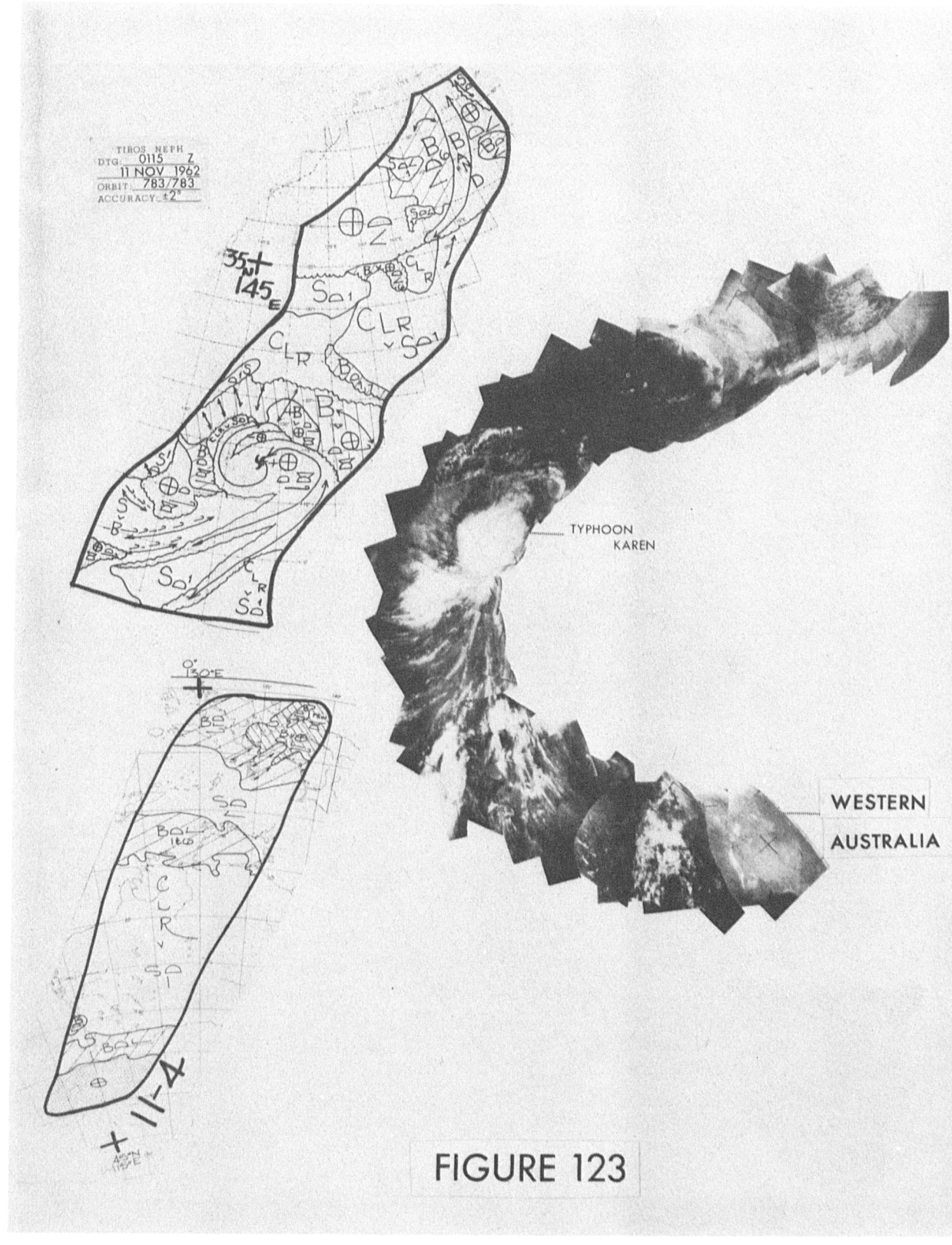
TIROS NEPH
DTG 0115 Z
11 NOV 1962
ORBIT 783/783
ACCURACY ±2°
35°
145°E
TYPHOON
KAREN
WESTERN
AUSTRALIA
11-4

FIGURE 123

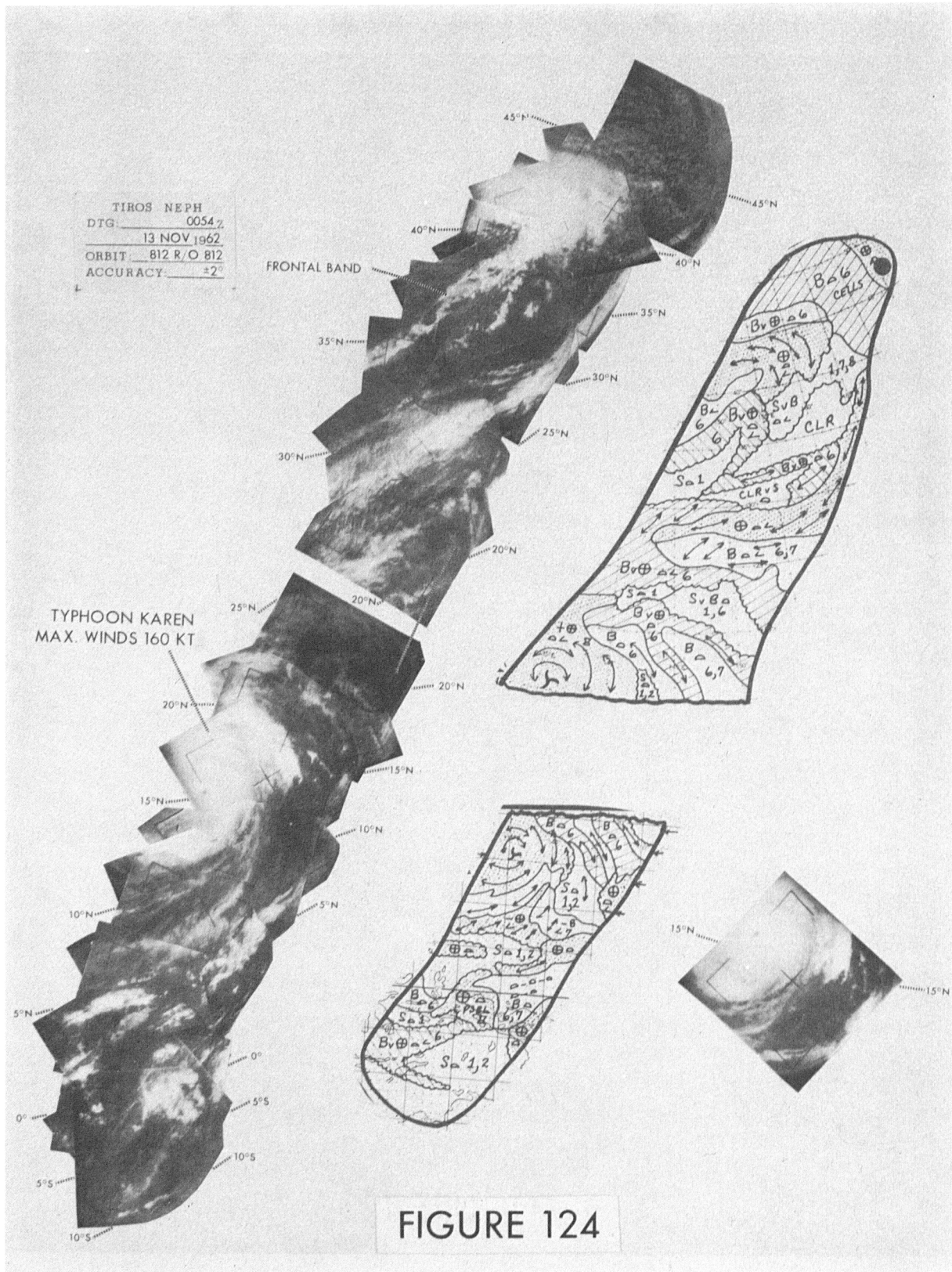
TIROS NEPH
DTG: 0054Z
13 NOV 1962
ORBIT: 812 R/O 812
ACCURACY: ±2°
FRONTAL BAND
TYPHOON KAREN
MAX. WINDS 160 KT
45°N
40°N
35°N
30°N
25°N
20°N
15°N
10°N
5°N
0°
5°S
10°S
Bv⊕ 6
B 6
CELLS
SvB
CLR
Sa 1
CLR VS
Sa 1,2
B 6,7

FIGURE 124

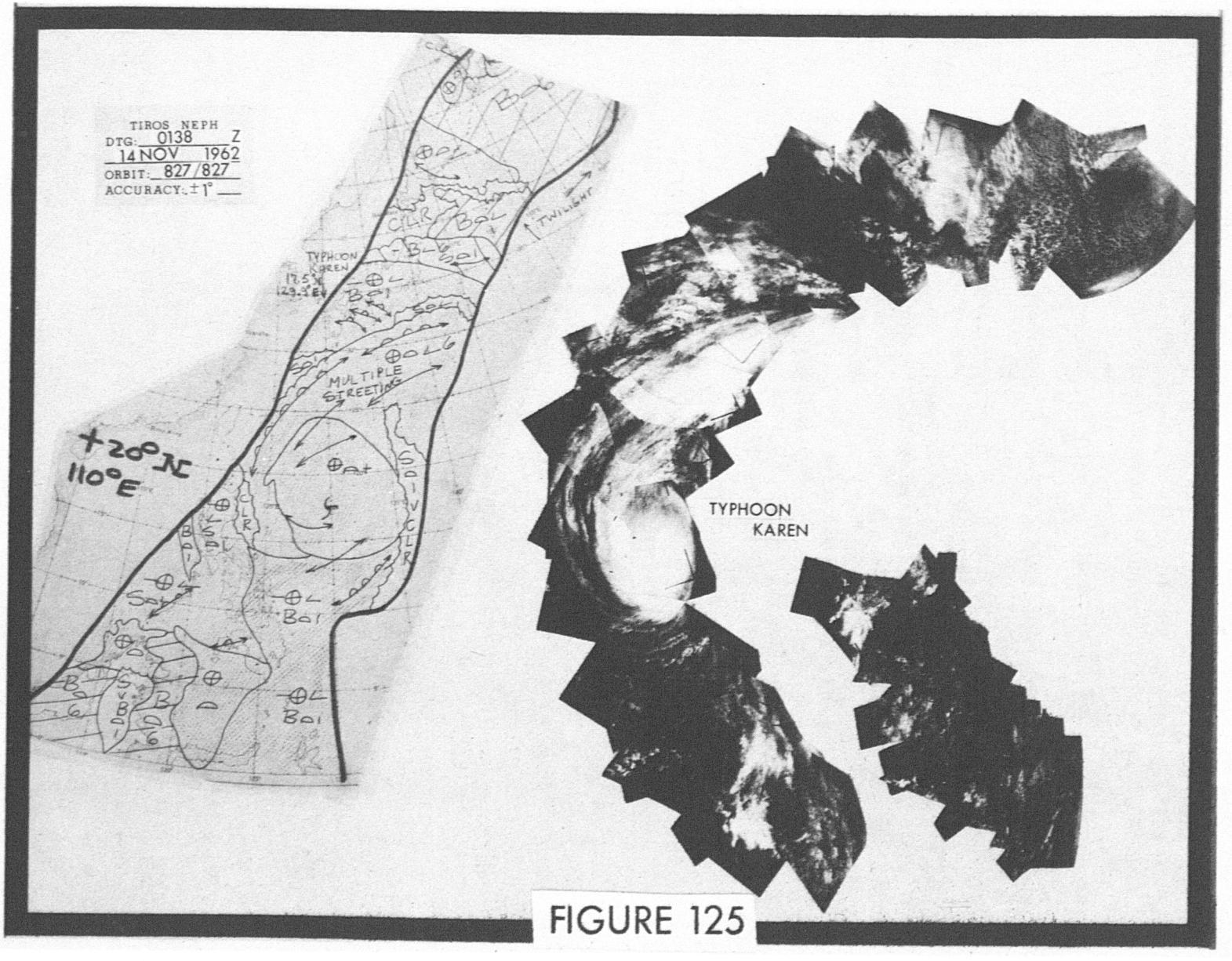


FIGURE 125

129 428

Number

17. On the Use of Redundancy in the Design of Operational Satellites, S. F. Singer, (April, 1963) PB 163 743 $1.60

18. An Analysis of CDA Station Effectiveness in Relation to Satellite Orbit, R. L. Pyle and S. F. Singer, (July, 1963) PB 163 744 $3.60

*19. An Investigation of Meteorological Satellite Characteristics for Continuous Earth Coverage, Thomas I. Gray, Jr., and S. F. Singer, (July, 1963) PB 163 745 $4.60

20. Conference on Satellite Ice Studies, Maurice D. Baliles and Herbert Neiss (Ed.), (June, 1963) PB 163 746 $9.10

21. Calculations of the Earth's Spectral Radiance for Large Zenith Angles, D. Q. Wark, J. Alishouse, and G. Yamamoto, (October, 1963)

22. Spectral Reflectance Photography of Earth from Mercury Spacecraft MA-8, Stanley D. Soules, (November, 1963)

*23. The Use of Satellite Cloud Photographs in Numerical Weather Prediction, Mary Ann Ruzecki, (December 1963) AD 428 269 $2.60

24. TIROS Cloud Pattern Morphology of Some Mid-Latitude Weather Systems, H. J. Broderick, Jr., (January, 1964)

25. Infrared Photography of the Earth from Mercury Spacecraft MA-9, Stanley Soules, (in preparation)

26. Meteorological Products from Digitized Satellite Vidicon Cloud Pictures, C. L. Bristor and W. M. Callicott, (March 1964) AD 600 078 $1.25

27, 28, In preparation

29. Tropospheric Conditions over the Tropical Atlantic as Observed by Two TIROS Satellites and Research Aircraft During 22 September 1962, H. M. Johnson and Captain R. W. Fett, (in press)

30. Lowlight Coverage from Polar and Sun-Synchronous Orbits, R. L. Pyle, (April, 1964) AD 600 970 $.75

31. Specular Spectral Reflectance of Paints from 0.4 to 40.0 Microns, W. Y. Ramsey, (April, 1964)